University of Alberta

Characterization of a *Vibrio cholerae* Type VI Secretion System Toxin/Immunity Pair

by

Sarah Tamiko Miyata

A thesis submitted to the Faculty of Graduate Studies and Research
in partial fulfillment of the requirements for the degree of

Doctor of Philosophy

in

Bacteriology

Department of Medical Microbiology and Immunology

Fall 2013
Edmonton, Alberta

Abstract

Vibrio cholerae is the Gram-negative bacterium responsible for the diarrheal disease cholera. In addition to the well-characterized virulence factors – cholera toxin and the toxin co-regulated pilus – used by this organism to cause watery diarrhea, *V. cholerae* uses the type VI secretion system (T6SS) to mediate host-pathogen and inter-bacterial interactions. The T6SS is the most-recently described mechanism by which Gram-negative bacteria export toxins across their cell envelope. This macromolecular structure assembles in the cytoplasm and consists of an outer sheath and inner tube. The inner tube is thought to be capped with three or more proteins possessing both structural and toxic functions. Upon contraction of the outer sheath, the inner tube and cap are ejected out of the bacterium and into neighboring prokaryotic or eukaryotic cells.

I discovered VasX – a T6SS toxin required for *V. cholerae* virulence toward the host model *Dictyostelium discoideum* and for killing Gram-negative bacteria. My Ph.D. work showed that VasX associates with structural T6SS proteins and has homology to pore-forming colicins. Secretion of VasX depends on certain structural T6SS proteins and VasW – a proposed VasX chaperone protein encoded upstream of *vasX*. Upon insertion into the cytoplasmic membrane of target cells, VasX disrupts the integrity of the membrane leading to a loss of the cell's membrane potential, permeability to propidium iodide, and lysis of the cell in the presence of detergent. Thus, I propose that VasX acts similar to pore-forming colicins by insertion into the cytoplasmic membrane followed by pore-formation, ultimately leading to the death of the target cell.

The VasX immunity protein TsiV2 mediates protection from an oncoming VasX attack generated by neighboring sister cells. TsiV2 localizes to the bacterial membrane and generates protection against VasX even when TsiV2 is present in the cell at low protein levels. Expression of *tsiV2* is influenced by a dual regulatory mechanism where one promoter is located upstream of the TsiV2-encoding operon and another promoter is located within the upstream gene (i.e. *vasX*). This dual regulation ensures *tsiV2* is constitutively expressed at basal levels when expression of other T6SS genes is turned off, mediating protection against T6SS attack from kin bacteria. Taken together, this thesis characterizes the function of a T6SS toxin and the mechanism by which *V. cholerae* protects itself from being killed by sister cells.

Acknowledgements

I would like to first thank my supervisor Dr. Stefan Pukatzki for his guidance and patience throughout my Ph.D. and for taking a chance on me as your first graduate student. I cannot stress enough that I am completing my Ph.D. because of you and your overwhelming support through the tough times my project has endured. You provided me with a great balance between supervision and independence, and challenged me to become a better scientist and writer and I am grateful for the changes I have undergone during my tenure in your lab.

Thank you to my supervisory committee members: Dr. Tracy Raivio and Dr. Bart Hazes for your guidance and support over the past six years. Both of you have an optimism and enthusiasm for science that I hope will influence my future endeavors. Thank you to Dr. Rebecca Case and Dr. Francis Nano for taking the time to be part of my thesis defense committee. I also want to thank our lab technician, Teresa Brooks, who was always someone I could bounce ideas off of. I would not have been able to accomplish many of these experiments without you and I am incredibly grateful for all your help. Thanks to Drs. Kim Ellison, Judy Gnarpe, and Mark Peppler for being wonderful teaching mentors.

To Kalia, Sarwin, Lisa, Christine, Kelly, and Kiera: I value our friendship and am glad we have managed to remain great friends even though we have been separated by a great distance for the past 6 years. Thanks to all the friends I have met during my Ph.D., especially Joel, Rachael, Steven, Elisabeth, Chad, Verena, and Teresa. I'll miss our ugly sweaters, crazy Christmas hats, Halloween costumes and Food Fighters volleyball games. Thank you to Anna Manalo for always being so kind, such a great source of support, and sending tasty treats to the lab. And to my slo-pitch friends Matt, Haley, Ryan, Ally, Garson, Brad, and all the members of the Whiskey Cats, Ice Beers, U of A Corporate Challenge, Nightmare, Shadow, Jumpin' Jack Smash, and Food Fighters teams - you have all given me an area of focus outside of science and an outlet for my pent-up science frustration. Thanks for all the good times!

To my parents Cathy and Kaz: thank you for always stressing the importance of education and being nothing but supportive of me (emotionally and financially) while I continued my education (for what seems like forever). I can't thank you enough for all your love and support over the years in all my life endeavors; whether it was teaching me how to read before starting school, driving me back and forth to my part-time job, or spending countless hours at the baseball diamond. As a person, I strive to be as selfless and giving as you both are. And to my brother, Kellen: you are the closest person to me in the world. I miss our movie-quoting and video game marathons and look forward to moving back to Ontario so we can spend more time together.

Finally, to my husband-to-be, Zack: I cannot put into words how much you have positively influenced my life in the past 8 years. As the spouse of a grad student, I think you have become just as deeply engrained in my project as I have. You have been my rock, my main support system throughout my Ph.D., and have gotten me through some of my most challenging years. I am so proud of you and all you have accomplished over the last few years. We have come so far together and I look forward to the next step in our lives as a married couple.

Table of Contents

List of Tables

List of Figures

List of Abbreviations

6xHis	Hexa-histidine tag
ABC	ATP-binding cassette
ACD	Actin cross-linking domain
Ace	Accessory cholera enterotoxin
ATP	Adenosine-5’-tri-phosphate
BLAST	Basic local alignment search tool
βME	β-mercaptoethanol
BSA	Bovine serum albumin
C-	Carboxy terminus
CaM	Calmodulin
cAMP	Cyclic adenosine monophosphate
CCCP	carbonyl cyanide *m*-chlorophenyl hydrazone
CF	Carboxyfluorescein
CFTR	Cystic fibrosis transmembrane conductance regulator
CFU	Colony-forming units
CT	Cholera toxin
CTXφ	Cholera toxin filamentous bacteriophage
CVEC	Conditionally-viable environmental cells
DiOC2(3)	3,3'-Diethyloxacarbocyanine, iodide
DNA	Deoxyribonucleic acid
DSP	dithiobis[succinimidylpropionate]
EtOH	Ethanol
GFP	Green fluorescent protein

Hcp	Hemolysin co-regulated protein
HRP	Horseradish peroxidase
IAHP	IcmF-associated homologous protein
Ids	Identity of self
kDa	Kilodaltons
LB	Luria-Bertani
LPA	Lysophosphatidic acid
LPC	Lysophosphatidylcholine
LPCx	Large protein complex
LPS	Lipopolysaccharide
LUV	Large unilammelar vesicle
MLV	Multilammelar vesicle
MOI	Multiplicity of infection
N-	Amino terminus
NADH	Nicotinamide adenine dinucleotide hydride
NCBI	National Centre for Biotechnology Information
ONPG	Ortho-Nitrophenyl-β-galactoside
OD	Optical density
PA	Phosphatidic acid
PBD	Peptidoglycan-binding domain
PBS	Phosphate buffered saline
PC	Phosphatidylcholine
PCR	Polymerase chain reaction
PE	Phosphatidylethanolamine
PH domain/PHD	Pleckstrin homology domain

PI	Propidium iodide
PIns	Phosphatidylinositol
PKA	Protein kinase A
PS	Phosphatidylserine
PIP	Phosphoinositide phosphate
PSI	Pounds per square inch
PVDF	Polyvinylidene fluoride
qRT-PCR	Quantitative real time PCR
QS	Quorum sensing
RFU	Relative fluorescence units
RGVC	Rio Grande *Vibrio cholerae*
Rhs	Rearrangement hot spot
RNA	Ribonucleic acid
RPM	Revolutions per minute
Rtx	Repeats in toxin
S1P	Sphingosine-1-phosphate
SDS	Sodium dodecyl sulfate
SDS-PAGE	Sodium dodecyl-sulfate polyacrylamide gel electrophoresis
Sec	General secretion
T1SS	Type I secretion system
T2SS	Type II secretion system
T3SS	Type III secretion system
T4SS	Type IV secretion system
T5SS	Type V secretion system
T6SS	Type VI secretion system

T7SS	Type VII secretion system
TA	Toxin/anti-toxin
TAT	Twin arginine translocation
TBS-T	Tris-buffered saline containing tween(20)
TCP	Toxin co-regulated pilus
TLE	Total liver extract
TM	Transmembrane
vas	Virulence-associated secretion
VgrG	Valine glycine repeat protein G
VPI	*Vibrio* pathogenicity island
WCL	Whole cell lysate
x-gal	5-bromo-4-chloro-3-indolyl-β-D-galactopyranoside
Zot	Zonula occludens toxin

CHAPTER 1

Introduction

1. General Introduction

1.1 *Vibrio cholerae* and Disease

Vibrio cholerae, a Gram-negative, curved rod bacterium, is the causative agent of the diarrheal disease cholera. This bacterium was first identified by Filipo Pacini in 1854 [1, 2] and was subsequently grown in pure culture and further characterized by Robert Koch in 1883 [2]. *V. cholerae* is an aquatic organism that commonly lives in biofilms in association with zooplankton in estuaries or brackish waters [3], but can also exist as a free-living planktonic organism. A single, sheathed, polar flagellum provides *V. cholerae* with motility for swimming in its natural habitat and for colonizing the human intestine [4-8].

V. cholerae can exist in a conditionally viable state (referred to as "conditionally viable environmental cells" or CVEC) in the environment that is associated with suboptimal sodium chloride concentrations and nutrient deprivation [9, 10]. Bacteria living in this semi-dormant state are found in both rod and coccoid morphology and are associated in clumps [9, 10]. These cells are capable of reverting to an infectious form when grown in rich medium or when inoculated into rabbit ileal loops [10]. Culturing of O1 *V. cholerae* from water samples using routine laboratory techniques indicates significantly lower levels of the pathogen are present than the concentration required to cause cholera. The formation of CVECs that are revived only under specific conditions likely accounts for this underrepresentation of O1 *V. cholerae* in water samples [10]. Furthermore, it is believed that these CVECs serve as a reservoir for *V. cholerae*

between cholera outbreaks and allow the bacteria to survive under suboptimal conditions.

Over 200 serogroups of *V. cholerae* have been identified based on different lipopolysaccharide (LPS) O-antigens on the bacterial surface [11, 12] and exposure to bacteriophages has undoubtedly shaped the evolution of the cholera bacterium. Not only are the two major virulence factors utilized by *V. cholerae* of phage origin, but vibriophages are thought to dramatically influence the genetic diversity of the species and the seasonality, severity, and duration, of cholera outbreaks [13-16]. *V. cholerae* is also known to undergo phase variation to alter the presentation of its O-antigen presumably to avoid predation by bacteriophages and the host immune system [17]. Furthermore, rough *V. cholerae* strains lacking an O-antigen are frequently isolated from convalescent cholera patients supporting the idea that altering or repressing presentation of the O-antigen may serve as a mechanism of immune system evasion [18, 19].

These ~200 serogroups can be divided into two classes – O1/O139 and non-O1/non-O139 – based on the potential for *V. cholerae* to cause large-scale cholera outbreaks. Strains belonging to the O1 and O139 serogroup are known to utilize cholera toxin (CT) and the toxin co-regulated pilus (TCP) as their critical virulence factors [20-25]. Although CT is known to be responsible for the voluminous watery diarrhea associated with cholera, pandemic strains in which the genes encoding CT were deleted still caused mild diarrhea in humans indicating that CT is not the sole virulence factor utilized by *V. cholerae* (discussed in subsequent chapters) [26, 27]. Furthermore, some non-O1/non-O139

serogroup strains possess the genes for TCP and CT; however these strains produce much less CT compared to their O1 serogroup strain counterparts likely due to differences in regulation [28-32].

The O1 serogroup can be further subdivided into two biotypes: classical and El Tor. The difference between these biotypes is based on specific phenotypes such as hemolysis of sheep blood, agglutination of chicken erythrocytes, Voges-Proskauer reaction, susceptibility to polymyxin B, and sensitivity to certain phages [33, 34]. Classical strains also produce more cholera toxin than those belonging to the El Tor biotype [35]. In addition to these phenotypic differences, classical and El Tor strains can be differentiated based on genotypic polymorphisms as well. Classical and El Tor biotypes are known to possess different alleles for *ctxB* (which encodes the B subunit of CT). However, the emergence of El Tor biotype strains that possess classical cholera toxin – so-called "hybrid strains" – impedes the simplicity of genotypic classification [36-39]. Both classical and El Tor biotypes can also be further grouped into three distinct serotypes – Ogawa, Inaba, and Hikojima (very rare) –based on variations (termed antigens A, B, and C) in their LPS O1-antigen [33, 40, 41]. The Ogawa serotype possesses A, B, and a small amount of C antigen. Strains of the Inaba serotype express A and C antigens, and those of the Hikojima express all three of A, B, and C [42]. The B and C antigens differ by the presence or absence, respectively, of a methyl group on the terminal sugar of the O-antigen [43]. The A antigen is a combination of the core and O-antigen polysaccharides [44].

The first five cholera pandemics occurred between 1817 and 1896 and it is believed that all five pandemics were caused by the classical biotype. In 1854, a physician named John Snow (with the assistance of Reverend Henry Whitehead) identified the source of a cholera outbreak in the London neighborhood of Soho to a communal water pump [45]. However, Snow was unable to observe or isolate the causative agent in water samples [45] – this feat was achieved by the Italian scientist Filippo Pacini in the same year [1, 2]. In 1883, Robert Koch became the first person to propagate *V. cholerae* in pure culture. Because *V. cholerae* was not identified as the causative agent of cholera until 1854, it is impossible to determine whether the classical biotype was, indeed, responsible for the first 5 cholera pandemics; however, this is presumed to be the case. The sixth cholera pandemic was caused the classical biotype, and lasted from 1899-1923.

The current seventh pandemic began in 1961in Indonesia and is associated with the El Tor biotype. Interestingly, prior to the 7^{th} pandemic, El Tor strains were only associated with sporadic diarrheal outbreaks [2] and the precise reason behind the disappearance of classical strains is unknown. It was demonstrated, however, that El Tor strains differ from classical strains in their by-products resulting from carbohydrate metabolism. Classical biotype strains exhibited a drop in medium pH and reduced viability as a result of acidic by-products [46]. El Tor biotype strains produced a neutral end product, thereby increasing its fitness compared to classical strains [46]. This difference in carbohydrate metabolism may account for the out-competition observed resulting in the El Tor biotype strains causing the current cholera pandemic.

The O139 serogroup gained recognition in 1992-1993 during an epidemic of cholera caused by a strain that failed to agglutinate with O1 antiserum. Horizontal gene transfer between an O1 El Tor serogroup strain and a non-O1 serogroup strain is the purported mechanism by which the O139 serogroup emerged [47]. Strains belonging to the O139 serogroup were responsible for a cholera epidemic associated with rapid spread and severe disease [48-52], but this outbreak failed to result in an outbreak of pandemic proportion.

Non-O1/non-O139 serogroup strains can also cause human illness and have been isolated from wound, ear, cerebral spinal fluid, urinary tract, and intestinal infections [53-56]. Small-scale cholera-like outbreaks have been attributed to infection with non-O1/non-O139 serogroup strains and this disease occurs in the absence of TCP and CT. Because these strains cause illness in the absence of the canonical virulence factors associated with cholera, they utilize other virulence factors that are poorly understood, or have yet to be identified.

The recent cholera outbreak in Haiti was largely reported to be caused by a *V. cholerae* O1 El Tor isolate [57, 58]. In contrast, one report indicates stool samples collected at the beginning of the epidemic contain a mixture of *V. cholerae* O1 and non-O1/non-O139 strains [59]. Hasan *et al*. suggest that the presence of non-O1/non-O139 serogroup strains serve as a reservoir for genetic diversity [59]; however it is also possible that in addition to serving as a genetic reservoir, these strains also contributed to disease among Haitians who experienced cholera-like symptoms during this outbreak.

Humans become infected with *V. cholerae* upon ingestion of contaminated food or water. Because *V. cholerae* is sensitive to the low pH of the stomach, a high infectious dose (~10^8-10^{11} organisms) is required for cholera to manifest [60]. Those that naturally produce less stomach acid, or are prescribed antacid medication are at a higher risk for contracting cholera because less bacteria (~10^4 organisms) are needed to cause disease [61]. In general terms, malnutrition is not thought to increase the risk for contracting cholera; however deficiency in vitamin A increases the probability of *V. cholerae* infection [62]. Persons with O-type blood group antigens are less likely to contract cholera, but the molecular reason for this is not known [63]. It is thought that *V. cholerae* survives passage through the acidic stomach due to its close-knit association in biofilms [64]. Upon colonization of the small intestine, *V. cholerae* produces CT [65] which results in disruption of the ion balance in intestinal epithelial cells (see section 1.2.1) resulting in water efflux from the cells and into the intestinal lumen. Large volumes of watery diarrhea, also referred to as "rice-water stools", are the hallmark of the disease cholera; however, vomiting also commonly occurs [66]. Persons infected with toxigenic *V. cholerae* can lose up to 20 liters of fluids per day and shed hypervirulent *V. cholerae* at a concentration up to 10^9 bacteria per milliliter in their stool [61, 67].

Prevention and Treatment of Cholera

The disease cholera manifests itself after ingestion of contaminated food or water and as a consequence, disease prevention is especially difficult in countries that lack proper water sanitation. Due to its association with zooplankton and its ability to form biofilms on aquatic particulate matter, *V. cholerae* infection rates can be reduced by filtering drinking water with cheesecloth which removes large particulate matter [68]. After infection with *V. cholerae*, one is naturally immune to re-infection by the same serogroup strain for approximately three years [69-71]. Two cholera vaccines (Dukoral and mORCVAX) are currently available that provide >50% protection for up to two years[72]. Although clinical trial data was accrued in areas where cholera is endemic, the vaccines are also marketed toward tourists to avoid contracting cholera while visiting foreign countries. Both vaccines are administered orally and contain killed whole *V. cholerae* bacteria, and persons that receive the vaccines reduce their risk of death from cholera by 50% [73, 74]. The vibriocidal immune response is generated largely against LPS [75, 76] and antibodies against CT do not elicit protective immunity [70]. There are several reasons accounting for the difficulties involved in developing an effective cholera vaccine including the short-lived memory B-cell response to LPS and a lack of understanding as to which antibody isotype provides the greatest protection [77-79].

The most crucial treatment for cholera patients is replacement of fluids and electrolytes; however, provision of clean drinking water or intravenous fluid replacement is problematic in developing countries, making it difficult to replace

the fluids lost from diarrhea and vomiting. Although infection with *V. cholerae* is self-limiting, cholera is a disease associated with high morbidity and mortality rates. Each year there are ~3-5 million cases of cholera resulting in 100,000-120,000 deaths (due to dehydration and shock) [80]. However, the actual number of cholera cases is presumed to be grossly underestimated due to poor record-keeping, those who do not seek medical intervention, and the lack of proper reporting by developing countries to avoid financial burdens due to loss of tourism.

Antibiotic treatment in combination with oral rehydration therapy can lessen the symptoms, and hasten recovery of cholera patients but is also more costly and warrants added consideration for the possibility of selecting for antibiotic resistant *V. cholerae* strains [81-84]. Quinolones (target DNA gyrase) and tetracyclines (inhibiting translation) are the most common antibiotics used to treat cholera infection [85, 86]; however, due to increasing antibiotic resistant strains, the use of antibiotics has been restricted for treatment of patients suffering from severe dehydration [84-86]. With all factors considered, ingestion of *V. cholerae* induces a vicious cycle of infection, dissemination, and re-infection in areas lacking proper hygiene, water sanitation, and access to medical care.

1.2 Virulence factors of *V. cholerae*

1.2.1 Cholera toxin and the toxin co-regulated pilus

The disease cholera manifests itself as a result of the secretion of CT – an $A:B_5$ toxin that disrupts the electrolyte balance within intestinal epithelial cells. Following ingestion of *V. cholerae* (via contaminated food or water), the bacteria traverse the stomach and colonize the small intestine. It is believed that the existence of environmental *V. cholerae* in biofilms provides protection for the bacteria during passage through the acidic conditions in the stomach [87]. Once in the small intestine, production of TCP facilitates interactions between *V. cholerae* cells resulting in microcolony formation [21, 88-90]. Although TCP is not required for colonization of the intestinal epithelium, it is an important virulence factor for *V. cholerae* during human infection and in the infant mouse model [20, 21]. The gene encoding the major pilin subunit *tcpA* is encoded, along with numerous other genes required for TCP biogenesis and regulation, within a ~41.2 kb genetic locus referred to as the *Vibrio* pathogenicity island (VPI) [20, 21, 91-97]. Also located within the VPI is *toxT* which encodes a transcriptional regulator required for expression of *V. cholerae* virulence genes such as those encoding TCP and CT [97]. The VPI is thought to have bacteriophage origins because it possesses integrase and transposase genes and is flanked by *att* sites [91]. However, Faruque and colleagues were unable to detect production of VPI phage particles in 46 TCP^+ *V. cholerae* strains grown in conditions known to induce phage particle production [98]. Interestingly, TCP, which is encoded

within VPI, serves as the receptor for the lysogenic, filamentous bacteriophage CTXφ.

Genomic DNA from CTXφ consists of two distinct regions: the RS2 region and the core. CTXφ DNA integrates at specific sites in the *V. cholerae* chromosome mediated by genes in the RS2 region [99] while the core possesses the genes *ctxA* and *ctxB* encoding the two subunits of CT. The core region also encodes the accessory cholera enterotoxin (Ace) and the zonula occludens toxin (Zot) [99]. Along with accessory roles in virulence, these two toxins are also important for the production of extracellular CTXφ particles[16]. Once integrated into the *V. cholerae* chromosome, CT becomes part of the ToxT regulon and expression of CT is upregulated when inside the host.

CT is secreted via the type II secretion system (T2SS, discussed in section 1.3) and the B portion binds GM_1 gangliosides on intestinal epithelial cells [100, 101]. Following endocytosis of the holotoxin, CT undergoes retrograde transport to the endoplasmic reticulum where the reduction of a di-sulfide linkage results in the release CT-A_1 [102]. CT-A_1, which carries out the enzymatic function of CT, is retrieved from the endoplasmic reticulum and escapes degradation by the degradasome thereby accessing the cytoplasm [103-107]. Association of CT-A_1 with host ADP-ribosylation factor exposes the active site of CT-A_1 leading to ADP-ribosylation of $G\alpha_s$ [103-105]. This modification locks $G\alpha_s$ in an active conformation resulting in exacerbated production of the second messenger cyclic adenosine monophosphate (cAMP) and increased activation of cytosolic protein kinase A (PKA). Phosphorylation of the cystic fibrosis transmembrane

conductance regulator (CFTR) by PKA results in ATP-mediated efflux of ions and secretion of water, out of the intestinal epithelial cells accounting for the large volumes of diarrhea associated with the disease cholera [108].

1.2.2 Quorum Sensing

Quorum sensing (QS) is a mechanism of bacterial communication via small diffusible chemical signals called autoinducers [109, 110]. The ability to communicate with one another provides single-celled organisms a means to coordinate gene expression and act similar to multicellular organisms. QS has been characterized in detail in the organisms *Pseudomonas aeruginosa* [111-118], *Staphylococcus aureus* [119-123], and *Vibrio harveyi* [124-131]. In these three cases, an increasing cell population results in a higher local concentration of autoinducer in the surrounding vicinity. Once autoinducer concentrations reach a certain threshold, the organisms coordinately increase expression of specific genes: virulence genes in the case of *P. aeruginosa* [113, 118, 132-136] and *S. aureus* [121, 137-139], and luciferase genes in the case of *V. harveyi* [110, 126-128, 130, 131, 140].

V. cholerae also uses QS as a communication mechanism to regulate expression of virulence genes; however, the QS regulatory circuit of this organism acts opposite to that of *P. aeruginosa* and *S. aureus* as virulence genes are down-regulated at high cell density. *V. cholerae* produces and responds to two autoinducers (CAI-1 and AI-2) using parallel QS circuits [124, 141-143]. At low

cell density, the autoinducer sensors, CqsS and LuxPQ, autophosphorylate and act as kinases resulting in phosphorylation of LuxO – an activator of the alternate sigma factor, σ^{54} [110, 124, 126, 127, 130, 144]. Phosphorylated (active) LuxO triggers a regulatory cascade that signals through the master regulator HapR, resulting in increased expression of genes belonging to the ToxT regulon and genes involved in biofilm production [130, 144-147].

At high cell density, an increase in autoinducer concentration reverses the LuxO-mediated regulatory cascade. LuxPQ and CqsS act as phosphatases, removing the phosphate from (inactivating) LuxO [142, 148] resulting in decreased expression of biofilm and virulence genes. It is believed that *V. cholerae* uses the small intestine of the human host to facilitate growth to high numbers after which the organism is flushed out of the intestine via the voluminous watery diarrhea [149]. After being purged from the body, *V. cholerae* exhibits a hyperinfectious phenotype (for at least 5 hours) associated with increased motility, increased expression of genes responsible for nutrient acquisition, and decreased expression of chemotaxis genes [150].

Thus at low cell density, expression of biofilm genes helps the organism to maintain colonization of the small intestine while virulence factors are coordinately expressed. Once the bacteria reach high titers in the intestine, biofilm and virulence genes are shut off allowing detachment from the intestinal epithelium and exit from the host. After being purged from the host, *V. cholerae* returns to its natural environment from where it can repeat its infectious cycle.

1.2.3 Additional virulence factors of *V. cholerae*

In addition to the well-characterized virulence factors CT and TCP, *V. cholerae* has an armament of other virulence factors at its disposal, some of which are strain specific. The zinc-metalloprotease, HapA, degrades host proteins such as mucin and disrupts tight junctions between epithelial cells [151-154]. The majority of *V. cholerae* isolates produce the *V. cholerae* cytolysin – a pore-forming toxin encoded by *hlyA* that causes a wealth of toxic effects toward host cells including apoptosis, autophagy, necrosis, and cell lysis [155-164]. The repeats-in-toxin A (RtxA) protein was also predicted to act as a pore-forming toxin; however, RtxA has since been shown to cause host cell-rounding resulting from covalent cross-linking of actin monomers into higher molecular weight structures [165, 166]. Infection of polarized epithelial cells with $RtxA^+$ *V. cholerae* results in perturbation of tight junctions, which could foster dissemination of the bacterium beyond the epithelial surface [167]. RtxA is secreted by an atypical type I secretion system (T1SS, described further in section 1.3) [168]. Interestingly, HlyA, RtxA, and HapA all contribute to persistent *V. cholerae* infection in the mouse intestine – a phenotype that occurs independently of CT or TCP[169].

As mentioned earlier, the core region of CTXφ encodes *ctxA*, *ctxB*, *ace*, and *zot*. Ace is an integral membrane protein that increases host cell ion permeability and Ace-mediated fluid accumulation was observed using the rabbit

ileal loop model [34, 170, 171]. Zot causes disruption of intestinal epithelial cells tight junctions and was implicated in causing mild diarrhea associated with a potential vaccine strain of *V. cholerae* lacking *ctxA* and *ctxB* [172].

V. cholerae are also known to use secretion systems (summarized in detail in section 1.3) to modulate host-pathogen interactions. The strain AM-19226 (O39 serogroup) utilizes the type III secretion system (T3SS) to cause intestinal damage in a rabbit infection model via translocation of at least four effector proteins into host cells[173-175]. Furthermore, the type VI secretion system (T6SS) is a recently described mechanism by which *V. cholerae* injects effector proteins into both eukaryotic and prokaryotic cells. This system will be described in detail in later sections.

1.3 Bacterial Secretion Systems

To date, six secretion systems (T1SS-T6SS) have been described in Gram-negative bacteria (Figure 1-1). A seventh secretion system was recently identified in Gram-positive *Mycobacterial* species (Figure 1-1). In general, all secretion systems share the ability to transport proteins across the bacterial cell envelope. However, secretion systems also differ from each other in their mechanism of secretion, the proteins they use to construct the secretion apparatus, and whether they release their substrates into the extracellular milieu or directly inject proteins into target cells. The ability to transport proteins is especially important for

bacterial pathogens to export or inject proteins that have toxic effects toward host cells.

1.3.1 The general secretory pathway and the twin arginine translocation pathway

Both the general secretory (Sec) pathway and the twin arginine translocation (TAT) pathway involve transporting proteins across the bacterial cytoplasmic membrane and are active in both Gram-positive and Gram-negative organisms. In the case of Gram-positive bacteria, Sec- and TAT-translocated proteins are exposed on the bacterial surface, or are proteolytically cleaved and released into the extracellular environment [176]. For Gram-negative bacteria, the Sec and TAT pathways locate proteins to the periplasm. Proteins destined for Sec translocation possess an N-terminal hydrophobic signal sequence (typically 5-30 amino acids long) that targets the protein to the cytoplasmic Sec translocation machinery that transports the protein across the membrane in an unfolded state [177]. Sec signal peptides display considerable diversity in length and sequence; however the structural and physiochemical functions are well-conserved [178, 179].

Proteins targeted to the TAT translocation machinery also possess an N-terminal signal sequence; however, the TAT signal sequence is rich in basic amino acids and contains two arginine residues (S/TRRXFLK) [180]. The TAT system transports folded proteins across the cytoplasmic membrane [180]. For

both the Sec and TAT systems, the N-terminal signal sequences can be cleaved as the proteins traverse the cytoplasmic membrane.

1.3.2 Sec- and TAT-dependent protein secretion mechanisms

The T2SS and T5SS are secretory mechanisms used exclusively by Gram-negative bacteria and both systems depend on protein translocation into the periplasm by either the Sec or TAT pathway. Once in the periplasm, proteins can be transported across the outer membrane using the T2SS translocation apparatus for which at least 12 additional proteins are involved[181]. Importantly, *V. cholerae* uses the T2SS to secrete CT and chitinase, and a T2SS mutant is defective in biofilm formation [182-186].

The T5SS is also referred to as the "auto-transporter" system because proteins mediate their own secretion across the outer membrane. Once proteins have been translocated across the inner membrane by the Sec or TAT system, the C-terminus of the protein folds into a β-barrel structure and inserts into the outer membrane forming a pore through which the remainder of the protein can be transported[187-189]. From there, the protein can remain tethered to the outer membrane or can be cleaved and released into the extracellular environment [187-189]. The T5SS is also involved in a form of microbial competition called contact-dependent growth inhibition (CDI) which will be discussed further in section 1.4.2.

1.3.3 Sec- and TAT-independent protein secretion mechanisms

The T1SS, T3SS, T4SS, T6SS, and T7SSs all possess the ability to transport proteins across the cell envelope in a Sec- and/or TAT-independent manner. The T1SS is used by Gram-negative bacteria to transport proteins from the cytoplasm to the extracellular environment, by-passing the periplasm. This system uses an inner membrane ATP-binding cassette (ABC) transporter to provide the energy for translocation. A membrane fusion protein bridges the cytoplasmic membrane and an outer membrane pore complex, providing a translocation channel that bypasses the periplasm to the extracellular milieu [190, 191].

The T7SS is responsible for secretion of at least two small proteins – ESAT-6 and CFP-10 – from *Mycobacterium tuberculosis* [192]. Both proteins are important for the virulence of this bacterium [192]; however it remains unclear exactly how these proteins are secreted across the *Mycobacterial* waxy cell wall.

The T3SS, T4SS, and T6SS are all proposed to form a molecular needle on the bacterial surface called the injectosome that is used to deliver bacterial toxins directly into the host or target cell [193-196]. T3SS injectosome structural proteins share similarity with flagellar apparatus proteins [195]. Two well-characterized T3SS belong to *Yersinia pestis* and *Salmonella enterica* serovar Typhimurium where both organisms use the T3SS to inject effector (toxin) proteins into host cells [197].

The T4SS injectosome proteins are homologous to bacterial conjugation machinery proteins and fittingly, this secretion system is known to transport both proteins and DNA [191, 198]. The stomach pathogen *Helicobacter pylori* injects the effector protein CagA into gastric epithelial cells using its T4SS[199], whereas *Agrobacterium tumefaciens* uses its T4SS to inject a protein-DNA complex into plant cells [200-202].

The T6SS is the most recently described mechanism by which Gram-negative bacteria inject proteins into target cells. In 2000, Das and colleagues observed up-regulation of the gene VCA0120 when the *V. cholerae* O1 El Tor strain N16961 was used to infect rabbit ileal loops [203]. VCA0120 is similar to *icmF*, the gene product of which is imperative for the T4SS of *Legionella pneumophila* [204-206]. Bioinformatic analyses identified a highly-conserved gene cluster in Gram-negative bacteria, all of which encoded this *icmF* homologue [207]. This cluster was referred to as the IcmF-associated homologous protein (IAHP) gene cluster until it was demonstrated that this gene cluster encodes a secretion apparatus that mediates toxicity toward the amoeboid host model *Dictyostelium discoideum* [194, 207]. Following this discovery, the IAHP cluster was designated the T6SS.

T6SS structural proteins share similarity with the tip of the T4 bacteriophage tail spike [208, 209] and thus, it is not surprising that bacteria use the T6SS to inject toxins into neighboring bacteria [210-221]. Interestingly, the T6SS also mediates virulence towards phagocytic eukaryotic cells like J774 murine macrophages or the amoeba *D. discoideum* [193, 194, 209, 213, 222-229].

The T6SS is a diverse mechanism that can target both eukaryotes and prokaryotes and will be discussed in detail in Chapters 3-6.

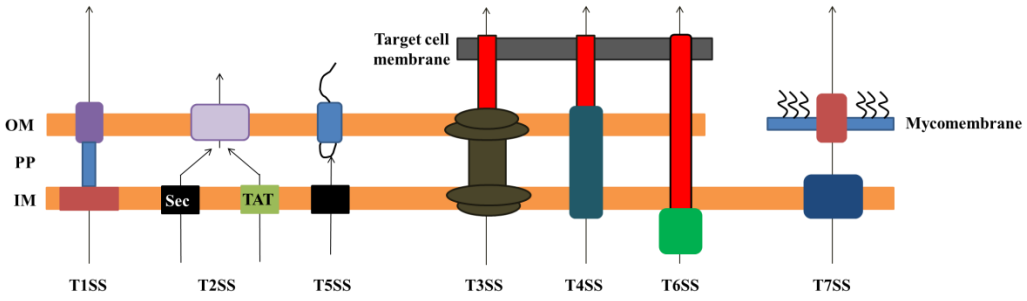

Figure 1-1. Schematic representation of the seven bacterial secretion systems described to date. OM; outer membrane, PP; periplasm, IM; inner membrane.

1.4 Microbial competition

1.4.1 Bacteriocins

Bacteriocins are peptides or proteins ranging in size from ~4-80 kDa that are produced and released by one bacterium for the purpose of killing closely related bacterial species [230, 231]. Several bacteriocins have been identified including colicins (produced by *E. coli*), pyocins (*P. aeruginosa*) [232], cloacins (*Enterobacter cloacae*) [233-235], marcescins (*Serratia marcescens*) [236], vibriocins (*V. cholerae*) [237-239] and megacins (*Bacillus megaterium*) [240]. This section will focus on colicin mechanisms of action because colicins are the most well-characterized type of bacteriocin.

Colicins have diverse mechanisms by which they exert their toxic effects including degradation of DNA and RNA [241-247], inhibition of murein synthesis [248], and pore-formation in the cytoplasmic membrane of the target cell [249-252]. Colicins are released into the extracellular environment and upon binding their target cell gain access to their cellular targets via sophisticated entry mechanisms. Importantly, colicin-mediated toxicity does not depend on cell-to-cell contact between the producing and target bacteria. Colicin production is triggered when the cell encounters a stress and activates the SOS response [253-255] as described in more detail below. This induces expression of the colicin-encoding operon including both the colicin itself and the colicin lysis protein (encoded downstream) [256-263]. The colicin lysis protein results in "quasilysis", and ultimately, death of the producer cell and release of colicins into the extracellular milieu [264-266]

The first step in colicin import into target cells is binding to an outer membrane protein on the cell surface by the central region of the colicin molecule [267-269]. The outer membrane protein bound varies depending on the colicin. For instance, colicins A and E1 bind BtuB (involved in vitamin B_{12} transport), colicin K binds Tsx (nucleoside transporter), and colicin U binds OmpA [231]. The presence of the outer membrane protein on the target cell is what determines specificity and susceptibility to certain colicins [270]. Translocation of the colicin across the cell envelope is mediated by the N-terminal domain and the enzymatic activity is carried out by the C-terminal domain [235, 271-276].

The presence of immunity proteins protects colicin-producing cells from suicide or auto-toxicity. DNase and RNase colicins are bound by their cognate immunity protein in the cytoplasm of the producing cell, and following secretion. Dissociation of the immunity protein only occurs after the colicin has bound the outer membrane receptor on its target cell [277-280]; however, the exact mechanism of dissociation remains unclear. On the other hand, immunity proteins to pore-forming colicins localize to the inner membrane where they either act as a plug, or prevent pore formation from occurring [231, 281].

Genes encoding colicins and their immunity proteins are organized in a conserved manner. All colicins are regulated via an SOS promoter that is repressed by the LexA protein [282-287]. Upon encountering a cellular stress such as UV radiation or chemical exposure, induction of the SOS response results in activation of RecA and cleavage of LexA leading to expression of colicin-encoding operons [287, 288]. Why colicin-encoding operons are regulated by the cell SOS response still remains unclear. For nuclease colicins, the immunity protein is encoded by a small gene located immediately downstream from (or even overlapping with) the stop codon of the toxin gene [241, 256, 258, 283, 289-292]. Importantly, transcription of nuclease colicin immunity genes is dually regulated with one promoter located upstream of the operon containing the colicin and immunity genes (polycistronic) and another promoter encoded within the toxin gene that strictly regulates expression of the immunity gene (monocistronic) [278, 282, 285, 293-297]. Pore-forming colicin genes are also regulated by the SOS response; however, the immunity gene for these colicins is canonically

located on the opposite strand of DNA in the inter-genic region between the colicin and lysis genes [231]. These immunity genes also have their own promoter ensuring that low-level expression of the immunity protein is maintained within the producer cell at all times in order to protect against autotoxicity[285].

The genetic organization and function of colicin and immunity genes is similar to that of bacterial toxin/anti-toxin (TA) systems. The significant difference between colicin/immunity and toxin/anti-toxin systems is that colicins are released into the environment to bind and kill target cells, whereas TA systems mediate killing from within the producing bacterium [298]. Furthermore, the genetic organization of TA cassettes is (generally speaking) opposite of colicin/immunity genes where the anti-toxin gene precedes that of the toxin [298, 299]. Three types of TA systems have been characterized; in each case, the toxin is a protein, but the anti-toxin can either be RNA (type I and III) or a protein (type II). TA systems are ubiquitous in nature and have been identified in the chromosome of nearly all free-living bacteria and archaea [300]. Initially, TA systems were described as plasmid-borne entities that ensured daughter cells each received a copy of the plasmid during bacterial growth and were thus referred to as "plasmid addiction systems" [301]. Both the toxin and anti-toxin are constitutively expressed within the cell and form a complex that inhibits the toxin's activity. Upon duplication, daughter cells receive the toxin/anti-toxin protein complex; however, if one of the cells fails to inherit the plasmid then no further anti-toxin can be produced. The anti-toxin is degraded at a higher rate than

the toxin and therefore, the daughter cell lacking the TA-encoding plasmid will release the toxin from this complex resulting in cell suicide [298, 302-304] . Chromosomally-encoded TA systems have also been identified and it has been suggested these function as a bacterial programmed cell death mechanism [298, 305].

1.4.2 Contact-dependent growth inhibition

Bacteria are commonly found in nature as part of complex microbial mixtures where communication via QS allows for cooperative behaviors. In stark contrast to this harmonious existence, bacteria must also compete for space and nutrients. It is thus not surprising that bacteria have evolved mechanisms not only to cooperate, but also to out-compete bacterial neighbors. CDI was first described in an *E. coli* strain (EC93) isolated from rat feces and involves delivery of an outer membrane-bound toxin from the producer cell to a receptor on the target cell surface [306-315]. CDI gene clusters include three genes: *cdiB*, *cdiA*, and *cdiI*. Together, CdiA and CdiB compose a two-partner secretion system (i.e. T5SS) where CdiB forms a β-barrel in the outer membrane through which the toxin CdiA is exported [306]. After translocation across the outer membrane, CdiA remains tethered to the producing cell. Upon interacting with its receptor on the target cell, BamA (a conserved outer membrane protein), the C-terminus of CdiA is cleaved and traverses the cell envelope to its cellular target [314, 316]. Similar to colicins, the CdiA producer cell is protected against autotoxicity and killing by sister cells due to the presence of the immunity protein CdiI [306, 307].

CDI is not restricted to *E. coli* EC93, but is present in numerous Gram-negative bacteria including plant, animal, and human pathogens [315]. CdiA is a protein with a polymorphic C-terminus. This diversity provides different CdiA proteins with the ability to target different cellular components [307, 314, 315]. The immunity protein CdiI also exhibits great diversity in different CDI^+ bacteria which is not surprising given that the immunity protein specifically inhibits the function of CdiA [307, 311, 312]. For example, CdiA from UPEC *E. coli* EC93 causes metabolic down-regulation of *E. coli* K-12 via pore-formation in the inner membrane [307]. Alternately, CdiA from UPEC *E. coli* 536 has tRNase activity and CdiA from the plant pathogen *Dickeya dadantii* 3937 possesses DNase activity [315].

Bioinformatic analyses suggested that CDI systems share similar features with "rearrangement hot spots" or Rhs elements [312, 317]. Rhs elements were initially described as repetitive DNA sequences resulting in genetic duplications [318]. Multiple Rhs elements can be found within the *E. coli* K-12 genome and are predicted to be the result of unequal recombination events between different Rhs elements [318]. Similar to CDI, Rhs loci encode a large protein followed by a small ORF that could represent a toxin/immunity pair. Indeed, two Rhs loci in the *D. dadantii* 3937 genome were shown to mediate growth inhibition of competitor cells [317]. Interestingly, Rhs-mediated growth inhibition by *D. dadantii* 3937 was dependent on a functional T6SS implying that the Rhs toxin was secreted in a T6SS-dependent manner [317].

Interestingly, the C-termini of Rhs toxins are polymorphic and share similar enzymatic activity to CdiA proteins and orphan *cdiA*/*cdiI* gene clusters have been located throughout the genome of CDI^+ bacteria [312, 317]. Furthermore, VgrG proteins (belonging to the T6SS) that possess C-terminal enzymatic activity also share similar features with Rhs elements [319]. Taken together, it seems that Rhs elements provide a basic mechanism for creating heterologous populations of enzymatic C-termini. Intra- and inter-bacterial recombination of Rhs C-termini could result in a diverse array of bacterial toxins that can be targeted for export from the cell by both CDI and the T6SS.

1.4.3 Self/non-self recognition

Proteus mirabilis is a Gram-negative, rod-shaped bacterium that is present in water and soil, and also as part of the normal human intestinal flora. This organism can also cause urinary tract infections in humans leading to the formation of bladder and/or kidney stones [320-322]. *P. mirabilis* exhibits swarming motility when grown on a semi-solid surface such as an agar plate. The ability to swarm is characterized by differentiation of the bacterium into an elongated, hyper-flagellated cell referred to as a "swarmer cell" [323-326]. When swarms consisting of two different *P. mirabilis* strains approach each other, a visible line or boundary is formed between the two encroaching swarms [323-326]. On the other hand, when two swarms of the same strain approach each other, boundaries do not form and the two swarms merge together [324, 327].

Although *P. mirabilis* is known to produce bacteriocins called proticines, proticine production is not the sole determinant that mediates boundary formation [325]. This was demonstrated using four individual strains of *P. mirabilis* that do not produce, and are not sensitive to, proticines. These strains maintained the ability to form boundaries with each other suggesting that other factors are involved in boundary formation [325, 328]. Boundary formation is based on the ability of *P. mirabilis* strains to differentiate between "self" and "non-self" and this is mediated by a set of proteins termed Ids for identity of self [326, 329]. Three *ids* genes – *idsA, idsB*, and *idsD* – share similarity with the T6SS genes *hcp, vgrG*, and *vasX* (Appendix Figure 9-1 and [326]). The *ids* gene cluster is transcribed as an operon and has a similar genetic organization as the T6SS gene cluster encoding VgrG-2, Hcp-2, and VasX (Appendix Figure 9-1 and [326, 329]). The VasX homologue, IdsD (Dr. B. Hazes, unpublished observation), was identified as a crucial determinant of self/non-self recognition [326]. When *idsD* is deleted, the wild-type *P. mirabilis* parent strain no longer recognizes the *idsD* mutant as "self" [326]. It is currently unclear how the Ids proteins mediate boundary formation, however, enlarged and rounded cells have been observed in the vicinity of the swarm boundary [323, 327]. Given the similarity between crucial Ids and T6SS proteins, it is feasible that *P. mirabilis* swarms engage in T6SS-like inter-bacterial interactions resulting in bacterial killing and boundary formation.

1.5 The type VI secretion system

The T6SS is the most recently described mechanism by which Gram-negative bacteria export proteins across their cell envelope. This secretion system is encoded by a diverse array of proteobacteria including numerous plant, animal, and human pathogens [216, 330-332]. Similar to the T3SS and T4SS, the T6SS is presumed to form a molecular syringe on the bacterial surface that punctures, and delivers toxins into, target cells. T6SS gene clusters encode at least 20 ORFs and a single bacterium has been found to encode up to six complete T6SS gene clusters. T6SS gene clusters from select Gram-negative bacteria are presented in Figure 1-2.

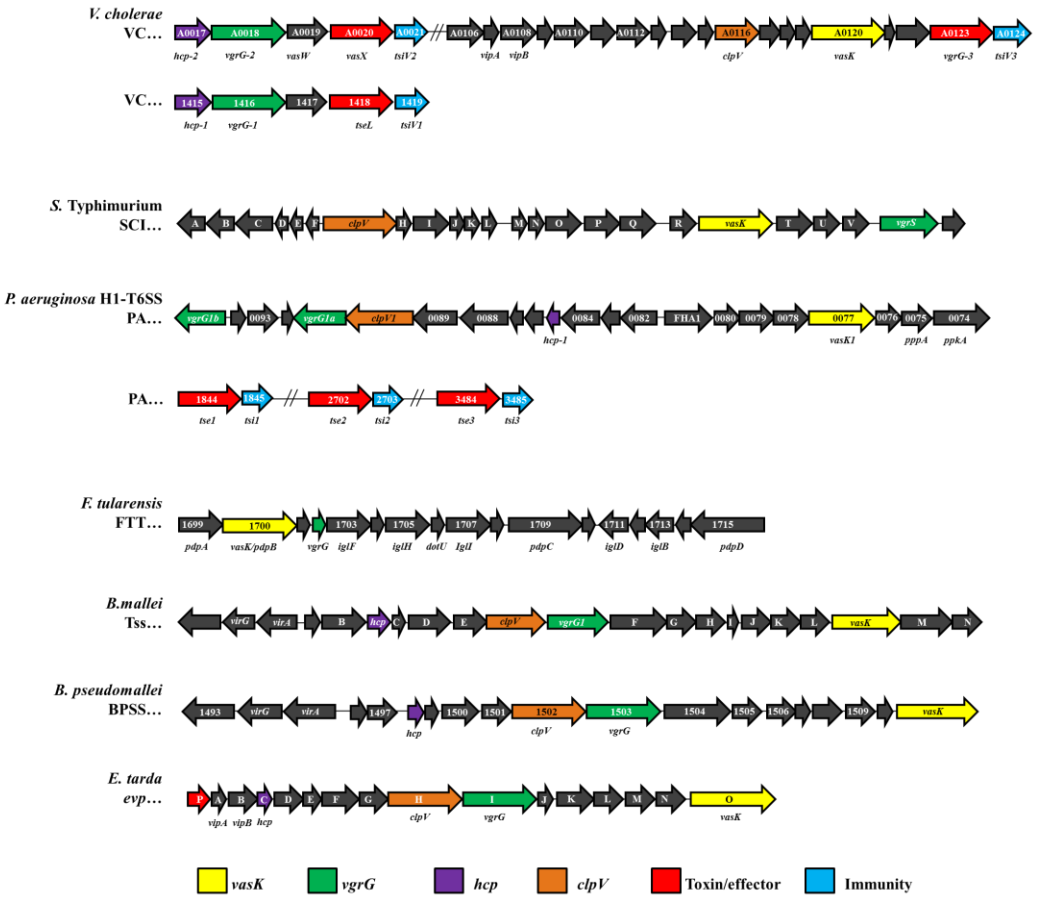

Figure 1-2. Schematic representation of T6SS gene clusters in select Gram-negative bacteria. Highlighted genes are indicated by the colour scheme presented in the legend.

1.5.1 T6SS-mediated killing of eukaryotes

The T6SS was initially described as a protein secretion apparatus used to target eukaryotes [193, 194]. Toxic phenotypes were observed upon infection of murine macrophages and the social amoeba *D. discoideum* with *V. cholerae* [193, 194, 209, 222-224, 333] and antibodies against T6SS proteins from cystic fibrosis patient sputum samples suggested *P. aeruginosa* uses the T6SS in chronic lung infections [193]. The ability to target eukaryotic cells using the T6SS has since

been demonstrated for a wealth of Gram-negative T6SS$^+$ bacteria including *Burkholderia cenocepacia, Burkholderia mallei, Burkholderia pseudomallei, Edwardsiella tarda, Edwardsiella ictaluri, Francisella tularensis* and *novicida, Salmonella* Typhimurium and Gallinarum, *A. hydrophila*, and *Helicobacter hepaticus* [224-229, 334-348].

One recurring theme in T6SS-mediated toxicity toward eukaryotes is the specific targeting of phagocytic cells like macrophages or *D. discoideum*. Ma *et al.* elegantly demonstrated that inhibition of phagocytosis using cytochalasin D prevented *V. cholerae* T6SS-mediated toxicity in J774 murine macrophages [222]. Furthermore, when non-phagocytic Chinese hamster ovary cells (which are normally resistant to T6SS-mediated effects) were engineered to induce opsonophagocytosis of *V. cholerae*, they became susceptible to killing by *V. cholerae* in a T6SS-dependent manner [222]. Other examples of phagocyte-specific phenotypes include actin rearrangements in ANA-1 murine macrophages by *B. cenocepacia*, increased intracellular replication and survival of *B. mallei* in RAW264.7 murine macrophages [226], formation of multinucleated giant cells by *B. pseudomallei* in RAW264.7 macrophages [225], survival of *S.* Gallinarum within murine and avian macrophage cell lines [349], and phagosomal escape and intracellular growth of *Francisella* species [345, 350, 351]. The reason for the T6SS utilization specifically following uptake by phagocytic cells is currently unclear; however, it has been demonstrated that acidic conditions, and other changes concomitant with the environment inside the phagolysosome induce T6SS-gene expression in certain bacterial species [334, 336, 352, 353]. This

implies that the conditions within the phagosome allow T6SS$^+$ bacteria to sense the host environment and up-regulate virulence factors accordingly.

1.5.2 The T6SS and microbial competition

The structural proteins that comprise the T6SS needle complex share homology with the tail spike of the T4 bacteriophage [208, 209]. Thus, it is not surprising that bacteria use the T6SS for inter-bacterial competition [211-214, 217, 354]. Characterization of the T6SS bacterial killing mechanism is still in its infancy; however both *V. cholerae* and *P. aeruginosa* secrete toxins that degrade the peptidoglycan of the target cell [210, 215]. Cell wall degradation appears to be a common theme in T6SS-mediated bacterial killing, as genes encoding similar toxins are found in β-, δ-, and ϒ-proteobacteria [216].

Lipase proteins are another common T6SS bacteria-targeting effector [216, 221, 332, 355] whose function has been demonstrated in *B. thailandensis*, *V. cholerae*, and *P. aeruginosa* [332]. In the case of *P. aeruginosa*, the lipase toxin (Tle5^{PA}) converts phosphatidylethanolamine (PE) into phosphatidic acid (PA) within the target cell inner membrane [332]. Although it is not clear at this time what specific toxic effect the conversion of PA confers, the authors also demonstrated that lipase toxins render target bacterial cells more permeable to propidium iodide (PI) and thus perturb the inner membrane [332].

Interestingly, some T6SS$^+$ bacteria are able to target both prokaryotes and eukaryotes. *V. cholerae* strain V52 possesses one T6SS gene cluster encoding

both prokaryotic and eukaryotic toxins and it has been demonstrated that this strain kills *D. discoideum*, murine macrophages, and a variety of Gram-negative bacteria [194, 209, 211, 223]. Furthermore, some bacterial genomes contain multiple evolutionarily distinct T6SS gene clusters including *P. aeruginosa*, *B. thailandensis*, *B. mallei*, and *B. pseudomallei* [213, 225, 226, 356-358]. In the case of *B. thailandensis* it was demonstrated that one of the T6SS clusters specifically targets eukaryotes, while another targets prokaryotes[213]. Figure 1-3 provides a summary of the different mechanisms used by bacteria to mediate microbial competition.

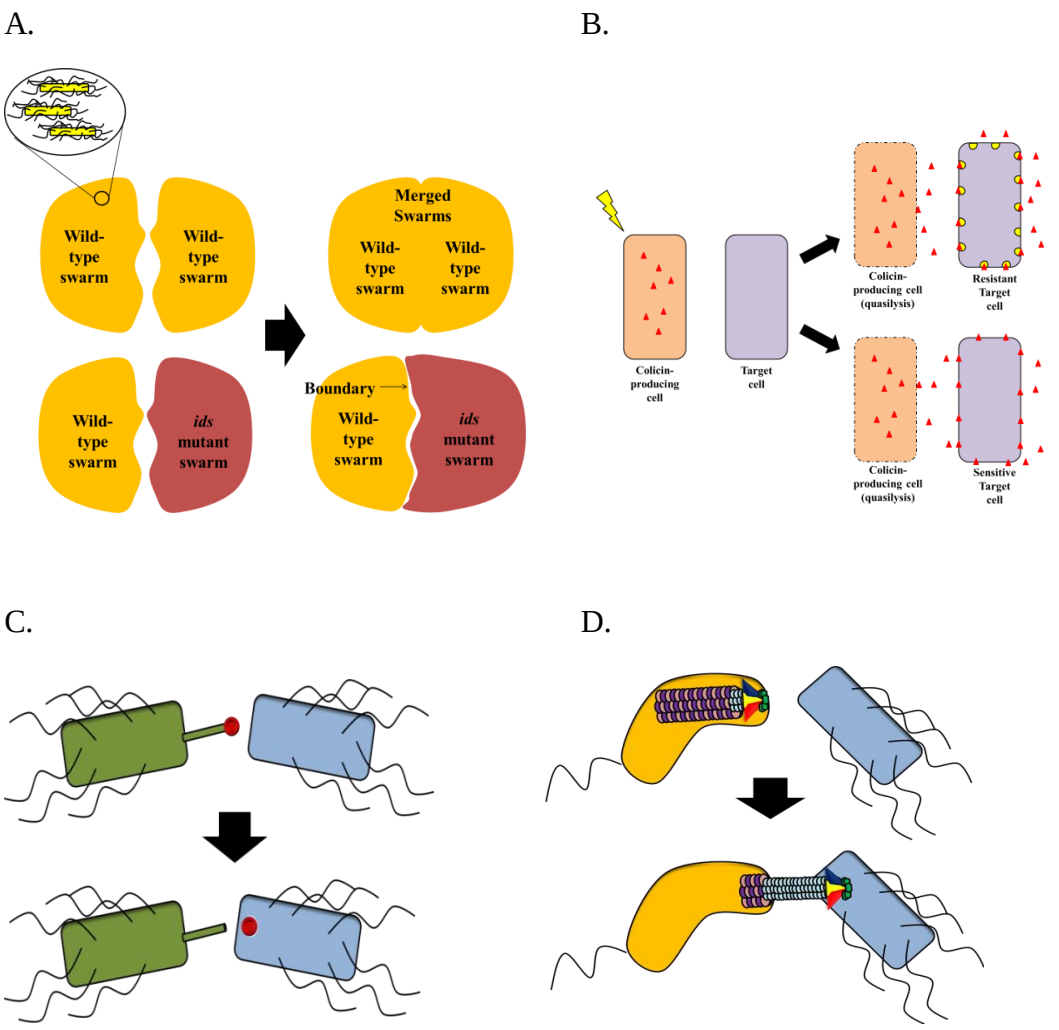

Figure 1-3. Different mechanisms utilized for microbial competition. (A) Swarms of *P. mirabilis* consist of elongated, hyperflagellated swarmer cells (circle inset). "Self/non-self" recognition by *P. mirabilis* results in boundary formation between two swarms (lower panel) when the genes encoding for "identity of self" (*ids*) are mutated. Two encroaching swarms of the wild-type strain recognize each other as "self" and do not form boundaries (top panel). (B) Colicins (red triangles) are produced following a cell stress event. Concomitant production of the colicin lysis protein results in "quasilysis" and permeates the producer cell resulting in colicin release into the extracellular medium. Neighboring cells that produce the colicin immunity protein (yellow half-moon) are protected while nearby cells that do not produce the immunity protein are susceptible to colicin-mediated killing. (C) "Toxin on a stick" model where the CDI^+ *E. coli* (green) delivers the toxin (red circle) to the target cell (blue). (D) The T6SS is a macromolecular machine produced in the cytoplasm of the $T6SS^+$ cell. The VipA/VipB sheath (purple) surrounds the Hcp tube (light blue) which is capped with VgrG proteins (yellow, blue, red triangles) and associates with T6SS toxins (green). The Hcp tube is ejected from the cell delivering the VgrGs and other toxins into the target bacterial cell (blue).

1.5.3 Formation of the T6SS molecular syringe – structural T6SS proteins

The structural proteins that comprise the T6SS needle complex share homology with the tail spike of the T4 bacteriophage [208, 209]. Within the bacterial cytoplasm, the T6SS assembles as long dynamic structures composed of VipA and VipB proteins. The VipA/B complex forms a contractile sheath that surrounds an inner tube composed of Hcp proteins. Hcp monomers (~18 kDa) interact to form hexameric rings that can stack on top of one another forming a tube [193]. The Hcp tube has an outer diameter of 85 Å and an internal diameter of 40 Å [208]. It is hypothesized that the Hcp tube (surrounded by the VipA/B sheath) is capped with a trimer consisting of VgrG proteins located in the bacterial envelope[220].

Upon contraction of the VipA/B sheath, the Hcp tube capped with VgrGs is believed to be ejected from the cell to puncture into target cells [208, 218-220]. At this time, the formation of the T6SS syringe on the bacterial surface has not been visualized; however, the hallmark of a functional T6SS is the secretion of Hcp into culture supernatants [193, 194, 224, 229, 359, 360]. This protein is likely sloughed from the needle complex resulting in its presence in culture supernatants. When the T6SS was first described, it was believed that the Hcp tube formed a conduit through which proteins were translocated into host cells; however, this has yet to be demonstrated. Therefore it is currently unclear whether T6SS effector proteins actually traverse the T6SS needle complex, or are ejected from the cell by physical association with the tip of the needle.

Finally, two proteins provide the energy for protein secretion and for disassembly of the secretion apparatus. The IcmF-like inner membrane protein, VasK, provides the energy to translocate proteins across the cytoplasmic membrane [361] and the AAA+ ATPase protein ClpV disassembles the sheath complex following contraction [362]. Importantly, strains lacking *vasK* are unable to secrete T6SS proteins and are used routinely as a T6SS-negative strain.

1.5.4 Toxins of the T6SS

Although it is known that a diverse array of bacteria utilize the T6SS to target prokaryotes and eukaryotes, only a few of the proteins mediating the toxic effects have been identified and/or characterized. In *P. aeruginosa*, three toxins have been identified: type six exported 1-3 (Tse1-3) [214, 215]. The molecular function of Tse2 is not known; however, cytoplasmic production of this protein in both prokaryotes and eukaryotes results in toxicity [214]. Tse1 and Tse3 on the other hand are specific to bacteria as they degrade the peptidoglycan acting as an amidase and a muramidase, respectively [215]. *P. aeruginosa* producing any of Tse1-3 is protected against its own toxins by the presence of anti-toxins or immunity proteins specific to each of the toxins [214, 215]. In each case, the immunity gene is located directly downstream of the gene encoding the toxin which is analogous to the genetic organization of certain colicins, and the CDI system.

Reports of other T6SS toxins are scarce. The plant pathogen *Rhizobium leguminosarum*, was shown to transport the small ribose-binding protein RbsB in a T6SS-dependent manner; but what advantage this confers to *R. leguminosarum* is unclear [363]. The fish pathogen *E. tarda* uses its T6SS to secrete a small protein called EvpP that has no conserved domains and no characterized homologous proteins [228, 229, 335]. EvpP is crucial for virulence of *E. tarda* toward blue gourami fish; however, the exact function of EvpP has not been elucidated [229].

VgrG-1, VgrG-3, VasX, and TseL are T6SS toxins utilized by *V. cholerae* to mediate bacterial-host and inter-bacterial interactions [209, 210, 221-223, 332, 333, 355] and these toxins will be described in detail in the following section.

1.6 The *V. cholerae* T6SS

All sequenced strains of *V. cholerae* encode the T6SS implying that this system has been selected for throughout evolution. The T6SS genes in this organism are dispersed among three different areas of the *V. cholerae* chromosome (Figure 1-4) with two copies of *hcp* (*hcp-1* and *hcp-2*), and three *vgrGs* (*vgrG-1*, *vgrG-2*, and *vgrG-3*) [194]. The Hcp proteins have identical amino acid sequences and are functionally redundant [194]. On the other hand, VgrG proteins have unique sequences and cannot complement one another [209]. All three VgrGs share a similar N-terminal core but have varied C-termini. VgrG-1 contains a C-terminal actin cross-linking domain, whereas VgrG-3 has a

C-terminal peptidoglycan degrading domain [208-210, 222, 333]. VgrG-2 does not possess a C-terminal extension and solely consists of the core [208, 209].

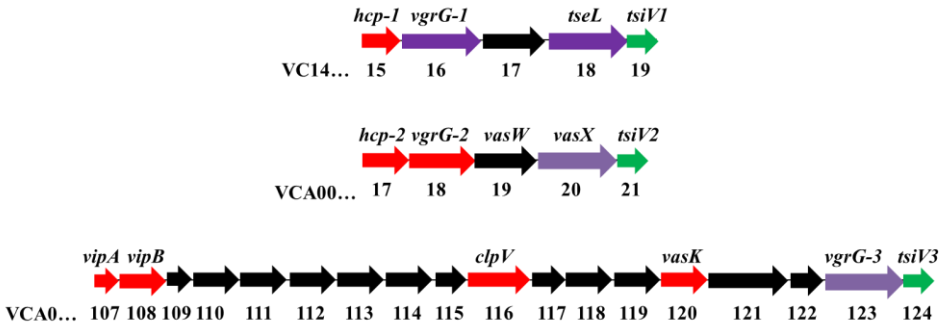

Figure 1-4. Schematic representation of the *V. cholerae* T6SS gene clusters. Genes encoding proteins with characterized functions are denoted in red, toxins are shown in purple, and immunity protein genes are green. Genes encoding T6SS proteins yet to be characterized are black.

1.6.1 Regulation of the *V. cholerae* T6SS

The regulatory mechanisms governing T6SS gene expression in *V. cholerae* are complex and are influenced by numerous regulatory pathways. To further complicate the subject, T6SS regulation varies between different *V. cholerae* strains. The O1 serogroup strains C6706 and N16961 both possess a full complement of T6SS genes; however, they are not known to express these genes under laboratory conditions. Fittingly, they also do not kill other bacteria, *D. discoideum*, or murine macrophages. T6SS genes of the strains A1552, AJ3 and AJ5 (O1 El Tor) are expressed in response to QS signals (i.e. at high cell density) [364]. Furthermore, the strains A1552, E7946, and 93Ag49 produce and secrete

Hcp when grown at 22 ^{o}C (as opposed to 37 ^{o}C) or when exposed to high salt concentrations [365] implying T6SS genes are expressed in these strains in conditions mimicking their natural habitat rather than during host infection. Interestingly, growing C6706 using these same conditions fails to induce Hcp production [365] and therefore, QS, low temperature, and high salinity are not universal T6SS activation cues that can be applied to all O1 *V. cholerae* strains.

C6706 is capable of expressing T6SS genes however, as evidenced by up-regulation of T6SS genes during colonization of the mouse small intestine [366] and the ability of C6706 to engage in T6SS-mediated bacterial killing in the presence of mucin (Dr. V. Bachmann, unpublished observation). Furthermore, production and secretion of Hcp can also be stimulated *in-vitro* via mutation of the QS regulator LuxO (i.e. mimicking high cell density conditions), and the global type six regulator A (TsrA) [367]. Although the cues inducing expression of T6SS genes in this strain are not fully understood at this time, the T6SS is functional and likely plays an important role during the lifecycle of C6706.

The *V. cholerae* O37 serogroup strain V52 was the causative agent of a cholera-like outbreak in Sudan in 1968 [368]. This strain possesses a constitutively-active T6SS when grown under standard laboratory conditions as evidenced by its ability to secrete Hcp into culture supernatants [194]. Furthermore, V52 uses its T6SS to kill murine macrophages, *D. discoideum*, and other Gram-negative bacteria [194, 209, 211].

V52 with its constitutive T6SS is not an anomaly, as *V. cholerae* isolates from the Rio Grande (RGVC strains) also constantly produce Hcp[369]. The reason behind the differences in regulation between V52 and the RGVC isolates compared to the O1 serogroup strains N16961, C6706, and A1552 is not clear. However, polymorphisms in the T6SS transcriptional activator VasH do not account for these differences [369, 370]. VasH is an activator of the alternate sigma factor, σ^{54} (RpoN) that binds promoters upstream of the two auxiliary T6SS gene clusters [370-372], making it the most downstream regulator of the T6SS regulatory cascade. There is debate in the literature as to whether VasH and RpoN regulate genes belonging to the large T6SS gene cluster. Bernard *et al.*, determined that VasH/RpoN positively regulates the large cluster (and the two satellite gene clusters) in *V. cholerae* strain O395 [371] while Dong *et al.*, observed that VasH/RpoN regulates only the two auxiliary T6SS gene clusters in *V. cholerae* V52 [372]. Nevertheless, VasH is an important T6SS regulator for *V. cholerae* even though different strains respond to a variety of extracellular signals leading to expression of T6SS genes.

1.6.2 *V. cholerae* and targeting eukaryotes

V. cholerae V52 deploys VgrG-1, VasX, and TseL using its T6SS to mediate virulence toward eukaryotic hosts [209, 221-223, 332, 333]. Following phagocytosis, V52 uses its T6SS to inject VgrG-1 into the cytoplasm of murine macrophages resulting in cell-rounding and eventually death [194, 209, 222]. As mentioned previously, VgrG-1 contains a C-terminal actin cross-linking domain

which catalyzes covalent attachment of host G-actin monomers to one another [209, 222]. *V. cholerae* causes inflammation and cross-links host cell actin in the intestine of infant mice [333] and causes macrophage cell-rounding [209]. Furthermore, a *vgrG-1* mutant of V52 is avirulent toward *D. discoideum* [373] presumably due to the inability to cross-link amoeboid actin; however this has not been experimentally demonstrated.

TseL is a phospholipase that disrupts phospholipid vesicles *in-vitro*[332] and is important for T6SS-mediated virulence as *V. cholerae* V52 lacking *tseL* is attenuated toward *D. discoideum* [221]. Presumably, TseL disrupts the cytoplasmic membrane of its target cells by cleaving phospholipids resulting in membrane instability.

VasX is another *V. cholerae* T6SS toxin and similar to TseL it appears to target the cytoplasmic membrane of host cells [223]. V52 lacking *vasX* is also attenuated in its virulence toward *D. discoideum*. VasX was the focus of my Ph.D. research and therefore, this toxin will be discussed in detail in the remaining chapters of this thesis.

1.6.3 *V. cholerae* and targeting prokaryotes

V. cholerae uses its T6SS to mediate inter-bacterial interactions resulting in the death of target cells [210, 211, 369, 370]. T6SS-mediated killing of other bacteria seems to be limited to Gram-negative organisms as V52 was unable to kill a panel of Gram-positive bacteria including *S. aureus, Enterococcus fecaelis*,

and *Listeria monocytogenes* (Appendix Figure 9-2 and [211]). Bacterial killing is an active process (i.e. heat-killed *V. cholerae* do not engage in killing) and occurs in a contact-dependent manner (Appendix Figure 9-3 and [211]). Interestingly, bacterial killing only occurs when the "predator" and "prey" bacteria are incubated together on an agar plate – that is, killing does not occur when the two bacteria are mixed in liquid culture[211]. A similar observation was made for bacterial competition involving *P. aeruginosa* [214].

We noted that *V. cholerae* V52 does not kill the *V. cholerae* O1 serogroup strains C6706, N16961, or O395 [211]. As mentioned previously, all of these strains encode T6SS genes but do not produce T6SS proteins under standard laboratory conditions [364, 365, 370]. Interestingly, RGVC isolates that constitutively produce T6SS proteins (refer to section 1.6.1) can kill *E. coli*, V52, and other non- *V. cholerae* environmental bacteria isolated from the Rio Grande (Appendix Figure 9-4 and [369]). This implies that these RGVC strains could use the T6SS for environmental fitness in their natural habitat and that the T6SS may provide a selective growth advantage in this setting. Furthermore, V52 uses its constitutively active T6SS to kill all RGVC isolates [369]. This T6SS bacterial killing has been termed "dueling" and time-lapse fluorescence microscopy has been used to visualize the VipA/VipB sheath contraction and (presumed) firing of the T6SS needle complex into neighboring bacterial cells [218-220].

Three toxins that mediate T6SS bacterial killing by *V. cholerae* have been identified: TseL, VgrG-3, and VasX. The phospholipase TseL is a versatile toxin with the ability to target both prokaryotes and eukaryotes [221, 332]. Russell *et*

al., determined that exposure to TseL alters the phospholipid composition of the target bacterium; however the specific effect this has on the bacterium is not yet understood[332]. VgrG-3 has both structural (see section 1.5.3) and toxin activity and acts by degrading the peptidoglycan of target cells [209, 210, 221]. Finally, VasX shares similarity with pore-forming colicins and disrupts the inner membrane of target bacteria, the mechanism for which will be discussed in detail in later chapters.

V. cholerae mediates T6SS-dependent killing of bacterial competitors using the three toxins described above; however some bacterial strains are resistant to killing by V52 such as *V. cholerae* N16961, O395, and C6706. Conversely, RGVC isolates are killed by V52. The mechanism behind this selective *Vibrio-Vibrio* killing involves specific toxin/immunity compatibility groups (D. Unterweger, submitted).

V. cholerae uses three toxins with unique mechanisms to kill other bacteria: TseL, VgrG-3, and VasX [210, 221, 332, 355]. Directly downstream of each toxin gene is a gene encoding the corresponding anti-toxin or immunity protein (Figure 1-4) that serves to protect *V. cholerae* from an attack by sister cells (D. Unterweger, unpublished observation and [374]). Each immunity protein specifically inhibits its cognate toxin (D. Unterweger, unpublished observation and [221]).

There appears to be diversity in the type of toxin/immunity pairs used by different *V. cholerae* strains which accounts for the ability of V52 to kill RGVCs,

and the inability of V52 to kill C6706 and N16961. That is, V52 has the same toxin/immunity sets as C6706 and N16961 and the immunity proteins provide C6706 and N16961 with protection against V52 toxins. RGVC isolates, on the other hand, utilize different toxins and immunity proteins and are therefore not protected against the toxins used by V52 (D. Unterweger, unpublished observation). Diversity in T6SS toxin/immunity pairs sets the stage for bacterial dueling and allows for inter- and intra-species bacterial competition.

1.7 Hypothesis and Aims

V. cholerae causes the devastating diarrheal disease cholera which is a major global health burden to this day. The cholera bacterium normally inhabits brackish water where it lives in mixed microbial populations. Following ingestion of the bacterium, *V. cholerae* colonizes the small intestine where it encounters the host microbiota and infiltrating host immune cells. Regardless of its environment, *V. cholerae* must compete for space and nutrients and we therefore hypothesize that the *V. cholerae* T6SS plays a role in the human disease cholera [375]. Our lab seeks to understand what role the *V. cholerae* T6SS plays in inter-bacterial and host-pathogen interactions with the ultimate goal of developing ways to inhibit or disable the T6SS for the betterment of human health. Recently, it was proposed that developing antimicrobial therapies that disable virulence factors rather than kill the bacterium would result in less selective pressure on the organism [376]. Ultimately, this would lead to a reduced frequency of resistance to these antimicrobial agents because the drugs do not kill the bacteria. The T6SS is one such virulence factor that could be targeted for development of novel antimicrobial therapies. Given that the T6SS mediates killing of macrophages and other bacteria we believe that *V. cholerae* uses its T6SS to establish infection in the human small intestine. Although a drug that disables *V. cholerae* of its T6SS would not prevent the index case of a cholera outbreak, such as drug could help reduce subsequent transmission of the organism by preventing intestinal colonization of people within a community and/or household.

At the outset of my graduate work, the focus of T6SS research involved the interaction of T6SS$^+$ bacteria and their host (eukaryotic) cell. The T6SS is a dynamic structure that forms in the bacterial cytoplasm consisting of an Hcp tube surrounded by a VipA/VipB sheath [193, 208, 218-220, 362]. Contraction of the sheath supposedly results in the ejection of the Hcp tube (capped with a VgrG trimer) out of the bacterium and into the target cell [208, 218-220]. I hypothesized that *V. cholerae* uses its T6SS needle complex to puncture host cells for the delivery of effector proteins through the Hcp tube and into the host cytoplasm. Using a proteomics approach, I identified the protein VasX which is secreted by V52 in a T6SS-dependent manner. The remainder of my Ph.D. thesis research focused on characterization of VasX, and proteins involved in VasX-mediated toxicity. The data chapters are organized by the questions addressed, and are as follows:

Chapter 1: What protein(s) are secreted by the T6SS?

I hypothesized that *V. cholerae* uses its T6SS to secrete effector proteins into host cells. To identify novel T6SS secreted proteins, I analyzed the protein composition of culture filtrates (in the presence or absence of the T6SS regulator VasH) by mass spectrometry and this led to the identification of VasX. To gain a better understanding of how VasX might function in the context of the T6SS, I carried out a series of biochemical and bioinformatic analyses.

Chapter 2: Is VasX required for *V. cholerae* virulence toward eukaryotes?

I hypothesized that VasX is important for T6SS-mediated virulence toward host cells. To test this, I analyzed virulence of V52Δ*vasX* toward both *D. discoideum* and murine macrophages. To gain a better understanding of the mechanism by which VasX acts, I tested the ability of VasX to bind membrane lipids using two independent techniques.

Chapter 3: Is VasX important for *V. cholerae* T6SS-mediated killing of bacteria?

To determine whether VasX is important for V52 T6SS-mediated bacterial killing, V52Δ*vasX* was used as the predator strain in a variety of bacterial killing assays. To determine the mechanism by which VasX kills bacteria I fused *vasX* to the sequence encoding the Sec signal peptide to target VasX to the periplasm. Cells expressing this fusion were used to determine toxicity of VasX to the producer cell, and whether VasX disrupts the membrane potential by perturbing the inner membrane.

Chapter 4: How does *V. cholerae* protect itself against VasX auto-toxicity?

I hypothesized that V52 produces an immunity protein that counteracts the toxic effects of VasX. To determine whether the small gene directly downstream of *vasX*, *tsiV2,* encodes the VasX immunity protein, *tsiV2* was deleted in the pandemic O1 strain C6706 which has a repressed T6SS under laboratory conditions. This mutant was tested for its sensitivity to V52 in a bacterial killing assay against V52. Subcellular localization experiments were performed to

determine where TsiV2 localizes within the bacterium. Promoter fusion experiments were performed to resolve the anomaly that C6706 is immune to VasX toxicity despite a lack of T6SS (i.e. *tsiV2*) gene expression. To determine whether VasX and TsiV2 interact, the two purified proteins were used for cross-linking studies and far western blotting.

Chapter 5: What role does VasW play in the *V. cholerae* T6SS?

Directly upstream of *vasX* on the V52 chromosome is the gene *vasW*. Because this protein is encoded within the gene cluster that encodes the important T6SS proteins Hcp-2, VgrG-2 and VasX, I hypothesized VasW is important for T6SS-mediated virulence. To gain insight into the role of VasW in the T6SS, V52Δ*vasW* virulence was assessed using the *D. discoideum* plaque assay and the bacterial killing assay. The secretion profile of V52Δ*vasW* was analyzed to determine whether this mutant strain retained the ability to secrete Hcp and VasX into culture supernatants.

The results of my study have revealed that VasX is an important toxin used by V52 to kill both eukaryotes and prokaryotes and has contributed to our knowledge of the versatility of the T6SS. VasX is the first T6SS toxin characterized that acts similar to pore-forming colicins and disrupts the inner membrane of target cells – a toxic mechanism (reliant on VasW) that is inhibited by its cognate immunity protein TsiV2.

CHAPTER 2

Identification and biochemical characterization of VasX

Portions of this chapter have been published as:

Miyata, S.T., Kitaoka, M., Brooks, T.M., McAuley, S.B., and Pukatzki, S. (2011) *Vibrio cholerae* Requires the Type VI Secretion System Virulence Factor VasX to Kill *Dictyostelium discoideum*. *Infection and Immunity*, 779(7):2941-9.

The experiment described in section 2.2.3 (qRT-PCR) was conducted by Maya Kitaoka.

2. Identification and biochemical characterization of VasX

2.1 Introduction

Secretion systems provide bacteria a means to transport proteins across their cell envelope. To date, seven unique secretion systems have been described in both Gram-positive and Gram-negative bacterial species. The T6SS is the most recently described secretion system for Gram-negative bacteria. This system is thought to resemble the T3SS and T4SS with the production of a molecular syringe protruding from the bacterial envelope for the purpose of injecting effector proteins into target cells.

V. cholerae V52 is a clinical isolate that belongs to the O37 serogroup. This strain has a constitutively-active T6SS under laboratory conditions and is known to secrete Hcp and VgrG proteins into culture supernatants [194, 209]. Neither VgrG nor Hcp possess canonical signal peptides. Hcp and VgrG are proposed structural proteins of the T6SS syringe apparatus and are crucial for secretion of other T6SS-associated proteins. Purified Hcp forms hexamers that stack on top of each other to form a tube-like structure *in-vitro*[193] that is believed to form the conduit through which T6SS secreted proteins are translocated. The VgrG proteins (VgrG-1, VgrG-2, and VgrG-3) interact to form an SDS-resistant, heat-sensitive multimeric complex that can be visualized as a high molecular weight protein band by western blotting [194, 209, 357]. This VgrG complex is believed to sit atop the Hcp tube and serve as the T6SS puncturing device [209]. The three VgrG proteins share a similar “core” but differ

with regards to their C-termini. VgrG-1 possesses a C-terminal actin cross-linking domain that causes cell rounding in murine macrophages [194, 209, 222, 223]. VgrG-2 consists solely of the VgrG core and does not have a C-terminal extension; however, the function of this protein cannot be complemented by VgrG-1 or VgrG-3, and VgrG-2 is imperative for secretion of Hcp [194, 209, 223]. The C-terminus of VgrG-3 has peptidoglycan degrading capabilities and is used by V52 to compromise the cell wall of microbial competitors [210, 374].

Two other proteins that are crucial for T6SS function are VasK and VasH. VasK is an inner membrane protein that provides the energy for translocation of T6SS proteins across the bacterial cell envelope. Importantly, *vasK* is crucial for the formation of the T6SS needle complex and thus V52Δ*vasK* is the equivalent of a T6SS-null strain. VasH is a transcriptional regulator that activates the alternate sigma factor, σ^{54} to drive transcription of T6SS genes. Conflicting reports attest to the ability of VasH to regulate the large and auxiliary T6SS gene clusters in *V. cholerae* [371, 377]. Using electromobility shift assays and β-glucuronidase fusions as a reporter of transcriptional activity, Bernard *et al.* determined that VasH/RpoN regulates the large T6SS gene cluster, as well as the small auxiliary clusters which encode T6SS secreted proteins in *V. cholerae* O395[371]. Contradictory to this, RNA-seq, ChIP-seq and qPCR data indicate that in strain V52, RpoN strictly regulates the smaller *hcp*-encoding clusters and not the large T6SS cluster[372]. Regardless of these contradictory data, VasH is known to regulate transcription of the two T6SS satellite gene clusters encoding Hcp-1 and VgrG-1, and Hcp-2 and VgrG-2[370-372, 378]. As such, a *vasH*

mutant is similar to a *vasK* mutant because it is unable to produce a functional T6SS apparatus due to the lack of Hcp and VgrG production [194, 370].

Secretion systems such as the T3SS, T4SS, and T6SS produce molecular syringes used to puncture, and deliver effector proteins into the target cell. My goal was to identify *V. cholerae* T6SS effector protein(s) by taking advantage of the T6SS regulator VasH. I hypothesized that over-expression of *vasH* would result in the over production and secretion of T6SS effector proteins into culture supernatants.

2.2 **Results**

2.2.1 Overexpression of *vasH* and identification of VasX.

My initial goal was to identify T6SS effector proteins; those that are translocated through the injectosome and into host cells to alter host cell function. Given that wild-type V52 constitutively expresses T6SS genes [194], the presence of host cells is not required to trigger secretion of T6SS proteins. Therefore, it was possible to analyze the V52 secretome by identifying proteins present in bacterial culture supernatants.

To identify T6SS-dependent secreted proteins, I took advantage of VasH; a T6SS transcriptional regulator and activator of σ^{54} [194, 370, 371, 379]. The *vasH* gene was cloned into pBAD24 downstream of an arabinose-inducible promoter (pBAD24-*vasH*) and the plasmid was transformed into V52Δ*vasH*. V52Δ*vasH*/pBAD24-*vasH* was grown in the presence and absence of arabinose

and the protein content of culture supernatants of the two strains was compared. To visualize total protein content, the supernatant samples were subjected to SDS-PAGE followed by silver staining. I observed multiple bands that were present under *vasH*-inducing conditions but absent under non-inducing conditions (Figure 2-1). Knowing that V52Δ*vasH* alone does not secrete Hcp [194], restoration of Hcp secretion upon *vasH* induction indicated proper complementation. To identify other proteins present strictly when *vasH* was over-expressed, both arabinose induced and non-induced lanes were excised and subjected to liquid chromatography/mass spectrometry (LC-MS/MS) analysis. Among other proteins (Table 2-1), mass spectrometry identified a protein encoded by VCA0020 in supernatants of VasH-producing bacteria that was not present in supernatants of bacteria lacking *vasH*. The VCA0020 gene product corresponded to a ~120 kD protein that we subsequently named VasX.

.

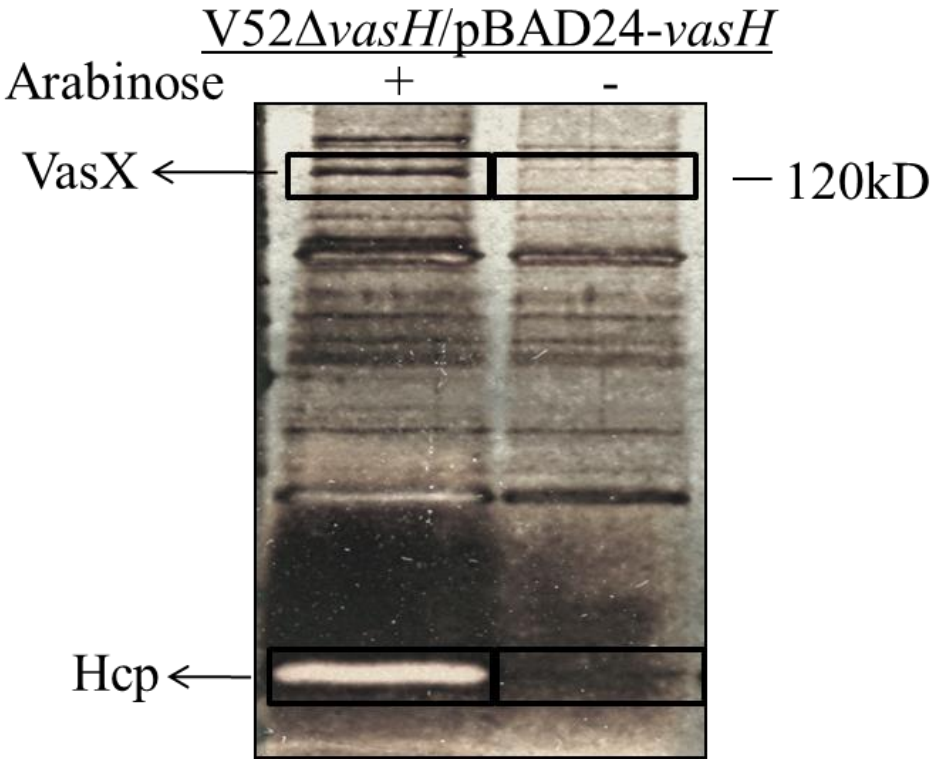

Figure 2-1. V52Δ*vasH*/pBAD24-vasH secretes VasX into culture supernatants strictly under inducing conditions. Silver-stained SDS-PAGE comparing supernatants of *V. cholerae* V52Δ*vasH*/pBAD24-vasH grown under inducing (+ arabinose) or non-inducing (- arabinose) conditions. Black boxes highlight proteins present under inducing conditions but absent under non-inducing conditions. Proteins from each lane were excised and identified by LC-MS/MS analysis.

Table 2-1. Proteins identified by mass spectrometry as present in culture supernatant strictly when *vasH* expression was induced.

Protein Designation	Mass (kDa)	Organism	Peptide sequences identified	Accession
VgrG-1	129	*V. cholerae* N16961	YEVQLASR EFCVQYR FVIEITNAK ESDIDFLHR GFGTSATPELR TQAEVSEVQLK SAQGDALFMLTK VSNLTAEQMVDK TVPNELQSYLPK HTLYFSDASDSLSK YKDDVNGAAFSQIR FDLQEHLDPAMNR YSNGNEQSSCWVR DFDGLIENDHTTVIR LAAEEGLVYSFVHEAGK TYHATNTPPYTLPEHK TETHQGEGFNELSFEDQAGK	gi 15641427
VgrG-2	78	*V. Cholerae* V52	YEVQLASR EFCVQYR ESDIDFLHR TQAEVSEVQLK VSNLTAEQMVDK GPAPVCEVCEEAK LDCSSEIGGSLQQK HTLYFSDASDSLSK YKDDVNGAAFSQIR FDLQEHLDPAMNR YSNGNEQSSCWVR DFDGLIENDHTTVIR LAAEEGLVYSFVHEAGK TYHATNTPPYTLPEHK TETHQGEGFNELSFEDQAGK	gi 121727991
VgrG-3	113	*V. cholerae* N16961	EFCVQYR SDEPLLLAGVR SSPSWWSDLK EFFSGLNPATK VDGLEDESLVVR DGQVVQQINGIVR EFNVVWQDIASR GFEGQESLSDSVWR DIAYQQPNYEHFDAPGR	gi 15600894
		V. cholerae RC385	EFCVQYR FVIEITNAK ESDIDFLHR GFGTSATPELR TQAEVSEVQLK SAQGDALFMLTK VSNLTAEQMVDK TVPNELQSYLPK HTLYFSDASDSLSK FDLQEHLDPAMNR YSNGNEQSSCWVR DFDGLIENDHTTVIR LAAEEGLVYSFVHEAGK TYHATNTPPYTLPEHK	gi 116216447
VCA0020	122	*V. cholerae* N16961	GQTIGLQITR DNSFIDEVR GGTPSLLANLR DTCTPSLPVEK VAQYPSWNPFK WSIEDNQPVYR LPAQPAYYQPQR EAVTPILINEQQGK WIEPAQSSFGALQK AGELDLQSAEANDIATR YAFDVYDDQGQALHPLPK	gi 15600791
Hcp	19	*V. cholerae* N16961	FTVALNK QENFFTTK AVPLLYNALSSGEK ITWDHVNAGTSGSDDWR LENASIVDIHCEMPHCQDPAK	gi 116217197
Putative porin (VC1854)	40	*V. cholerae* N16961	VDSANNFGIGAR SDAGTVDFYGQLR YGTLSDALHDSQVK FLEDKDPTIGSGSSR	gi 15641856
Heme transport portein (HutA)	78	*V. cholerae* N16961	LFAQISQGFR TFSESIALANK SGDLESLVAYTR NNVIFYIPNASEK	gi|15601335

VasX is encoded on the *V. cholerae* small chromosome and is part of a T6SS operon encoding two essential T6SS genes, *hcp-2* and *vgrG-2* (VCA0017 and VCA0018, respectively) (Figure 2-2). NCBI denotes VasX as a hypothetical protein and BLASTP analysis revealed that VasX homologs are present in Gram-negative bacteria such as *Pseudomonas syringae* (25% identity, 43% similarity), *Photobacterium damselea* (28% identity, 45% similarity), and *Aeromonas hydrophila* (33% identity, 50% similarity). PSI-BLAST analysis also indicated homology to the protein IdsD from *P. mirabilis* (12% identity, 26% similarity) (Dr. B. Hazes, personal communcation). The hypothetical, uncharacterized genes VCA0019 (*vasW*), VCA0021 (*tsiV2*), and VCA0022 also belong to the VasX-encoding operon.

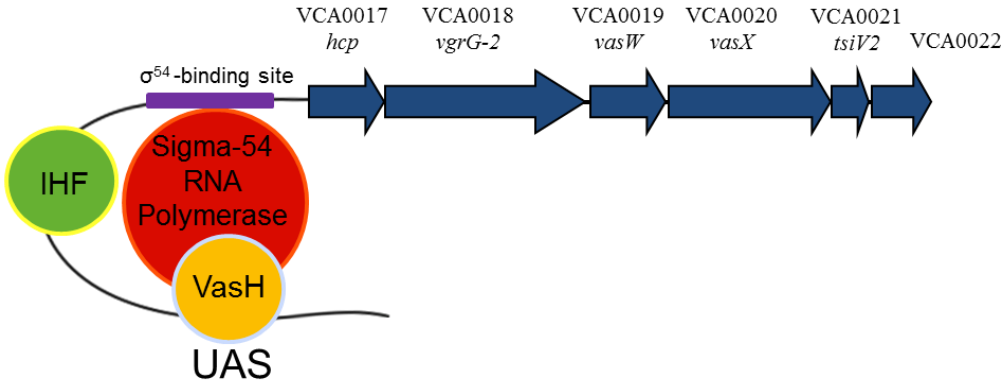

Figure 2-2. Schematic representation of the VasX-encoding gene cluster. *vasX* is located in a T6SS satellite gene cluster along with *hcp-2* (VCA0017), *vgrG-2* (VCA0018), *vasW* (VCA0019), *tsiV2* (VCA0021), and VCA0022. VasH is an activator of the alternate sigma factor σ^{54} that acts at a promoter located upstream of *hcp-2*. IHF; integration host factor, UAS; upstream activation sequence.

2.2.2 VasX production depends on the σ^{54}-dependent transcriptional activator VasH

Our finding that VasX was present exclusively in supernatants of VasH-producing *V. cholerae* (Figure 2-1) suggests that VasH regulates the production of VasX. This hypothesis is supported by our observation that VasX cannot be detected in V52Δ*vasH* culture supernatants by western blotting with VasX antiserum, and that VasX levels are significantly reduced in pellet fractions (Figure 2-3). Importantly, DnaK, a cytoplasmic heat-shock protein [380] was present only in bacterial pellet samples, indicating that the bacteria were intact, and thus VasX is actively secreted and not released by cell lysis.

To investigate the relationship between VasH and the physically linked genes *hcp-2* and *vasX* (Figure 2-2), we used western blotting with polyclonal antibodies to detect Hcp and VasX in the complemented *vasH*-deletion mutant. No Hcp and significantly reduced levels of VasX could be detected in pellets or concentrated supernatants when *vasH* was not expressed; however, upon induction of *vasH* expression, Hcp and VasX production within the cell and secretion into culture supernatants was restored (Figure 2-3). These data indicate that VasH plays an integral role in regulating both Hcp and VasX, supporting our hypothesis that *hcp-2*, *vgrG-2*, and *vasX* belong to the same T6SS regulon.

To determine if the difference in protein levels was due to VasH-induced transcript levels, we used semi-quantitative real-time PCR (qRT-PCR) to measure the *vasX* transcript levels in the complemented V52Δ*vasH* strain grown under inducing (+ arabinose) and non-inducing (-arabinose) conditions relative to the

transcription of the outer membrane protein OmpW. It was previously demonstrated that the presence of arabinose does not affect the expression of OmpW [381]. When *vasH* expression was induced with arabinose, *vasX*-transcript levels increased ~10-fold (Figure 2-3). We propose that VasH acts directly at the promoter located immediately upstream of the T6SS satellite cluster encoding Hcp-2, VgrG-2, and VasX in *V. cholerae* V52.

A.

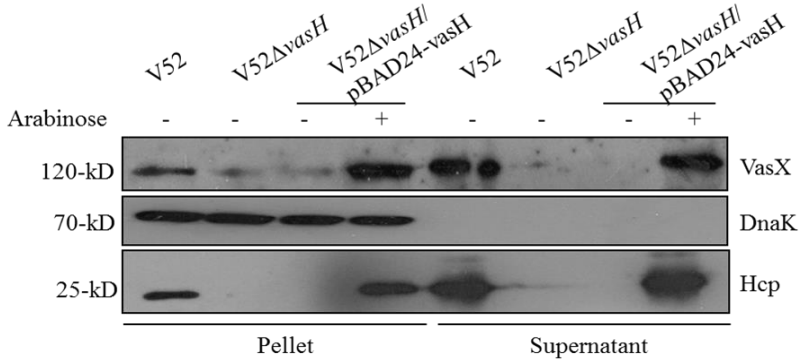

B.

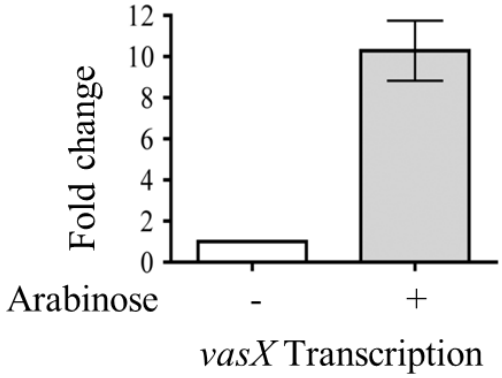

Figure 2-3. VasX production depends on the T6SS regulator VasH. (A) Western blot demonstrating that *trans* expression of *vasH* restores production of both Hcp and VasX. Pellet and supernatant fractions were prepared from mid-logarithmic cultures and subjected to SDS-PAGE followed by western blotting with VasX, Hcp, and DnaK (lysis and loading control) primary antibodies. (B) VasH regulates the expression of *vasX*. V52Δ*vasH* carrying pBAD24-vasH to allow arabinose-controlled complementation was grown to mid-logarithmic phase in the presence or absence of arabinose. VasX transcript levels were determined by qRT-PCR using the gene encoding the *V. cholerae* outer membrane protein OmpW (*ompW*) as an internal control. Error bars indicate the standard deviation.

2.2.3 VasX secretion depends on the T6SS proteins Hcp, VasK, and VgrG-2

As a secreted protein that is dependent on the T6SS regulator VasH for expression, I hypothesized that VasX is a protein secreted by the T6SS. Therefore, I tested whether T6SS structural proteins were required for VasX secretion. To test this, I employed the T6SS deletion mutants V52Δ*hcp1,2* (which lacks both chromosomal copies of *hcp*), V52Δ*vgrG-1*, V52Δ*vgrG-2*, V52Δ*vgrG-3*, and V52Δ*vasK*[194]. VasX was secreted by wild-type V52, V52Δ*vgrG-1*, and V52Δ*vgrG-3*, but not by V52Δ*vasK*, V52Δ*hcp1,2*, or V52Δ*vgrG-2* (Figure 2-4). Furthermore, VasX and Hcp were dependent on the same T6SS proteins for secretion from the bacterial cell (Figure 2-4). VgrG-2 was the only one of the three VgrG proteins absolutely required for secretion of both Hcp and VasX (Figure 2-4). The absence of VasX in culture supernatants was not due to a failure to produce VasX within the cell as VasX was present in bacterial pellet samples of all T6SS mutants tested (with the exception of the in-frame deletion mutant V52Δ*vasX*) (Figure 2-4). Deletion of *vasX* did not affect secretion of Hcp (Figure 2-4) and thus, VasX does not appear necessary for the formation of the T6SS structural apparatus.

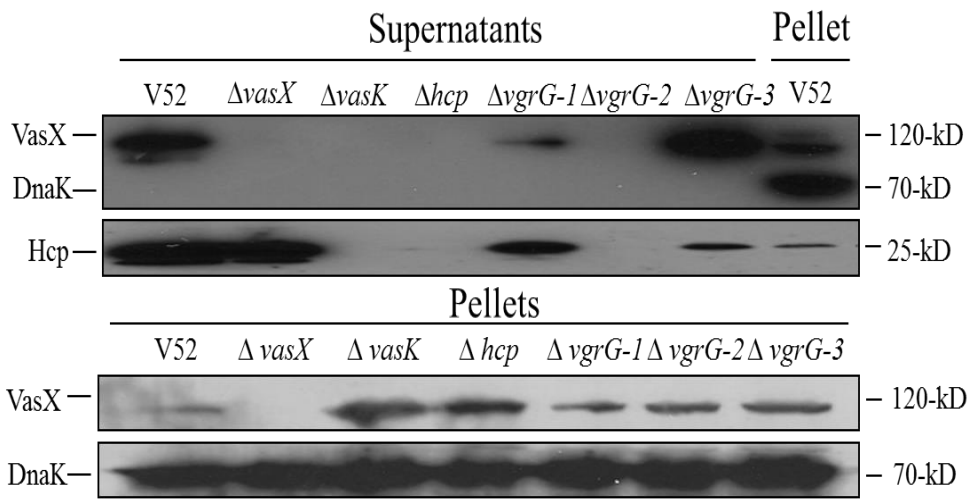

Figure 2-4. Secretion of VasX is T6SS dependent. Western blot of VasX and Hcp from culture supernatants and bacterial pellets. Supernatant and pellet fractions were harvested from mid-logarithmic cultures and subjected to western blotting using the indicated antibody types (listed to the left of the blot). Molecular masses are shown to the right of both blots. Blotting for the cytoplasmic protein DnaK serves as a loading and lysis control.

2.2.4 Bioinformatics and Secondary structure prediction of VasX

The SignalP server predicted that *vasX* does not encode a canonical secretion signal peptide and interestingly, the subcellular localization prediction tool PSORTb suggested that VasX localizes to the cytoplasmic membrane. The hidden Markov model homology search program HHpred[382] identified an N-terminal pleckstrin homology (PH) domain (E = 0.5, P = 5E-5) and a C-terminal colicin-like domain (E = 0.5, P = 3E-5) (Figure 2-5). Although the E-values identified by HHpred are large, further protein structure prediction of the candidate PH domain (amino acids 73–166) in VasX by the Phyre server[383, 384] also indicated a canonical PH domain structure consisting of a stretch of 100-200 amino acids containing two β-sheets followed by an α-helix[385]. Since

PH domain-containing proteins are frequently involved in signal transduction in eukaryotic cells, these predicted structural features in VasX raise the possibility that it may engage in molecular mimicry by utilizing its PH domain to attach itself to host cell structures such as biological membranes.

The bioinformatics programs TMHMM, Phobius, and SOSUI were used to provide further predictions of VasX secondary structure. TMHMM and Phobius both predicted the presence of three transmembrane domains (Figure 2-5 and Table 2-2) with the N-terminal portion of VasX outside of the cell (i.e. in the periplasm) and the C-terminus facing the cytoplasm. SOSUI suggested that VasX contains 5 transmembrane helices (Table 2-2). A summary of the transmembrane regions predicted by these programs is presented in Table 2-2. These bioinformatics predictions suggest that VasX is a membrane protein which I further investigated using subcellular fractionation experiments.

Table 2-2. Bioinformatic predictions for VasX. The indicated programs were used to predict the topology within the cell membrane, and the number of transmembrane domains possessed by VasX. Full length VasX is 1085 residues. TM; transmembrane.

Prediction Program	Number of TM Domains Predicted	Coordinates (amino acids) of Predicted TM Domains
TMHMM	3	757-779 860-882 886-908
SOSUI	5	713-735 758-780 807-829 847-869 884-906
Phobius	3	808-826 846-885 886-908

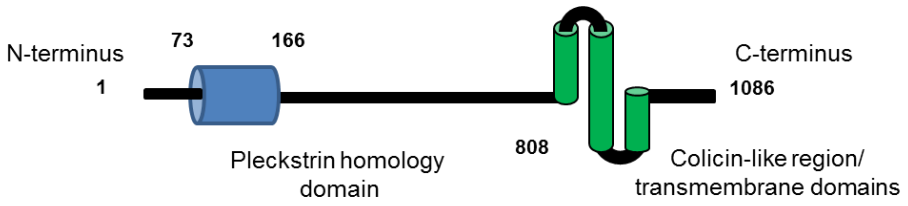

Figure 2-5. Schematic representation of VasX based on bioinformatic analyses indicating VasX possesses an N-terminal PH domain (blue cylinder) and a C-terminal colicin-like domain with 3 transmembrane domains (green cylinders). Numbers indicate corresponding amino acid residues.

2.2.5 VasX localizes to the bacterial membrane

Bioinformatic analyses suggested that VasX localizes to the bacterial inner membrane. To investigate the localization of VasX and Hcp within the bacterium, I performed subcellular fractionation experiments. V52 was transformed with the β-lactamase-encoding plasmid pBAD24 for subcellular fractionation experiments to use β-lactamase as a periplasmic control. Other fractionation controls included DnaK (cytoplasm) and OmpU (membrane). I observed that Hcp localizes to all cellular compartments, whereas VasX localizes specifically to the cytoplasmic and membrane fractions (Figure 2-6). It should be noted that Hcp is present in the periplasm at high abundance, while VasX cannot be detected in this compartment (Figure 2-6). Therefore, VasX either is present in the periplasm transiently and at very low levels, or VasX employs a strategy to by-pass the periplasm *en-route* out of the cell.

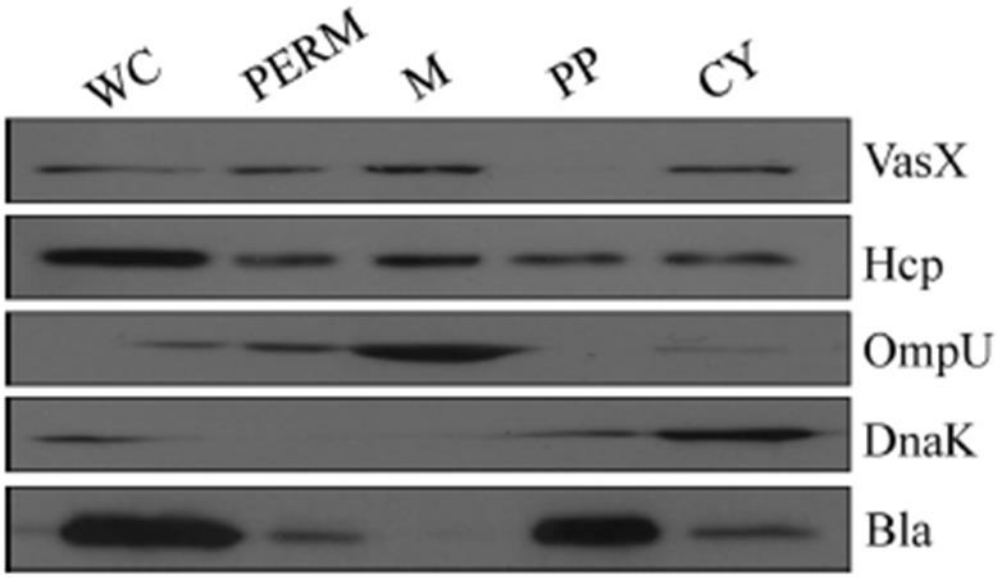

Figure 2-6. VasX localizes to the bacterial membrane. V52/pBAD24 was grown to mid-logarithmic phase and subjected to subcellular fractionation. Various fractions (whole cell [WC], permeabilized V52 [PERM], membrane [M], periplasm [PP], and cytosol [CY]) were separated by SDS-PAGE followed by western blotting with VasX, Hcp, OmpU (membrane control), DnaK (cytosol control), and β-lactamase (Bla; periplasm control) primary antibodies.

According to my subcellular fractionation data, VasX is abundant in the membrane fraction; however, it was not clear from this experiment whether VasX localized to the inner or outer membrane. Bioinformatic analysis using PSORTb suggested that VasX is an inner membrane protein (see section 2.2.2). To confirm this prediction, V52 and V52Δ*vasK* were grown in liquid culture and the total membrane fraction was isolated. Since VasX is a secreted protein, I included the strain V52Δ*vasK* which is incapable of VasX secretion (Figure 2-4). By using this control, I wanted to determine whether VasX localizes to the cytoplasmic membrane following synthesis in the cytosol, or whether VasX was first secreted by V52 following which it could insert into the neighboring cell membrane. Total

membranes were subjected to sucrose gradient fractionation to separate the inner and outer membranes. Fractions were collected and a portion of each fraction was subjected to NADH oxidase activity to distinguish inner and outer membrane fractions. The remainder of each fraction was boiled with 4x protein sample buffer, and subjected to SDS-PAGE followed by western blotting. OmpU and EpsL (an inner membrane protein of the T2SS [386]) antibodies were used to detect the outer and inner membrane fractions, respectively. VasX was visualized using α-VasX antibody. The resulting western blot indicated that in both V52 and V52Δ*vasK,* VasX is concentrated in the same sucrose fractions as EpsL (Figure 2-7). NADH oxidase activity was also highest in the same fractions EpsL. This suggests that VasX localizes to the bacterial inner membrane after synthesis in the cytoplasm.

A.

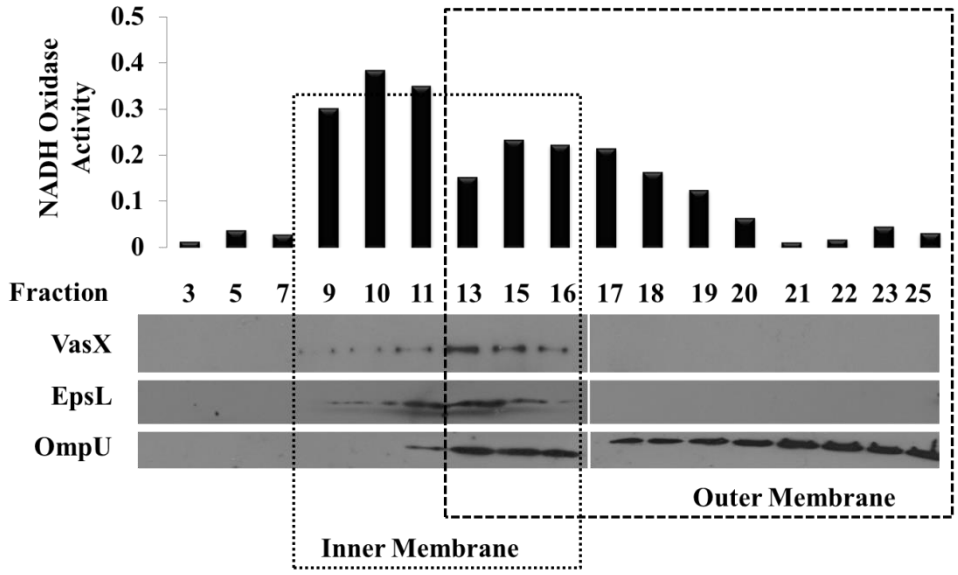

B.

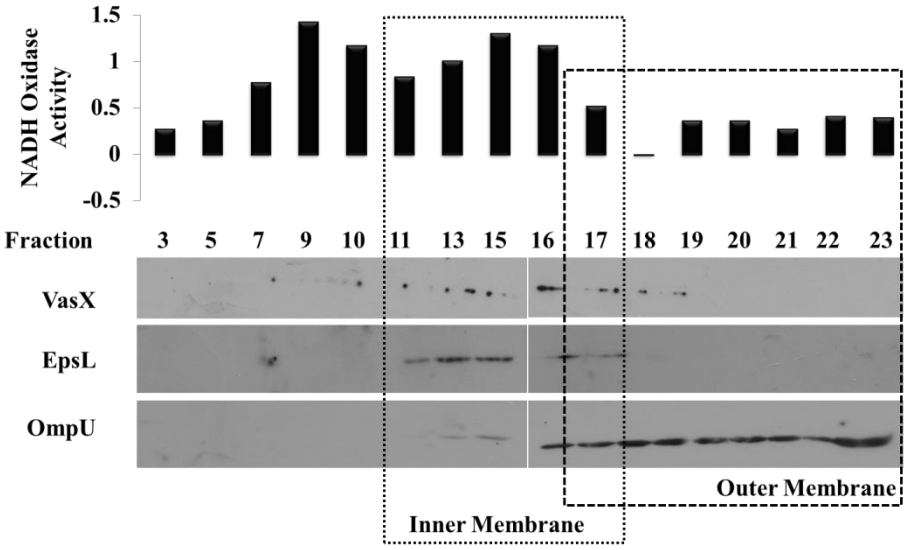

Figure 2-7. VasX localizes to the bacterial inner membrane. V52 (A) and V52Δ*vasK* (B) total membranes were isolated and subjected to sucrose gradient fractionation. Samples were collected in 200 µL aliquots and subjected to western blotting with EpsL (inner membrane), OmpU (outer membrane), and VasX primary antibodies. The NADH oxidase activity of the corresponding fractions is plotted above the western blot.

2.2.6 VasX interacts with T6SS structural proteins VgrG-1, VgrG-2 and Hcp-2

Given that VasX is encoded within a T6SS operon and depends on structural T6SS components for export out of the bacterial cell (Figure 2-4), I wondered whether VasX physically interacts with other T6SS proteins. To test this, 6xHistidine tags were fused to the C-termini of VgrG-1, VgrG-2, and Hcp-2 and the fusions were cloned into pBAD24 (pBAD24-vgrG-1::6xHis, pBAD24-vgrG-2::6xHis, pBAD24-hcp-2::6xHis). Empty vector pBAD24 was used as a negative control. Plasmids were transformed into V52 and the strains were grown in selective LB in the presence of 0.1% arabinose to induce expression from the P_{BAD} promoter. 6xHis-tagged proteins were pulled down using Ni^{2+} NTA resin and subjected to western blotting using α-VasX and α-6xHis antibody. The resulting immunoblots indicated that VasX indeed interacts with VgrG-1, VgrG-2, and Hcp-2 and this interaction was not observed in the empty vector negative control samples (Figure 2-8).

A.

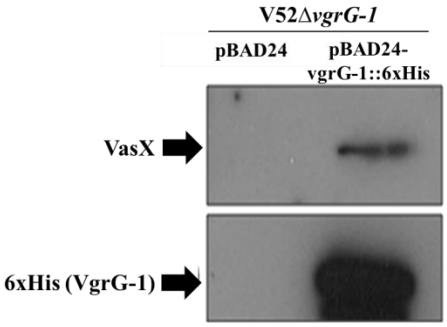

B.

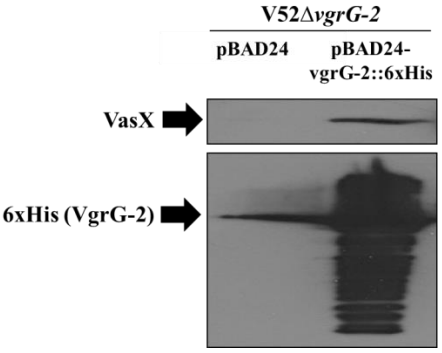

C.

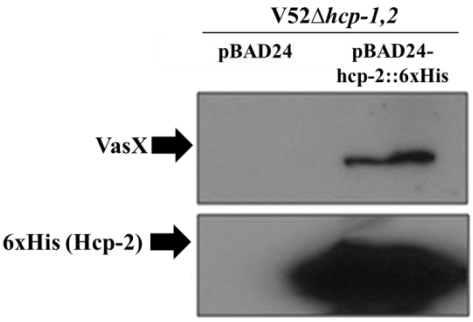

Figure 2-8. VasX interacts with T6SS structural proteins. Cells producing 6xHis-tagged VgrG-1(A), VgrG-2 (B), or Hcp-2 (C) were lysed and 6xHis-tagged proteins were pulled down using Ni^{2+} NTA resin. Cells harboring the empty vector pBAD24 served as a negative control. Pull-down samples were subjected to western blotting with VasX and 6xHis primary antibodies.

2.2.7 VasX forms a large protein complex

During analysis of culture supernatants from various T6SS mutants by SDS-PAGE and silver staining I noticed the presence of a high molecular weight protein band present in V52 culture supernatants but absent from supernatants of V52Δ*vasK* and V52Δ*vasX* (Figure 2-9). This band is also dependent on the T6SS regulator VasH as the band appears in culture supernatants of V52Δ*vasH*/pBAD24-vasH in the presence, but not the absence, of arabinose (Figure 2-9). I hypothesized that this band was a protein multimer that contained VasX (either as one protein in a multi-protein complex, or as a homo-multimer) which I henceforth refer to as the VasX large protein complex (LPCx)

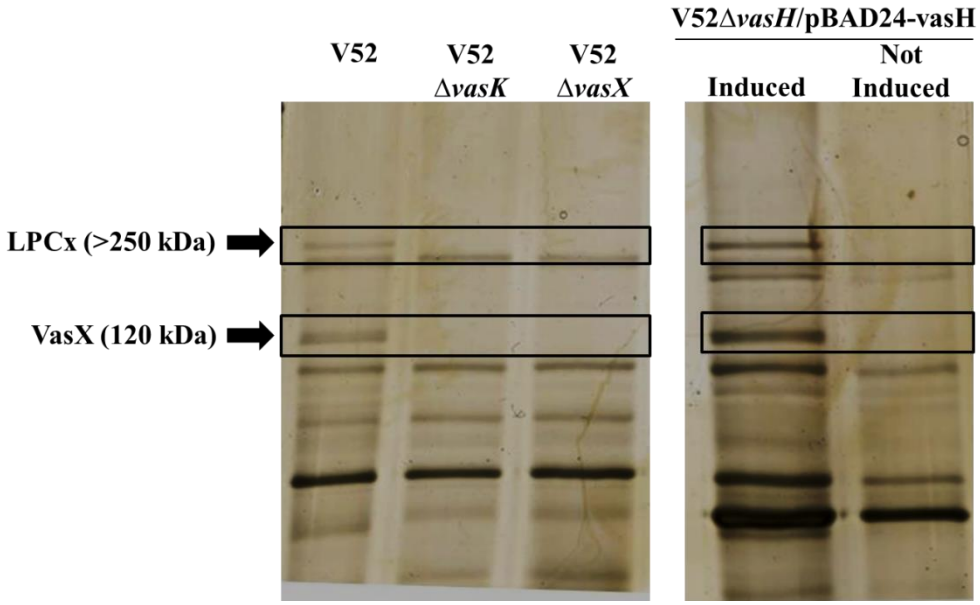

Figure 2-9. VasX is part of a LPCx. Concentrated supernatant samples from the strains noted at the top of figure were subjected to SDS-PAGE followed by silver staining to visualize secreted proteins. Black boxes indicate the presence/absence of monomeric VasX (120 kDa) and the LPCx (>250 kDa).

Previous studies have demonstrated the presence of multimeric T6SS protein complexes present in the bacterial membrane that are heat-sensitive [357, 387]. Therefore, I resuspended V52 pellet samples in SDS protein sample buffer and boiled, or did not boil the sample. The samples were subjected to SDS-PAGE followed by western blotting using α-VasX antibody. I observed the presence of a high molecular weight band present in non-boiled samples (>250 kDa) but this band disappeared in the boiled samples (Figure 2-10). Therefore, V52 produces a LPCx that is heat-sensitive but SDS-resistant. Because this complex is recognized by the VasX antibody, VasX is either a component of the complex, or the complex is a VasX homo-multimer.

Bacterial secretion systems are multi-protein complexes that protrude from the bacterial cell envelope. Because I previously observed that VasX interacts with T6SS structural proteins, I hypothesized that formation of the VasX-containing LPCx would require other T6SS structural components such as VgrG-2, Hcp-1, Hcp-2, or VasK. To test this, I prepared boiled and non-boiled whole cell lysate samples using V52, V52Δ*vasK*, V52Δ*vgrG-2*, and V52Δ*hcp-1,2*. Following western blotting with VasX antibody I observed the LPCx in all non-boiled protein samples (Figure 2-10). Therefore T6SS structural proteins VgrG-1, VgrG-2, VgrG-3, VasK, and Hcp-1,2 are not required for the formation of the protein oligomer. This means that the LPCx is composed strictly of VasX, or contains other proteins (T6SS-related, or unrelated) that have yet to be identified.

To determine whether the VasX LPCx can form in a T6SS$^-$ bacterium, I over-expressed *vasX* in the *E. coli* strain DH5α which does not possess T6SS

genes. Boiled and non-boiled pellet samples were subjected to SDS-PAGE followed by western blotting with VasX primary antibody. I observed the presence of the VasX LPCx in DH5α (Figure 2-10) suggesting that no other *Vibrio*-specific, or T6SS, proteins complex with VasX to form the LPCx.

A.

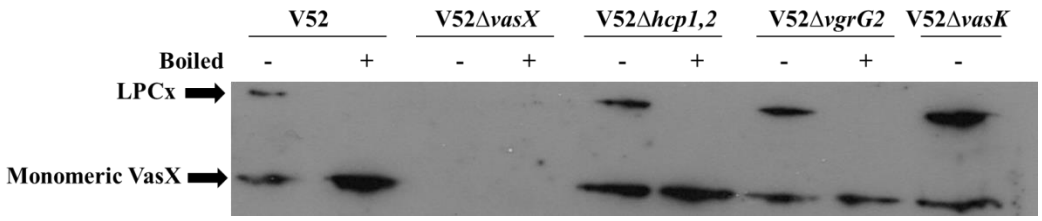

B.

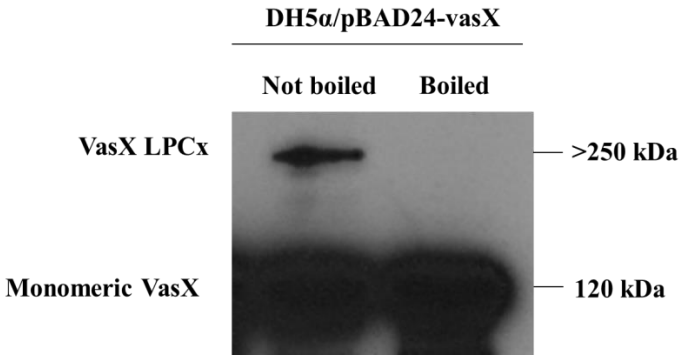

Figure 2-10. The VasX LPCx is present in *V. cholerae* T6SS mutants and DH5α. (A and B) Bacterial pellet samples from the indicated strains were boiled, or not boiled, in protein sample buffer were subjected to SDS-PAGE followed by western blotting with VasX primary antibody. The strain DH5α/pBAD24-vasX was grown in the presence of 0.1% arabinose to induce expression from the P_{BAD} promoter.

To identify what other proteins (if any) are part of this complex, V52Δ*vasX*/pBAD24-vasX::6xHis was used for over-expression of 6xHis-tagged *vasX* and I pulled down the LPCx using Ni^{2+} NTA resin. As a negative control, the cell lysate of V52Δ*vasX*/pBAD24 was also subjected to pull-down using Ni^{2+} NTA resin. Isolation of the LPCx was confirmed by SDS-PAGE followed by coomassie staining. The LPCx band was excised from the gel, as well as the corresponding molecular weight gel fragment from the negative control sample and both were submitted for protein identification by LC-MS/MS analysis. Identified proteins that were unique to the sample where VasX::6xHis was produced are presented in Table 2-3. The majority of peptides identified corresponded to VasX (Table 2-3). Two peptides were matched to the cAMP regulatory protein (VC2614). This data suggests that VasX either associates with itself forming a homo-multimer, or forms a complex with the cAMP regulatory protein.

Table 2-3. Proteins identified by mass spectrometry following Ni^{2+} NTA pull-down of the VasX LPCx.

Protein Designation	Mass (kDa)	Organism	Peptide sequences identified	Accession
VasX	120	*V. cholerae* N16961	LLLVESLVR GGTPSLLANLR QPLIGIIPVR AITEYCATAK EEAVLQHNPK EAVTPILINEQQGK WIEPAQSSFGALQK AGELDLQSAEANDIATR LGQLLSSELPMMLTLK TGQTNDAQNPASACPFK IDWSDDEANKPTHER KLGQLLSSELPMMLTLK WADLDNFLVEHYTELK ESWQAVMELLFPYQNQPK LNAILQEMNDALELKPGNVSPK	gi 15600791
cAMP-regulatory protein	23.5	*V. cholerae* N16961	VGDLAFLDVTGR QLIQVNPDILMR	gi 15642609

Multimerization of protein toxins has been shown to occur in the membrane [159, 357, 387-389]. Thus, I hypothesized that VasX inserts into the inner membrane from the cytoplasm and forms the LPCx. To test this, I isolated total bacterial membranes from V52. Boiled and non-boiled membrane samples were analyzed for the LPCx by western blotting with VasX antibody. In the non-boiled membrane sample, VasX was present strictly in the LPCx form (Figure 2-11). In the boiled samples, only monomeric VasX was observed. This suggests that when VasX localizes to the inner membrane it is present exclusively as the LPCx.

Bioinformatics analysis predicted that VasX contains C-terminal transmembrane domains which likely mediate its association with the inner membrane and thus, LPCx formation. I hypothesized that the C-terminus of VasX would be sufficient to form LPCxs. To test this I created FLAG-tagged versions of VasX: full length (amino acids 1-1085), and truncated forms corresponding to amino acids 1-218, 1-542, 76-542, 167-700, and 543-1085. These specific fragments were chosen based on the TMHMM and HHpred bioinformatics output. Region 1-218 contains the putative N-terminal PH domain, 1-542 is the N-terminal half of the protein, 76-542 contains the PH domain and the remaining N-terminal half of VasX. Section 167-700 lacks the PH domain and predicted transmembrane segments, and region 543-1085 is the C-terminal half of the protein which includes the transmembrane domains. Bacterial pellet samples were harvested and boiled or not boiled in sample buffer.

Samples were subjected to SDS-PAGE followed by western blotting with anti-FLAG primary antibody. I observed LPCx formation using VasX 1-1085, 167-700, and 543-1085 but not with 1-218, 1-542, or 76-542 (Figure 2-11). This suggests that only the fragments containing the putative transmembrane domains are capable of forming LPCxs.

A.

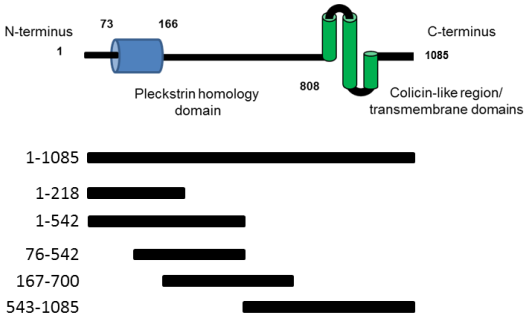

B.

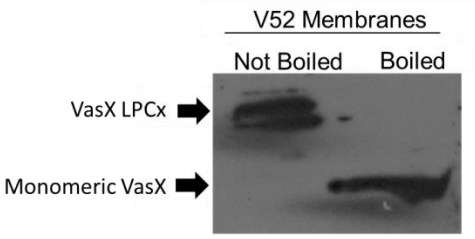

C.

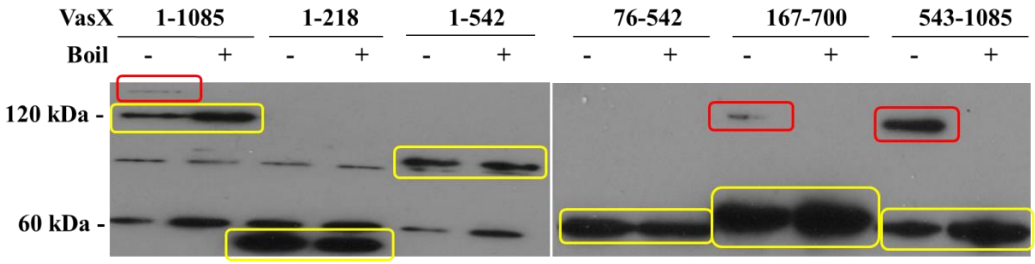

Figure 2-11. The VasX LPCx forms in cell membranes and is mediated by the C-terminal half of the protein. (A) Schematic representation of the *vasX* truncation mutants used in this experiment. Amino acid residues are indicated by the numbers to the left of each truncation. (B) VasX is present exclusively as the LPCx in the membrane fraction. Cell membranes were isolated and boiled or not boiled with protein sample buffer. Samples were subjected to SDS-PAGE followed by western blotting with VasX primary antibody. (C) Pellet samples were prepared using V52Δ*vasX* expressing full length *vasX* or FLAG-tagged truncated forms of *vasX* and boiled or not boiled in protein sample buffer. Samples were subjected to SDS-PAGE followed by western blotting with FLAG primary antibody. The amino acid residues corresponding to the VasX constructs are indicated at the top of the figure. Red boxes denote LPCxs and yellow boxes indicate bands corresponding to the expected monomeric molecular weight of the protein. The molecular weight is indicated at the left of the blot.

2.3 **Discussion**

Using its constitutively active T6SS, V52 secretes the structural proteins Hcp and VgrG into culture supernatants and the secretion of Hcp is the hallmark of a functional T6SS [193, 194]. The secretion of putative effector proteins by the T6SS has been seldom described. In an attempt to identify unique substrates of the *V. cholerae* T6SS, we took advantage of the T6SS transcriptional regulator VasH. Along with RpoN (σ^{54}), VasH activates transcription of the two T6SS satellite gene clusters in *V. cholerae* [370-372, 378]. Using a proteomics approach, I identified a ~120 kDa protein that I named VasX (Figure 2-1). VasX is encoded within a T6SS satellite gene cluster and *vasX* expression is regulated by the T6SS transcriptional activator VasH (Figure 2-3) suggesting that this protein is involved in T6SS function.

The inner tube of the T6SS secretory apparatus is predicted to be comprised of an Hcp tube that is capped with a VgrG-1/2/3 trimer [208]. The VgrG trimer does not have a pore through which putative effectors can pass [208]. And thus, if T6SS effector proteins are indeed translocated through the Hcp tube, removal of the VgrG cap must precede secretion of effectors. Using Ni^{2+} NTA resin to pull down 6xHis-tagged VgrG-1, VgrG-2, and Hcp-2 from crude bacterial lysates, I demonstrated that VasX interacts with all three of these structural proteins (Figure 2-8), although I cannot conclude from this experiment that these interactions were direct. Hcp and VgrG-2 were previously shown to be co-dependent for secretion, and deletion of either gene in V52 abrogated virulence toward *D. discoideum* [194]. Interestingly, secretion of VasX was also dependent

on Hcp and VgrG-2 (as well as VasK) and VasX and Hcp share the same secretion requirements (Figure 2-4). Taken together, these data suggest that VasX may be part of the T6SS structural apparatus, or VasX could be a T6SS effector protein that associates with structural proteins *en route* out of the bacterium (rather than traversing the Hcp tube). Structural analysis of a *P. aeruginosa* T6SS effector supports the idea that T6SS effectors are not translocated through the Hcp tube because the two toxins analyzed are too large to traverse the tube and would require significant molecular rearrangements to their native structures [390]. Importantly, Figure 2-4 provides evidence refuting the idea that VasX is a structural T6SS protein because V52Δ*vasX* secretes Hcp and therefore is not required for the proper formation of the T6SS needle complex. Therefore, based on these data I propose that VasX is a T6SS effector protein that is delivered into host cells.

Bioinformatics and secondary structure predictions suggested that VasX possesses an N-terminal PH domain; a domain typically found in eukaryotic and not prokaryotic cells [391]. PH domains are canonically associated with binding phosphoinositides on the inner leaflet of the eukaryotic cell membrane where they alter cell signaling events [392, 393]. The V52 T6SS mediates virulence toward both murine macrophages and *D. discoideum* purportedly by injection of effector proteins into the host cytoplasm following uptake into phagocytic vesicles [194, 209, 222]. Given that VasX depends on T6SS structural proteins for secretion (Figure 2-4), we predicted that VasX is injected into the host cytoplasm along

with VgrG-1 (actin cross-linking) where it could bind phosphoinositides and disrupt cell signaling events.

Bioinformatics analyses suggested that VasX localizes to the cytoplasmic membrane and has three (or five) C-terminal transmembrane domains (Figure 2-5 and Table 2-2). Using subcellular fractionation I observed that VasX is present in the bacterial cytoplasm and inner membrane but not the periplasm (Figures 2-6 and 2-7) whereas Hcp was observed in each fraction. This suggests that VasX by-passes the periplasm during transit out of the bacterium, or is present transiently at levels undetectable by western blotting. One possibility is that VasX is translocated through the Hcp tube spanning the inner membrane, periplasm, and outer membrane which would prevent VasX exposure to the periplasmic space.

Sucrose gradient separation of inner and outer bacterial membranes suggested that VasX does, in fact, localize to the inner membrane and this occurs in both wild-type V52 and V52Δ*vasK* (Figure 2-7). It is contradictory that VasX was identified as a secreted protein, yet VasX is also a membrane-localized protein. Thus, VasX has amphipathic properties allowing it to be present as a soluble and membrane-bound entity. Interestingly, the ability to exist in both water-soluble and membrane-bound forms has been described previously for pore-forming colicins [231, 394] and coincidentally, HHpred predicted that VasX possesses a C-terminal colicin-like domain.

It was reported that some T6SS proteins in *B. cenocepacia* and *P. aeruginosa* form high molecular weight protein complexes [357, 387]. These

multi-protein complexes are SDS-resistant but heat-sensitive [357, 387]. I observed that VasX also formed an SDS-resistant, heat-sensitive LPCx via its C-terminus (Figures 2-9, 2-10, 2-11). Surprisingly, this complex formed in the absence of the crucial T6SS proteins VasK, VgrG-2, and Hcp-1,2 and in the T6SS$^-$ bacterium DH5α, implying that the LPCx did not represent an aggregation of T6SS structural proteins for assembly of the needle complex. Following purification and analysis of the LPCx protein content via mass spectrometry, a large proportion of the identified peptides corresponded to VasX (Table 2-3) suggesting that the LPCx is a VasX homo-multimer. However, two peptides from the cAMP regulatory protein were also identified, implying this protein may associate with VasX to form the LPCx. I do not believe this to be the case for several reasons discussed here: Formation of the LPCx in *E. coli* DH5α indicates that other *Vibrio* proteins are not part of the LPCx (but I cannot rule out the possibility that a cAMP regulatory protein of DH5α can be substituted in this case). In a previous, unrelated VasX::6xHis nickel pull-down experiment, mass spectrometry analysis identified this cAMP regulatory protein in both samples containing VasX::6xHis and in the empty vector negative control and thus, not identifying the cAMP regulatory protein in the negative control may be an anomaly of this particular experiment. Furthermore, mutation of the gene encoding the cAMP regulatory protein does not impede T6SS-mediated killing by *V. cholerae* (Dr. V. Bachmann, unpublished observation), and I have observed that purified, recombinant VasX forms high molecular weight complexes in

solution (Section 5.2.10, Figure 5-16). For the reasons discussed here I postulate that the LPCx is composed strictly of VasX.

Multimerization of proteins in cell membranes has commonly been described for pore-forming toxins [159, 389, 395]; however, multimerization of pore-forming toxins generally occurs following secretion, once the proteins have inserted into their target cell. Conversely, VasX forms LPCxs in the membrane of the producing cell. Interestingly, the LPCx is also present in culture supernatants implying that VasX is secreted in this multimeric form.

Taken together, the data presented in this chapter present the identification and biochemical characterization of VasX. VasX is a secreted protein with amphipathic characteristics encoded within a satellite T6SS gene cluster that is regulated by the σ^{54} activator VasH. Based on the data presented in this chapter, I provide a model whereby VasX is a T6SS effector protein that localizes to the inner membrane and forms a LPCx. This LPCx interacts with VgrG proteins in the membrane during formation of the T6SS injectosome in the bacterial cytoplasm. Because Hcp is thought to be ensheathed with VipA/VipB proteins I propose that the interaction of VasX and Hcp is indirect and is mediated via the VgrG cap atop the Hcp tube. Upon contraction of the VipA/VipB sheath, VasX along with the VgrG protein cap and the Hcp tube are expelled from the cell and injected into the cytoplasm of host cells. I hypothesize that VasX is not translocated through the Hcp tube but rather is ejected from the cell as part of the tip of the T6SS needle complex. Once introduced into the host cytoplasm, the PH domain localizes VasX to the inner leaflet of the host membrane and disrupts cell

signalling. Figure 2-12 is a model summarizing the characteristics described for VasX thus far.

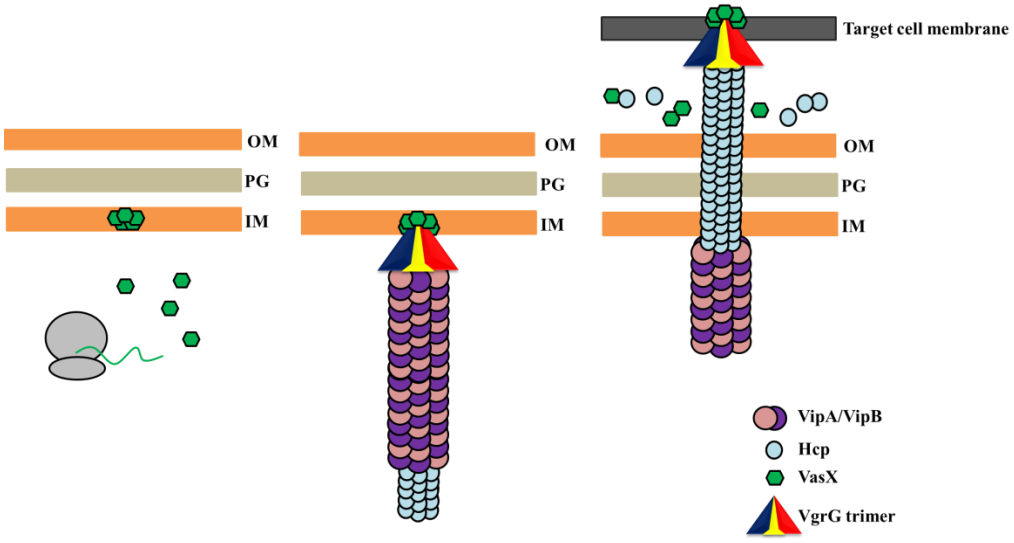

Figure 2-12. Proposed model for VasX export from the bacterial cell. VasX is produced in the cytoplasm and localizes to the inner membrane following which it self-associates forming the LPCx (left panel). The T6SS needle complex forms with the VgrG trimer cap associating with VasX, Hcp, and the VipA/VipB sheath (centre panel). Following contraction of the outer sheath, the inner Hcp tube, VgrG cap, and VasX LPCx are ejected from the cell and into the target cell (right panel). Ejection of the T6SS needle complex results in sloughing of VasX and Hcp into the extracellular space. OM; outer membrane, PG; peptidoglycan, IM; inner membrane.

CHAPTER 3

VasX is required for *Vibrio cholerae* virulence toward *Dictyostelium discoideum*

Portions of this chapter have been published as:

Miyata, S.T., Kitaoka, M., Brooks, T.M., McAuley, S.B., and Pukatzki, S. (2011) *Vibrio cholerae* Requires the Type VI Secretion System Virulence Factor VasX to Kill *Dictyostelium discoideum*. *Infection and Immunity*, 779(7):2941-9.

The experiment described in Figure 3-6 was conducted by Steven McAuley.

The data for Figures 3-7 and 3-8 were supplied by Teresa Brooks.
Purification of recombinant VasX and VasX(1-200) was performed by Teresa Brooks.

3. VasX is required for *V. cholerae* virulence toward *D. discoideum*

3.1 Introduction

The *V. cholerae* T6SS was first identified based on the ability of V52 to avoid predation by the social amoeba *D. discoideum* [194]. A transposon library of V52 was used to screen for mutants that became susceptible to predation by *D. discoideum* and this led to the identification of the crucial T6SS components VasH, VasK, Hcp, and VgrG [194]. The use of *D. discoideum* as a host model has proven useful for the identification of virulence factors [194, 224, 355, 373]; however, the specific mechanism by which V52 kills *D. discoideum* using its T6SS has not been elucidated. The interaction of V52 and *D. discoideum* was characterized by means of a plaque assay. Here, V52 was mixed with *D. discoideum* and plated on nutrient agar [396] which is able to support the growth of bacteria but not the amoebae. To survive, amoebae must prey on the bacteria resulting in plaque formation in the bacterial lawn. However, *V. cholerae* strains expressing a functional T6SS, such as V52, are virulent towards amoebae and can resist predation, thus preventing plaque formation [194]. Importantly, T6SS-mediated virulence toward *D. discoideum* is an active process that results in a loss of viable amoebae rather than the inability of *D. discoideum* to feed on V52[194].

VgrG-1 is an important T6SS protein that has a C-terminal actin cross-linking domain (ACD) [194, 209, 222]. This protein is crucial for V52 virulence towards phagocytic eukaryotic cells such as *D. discoideum* and RAW 264.7 murine macrophages [194, 209, 222]. VgrG-1 causes cell-rounding mediated by

the cross-linking of monomeric G actin in the host cell cytoplasm[209, 222]. Presumably, VgrG-1 mediates actin cross-linking in *D. discoideum* as well given that V52Δ*vgrG-1* is avirulent in the plaque assay [194]. The polymerization of host actin molecules can be visualized by western blotting with α-actin antibody where a laddering effect is observed when actin is cross-linked [209, 222]. Ma and colleagues demonstrated that phagocytosis is required for VgrG-1 translocation into the host cytosol and subsequent actin cross-linking[222]. Importantly, T6SS-mediated virulence by V52 has only been documented for professional phagocytes [194] and whether V52 translocates proteins other than VgrG-1 into the host cytoplasm remains undetermined.

In the following set of experiments I characterized the role of VasX in the context of T6SS-mediated killing of the eukaryotes *D. discoideum* and RAW 264.7 murine macrophages. Bioinformatics analysis suggested the presence of an N-terminal PH domain within VasX (section 2.2.2). Canonically, PH domains are present in eukaryotic, not prokaryotic, proteins and are involved in signal transduction. The secondary structure of typical PH domains consists of two β-sheets, followed by an α-helix that contains a conserved tryptophan residue [385, 397, 398]. Based on these secondary structure predictions, we hypothesized that VasX engages in molecular mimicry by utilizing its PH domain to attach itself to host cell structures such as biological membranes.

3.2 **Results**

3.2.1 VasX is required for V52 virulence toward *D. discoideum*

To test whether VasX is important for T6SS-mediated virulence toward eukaryotes, I created a *vasX* deletion strain (V52Δ*vasX*) and complemented the mutation *in-trans* by expressing *vasX* from the P_{BAD} promoter in the plasmid pBAD24 [399] (V52Δ*vasX*/pBAD24-*vasX*). To ensure VasX was produced and secreted in this strain, V52Δ*vasX*/pBAD24-*vasX* was grown in selective LB broth in the presence or absence of arabinose. Bacterial pellet and supernatant fractions were subjected to SDS-PAGE and western blotting with VasX antibody demonstrated that VasX was expressed and secreted by this strain under inducing conditions (Figure 3-1). It appears that over-expression of VasX does not result in larger amounts of secretion into culture supernatants as the amount of secreted VasX was similar for wild-type V52 and V52 over-expressing VasX (Figure 3-1).

A.

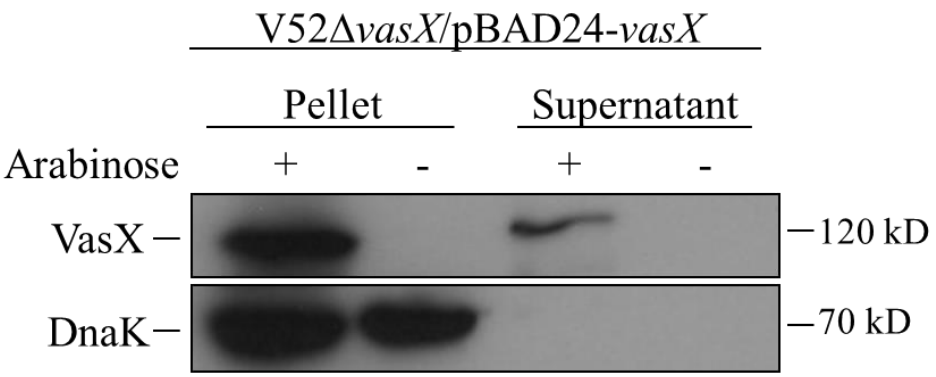

B.

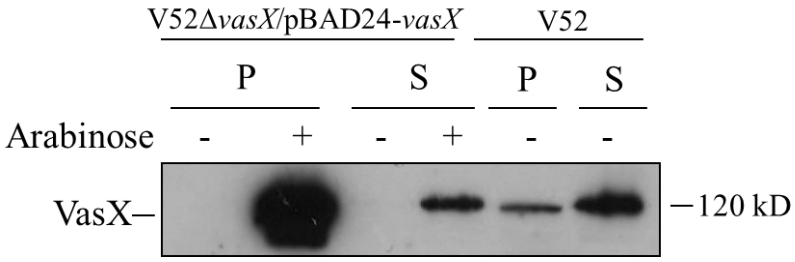

Figure 3-1. Episomal expression of *vasX* restores secretion of VasX to wild-type levels. Bacterial pellet and supernatants samples were harvested from mid-logarithmic cultures and subjected to SDS-PAGE followed by western blotting with VasX and DnaK primary antibody. (A) Episomal expression of *vasX* restores production and secretion in V52Δ*vasX*. DnaK is a cytoplasmic protein that serves as a loading and lysis control. (B) Over-expression of *vasX* does not result in increased secretion into culture supernatants. Molecular weights are shown to the right of each blot. P; pellet sample, S; supernatant sample.

V52Δ*vasX*/pBAD24-vasX was then used in a plaque assay to determine whether VasX is important for virulence toward the amoeboid host model *D. discoideum* [373, 400, 401]. No plaques were observed on plates with wild-type V52; however, plaques developed after a four-day incubation with V52Δ*vasX,* V52Δ*vasK,* and V52Δ*vgrG-1* (Figure 3-2). The number of plaques in a lawn of V52Δ*vasX* was significantly fewer than in lawns of V52Δ*vasK* and V52Δ*vgrG-1* (*P*-value < 0.001). V52Δ*vgrG-1* exhibited a stronger plaque phenotype than V52Δ*vasX*; however, both VasX and VgrG-1 contribute to T6SS-mediated virulence towards *D. discoideum* (Figure 3-2).

A.

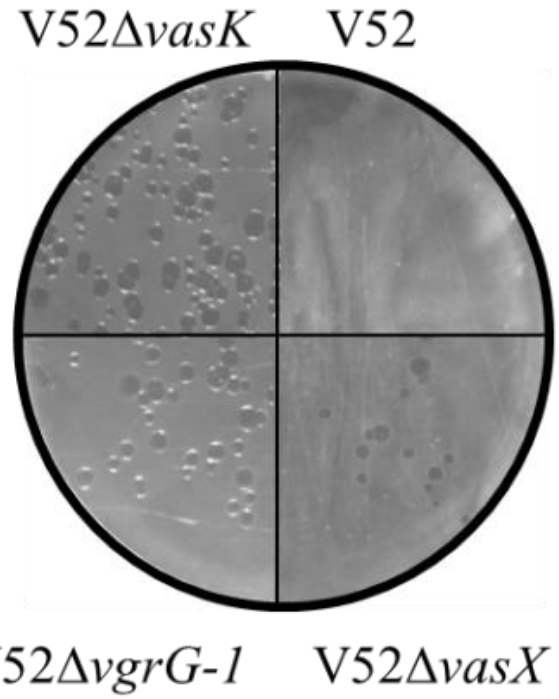

B.

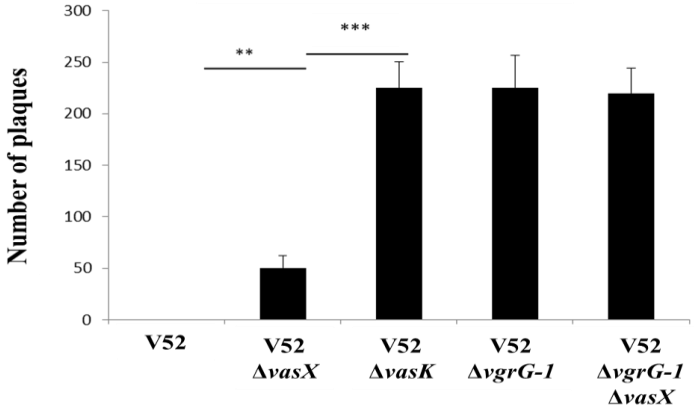

Figure 3-2. V52Δ*vasX* virulence is attenuated towards *D. discoideum*. Bacterial cultures of the strains indicated on the *x*-axis were mixed *D. discoideum* amoebae and spread onto SM/5 nutrient agar plates. Following 4-day incubation, plaques were photographed (A) and quantified (B). *** = $p < 0.001$, ** = $p < 0.01$. Error bars indicate the standard deviation.

Previously it was determined that VgrG-1 is imperative for V52 virulence toward *D. discoideum* [194]. To determine if VgrG-1 and VasX act synergistically, we created a *vgrG1/vasX* double-knockout strain (V52Δ*vgrG-1*Δ*vasX*) and tested its plaque assay phenotype. The number of plaques in a lawn of V52Δ*vgrG-1*Δ*vasX* are not significantly different from those in a lawn of V52Δ*vgrG-1* but do differ significantly compared to V52Δ*vasX* (Figure 3-2). Therefore, although VasX is important for T6SS-mediated virulence towards *D. discoideum*, VasX and VgrG-1 do not appear to have additive toxic effects.

To confirm that VasX was responsible for the plaque-forming phenotype, plaque assays were carried out with V52Δ*vasX*/pBAD24-*vasX* under inducing (0.1% arabinose) and non-inducing (absence of arabinose) conditions. Plaques developed when *vasX* was not expressed; however, no plaques developed under inducing conditions (Figure 3-3). Transformation of V52Δ*vasX* with pBAD24 (plasmid control) did not affect the plaque phenotype in the absence or presence of arabinose. Taken together, these complementation experiments confirm that the attenuated virulence of the *vasX* mutant was due to the removal of *vasX* and not to another variable such as an effect on downstream genes (polarity), indicating a role for VasX in T6SS-mediated virulence towards *D. discoideum*.

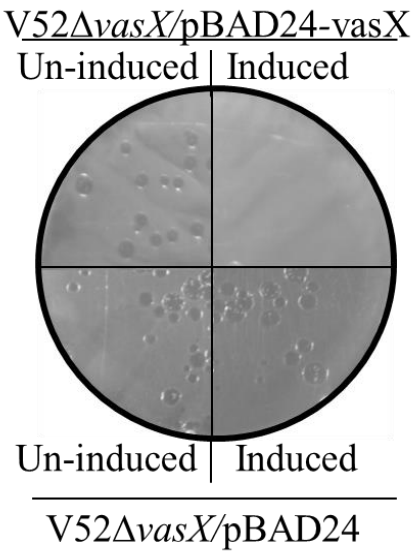

Figure 3-3. Episomal expression of *vasX* restores virulence of V52Δ*vasX* toward *D. discoideum*. V52*vasX*/pBAD24-*vasX* and the plasmid control (V52*vasX*/pBAD24) were mixed with amoebae, spread and spread on nutrient agar (with or without 0.1% arabinose), and incubated for 4 days at 22°C to allow for plaque formation.

3.2.2 The PH Domain is important for VasX-mediated virulence

PH domain-containing proteins are associated with modifying cell signaling events in eukaryotes. Therefore, I hypothesized that VasX, following T6SS-dependent delivery into the cytoplasm of the host cell, disrupts cell signaling cascades by binding phosphoinositides via its putative PH domain. I created a mutant form of *vasX* that lacks the PH domain-encoding region (Figure 3-4) and used this strain (V52ΔPHDomain) in a plaque assay. I observed that V52 lacking the PH domain was attenuated in its virulence toward *D. discoideum* (Figure 3-4) and that this could be complemented by expression of full-length *vasX in-trans* (Figure 3-4). This implies that the PH domain region is an important factor for VasX-mediated killing of amoebae.

A.

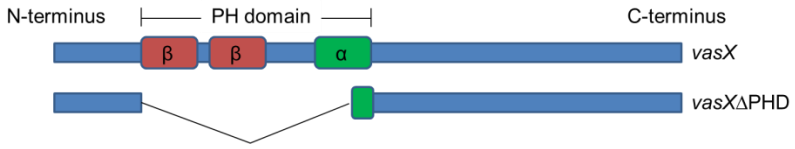

B.

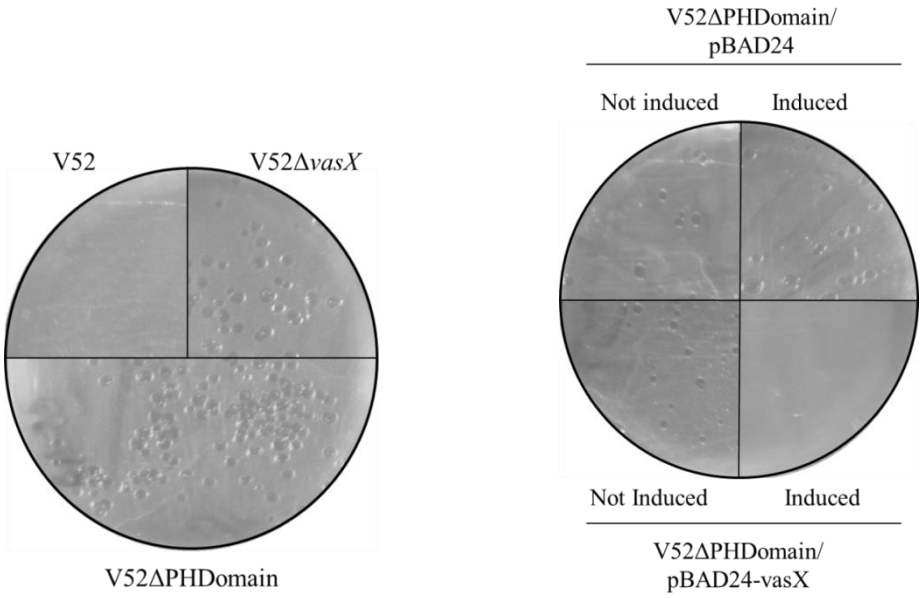

Figure 3-4. The PH domain is crucial for VasX-mediated virulence. (A) Schematic representation of VasX and the mutated form lacking the PH domain. The β-sheets and α-helix predicted by HHpred are shown in red and green, respectively. (B) Plaque assay demonstrating deletion of the PH domain renders V52 attenuated in its virulence toward *D. discoideum*. The indicated bacterial strains were mixed with *D. discoideum* and spread onto nutrient agar plates (+/- arabinose to induce expression from the P_{BAD} promoter). The formation of plaques in the bacterial lawn indicates the amoebae preyed upon the bacteria.

Eukaryotic PH domains share a conserved tryptophan residue within the α-helical region which, when mutated, reduces the protein's ability to interact with phosphoinositides [402]. VasX contains two tryptophan residues, Tryp144 and Tryp146, within the predicted PH domain α-helix. Therefore, I performed site-

directed mutagenesis using the plasmid pBAD24-vasX and (independently) substituted Tryp144 and Tryp146 for alanine. The plasmids pBAD24-vasX(W144A)::FLAG and pBAD24-vasX(W146A)::FLAG were each transformed into V52Δ*vasX* creating strains V52Δ*vasX*/pBAD24-vasX(W144A)::FLAG and V52Δ*vasX*/pBAD24-vasX(W146A)::FLAG. These strains were used in a plaque assay to determine if the mutant forms of VasX could complement the *vasX* deficiency. I observed that both *vasX* mutants were able to complement V52Δ*vasX* virulence toward *D. discoideum* (Figure 3-5) to the same extent as expressing wild-type *vasX in-trans*. Therefore, mutation of the tryptophan residues within the putative PH domain does not alter the toxic activity of VasX.

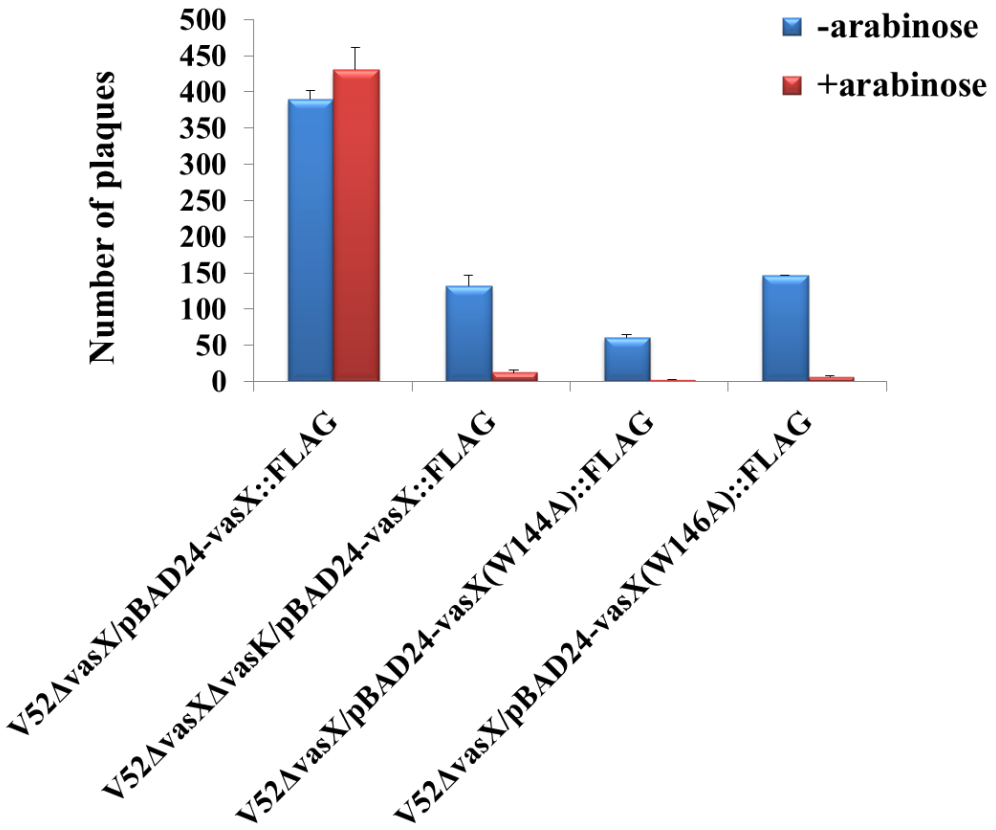

Figure 3-5. Quantification of plaques in lawns of V52 with site-directed mutagenesis of the PH domain in VasX. V52Δ*vasX* harboring plasmids with wild-type *vasX*, or the *vasX* site-directed mutants was mixed with *D. discoideum* and incubated on a nutrient agar plate under inducing (+arabinose) or non-inducing (- arabinose) conditions. The number of plaques formed in the bacterial lawn was quantified. Error bars indicate the standard deviation.

3.2.3 VasX is not required for V52 actin cross-linking

In addition to its virulent phenotype toward *D. discoideum*, *V. cholerae* uses its T6SS to crosslink actin in RAW 264.7 macrophages [209, 222, 333]. Actin crosslinking is achieved by the VgrG-1 protein; a large protein possessing a C-terminal actin cross-linking domain that is translocated into host cells via the

T6SS [209, 222, 333]. To test whether VasX was required for VgrG-1-mediated cross-linking of host cell actin, murine RAW 264.7 macrophages were infected with wild-type V52, V52Δ*hcp1,2*, V52Δ*vasK*, V52Δ*vgrG-1*, or V52Δ*vasX* for 2 hours. Following infection, cells were collected, lysed and resolved by SDS-PAGE followed by western blotting using α-actin antibody. Actin crosslinking was visualized by a "laddering" effect of actin bands as monomeric units of G-actin are covalently attached to one another forming higher molecular weight structures [209]. We observed that wild-type V52 and V52Δ*vasX* strains were capable of crosslinking RAW 264.7 cell actin (Figure 3-6). Thus, deletion of *vasX* did not affect the assembly or the enzymatic function of the T6SS physical translocon complex.

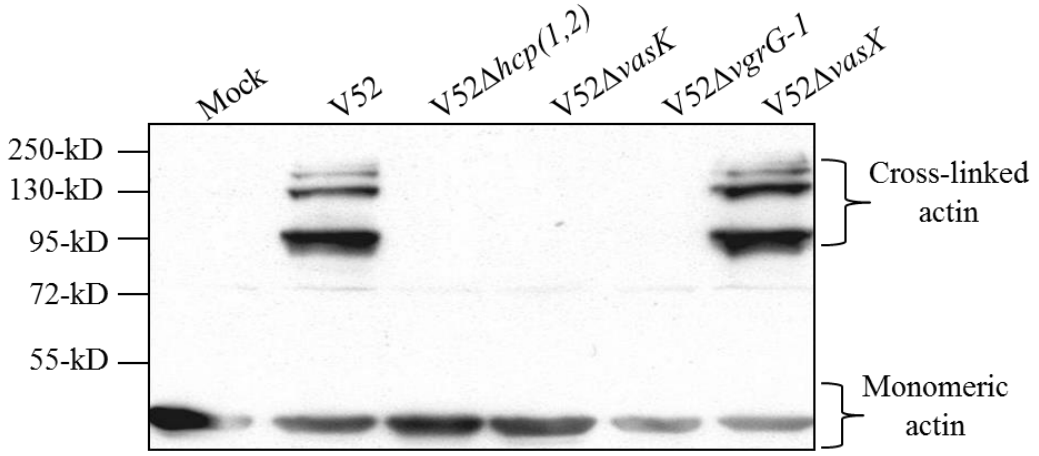

Figure 3-6. VasX is not required for T6SS-mediated cross-linking of murine macrophage actin. RAW 264.7 macrophages were infected with the strains indicated at the top of the figure. Cell lysates were subjected to SDS-PAGE followed by western blotting using actin primary antibody. Molecular mass markers are shown to the left of the blot. The *hcp* deletion strain V52Δ*hcp-1,2* has both chromosomal copies of *hcp* deleted.

3.2.4 VasX is a lipid-binding protein

PH domain-containing proteins have canonically been characterized as lipid-binding proteins. More specifically, PH domains bind phosphoinositides on the inner leaflet of the eukaryotic cell membrane and alter many cellular processes [392, 393]. Because VasX contains an N-terminal PH-like domain, we wanted to test whether VasX binds lipids. We performed far-western blots using nitrocellulose membranes spotted with a variety of membrane lipids (Figure 3-7). Lipid-bound membranes were probed with purified VasX to determine its ability to interact with cell membrane phospholipids. We noted that VasX interacts with membrane phospholipids that bear a phosphorylated head group and carry two acyl chains, namely phosphatidic acid (PA) and each of the phosphatidylinositol phosphates (PIP). However, VasX does not bind phosphatidylinositol (PIns), phosphatidylserine (PS), phosphatidylethanolamine (PE), phosphatidylcholine (PC), lysophosphatidic acid (LPA), lysophosphatidylcholine (LPC) or sphingosine-1-phosphate (S1P). We also tested whether the first 200 residues of VasX, which encode the putative PH domain, retained the ability to bind membrane lipids. VasX(1-200) exhibited the same lipid-binding pattern as full-length VasX (Figure 3-7). The positive control represents purified protein (either full length or truncated VasX) spotted directly onto the membrane.

We previously determined that *V. cholerae* uses its T6SS to kill other bacteria [211]. Because VasX is a T6SS toxin that binds eukaryotic lipids, we wanted to test whether VasX could bind bacterial LPS. Purified *E. coli* LPS (Sigma-Aldrich) was spotted onto a PIP strip at the same concentration as each of

the membrane lipids on the strip (100 pmol). Full-length VasX retained the ability to bind PA and each PIP (Figure 3-7); however, VasX did not bind to bacterial LPS.

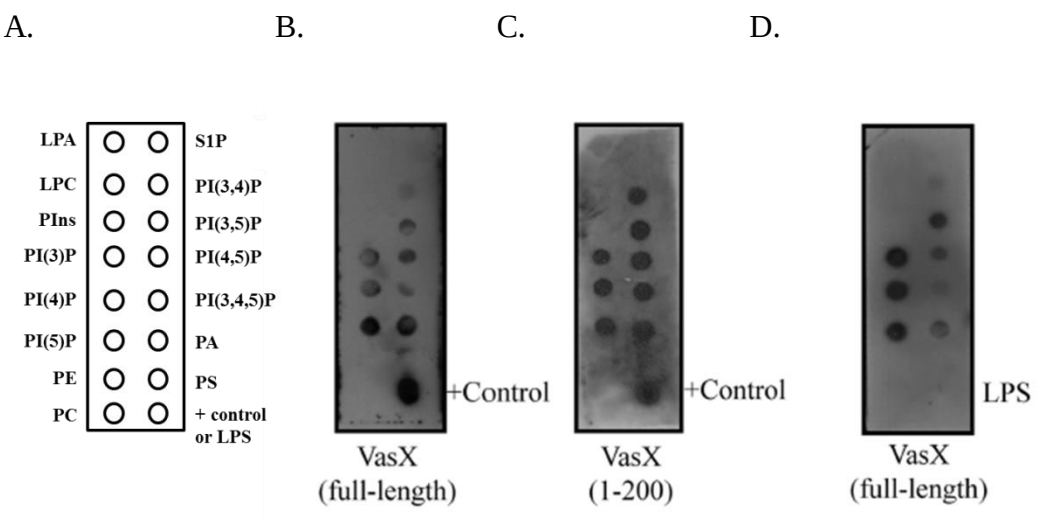

Figure 3-7. VasX binds phosphoinositides but not LPS. (A) Schematic representation of the various biological membrane lipids present on PIP Strips, including PA, PI, PIP, PS, PE, PC, LPA, LPC, and S1P. (B, C, and D) Purified full-length VasX or a truncated version consisting of residues 1 to 200 (containing the PH domain) was used to probe PIP Strips for lipid binding. Bound protein was detected using His primary antibody. The positive control (+) included purified VasX spotted directly onto the PIP Strip membrane. In panel D, *E. coli* LPS was spotted in place of the positive control on the PIP Strip.

To determine whether these interactions also occurred in aqueous solution, multilamellar vesicles (MLV) of PA, LPA and a natural mixture of bovine total liver lipids extracts (TLE, which does not contain a significant amount of PA or PIPs according to the composition indicated by the manufacturer – Avanti Polar Lipids) were prepared in PBS and mixed with purified full-length VasX, VasX(1-200) or BSA (negative control). These large lipid vesicles, and any associated

proteins, can be pelleted by centrifugation, creating total, pellet, and supernatant fractions for SDS-PAGE analysis. We observed that VasX was found in the pellet (lipid pull-down) fractions when mixed with PA, but not when mixed with TLE, LPA or PBS (Figure 3-8). Similarly, the truncated version of VasX, containing the predicted PH domain showed the same pattern of lipid-binding as full-length VasX in MLV experiments (Figure 3-8). As expected, BSA was not pulled down with any of the membrane lipids tested. These results suggest that VasX interacts with phosphorylated membrane lipids via its PH domain.

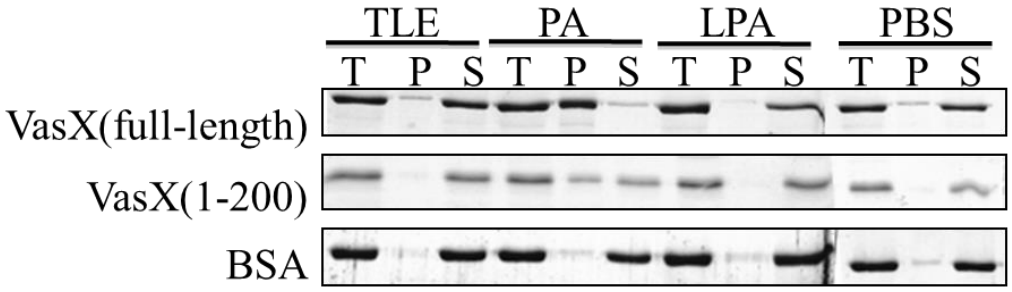

Figure 3-8. MLV pulldown of purified recombinant VasX and the N-terminal fragment of VasX(1–200). Full-length VasX, VasX(1–200), and BSA (negative control) were mixed with MLV of TLE, PA, LPA, or PBS (as a technical control) and divided into total (T), pellet (P), and supernatant (S) fractions by centrifugation. The partitioning of protein into each fraction was visualized by SDS-PAGE and Coomassie blue staining.

3.2.5 VasX is not translocated into the cytoplasm of host cells

To test whether VasX is injected directly into the cytosol of infected host cells, I fused *vasX* to the DNA sequence encoding the N-terminal enzymatic portion of the *Bordetella pertussis* adenylate cyclase toxin CyaA. Similar fusions have been used extensively to demonstrate translocation of effector molecules into the cytosol of infected cells [403-406]. CyaA converts adenosine triphosphate (ATP) into cAMP only in the presence of calmodulin (CaM) which is found strictly in the cytosol of eukaryotic cells (and not within prokaryotic cells). Therefore, if VasX::CyaA is translocated into the cytosol, a significant increase in intracellular cAMP will result.

The *vasX::cyaA* fusion was introduced into pBAD24 under the control of an arabinose-inducible promoter and was transformed into both V52Δ*vasX* (creating the strain V52Δ*vasX*/pBAD24-vasX::cyaA) and the T6SS-null mutant V52Δ*vasX*Δ*vasK* (creating strain V52Δ*vasX*Δ*vasK*/pBAD24-vasX::cyaA). To test expression and T6SS-dependent secretion of these fusions, V52Δ*vasX*/pBAD24-vasX::cyaA and V52Δ*vasX*Δ*vasK*/pBAD24-vasX::cyaA were grown to late logarithmic phase in the presence or absence of arabinose. Cell pellet and supernatant fractions were collected and analyzed by western blot with CyaA antibodies. The *vasX::cyaA* fusion is expressed in both strains, and the VasX::CyaA fusion is secreted from the bacterial cell in a T6SS-dependent manner (Figure 3-9). Importantly, plaque assays with *D. discoideum* indicated that expression and secretion of VasX::CyaA complemented the *vasX* deletion (Figure 3-9).

A.

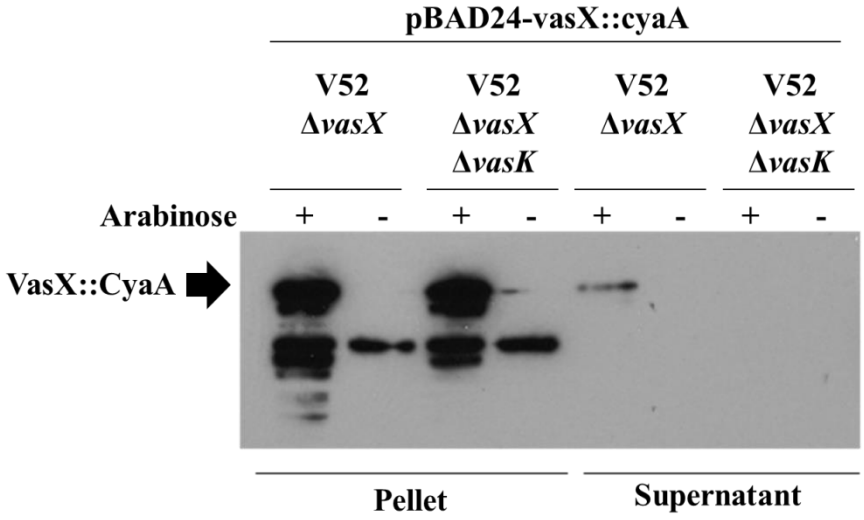

B.

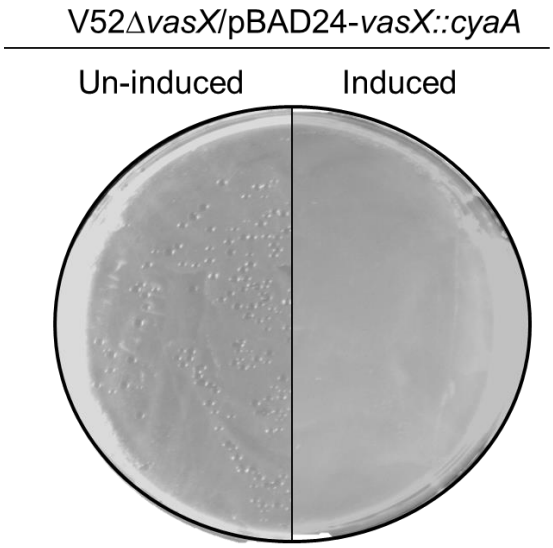

Figure 3-9. VasX::CyaA is secreted in a T6SS-dependent manner and complements V52Δ*vasX*. (A) Pellet and supernatant samples were harvested from mid-logarithmic cultures of the strains indicated. Samples were subjected to SDS-PAGE followed by western blotting with α-CyaA primary antibody. (B) V52Δ*vasX*/pBAD24-vasX::cyaA was mixed with *D. discoideum* and spread onto nutrient agar (+/- arabinose). Plaque formation in the bacterial lawn indicates the amoebae were able to prey on the bacteria.

I then tested the ability of V52Δ*vasX*/pBAD24-vasX::cyaA and V52Δ*vasX*Δ*vasK*/pBAD24-vasX::cyaA lysates to catalyze cAMP production in the absence of host cells to ensure this fusion protein produced functional CyaA. V52Δ*vasX*/pBAD24-vasX::cyaA and V52Δ*vasX*Δ*vasK*/pBAD24-vasX::cyaA lysates were incubated in the presence/absence of ATP and CaM and the cAMP levels were analyzed using the same method as for infected macrophages. I observed that VasX::CyaA possesses functional adenylate cyclase activity because both V52Δ*vasX*/pBAD24-vasX::cyaA and V52Δ*vasX*Δ*vasK*/pBAD24-vasX::cyaA lysate samples were able to catalyze the production of cAMP in the presence of ATP and CaM (Figure 3-10).

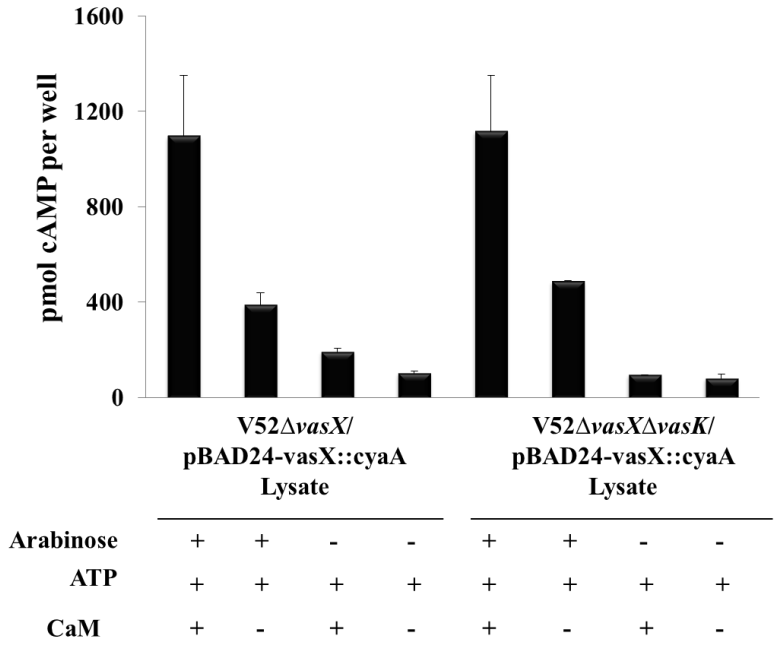

Figure 3-10. VasX::CyaA is a functional fusion capable of stimulating cAMP production. The bacterial strains listed on the *x*-axis were grown in the presence or absence of arabinose to induce expression of *vasX::cyaA*. Bacterial cell lysates were incubated in the presence or absence of ATP and CaM and the cAMP levels were assayed using the cAMP EIA Kit (New East Biosciences). Error bars indicate the standard deviation.

Knowing that the VasX::CyaA fusion protein is expressed and secreted and that it complements the *vasX* deletion mutant, I then tested whether expression of this fusion protein caused an increase in *D. discoideum* cAMP levels. Upon infecting *D. discoideum* in liquid culture with V52Δ*vasX*/pBAD24-vasX::cyaA or V52Δ*vasX*Δ*vasK*/pBAD24-vasX::cyaA under inducing or non-inducing conditions, we did not observe an increase in intracellular cAMP levels in cells infected with either of the two strains (Figure 3-11). This indicates that the *vasX::cyaA* fusion is not present at abundant levels in the cytoplasm of the amoebae.

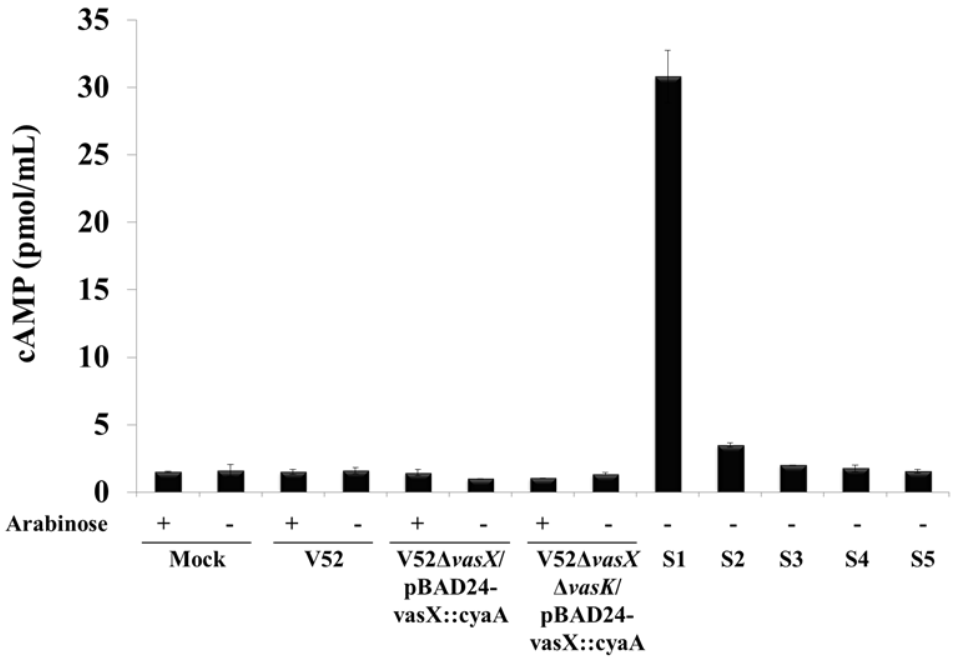

Figure 3-11. VasX::CyaA does not stimulate cAMP production upon infection of *D. discoideum*. The bacterial strains listed on the *x*-axis were used to infect *D. discoideum* grown in liquid culture in the presence or absence of arabinose. Cell lysates were harvested following a 1.5-hour infection and assayed for cAMP concentration using the cAMP EIA Kit (New East Biosciences). Error bars indicate the standard deviation. S1-S5; cAMP standards provided with the cAMP EIA kit.

I then tested whether VasX::CyaA could cause increased cAMP levels within the cytosol of RAW 264.7 murine macrophages. As a positive control, I used Enteropathogenic *E. coli* (EPEC) strain E2348/69 transformed with pACYC184-espF::cyaA. EspF is an EPEC effector protein that is translocated into host cells via the T3SS [406]. Following macrophage infection, the intracellular cAMP levels increased approximately 250-fold when infected with this EPEC/pACYC184-espF::cyaA (Figure 3-12). However, when macrophages were infected with EPEC containing the empty vector, cAMP levels did not increase (Figure 3-12). Upon infecting RAW 264.7 macrophages with V52Δ*vasX*/pBAD24-vasX::cyaA or V52Δ*vasX*Δ*vasK*/pBAD24-vasX::cyaA under inducing or non-inducing conditions, we did not observe an increase in intracellular cAMP levels in cells infected with either of the two strains, indicating that the *vasX::cyaA* fusion is not present at abundant levels in the cytoplasm of host cells (Figure 3-12). Taken together these data indicate that VasX::CyaA does not gain access to the host cell cytoplasm following infection of *D. discoideum* or murine macrophages.

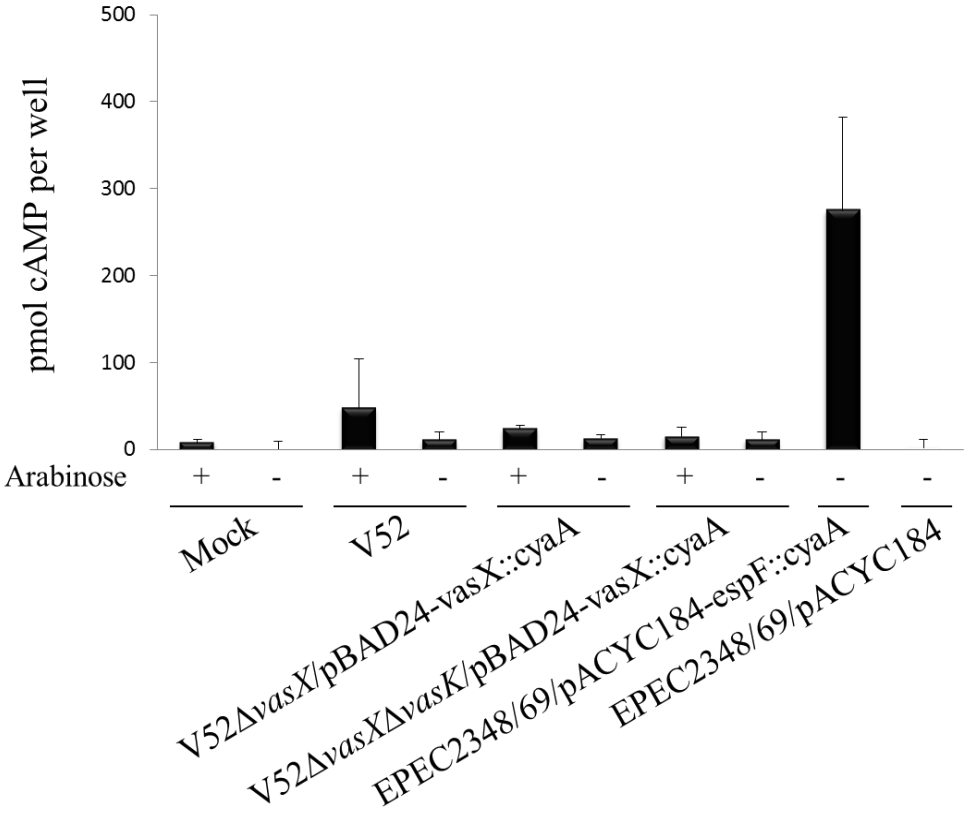

Figure 3-12. VasX::CyaA does not stimulate cAMP production upon infection of murine macrophages. The bacterial strains listed on the *x*-axis were used to infect RAW 264.7 macrophages in the presence or absence of arabinose. Cell lysates were assayed for cAMP concentration using the cAMP EIA Kit (New East Biosciences). Error bars indicate the standard deviation.

3.2.6 VasX does not cleave phosphate from phosphoinositides

VasX binding to phosphoinositides (Figure 3-7) is mediated by the N-terminal 200 residues containing the putative PH domain. Some proteins that bind phosphoinositides act as phosphatidylinositol phosphatases which can result in membrane blebbing and destabilization [407-410] and I therefore set out to determine whether VasX can cleave phosphate from PIPs. I used the Malachite Green Phosphatase Assay (Caymen Chemical) to determine whether VasX, or

more specifically the PH domain, can cleave phosphoinositides. This colorimetric assay measures the amount of inorganic phosphate bound to malachite green molybdate under acidic conditions and can be measured by reading the OD_{620}. Purified, recombinant VasX or VasX(1-200) was incubated by itself, or in combination with phosphatidylinositol(4,5)bisphosphate ($PI(4,5)P_2$) – a lipid to which VasX binds (Figure 3-7). I observed that the incubation of VasX alone resulted in the same amount of free inorganic phosphate as VasX mixed with $PI(4,5)P_2$ (Figure 3-13). Similarly, VasX(1-200) mixed with $PI(4,5)P_2$ had a similar amount of inorganic phosphate release compared to VasX(1-200) alone (Figure 3-13). Incubation of $PI(4,5)P_2$ alone had the highest amount of free inorganic phosphate (~0.3 nmol phosphate per 50 µL) compared to other experimental samples (Figure 3-13). Therefore, incubation with VasX or VasX(1-200) does not result in the cleavage of phosphate from $PI(4,5)P_2$.

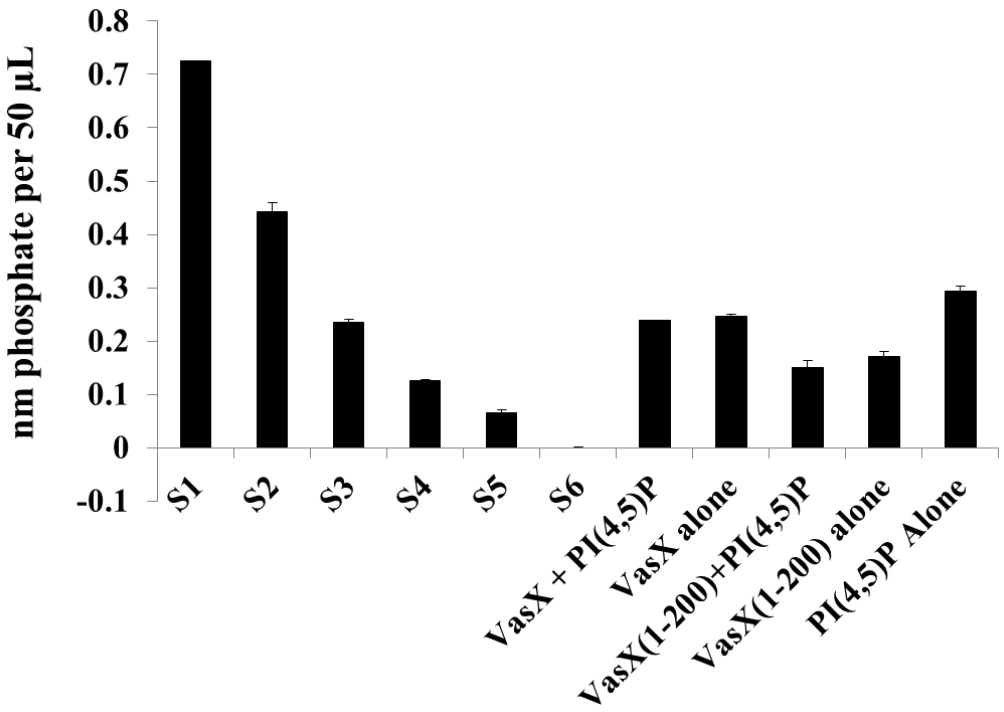

Figure 3-13. VasX does not cleave phosphate from phosphoinositides. Purified, recombinant VasX or VasX(1-200) were incubated in the presence or absence of $PI(4,5)P_2$. The resulting concentration of free inorganic phosphate was measured using the Malachite Green Phosphatase Assay (Caymen Chemical) and plotted. S1-S6; experimental standards containing decreasing concentrations of inorganic phosphate.

3.3 **Discussion**

The data presented in this chapter identified VasX as a virulence determinant for V52 against *D. discoideum* (Figures 3-2 and 3-3) and demonstrated VasX's lipid-binding ability (Figures 3-7 and 3-8). Because inositol phosphates are rarely found in bacteria [391], we initially postulated that the PH domain of VasX has a role in binding to host membrane lipids. Indeed, we found that VasX and a truncated version of VasX consisting of residues 1-200 (encompassing the putative PH domain) bind to membrane lipids, including

various phosphatidylinositol phosphates and phosphatidic acid using two independent methods (Figures 3-7 and 3-8). The mechanism behind the specificity of lipids bound by VasX (e.g. VasX bind phosphatidic acid but not lysophosphatidic acid) remains unclear; however, interference with host cell phosphoinositide metabolism and signaling by pathogenic bacteria is not uncommon and has been previously demonstrated for other enteric bacterial pathogens [410-412]. Based on the results of the malachite green phosphatase assay, it does not appear that cleavage of phosphoinositides is the mechanism by which VasX acts (Figure 3-13).

Results of my plaque assays with *D. discoideum* indicated that VasX is required for virulence toward amoebae. Restoration of the virulent phenotype was observed upon expression of *vasX in-trans* confirming that attenuation of V52Δ*vasX* toward amoebae is not due to a polar mutation (Figure 3-3). Interestingly, the number of plaques that formed in V52Δ*vasX* lawns was significantly less than the number of plaques that developed in lawns of V52Δ*vasK,* V52Δ*vgrG-1*, and V52Δ*vgrG-1*Δ*vasX*. The smaller number of plaques formed by V52Δ*vasX* could suggest that VgrG-1 is a more potent amoeboid toxin than VasX. Even though VgrG-1 was dispensable for VasX secretion *in-vitro* (Figure 2-4) and VasX is not required for the actin cross-linking activity of VgrG-1, both VgrG-1 and VasX are required for virulence toward amoebae (Figure 3-2). Since V52Δ*vgrG-1* and V52Δ*vgrG-1*Δ*vasX* have a more severe plaque-forming phenotype than V52Δ*vasX*, I conclude that V52Δ*vgrG-1*

has a dominant plaque phenotype and VasX and VgrG-1 do not appear to act synergistically.

Deletion of the VasX PH domain also resulted in plaque formation in the V52ΔPHDomain bacterial lawn similar to the phenotype observed with V52Δ*vasX* bacterial lawns suggesting that the PH domain is crucial for VasX function. It is also possible that deletion of the PH domain resulted in a mutant version of VasX that was unable to fold and function properly producing a similar phenotype than that observed. In an attempt to circumvent this improper folding possibility, I performed site-directed mutagenesis on two individual tryptophan residues within the putative PH domain α-helix region (W144 and W146) as tryptophan residues within PH domains α-helices are crucial for PH domain function [398, 413]. Mutation of tryptophan residue 144 or 146 to alanine did not affect the toxicity of VasX in the *D. discoideum* plaque assay (Figure 3-5) suggesting that neither tryptophan residue is crucial for VasX-mediated virulence. These data suggest that the secondary structure prediction for VasX is incorrect or that the N-terminus of VasX appears similar to a PH domain but functions in a unique manner.

Although VasX is important for virulence toward *D. discoideum,* VasX is not required for VgrG-1 to gain access to the host cytoplasm as V52Δ*vasX* was able to cross-link macrophage actin to the same extent as wild-type V52 (Figure 3-6). It is possible that the actin cross-linking phenotype is too dominant of an effect to witness small decreases in virulence mediated by VasX and therefore we still entertained the possibility that VasX was an effector protein translocated into

the host cell cytoplasm. By fusing *vasX* to *cyaA* we tested whether VasX was translocated into the cytoplasm of both *D. discoideum* and murine macrophages. Although VasX::CyaA was secreted (Figure 3-9), functional (Figure 3-10), and could complement virulence of V52Δ*vasX* in a plaque assay (Figure 3-9), this fusion protein failed to elicit an increase in the cytosolic cAMP levels in *D. discoideum* and macrophage infection assays (Figures 3-1 and 3-12). This implies that VasX::CyaA was not introduced into the host cytoplasm. I propose the following scenario to explain why VasX – a secreted protein that is not introduced into the host cytoplasm – is important for virulence toward *D. discoideum* but not macrophages.

I previously presented data indicating that VasX possesses C-terminal trans-membrane domains and localizes to the bacterial inner membrane (Figures 2-5 and 2-7). Furthermore, the N-terminus of VasX possesses a putative PH domain which we demonstrated mediates binding to membrane lipids. Generally speaking, PH domains are found in proteins associated with the membrane, but possess no catalytic activity themselves. It was proposed that these domains serve to tether proteins to the membrane surface [414, 415]. Therefore, both the N- and C-termini of VasX may target the protein to the membrane.

It has been established that phagocytic uptake is required for T6SS-mediated virulence toward macrophages [222]; however, this has not been determined in the case of *D. discoideum*. It is also currently unclear whether VgrG-1 cross-links actin during V52 infection of *D. discoideum*. It is possible that T6SS-mediated virulence toward amoebae, at least in the case of VasX, could

result from the T6SS puncturing across the cytoplasmic membrane from the extracellular milieu. According to the model presented in Figure 2-12, VasX is ejected from the bacterium in association with the T6SS needle complex and into the target cell. Rather than being introduced into the cytoplasm of the host cell, VasX may become tethered to the outer leaflet of the host plasma membrane via the PH-like domain and then insert into the host membrane via its transmembrane domains. This model is supported by my data that VasX::CyaA is secreted but does not increase cytoplasmic cAMP levels because the fusion protein is not introduced into the cytoplasm of host cells, but rather is delivered to the membrane with its topology such that CyaA does not reach the cytoplasm. Because secondary structure predictions suggested VasX is similar to pore-forming colicins, I propose that VasX toxicity is caused by disruption of the membrane integrity of *D. discoideum*.

In the case of macrophages, I hypothesize that phagocytic uptake of the bacteria allows for the T6SS needle complex to puncture the phagosomal membrane delivering VgrG-1 into the cytoplasm where it cross-links host actin. Puncturing of the phagosomal membrane by the T6SS needle complex results in VasX insertion into the membrane of the phagosome and therefore does not perturb cytoplasmic membrane integrity. This model is summarized in Figure 3-14.

A.

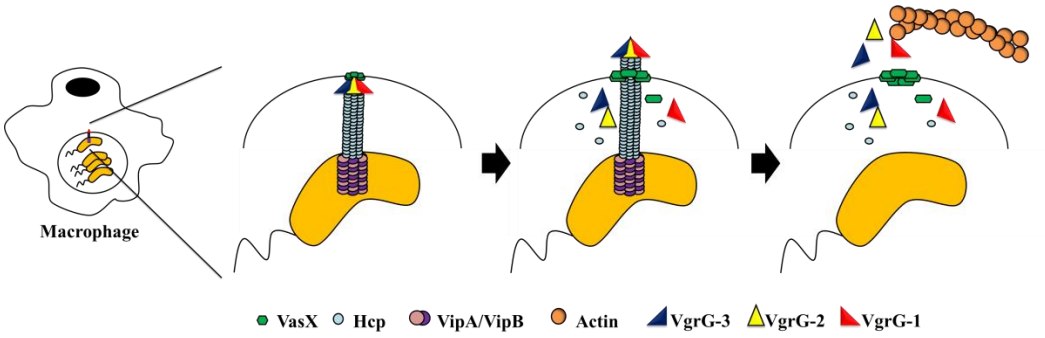

B.

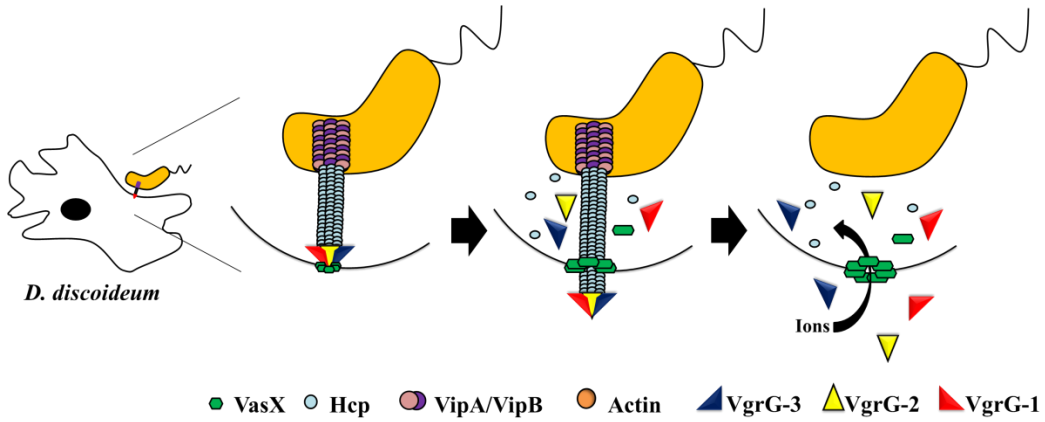

Figure 3-14. Model summarizing proposed mechanism by which VasX is required for virulence toward *D. discoideum* but not murine macrophages. (A) *V. cholerae* is phagocytosed by a macrophage and translocates the T6SS secretory complex through the phagosome membrane. VasX is deposited into the phagosomal membrane and forms a pore. VgrG-1 reaches the macrophage cytoplasm where it cross-links host actin. (B) *V. cholerae* punctures *D. discoideum* without being phagocytosed. VasX is deposited into the cytoplasmic membrane and forms a pore through which ions can leak from the cell resulting in death of the amoeba. It is currently unknown whether VgrG-1 cross-links actin during infection of *D. discoideum*.

CHAPTER 4

VasX is a bacterial toxin that targets the inner membrane of prey cells

The data for Figures 4-1B and 4-2 was provided by Daniel Unterweger.

The data for Figure 4-11 was provided by Teresa Brooks.

Flow cytometry in Figure 4-8 was performed by Dr. Karen Poon (University of Calgary).

4. VasX is a bacterial toxin that disrupts the inner membrane of target cells

4.1 Introduction

During their lifecycle, bacteria are often found in complex communities where they interact with their sister cells, other bacterial strains, protozoan predators/hosts and higher eukaryotes. In some cases, such as with biofilm formation and QS, bacteria work together and can function like a multi-cellular organism to achieve a specific goal [149, 416, 417]. On the other hand, bacteria can also compete with neighboring cells for living space or nutrient acquisition purposes [231, 315, 418, 419]. Inter-bacterial interactions can occur in the environment or during host colonization as evidenced by *V. cholerae*. *V. cholerae* typically lives in biofilms formed on crustaceans such as copepods in its natural aquatic reservoir [420]. Upon human infection, *V. cholerae* encounter another set of microbial competitors, the resident intestinal microbiota, as it colonizes the small intestine. Therefore, the ability to compete with microbial neighbors likely provides an advantage for the bacterium in establishing and maintaining its ecological niche.

Three notable strategies employed by bacteria to fend off microbial competitors include the production of bacteriocins (reviewed in [231]), CDI [306-308, 311, 312, 314-316], and the T6SS [211, 212, 214, 218, 219, 374, 421]. Each mechanism involves the use of toxins and immunity proteins to confer toxicity toward their target bacteria. Bacteriocins are small proteins produced by one

bacterium for the purpose of killing closely-related bacterial species. Colicins are a well-characterized type of bacteriocin and are produced by *E. coli* species. [230]. The mechanisms by which colicins exert their toxic function are diverse and include pore-formation in the target cell's inner membrane, DNase and RNase activity, and inhibition of murein synthesis [243-245, 247, 248, 279, 422-425]. Pore-forming colicins are produced in the cytoplasm and then released, or secreted, into the extracellular milieu. Upon binding the outer membrane of the target cell, these colicins traverse the outer membrane and insert into the inner membrane resulting in formation of a voltage-dependent ion channel [250, 422, 423]. This pore-formation destroys the cell's membrane potential and leads to cell death [249, 272, 423, 426, 427]. The producer cell does not experience autotoxicity due to the production of pore-forming colicins themselves because these types of colicins can only insert when presented to the cell from the periplasmic face. This insertion specificity is presumed to be due to the orientation of the membrane potential [231, 422, 428, 429]. The potential generated across physiological membranes results in a negative charge inside the cell and a positive charge outside the cell and the insertion of proteins that form voltage-dependent ion channels require a *cis*-positive charge to be activated [428, 429]. Therefore, insertion of pore-forming colicin molecules is only toxic to cells when presented from the outside (periplasmic face) of the cell.

The T6SS of *V. cholerae, P. aeruginosa, C. rodentium, Acinetobacter baumannii, B. thailandensis,* and *S. marcescens* all have reported antibacterial activity [211-215, 217, 354, 369]. We previously reported that *V. cholerae* V52

uses its constitutively-active T6SS to target other Gram-negative bacteria including *E. coli*, *C. rodentium*, *S. enterica*, and environmental *V. cholerae* isolates (Appendix Figure 9-5 and [211, 369]). We also observed that certain *V. cholerae* strains such as C6706, N16961, and O395 were resistant to killing by V52 [211]. Using a C6706 transposon library [430], we identified three putative T6SS-encoded toxin/immunity systems in *V. cholerae*: VCA0123 and VCA0124 (*vgrG-3* and *tsiV3*, respectively), VC1418 and VC1419 (*tseL* and *tsiV1*, respectively), and VCA0020 and VCA0021 (*vasX* and *tsiV2*, respectively). Importantly, an in-frame deletion of *tsiV2* in C6706 renders this strain susceptible to killing by V52 (to be discussed in detail in chapter 5). We demonstrated that VgrG-3 is a bacterial toxin that degrades peptidoglycan of its target cell and the enzymatic activity of VgrG-3 can be inhibited by its cognate anti-toxin, or immunity protein, TsiV3 [210]. TseL is a putative class III lipase and is crucial for V52 to kill target bacteria [374]. Given that the C-terminus of VasX shares similarity with pore-forming colicins and that *vasX* is located directly upstream of its putative immunity protein-encoding gene *tsiV2*, I hypothesized that VasX is a *V. cholerae* T6SS toxin that targets prokaryotes.

4.2 **Results**

4.2.1 VasX is sufficient, but not required for V52 to kill *E. coli*

I have previously demonstrated that *V. cholerae* V52 kills other Gram-negative bacteria like *E. coli* [211]. This killing occurs in a T6SS-dependent

manner as a V52 *vasK* deletion mutant fails to kill bacteria and this phenotype can be complemented by expressing *vasK in-trans* [211]. Therefore, we wondered whether VasX is important for T6SS-mediated killing of *E. coli*. To test this, we performed a killing assay using V52, V52Δ*vasK*, and V52Δ*vasX*/pBAD24-vasX predator and *E. coli* as prey. V52Δ*vasX* retained the ability to kill *E. coli* to the same extent as wild-type V52 (Figure 4-1). Thus, we concluded that VasX is not required for V52 to kill *E. coli*. We hypothesized that VasX was not required for V52 to kill *E. coli* because the other two T6SS bacterial toxins VgrG-3 and TseL are able to mask the absence of VasX. To test whether VasX is important for killing *E. coli* in the absence of VgrG-3 and TseL, we performed a killing assay with V52Δ*vgrG-3*Δ*tseL* predator. We observed that this strain was still able to reduce the number of viable *E. coli* by ~1-log compared to V52Δ*vasK* or V52Δ*vgrG-3*Δ*tseL*Δ*vasX* which lacks all three T6SS toxin genes (Figure 4-1).

We noted that the triple toxin mutant V52Δ*vgrG-3*Δ*tseL*Δ*vasX* is unable to kill *E. coli* (Figure 4-1). This lack of killing could occur because the strain lacks all three T6SS toxins, or because the strain fails to properly assemble the T6SS needle apparatus. To determine whether each of the mutants used in Figure 4-1 produced a functional T6SS complex, we tested whether these strains secreted Hcp into culture supernatants. We observed that the triple toxin mutant was incapable of secreting Hcp, whereas each of the individual toxin mutants secreted Hcp (Figure 4-2). The double toxin mutants V52Δ*vgrG-3*Δ*vasX* does not secrete Hcp, whereas V52Δ*vgrG-3*Δ*tseL* and V52Δ*tseL*Δ*vasX* secrete Hcp albeit at reduced levels compared to wild-type V52 (Figure 4-2, discussed further in

Chapter 6). A similar finding was reported in an independent study, further confirming these results [221]. Taken together, these data suggest VasX is sufficient to kill *E. coli* when it is the sole toxin utilized by V52, but VgrG-3 and TseL can compensate for the lack of *vasX* toxicity in V52Δ*vasX*. Furthermore, the VgrG-3, TseL, and VasX appear to function as both toxins and structural proteins important for formation of the T6SS injectosome.

A.

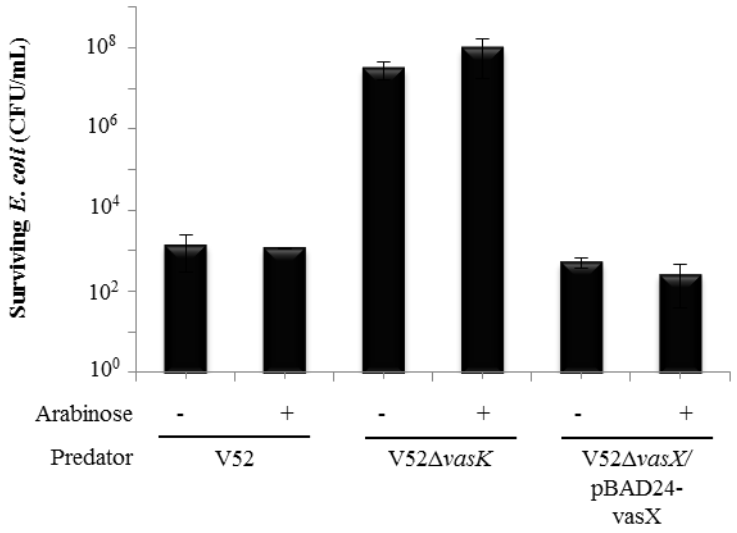

B.

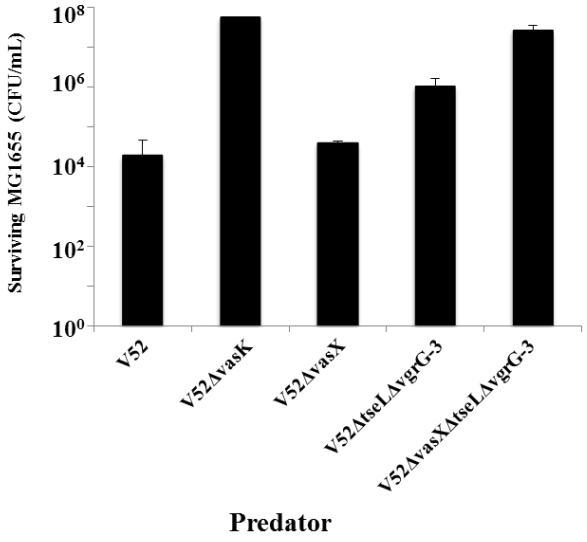

Figure 4-1. VasX is a T6SS bacterial toxin that acts in concert with TseL and VgrG-3. (A and B) Results of a bacterial killing assay showing surviving CFU/mL of rifampicin-resistant *E. coli* MG1655 prey following exposure to rifampicin-sensitive predator (listed on the *x*-axis). Arabinose was used to induce expression from the P_{BAD} promoter where indicated. Error bars indicate the standard deviation.

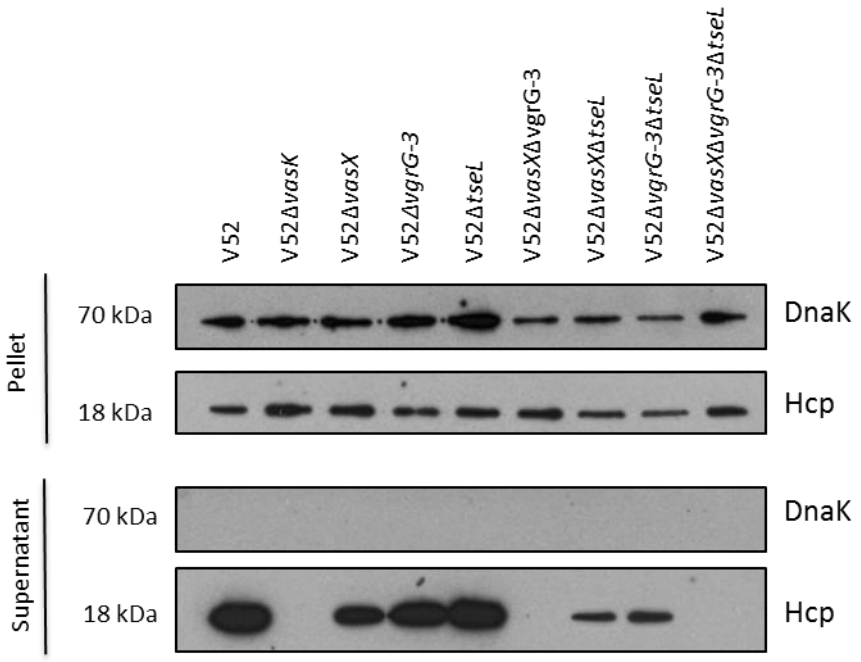

Figure 4-2. V52 toxin mutants have varied abilities to secrete Hcp. Cell pellet and supernatant samples were collected from mid-logarithmic cultures and subjected to SDS-PAGE followed by western blotting with α-Hcp and α-DnaK (loading and lysis control) antibodies.

4.2.2 VasX is required for maximal killing of *Vibrio parahaemolyticus*, *Vibrio fischeri*, and *Vibrio alginolyticus*, but not *Vibrio mimicus*.

Because bacteriocins specifically target closely related bacterial species, we decided to test whether VasX was required for killing other *Vibrio* species such as *V. parahaemolyticus, V. fischeri,* and *V. alginolyticus.* Using a bacterial killing assay, we observed that when exposed to V52, there was a ~4-5 log reduction in surviving prey (for all prey strains tested) compared to prey exposed to V52Δ*vasK* predator. Isogenic deletion of *vasX* rendered V52 attenuated toward

three of the four *Vibrio* species tested, namely *V. fischeri*, *V. alginolyticus*, and *V. parahaemolyticus* (Figure 4-3). In the susceptible strains, deletion of *vasX* did not completely abrogate the ability to kill these strains (Figure 4-3). Expressing *vasX* in V52Δ*vasX* (V52Δ*vasX*/pBAD24-vasX) restored the killing phenotype to levels comparable to wild-type V52. These results suggest that VasX is important for V52 to kill other *Vibrio* species, but not *V. mimicus*.

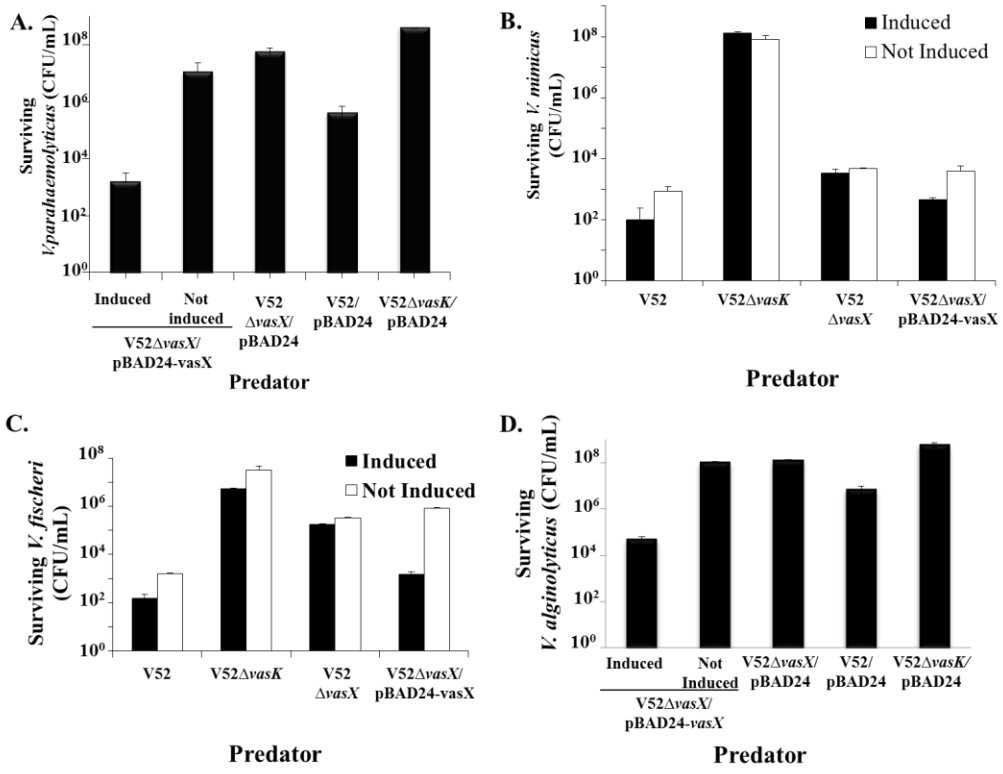

Figure 4-3. VasX is required for V52 to kill other *Vibrio* species. Results of a bacterial killing assay showing surviving CFU/mL of rifampicin-resistant *V. fischeri* (A), *V. alginolyticus* (B), *V. parahaemolyticus* (C), and *V. mimicus* (D) prey following exposure to rifampicin-sensitive predator (listed on the *x*-axis). Arabinose was used to induce expression from the P_{BAD} promoter where indicated (induced/not induced). Error bars indicate the standard deviation.

4.2.3 V52 uses VasX, TseL, and VgrG-3 to kill *V. parahaemolyticus*

I observed that VasX is important for V52 to kill *V. parahaemolyticus* (Figure 4-3); however, V52Δ*vasX* is not completely attenuated toward *V. parahaemolyticus* like the T6SS-null strain V52Δ*vasK*. I hypothesized that the other two bacterial toxins utilized by V52, TseL and VgrG-3, were responsible for the intermediate killing of *V. parahaemolyticus* that occurred using V52Δ*vasX* predator. To test this, I performed a killing assay using *V. parahaemolyticus* prey and a variety of V52 toxin mutants as predator. As previously observed, V52Δ*vasX* has an intermediate ability to kill *V. parahaemolyticus* compared to wild-type V52 and V52Δ*vasK*. V52Δ*vgrG-3* had a similar killing ability compared to V52Δ*vasX* whereas V52Δ*tseL* killed *V. parahaemolyticus* to the same extent as V52 (Figure 4-4). A V52 double mutant lacking both *vasX* and *vgrG-3* was completely attenuated toward *V. parahaemolyticus* as was the triple toxin mutant V52Δ*vasX*Δ*vgrG-3*Δ*tseL* (Figure 4-4). As noted earlier, the triple toxin mutant lacks the ability to secrete Hcp into culture supernatants (Figure 4-2) and therefore we cannot conclude whether this lack of killing is due to the lack of toxins, or to the lack of Hcp secretion. Finally, using V52Δ*vasX*Δ*tseL* or V52Δ*vgrG-3*Δ*tseL* predator resulted in an increased number of surviving *V. parahaemolyticus* compared to either of the corresponding V52 single mutants (Figure 4-4).

Since *V. parahaemolyticus* encodes two T6SSs [431], I also selected for surviving predator cells following the 4-hour incubation to determine whether *V. parahaemolyticus* was reciprocally killing V52. I did not observe a decrease in

the number of surviving V52 following incubation with *V. parahaemolyticus* (Figure 4-4). Therefore, although *V. parahaemolyticus* is T6SS^{+}, it does not kill V52 using these experimental conditions.

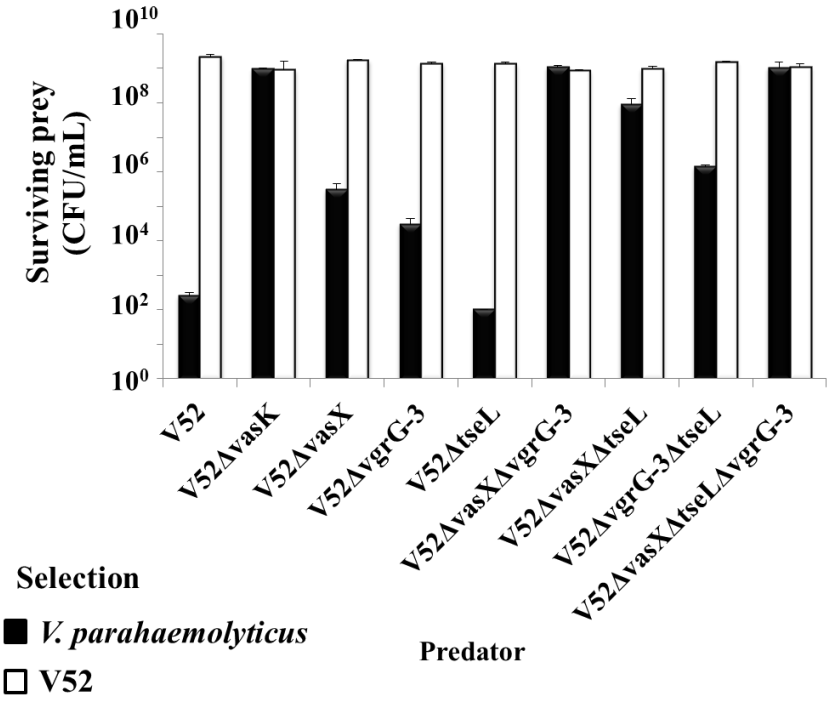

Figure 4-4. *V. cholerae* V52 uses TseL, VasX, and VgrG-3 to kill *V. parahaemolyticus.* Results of a bacterial killing assay showing surviving CFU/mL of *V. parahaemolyticus* and the predator strains listed on the *x*-axis following a 4-hour co-incubation. White bars indicate surviving V52 derivative and black bars indicate surviving *V. parahaemolyticus*. Error bars indicate the standard deviation.

4.2.4 Truncated forms of VasX cannot complement V52Δ*vasX* in a bacterial killing assay

We previously determined that the N-terminus of VasX (residues 1-200) binds lipids via its putative PH domain (Figures 3-7 and 3-8) and the C-terminus is involved in LPCx formation and membrane localization (Figure 2-11) presumably via its trans-membrane domains (Figure 2-5). Given that the C-terminus contains the colicin-like region, I asked whether the C-terminus alone was sufficient to mediate bacterial killing. The *vasX* truncation mutants consisting of residues 1-542 (N-terminal half) and 543-1085 (C-terminal half) were used to test whether the truncations could complement V52Δ*vasX* in a killing assay against *V. parahaemolyticus* prey. Expression of *vasX*(1-542) or *vasX*(543-1085) in V52Δ*vasX* did not restore the ability to kill *V. parahaemolyticus* (Figure 4-5). Thus, the C-terminal half of VasX is not sufficient to mediate the killing ability of VasX.

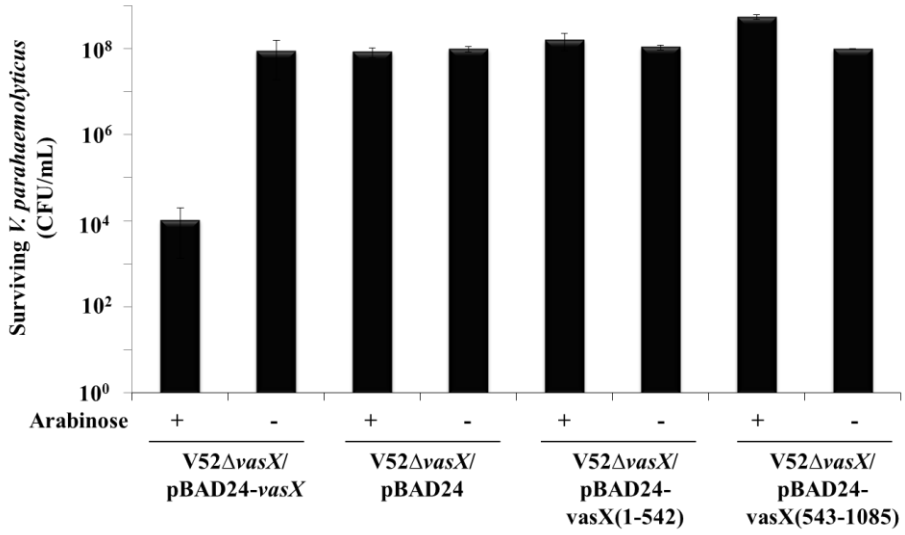

Figure 4-5. Truncated versions of VasX cannot complement the killing ability of V52Δ*vasX*. Surviving CFU/mL of *V. parahaemolyticus* prey were recovered following co-incubation with the strains listed on the *x*-axis. Arabinose was used to induce expression from the P_{BAD} promoter where indicated. Error bars indicate the standard deviation.

4.2.5 Targeting VasX to the Periplasm is Toxic

Voltage-dependent pore-forming colicins are not toxic to the producing cell because cytoplasmic localization of the protein does not allow for insertion into the inner membrane due to the orientation of the trans-membrane potential [432]. Previously it has been demonstrated that targeting a pore-forming colicin to the periplasm results in auto-toxicity [422]. When presented to the cell from the periplasmic face, colicins then can insert into the inner membrane and form a pore that dissipates the membrane potential [422, 432]. Given that VasX is found in the cytoplasm, but not the periplasm, of mid-logarithmic wild-type *V. cholerae* V52 (Figure 2-6 and [223]) we decided to test whether targeting VasX to the

periplasm would result in autotoxicity. First, as a proof-of-principle I tested whether episomal expression of *vasX* was toxic to C6706Δ*tsiV2*. C6706Δ*tsiV2* is susceptible to VasX-mediated killing because it lacks the gene encoding the VasX immunity protein, *tsiV2*. The role of TsiV2 will be discussed in detail in chapter 5. I performed a growth curve over 8 hours using C6706Δ*tsiV2* harboring pBAD24-vasX or the empty vector control and grew the strains under inducing and non-inducing conditions. At the 7 hour time point, a bacterial lysate sample was collected from each strain for western blot analysis. I observed that each strain grew equally well in the presence or absence of arabinose (Figure 4-6). Western blot analysis confirmed that VasX was indeed expressed where expected (Figure 4-6). This indicated that episomal expression of *vasX* was not toxic to C6706Δ*tsiV2*.

I then fused *vasX* the DNA sequence encoding the Sec signal peptide in the plasmid pBAD24 (pBAD24-LS::vasX) and was introduced into C6706Δ*tsiV2*. This strain (C6706Δ*tsiV2*/pBAD24-LS::vasX) was routinely grown in LB containing 0.2% glucose to prevent leaky expression from the P_{BAD} promoter in the case that LS::vasX was highly toxic to the producer cell. When C6706Δ*tsiV2*/pBAD24-LS::vasX was grown in the presence of 0.1% arabinose (no glucose), the bacteria increased in numbers up until the 2 hour time point, and then begin to die (Figure 4-6). The decrease in surviving CFU/mL plateaued when the cells reached their starting concentration. This phenotype was not observed in C6706Δ*tsiV2*/pBAD24-LS::vasX grown in the presence of 0.2% glucose (Figure 4-6). Furthermore, autotoxicity was not observed with the empty

vector control (LS) or C6706Δ*tsiV2* producing VasX lacking the Sec signal peptide (ie. non-periplasmic). An additional control for this experiment was C6706Δ*tsiV2* harboring pBAD24-LS::core. This plasmid results in production of the Sec signal peptide fused to the core of the VgrG-3 protein (lacking the peptidoglycan binding domain) and serves as a negative control demonstrating that in general, exporting proteins to the periplasm is not toxic to these cells (Figure 4-6). Thus, similar to colicins, targeting VasX to the periplasm is toxic to the producing cell.

A.

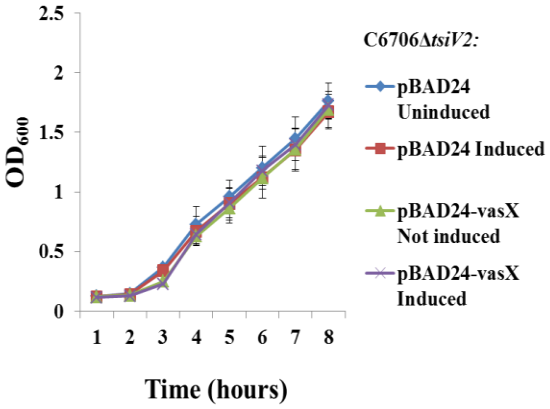

B.

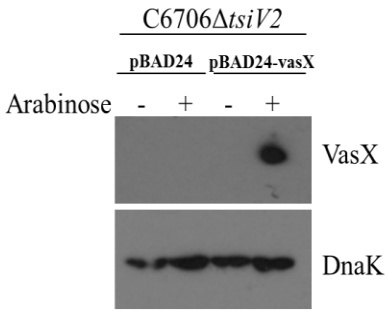

C.

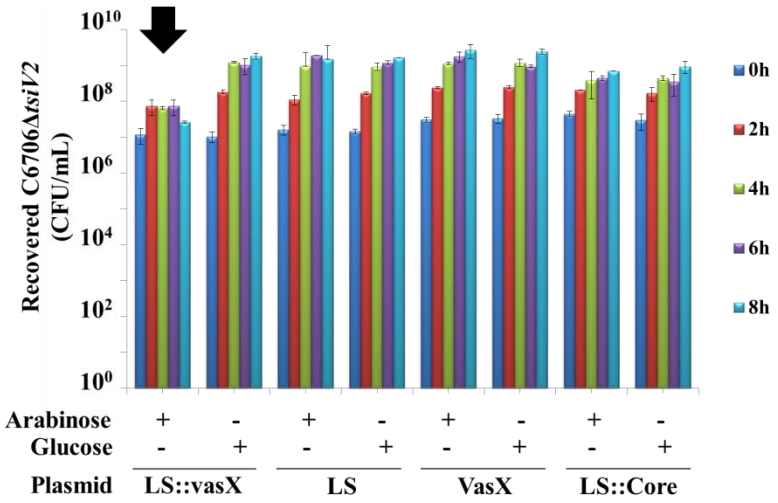

Figure 4-6. Production of LS::vasX, but not VasX, results in auto-toxicity. (A) Growth curve of C6706Δ*tsiV2* harboring pBAD24 (empty vector) or pBAD24-vasX. Arabinose was included where indicated (i.e. inducing conditions) to drive expression from the P_{BAD} promoter. OD_{600} readings were taken every hour. Error bars indicate the standard deviation. (B) A whole cell lysate sample from each strain in (A) was taken at the 7 hour time point and used for western blotting analysis with α-VasX and α-DnaK (loading control) antibodies. (C) Liquid cultures of C6706Δ*tsiV2* harboring the plasmids indicated were grown for 8 hours. Samples were harvested at 0, 2, 4, 6, and 8 hours and the recovered CFU/mL were enumerated. Arabinose and glucose were added where indicated for induction, and repression (respectively), of the P_{BAD} promoter. Error bars indicate the standard deviation.

4.2.6 SDS Sensitivity Assay

Knowing that periplasmic localization of VasX resulted in autotoxicity, I hypothesized that VasX disrupts the integrity of the inner membrane of target cells. Pore-forming colicins have been shown to insert into the inner membrane of target cells thereby compromising the integrity of the bacterial membrane and dissipating the membrane potential. To determine whether expression of LS::vasX compromised the inner membrane of the producing cell, I performed an SDS lysis assay [422]. Bacterial strains were grown under inducing conditions and then incubated in the presence or absence of SDS. Disruption of the bacterial inner membrane results in increased susceptibility to lysis in the presence of SDS [422] and I observed that expression of LS::vasX resulted in a significant increase in sensitivity of C6706Δ*tsiV2* toward SDS compared to the control strains (Figure 4-7). Therefore, production of VasX targeted to the periplasm results in disruption of the inner membrane of the producer cell.

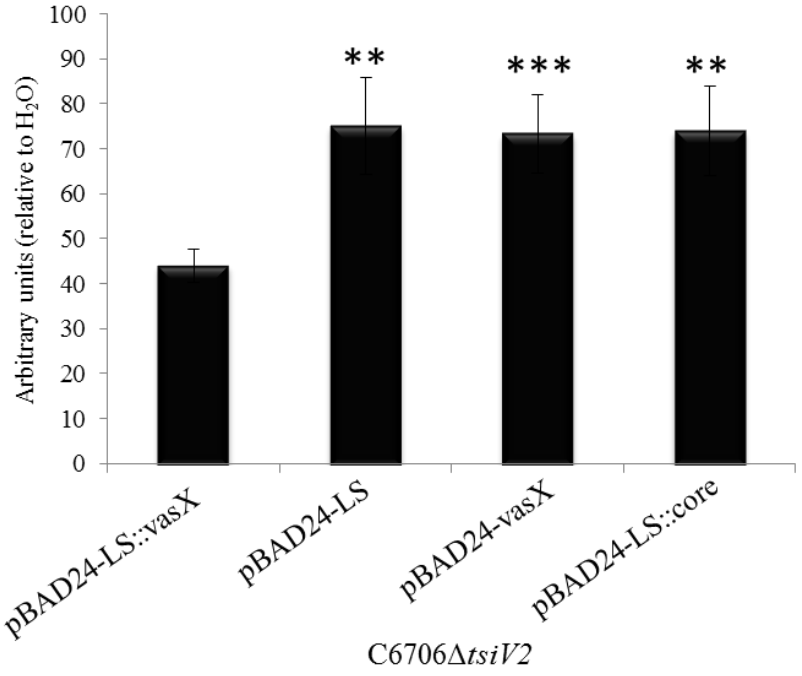

Figure 4-7. SDS sensitivity assay. Bacterial cultures of the strains indicated were grown under inducing conditions followed by the addition of SDS or water (diluent). Ratios were calculated based on OD_{600} readings for the SDS and H_2O samples and plotted. LS::vasX; *vasX* fused to a sequence encoding the Sec signal peptide. LS; empty vector, VasX; *vasX* lacking periplasmic signal sequence, LS::core; *vgrG-3* core sequence fused to a sequence encoding the Sec signal peptide. ***= $p < 0.001$, **= $p < 0.005$ relative to LS::vasX. *P*-values were calculated using the Student's one-tailed paired T-test. Error bars indicate the standard deviation.

4.2.7 VasX dissipates the membrane potential in target cells

Knowing that periplasmic VasX compromises the integrity of the inner membrane I subsequently hypothesized that this disruption of the inner membrane depleted the cell's membrane potential. To test this, I used the BacLight Bacterial Membrane Potential Kit (Molecular Probes). For this experiment, the fluorescent dye 3,3'-Diethyloxacarbocyanine, iodide ($DiOC_2(3)$) is used to stain all cells

green. If the cell is healthy and possesses a membrane potential, the dye accumulates within the cell and shifts towards red emission. Stained cells are analyzed by flow cytometry using Texas Red and FITC filters and the red/green ratio is indicative of the strength of the membrane potential in analyzed cells. The chemical carbonyl cyanide *m*-chlorophenyl hydrazone (CCCP), which uncouples the proton gradient, serves as a positive control for dissipation of membrane potential.

Upon analysis using flow cytometry, I observed that C6706Δ*tsiV2*/pBAD24-LS::vasX exhibited a lower red fluorescence compared to C6706Δ*tsiV2* expressing wild-type VasX (pBAD24-vasX), LS::core (pBAD24-LS::core), or the empty vector control (LS) (Figure 4-8). When CCCP was added to C6706Δ*tsiV2*/pBAD24-vasX, C6706Δ*tsiV2*/pBAD24-LS, or C6706Δ*tsiV2*/pBAD24-LS::core, the red fluorescence intensity decreased to levels comparable to C6706Δ*tsiV2*/pBAD24-LS::vasX (Figure 4-8). This implies that LS::vasX disrupts the membrane potential to the same extent as CCCP. From this data, the red/green ratios for all cells were calculated and plotted (Figure 4-8). According to these data, the membrane potential for cells expressing LS::vasX is significantly reduced compared to controls. Furthermore, LS::vasX uncouples the proton gradient to the same extent as the positive control CCCP. Taken together these data indicate that VasX, when targeted to the periplasm of the producer cell, compromises the integrity of the inner membrane and dissipates the membrane potential. We thus conclude that VasX is a bacterial toxin that targets the inner membrane of prey cells

A.

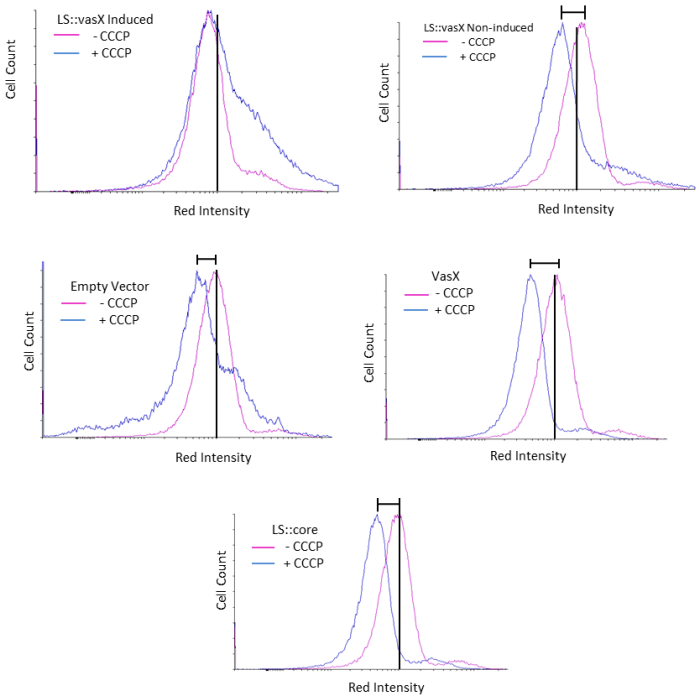

B.

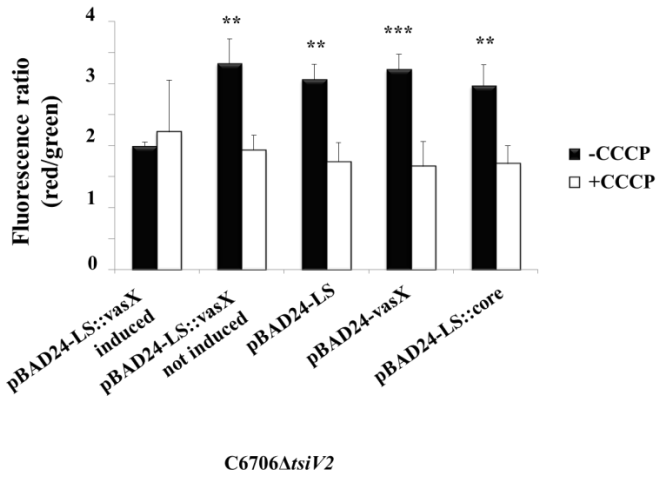

Figure 4-8. Periplasmic VasX dissipates the membrane potential of target cells. (A) VasX dissipates cell membrane potential. Overnight cultures of the strains indicated were were stained using the dye $DiOC_2(3)$ and analyzed by flow cytometry for a change in red emission. CCCP is a chemical that uncouples the proton gradient and was used as a positive control for dissipation of membrane potential in this experiment. (B) Quantification of flow cytometry data. Based on the data presented in (A), red/green fluorescence ratios were calculated for each condition and plotted. Error bars indicate standard deviation. ***= $p < 0.001$, **= $p < 0.005$ relative to LS::vasX (induced, -CCCP). *P*-values were calculated using the Student's one-tailed, paired T-test.

4.2.8 Periplasmic VasX does not result in cell lysis

Thus far, the data presented suggest that VasX targets the inner membrane of prey bacteria (Figures 4-7 and 4-8). However, it remained unclear whether disruption of the inner membrane resulted in lysis of the bacterium. To test whether VasX membrane disruption results in lysis of the cell I tested whether expression of *LS::vasX* resulted in contamination of culture supernatants with the cytoplasmic heat-shock protein DnaK [380]. C6706Δ*tsiV2* harboring pBAD24-LS::vasX, pBAD24-vasX, pBAD24-LS::core, or pBAD24-LS empty vector, were grown in the presence or absence of arabinose until mid-logarithmic phase. Culture supernatants were concentrated and subjected to SDS-PAGE followed by western blotting with α-DnaK antibody. The whole cell lysate of C6706Δ*tsiV2*/pBAD24-LS::VasX was included on the gels as a positive control for the DnaK western blot. DnaK was not present in any of the supernatant samples tested but was present in the whole cell lysate (Figure 4-9). This indicates that expression of LS::VasX does not result in lysis of the producing bacterium.

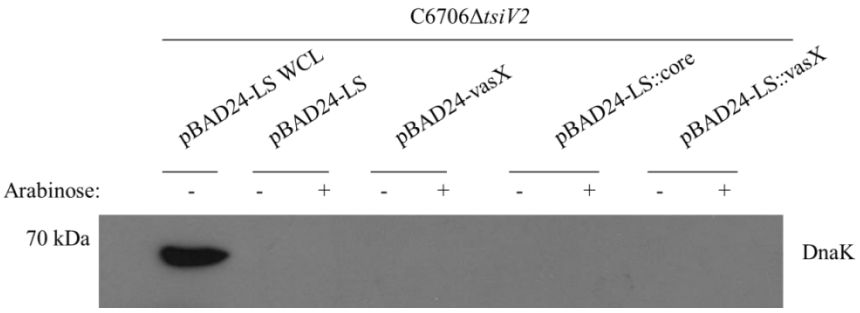

Figure 4-9. Expression of LS::vasX in C6706Δ*tsiV2* does not cause cell lysis. Pellet and supernatant samples were harvest from mid-logarithmic cultures of the indicated strains. Samples were subjected to SDS-PAGE followed by western blotting with α-DnaK primary antibody. WCL; whole cell lysate positive control.

4.2.9 Cells expressing periplasmic VasX are permeable to propidium iodide

Propidium iodide (PI) is an intercalating agent bound to a fluorescent molecule that binds DNA. Normally, PI is used to assess bacterial cell viability because it is membrane impermeant and does not penetrate healthy cells. However, in the case of dead cells, or those with damaged membranes, PI enters the cell and binds DNA. In previous sections I provided evidence that VasX disrupts the bacterial inner membrane (Figure 4-7 and 4-8) but does not result in cell lysis (Figure 4-9). Based on these data I propose that VasX permeabilizes the inner membrane in a manner that does not result in cell lysis. I hypothesized that cells expressing LS::VasX would be permeable to PI because they have damaged membranes. C6706Δ*tsiV2* harboring pBAD24-LS::vasX or pBAD24-vasX were grown in liquid culture until mid-logarithmic phase and then incubated with PI. As a positive control for PI uptake, both strains were killed by incubation in ethanol following incubation with PI. Cells were analyzed by flow cytometry to

assess the permeability of these cells on a population level. I observed that cells producing LS::vasX had ~30% greater uptake of PI compared to those producing VasX (Figure 4-10).

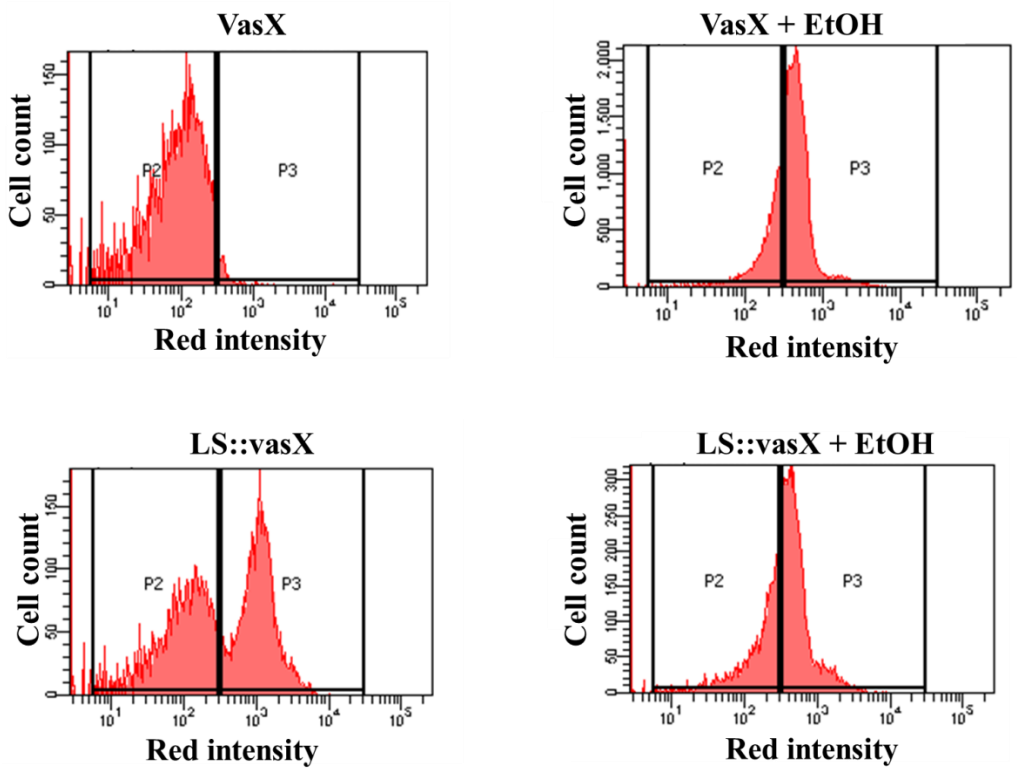

Figure 4-10. Cells producing LS::vasX become permeable to PI. C6706Δ*tsiV2* harboring pBAD24-vasX (VasX) or pBAD24-LS::vasX (LS::vasX) was grown in the presence of arabinose to induce expression from the P_{BAD} promoter and stained with PI. Cells were analyzed by flow cytometry to determine the percentage of cells that became permeable to PI as a result of membrane damage. Ethanol-killed cells (VasX + EtOH and LS::vasX + EtOH) were used as a positive control for PI permeability. The P2 population represents cells with intact membranes whereas the P3 population indicates cells that are permeable to PI.

4.2.10 Recombinant VasX causes leakage of carboxyfluorescein from lipid vesicles

My data thus far indicate that when VasX is targeted to the periplasm of the producing cell, these cells are more susceptible to lysis by SDS and their membrane potential is disrupted. Furthermore, the cells do not lyse but are permeable to PI. To further confirm our hypothesis that VasX is a membrane-disrupting protein, we tested whether purified, recombinant VasX could disrupt unilammelar vesicles composed of *E. coli* polar lipids. Large unilammelar vesicles (LUVs) encapsulating carboxyfluorescein (CF) were purchased from Avanti Polar Lipids. At high concentrations (such as inside LUVs), the fluorescence of CF is self-quenching; however, leakage of CF into the solvent upon LUV disruption results in an increase in fluorescence.

VasX, buffer alone, BSA, Triton X-100, or purified, recombinant TsiV3 (VgrG-3 immunity protein) were added to CF-encapsulating LUVs (CF-LUVs) and the relative fluorescence units (RFUs) were measured. LUV disruption by 0.1% triton X-100 was used as a control for maximal fluorescence. We observed that addition of VasX to CF-LUVs resulted in a significant increase in fluorescence compared to buffer alone, or addition of BSA, or purified, recombinant TsiV3 (negative controls) (Figure 4-11). TsiV3 is predicted to act in the periplasm to protect against peptidoglycan degradation and therefore, was not expected to perturb LUVs. These data indicate that VasX is able to disrupt LUVs to the extent that the encapsulated CF was released into the external environment.

This lends credence to our hypothesis that VasX acts similar to pore-forming colicins that target the inner membrane of their prey bacteria.

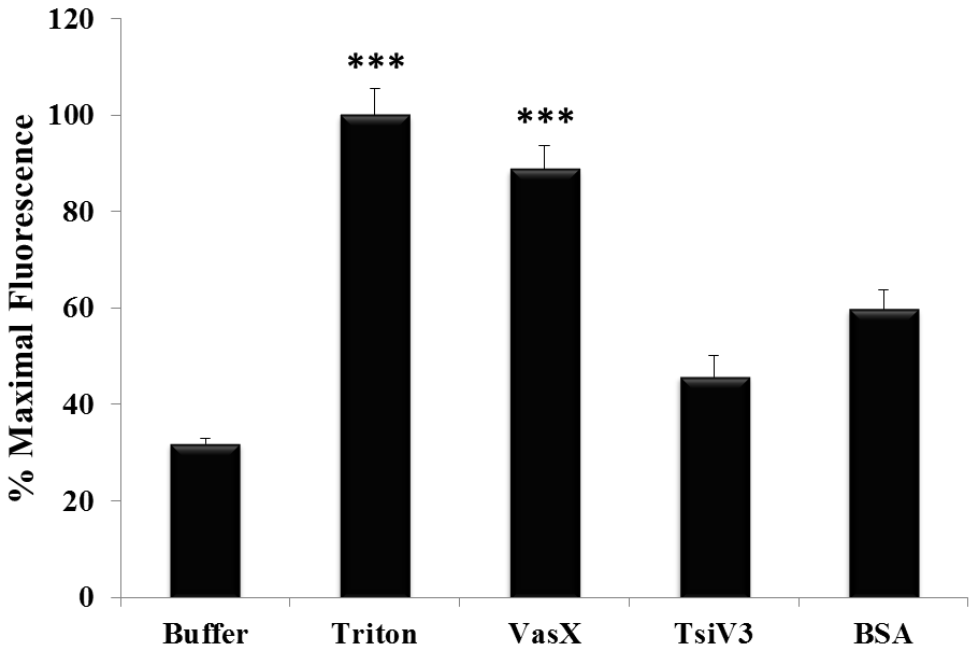

Figure 4-11. VasX disrupts large unilamellar vesicles resulting in the release of carboxyfluorescein. The substrates listed on the *x*-axis were mixed with CF-encapsulating LUVs followed by measurement of the fluorescence intensity. The detergent Triton X-100 is a positive control for LUV disruption and this sample was used as the value for maximal fluorescence. Buffer alone, purified, recombinant TsiV3, and BSA constitute negative controls. Error bars indicate the standard deviation. *** denotes $p < 0.001$ relative to BSA control.

4.2.11 Addition of purified, recombinant VasX and TseL to *E. coli* does not result in cell lysis.

Russell *et al*. recently determined that the phospholipase Tle5 produced by *P. aeruginosa* causes a shift in target cell membrane phospholipid composition [332]. Specifically, an increase in PA and a decrease in PE was observed upon exposure to Tle5 [332]. Using two different methodologies, I observed that VasX

binds phosphatidic acid (Figures 3-7 and 3-8). Although I do not question that VasX and TseL (the *V. cholerae* lipase) can function as independent toxins, I entertained the hypothesis that TseL-mediated concentration of phosphatidic acid in the *V. cholerae* membrane can increase the efficiency of VasX insertion into the inner membrane. To test this, I added purified, recombinant VasX and/or TseL to *E. coli* cells in the presence and absence of polymyxin B to permeabilize the *E. coli* outer membrane. The OD_{600} at t=0 and t=5 minutes was used to calculate the percent lysis. This technique was previously used to determine that the peptidoglycan-binding domain (PBD) of VgrG-3 caused cell lysis (via peptidoglycan degradation) [210].

I observed ~20% lysis in the presence of polymyxin B alone which was also observed by Brooks *et al.* [210] . Unexpectedly, addition of VasX and TseL individually or in combination +/- polymyxin B did not result in a greater amount of lysis compared to polymyxin B alone (Figure 4-12). It is thus not possible to determine whether TseL exacerbates the effects of VasX.

As mentioned previously, VgrG-3 causes lysis of *E. coli* via peptidoglycan degradation [210, 221]. I hypothesized that TseL and VasX did not cause lysis of *E. coli* because they could not cross the cell wall and that, at least in this experimental set-up, that VgrG-3 is required to degrade peptidoglycan prior to TseL and VasX reaching their cellular target – the inner membrane. To test this I added purified, recombinant VasX and/or TseL and/or PBD in the presence or absence of polymyxin B. I observed that in the presence of polymyxin B, PBD caused ~35% lysis and the same amount of lysis was observed when polymyxin

B, VasX, TseL, and PBD were added together (Figure 4-12). This indicates that PBD is capable of lysing *E. coli* when the outer membrane is permeabilized; however, addition of the other two toxins, VasX and TseL, does not result in increased lysis. Therefore, it appears that VasX and TseL are incapable of exerting their toxic effects when added exogenously.

A.

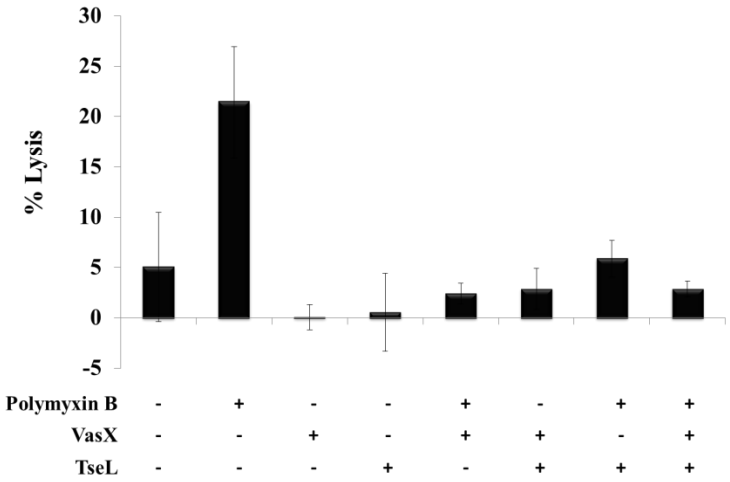

B.

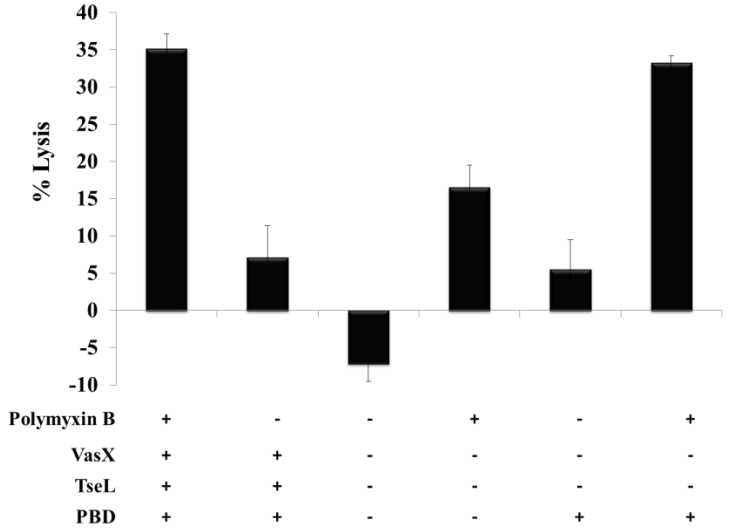

Figure 4-12. Addition of purified, recombinant VasX and TseL to *E. coli* does not result in cell lysis. (A) VasX and TseL were incubated with *E. coli* in the presence or absence of polymyxin B to permeabilize the outer membrane. The percent lysis was determined by measuring the OD_{600} at t=0 and t=5 minutes. (B) VasX, TseL, and PBD were incubated with *E. coli* in the presence or absence of polymyxin B. The percent lysis was calculated and plotted. Error bars for both (A) and (B) indicate the standard deviation. PBD; peptidoglycan-binding domain of VgrG-3.

4.3 **Discussion**

The data presented in this chapter indicate that VasX not only has a role in T6SS-mediated virulence toward *D. discoideum* but is used to kill bacteria as well. We previously showed that *V. cholerae* V52 uses its T6SS to kill *E. coli* [211]; however, in-frame deletion of *vasX* did not alter the ability of V52 to kill *E. coli* (Figure 4-1). A similar conclusion was reached by Dong *et al.* such that VasX is sufficient but not required for V52 to kill *E. coli* [221]. Because V52 encodes two other bacterial toxins (VgrG-3 and TseL), we created V52Δ*vgrG-3*Δ*tseL* in which VasX is presumably the only functional T6SS bacterial toxin. Using this strain as the predator in a killing assay against *E. coli* showed that V52Δ*vgrG-3*Δ*tseL* was still able to reduce the number of surviving *E. coli* by ~ 10-fold. This implies that VasX alone is sufficient to kill *E. coli* but the killing phenotype is drastically increased in the presence of VgrG-3 and TseL. Furthermore, because V52Δ*vasX* kills *E. coli* to the same extent as wild-type V52, the presence of TseL and VgrG-3 can compensate for the absence of *vasX* and together are highly toxic to prey bacteria (Figure 4-1).

Interestingly, when other *Vibrio* species such as *V. parahaemolyticus*, *V. fischeri*, and *V. alginolyticus* were used as prey, VasX has a much stronger phenotype (Figure 4-3). However, V52Δ*vasX* is not completely attenuated like the T6SS-null mutant V52Δ*vasK* and this discrepancy is attributed to the activity of VgrG-3 and/or TseL (Figure 4-4). In this case, VasX was a more effective toxin against *V. parahaemolyticus* and C6706, but less effective for killing *E. coli*. The specific reason behind this phenomenon remains to be determined, but could

be due to a number of factors including the requirement for specific receptors on target cells, varying degrees of susceptibility to T6SS effectors, the presence/absence of T6SS immunity proteins, or a combination of these factors.

Figure 4-2 indicated that deleting certain combinations of T6SS toxin-encoding genes results in a lowered ability to secrete Hcp (V52Δ*vasX*Δ*tseL* or V52Δ*tseL*Δ*vgrG-3*), or a complete lack thereof (V52Δ*vasX*Δ*vgrG-3*, or V52Δ*vasX*Δ*vgrG-3*Δ*tseL*). It appears that these toxins are required for the production of a functional secretion complex and when all three toxins are missing, ejection of the Hcp tube does not occur. This type of "checkpoint" system has also been described for the ordered assembly of the bacterial flagella [433] and may have a role in the translocation of T3SS effector proteins [434]. Therefore, VasX, VgrG-3, and TseL serve as T6SS toxins but also have a structural role in T6SS ejection.

Previously, VasX was reported to have homology to colicins (Figure 2-5 and [355]): secreted proteins that are toxic against closely-related bacterial species [230]. The mechanism of colicin killing can range from nuclease activity, to inhibition of murein synthesis, to pore-formation in the target cell inner membrane resulting in dissipation of membrane potential [241-252]. In some cases, colicin insertion into the membrane results in formation of a LPCx [425]. Although the C-terminus of VasX contains the colicin-like region and is capable of forming a LPCx, it is not sufficient for bacterial killing (Figure 4-5). This implies that the N-terminus of VasX plays a crucial role in VasX-mediated toxicity. The N-terminal half of the protein could be required for secretion of

VasX, interactions with structural T6SS proteins, or tethering VasX to the target cell membrane. Of note, multiple attempts to determine if any of the VasX truncation mutants were secreted failed to produce consistent results.

The mechanism by which colicins are delivered likely differs from delivery of T6SS toxins into target cells. T6SS-dependent bacterial killing is a contact-dependent phenotype [211], whereas colicins themselves possess sophisticated, cell contact-independent, mechanisms to gain entry into target cells [269, 435-437]. Indeed, exogenously added VasX and TseL were unable elicit toxic activity toward *E. coli* and the PBD requires permeabilization of the *E. coli* outer membrane to cause significant bacterial lysis (Figure 4-12). Chou *et al*. also suggested that in order to effectively intoxicate target bacteria, the toxins require delivery by the T6SS secretory apparatus to reach an effective concentration at their cellular target [390]. Thus, I propose that in order to kill other bacteria, the *V. cholerae* T6SS toxins must be injected into the target cell.

Cytoplasmic production of pore-forming colicins does not result in toxicity because pore-formation can only occur when the colicin is presented to the cell from the periplasmic face [231, 422, 432]. This is presumed to be due to the orientation of the transmembrane potential [231, 432]. We observed that episomal expression of VasX (lacking the Sec leader sequence) was not toxic to V52 (Figure 3-1) or C6706Δ*tsiV2* (Figure 4-6) implying that production of this protein does not kill the producing cell. Therefore, we designed a system whereby VasX is targeted to the periplasm of the producing cell by fusing VasX to a Sec signal peptide (LS::vasX). Production of LS::vasX in C6706Δ*tsiV2* was

toxic to the producing cells but did not cause complete cellular lysis (Figures 4-6 and 4-9). LS::vasX production imparted a disruption in the inner membrane as indicated by the results of the SDS assay, membrane potential analysis, CF release from LUVs, and permeability to PI (Figures 4-6, 4-7, 4-8, 4-10, and 4-11). That cells producing LS::vasX become permeable to PI but do not release DnaK implies that LS::vasX forms pores in the inner membrane large enough to permit influx of PI (~0.7 kDa) but small enough to prevent efflux of DnaK (~70 kDa). Taken together, these data suggest that VasX forms pores in the inner membrane of target cells capable of dissipating the membrane potential and halting cellular respiration. Further to this, my subcellular fractionation data presented in Chapter 2 demonstrated that VasX is a secreted protein that is present in the cytoplasm, and membrane fractions of V52; however, VasX is not present (to detectable levels) in the periplasmic fraction (Figure 2-6). It appears that VasX either by-passes the periplasm, or is present transiently in small quantities *en-route* out of the cell, as its presence in the periplasm could be auto-toxic.

Because T6SS-mediated bacterial killing is a contact-dependent phenotype [211], I propose a model where VasX is injected into the periplasm of target cells along with T6SS structural proteins and other putative toxins. From there, VasX can insert into the inner membrane and disrupt the target cell's membrane potential. Importantly, both prokaryotes and eukaryotes possess a cytoplasmic membrane and I postulate that this commonality is the reason behind the promiscuity of VasX killing. In the case of *D. discoideum*, I propose that pore-formation in the cytoplasmic membrane is responsible for the VasX-mediated

phenotype observed with this eukaryotic host. Targeting the membrane (or peptidoglycan) as opposed to a single protein/receptor is an evolutionarily advantageous mechanism employed by bacterial toxins since developing resistance to this toxic mechanism would prove challenging for target cells. A model for VasX function as a prokaryotic toxin is presented in Figure 4-13.

A.

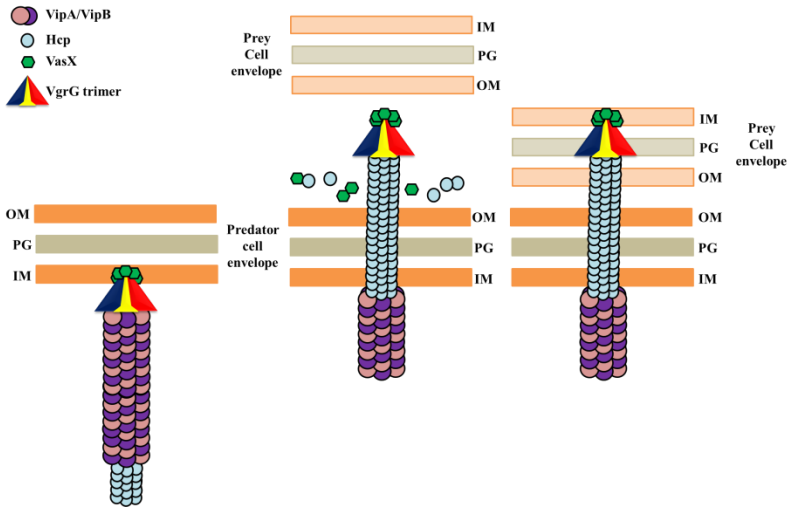

B.

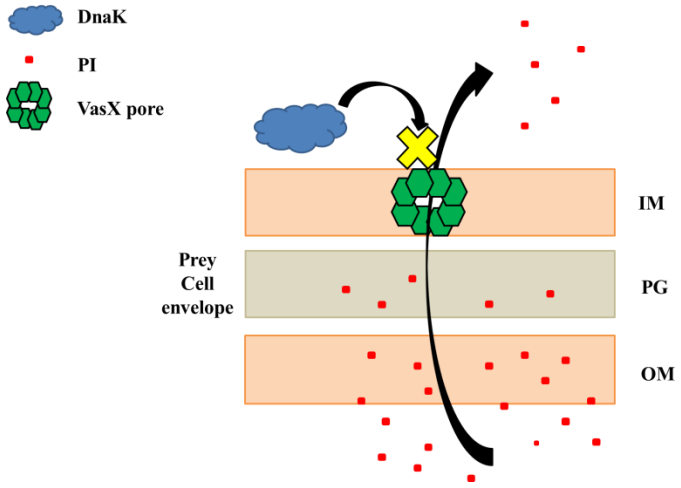

Figure 4-13. Model of VasX-mediated toxicity toward Gram-negative bacteria. (A) VasX accumulates in the inner membrane of the predator cell as a LPCx and associates with VgrG proteins ate the tip of the secretory apparatus (left panel). The T6SS needle is ejected from the predator cell where proteins are sloughed into the extracellular milieu (centre panel). The injectosome punctures the prey/target cell delivering VasX (and other T6SS toxins) to its cellular target, the inner membrane. (B). The VasX LPCx forms a pore in the prey cell inner membrane that is permeable to PI but does not allow passage of large molecules such as the cytoplasmic protein DnaK. Perturbation of the inner membrane by VasX pores leads to dissipation of the membrane potential and ultimately death of the target cell.

CHAPTER 5

TsiV2 is the VasX immunity protein

The experiments described in Figure 5-6 and 5-14B were conducted by Daniel Unterweger.

The data presented in Figure 5-21, and purified, recombinant VasX::6xHis and TsiV2::6xHis were provided by Teresa Brooks.

Figure 5-14A was provided by Dr. Karlene Lynch.

5. TsiV2 is the VasX immunity protein

5.1 Introduction

Bacteria that produce toxins targeted toward other closely related species must have a means to protect themselves from self-intoxication or being killed by neighboring sister cells. Immunity is mediated by the presence of anti-toxins or immunity proteins that counteract the function of their cognate toxins [210, 215, 216, 221, 246, 278, 279, 293, 298-300, 305, 307, 312, 315, 423, 432, 438, 439]. Genes encoding immunity proteins are typically located immediately downstream from (or even overlapping with) the stop codon of the toxin gene [241, 256, 258, 283, 289-292] and are subject to a unique regulatory mechanism.

Constitutive, low-level expression of immunity protein-encoding genes is important for bacteriocin-producing cells to protect against autotoxicity [285]. Commonly, transcription of the immunity protein-encoding gene is dually regulated with one promoter located upstream of the operon containing the toxin and immunity protein-encoding gene (polycistronic) and another promoter encoded within the toxin gene that strictly regulates expression the immunity gene (monocistronic) [278, 282, 285, 293-297].

In the case of pore-forming colicins, immunity proteins localize to the inner membrane where they counteract the toxic effects of the incoming colicin molecule. It is speculated that immunity proteins for pore-forming colicins either block pore-formation from occurring, or plug the ion channel created by the colicin, thereby preventing cell death [231, 423, 432].

As mentioned in Chapter 4, we and others identified three putative toxin/immunity systems used by *V. cholerae* to kill other bacteria (Miyata et al., submitted and [374]). In-frame deletion of *tsiV1, tsiV2*, or *tsiV3* in *V. cholerae* C6706 rendered this T6SS-silent strain susceptible to killing by V52 (Miyata *et al.*, submitted and [221]. We also demonstrated that TsiV3 specifically inhibits the peptidoglycan degrading ability of VgrG-3 [210]. Given that VasX is a bacterial toxin and *tsiV2* is encoded directly downstream of *vasX*, I hypothesized that VasX and TsiV2 are a toxin/immunity pair. The following experiments were aimed at characterizing TsiV2 as the VasX immunity protein.

5.2 **Results**

5.2.1 TsiV2 is the VasX immunity protein

Encoded directly downstream of *vasX* on the V52 chromosome is the gene VCA0021 which was named type six secretion immunity gene in *Vibrio* 2 (*tsiV2*) [221]. Given that colicins are genetically organized with the immunity gene directly downstream from the colicin gene, we hypothesized that *tsiV2* encodes the VasX immunity protein. To test this, we took advantage of the *V. cholerae* strain C6706 which possesses a full complement of T6SS genes and is immune to killing by V52 [211]. Importantly, C6706 does not activate its T6SS under standard laboratory conditions [365, 370, 375] which made it possible to create in *in-frame tsiV2* deletion mutant (C6706Δ*tsiV2*) without C6706 engaging in sororicide. When challenged against V52 in a killing assay, C6706Δ*tsiV2* was

killed by V52 but not by V52Δ*vasK* or V52Δ*vasX* (Figure 5-1). This data suggests that TsiV2 is required for C6706 immunity to V52, and that VasX is involved in this killing phenotype.

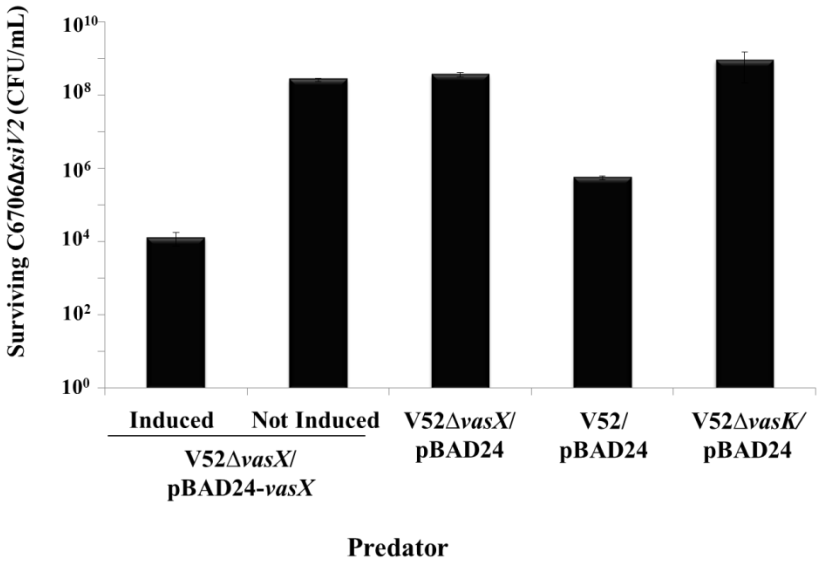

Figure 5-1. TsiV2 is the VasX immunity protein. Predator bacteria (listed on the *x*-axis) were mixed with C6706Δ*tsiV2* and surviving rifampicin-resistant prey bacteria were enumerated. Arabinose was included to induce expression from the P_{BAD} promoter (inducing conditions) where indicated. Error bars indicate the standard deviation.

5.2.2 Complementation of C6706Δ*tsiV2*

For complementation, *tsiV2* was cloned downstream of an arabinose-inducible promoter in the vector pBAD24 with a C-terminal FLAG tag (pBAD24-tsiV2::FLAG) and transformed into C6706Δ*tsiV2*. This strain, C6706Δ*tsiV2*/pBAD24-*tsiV2::*FLAG was used as prey in a killing assay with V52

predator on plain LB plates, or LB plates containing arabinose (to induce expression from the P_{BAD} promoter) or glucose. Addition of glucose is known to tightly repress expression from the P_{BAD} promoter [399, 440]. I observed that C6706Δ*tsiV2*/pBAD24-tsiV2::FLAG was protected from killing by V52 regardless of the presence of arabinose or glucose (Figure 5-2). As expected, wild-type C6706 remained immune, and the empty vector control remained sensitive to killing under all three conditions (Figure 5-2). Furthermore, the T6SS-null predator strain, V52Δ*vasK*, did not kill any of the C6706Δ*tsiV2* prey strains tested (Figure 5-2). I also noted that under inducing conditions, the number of surviving C6706Δ*tsiV2*/pBAD24-tsiV2::FLAG was less than the same strain exposed to non-inducing conditions (indicated by the arrows in Figure 5-2).

Because I observed protection mediated by pBAD24-tsiV2::FLAG under all three conditions tested, I performed a western blot using cell lysates from killing spots consisting of V52Δ*vasK* predator and C6706Δ*tsiV2*/pBAD4-tsiV2::FLAG prey from the three different agar plates tested. Here, I wanted to determine whether expression of TsiV2::FLAG was only detectable in the presence of arabinose. As shown in Figure 5-2, TsiV2::FLAG was only detected in cells incubated on LB plates containing arabinose. DnaK was used as a loading control and was present in each of the samples tested implying that bacteria were present in each sample. Therefore, even by repressing transcription from the P_{BAD} promoter (i.e. in the presence of glucose) pBAD24-tsiV2::FLAG was protective against killing by V52. Taken together, these data indicate that although we can complement C6706Δ*tsiV2* immunity by providing *tsiV2 in-trans*, expression of

the gene encoding the immunity protein is slightly toxic to the producer cell and very small amounts of TsiV2 are sufficient to be protective. It is also possible that the protective mechanism of *tsiV2* could be DNA-, and not protein-mediated.

A.

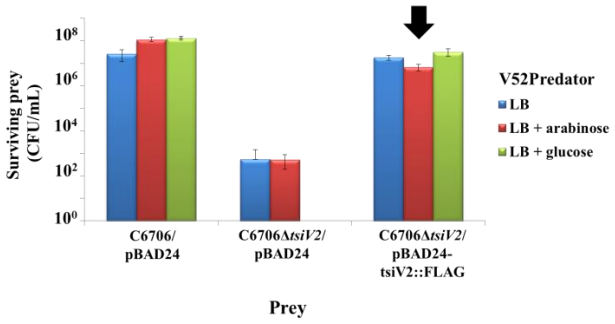

B.

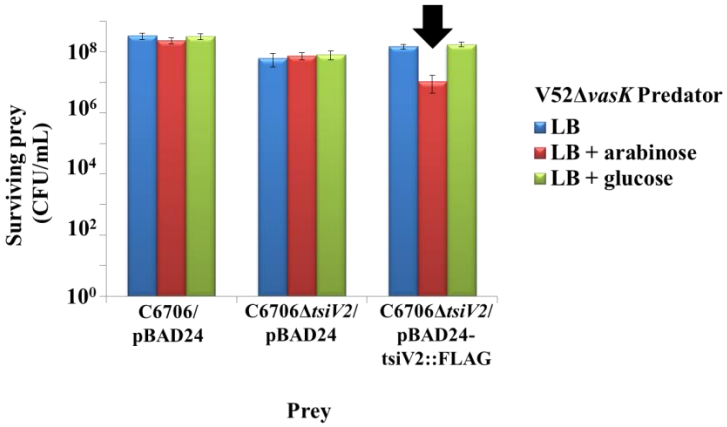

C.

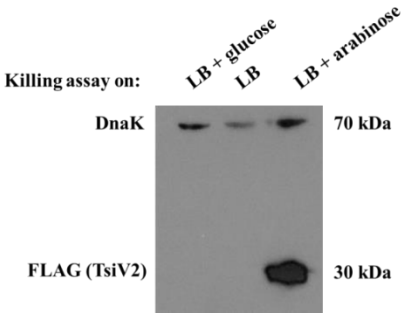

Figure 5-2. Episomal expression of *tsiV2* restores immunity to C6706Δ*tsiV2*. Surviving prey bacteria listed on the *x*-axis were recovered following co-incubation with the predator strain V52 (A) or V52Δ*vasK* (B). Arabinose or glucose was used to induce or repress expression from the P_{BAD} promoter, respectively, where indicated. Error bars indicate the standard deviation. (C) Bacterial lysate samples were harvested from killing spots in (B) and used for western blotting with FLAG and DnaK (loading control) antibodies. Molecular weights are indicated to the right of the blot.

5.2.3 Low amounts of TsiV2 provide protection against VasX

To investigate whether the protective phenotype of *tsiV2* could be DNA-mediated, I took advantage of two plasmids I had previously constructed. The gene *tsiV2* was cloned into pJET1.2/blunt (Thermo Fisher) which contains a T7 promoter that is not active in *V. cholerae* [441]. The first vector consisted of full-length *tsiV2* fused to a C-terminal FLAG tag (pJET-tsiV2::FLAG) and the second construct was *tsiV2* lacking a start codon fused to a C-terminal 6xHis tag (pJET-tsiV2(ΔATG)::6xHis).

pJET1.2/blunt is a blunt-ended vector and therefore blunt PCR products can be ligated into pJET1.2/blunt in a forward or reverse orientation. Restriction analysis and sequencing of pJET-tsiV2::FLAG and pJET-tsiV2(ΔATG)::6xHis indicated that both *tsiV2::FLAG* and *tsiV2(ΔATG)::6xHis* were in the reverse orientation relative to the T7 promoter. Therefore, not only should the T7 promoter be silent in *V. cholerae*, but the genes were cloned in the reverse orientation. Both of these plasmids were transformed into C6706Δ*tsiV2* and I hypothesized that neither vector would be protective when this strain was challenged with V52 predator.

I performed killing assays using V52 or V52Δ*vasK* predator and C6706Δ*tsiV2* harboring pBAD24 (empty vector), pBAD24-tsiV2::FLAG, pJET-tsiV2::FLAG, or pJET-tsiV2(ΔATG)::6xHis as prey. As I observed previously, pBAD24 alone was not protective for C6706Δ*tsiV2* whereas pBAD24-tsiV2::FLAG was protective (Figure 5-2 and 5-3). Interestingly, pJET-tsiV2::FLAG was also able to protect C6706Δ*tsiV2* from V52 whereas pJET-tsiV2(ΔATG)::6xHis was not protective against V52 (Figure 5-3). Therefore,

even when cloned in the reverse orientation downstream of a T7 promoter, *tsiV2* can mediate protection for C6706Δ*tsiV2* and protection does not occur when the gene lacks a start codon. This implies that TsiV2 protection is protein-mediated at low expression levels.

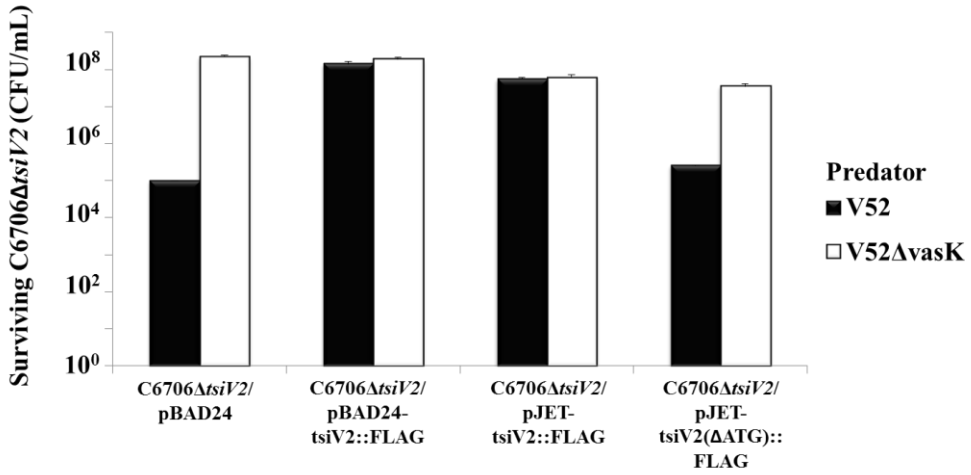

Figure 5-3. pJET-tsiV2::FLAG protects C6706Δ*tsiV2* from killing by V52. Survival of rifampicin-resistant prey (listed on the *x*-axis) was determined by enumerating the CFU following exposure to the indicated rifampicin-sensitive predator (legend). Error bars indicate the standard deviation.

To further confirm the results in Figure 5-3, we performed site-directed mutagenesis on *tsiV2* to change residues 14, 127, and 164 of TsiV2 to stop codons. The plasmid pBAD24-tsiV2::FLAG was used as the backbone for mutagenesis creating plasmids pBAD24-tsiV2::FLAG*14, pBAD24-

*tsiV2::*FLAG*127, and pBAD24-*tsiV2::*FLAG*164. These plasmids were transformed into C6706Δ*tsiV2* and were challenged in a killing assay with V52 or V52Δ*vasK* predator. While all strains exposed to V52Δ*vasK* survived as expected, all *tsiV2* site-directed mutants lost their immunity to V52 (Figure 5-4). Thus, immunity provided by *tsiV2* is not DNA-mediated and we therefore conclude that *tsiV2* must be translated into a (full length) protein to provide immunity to V52 killing.

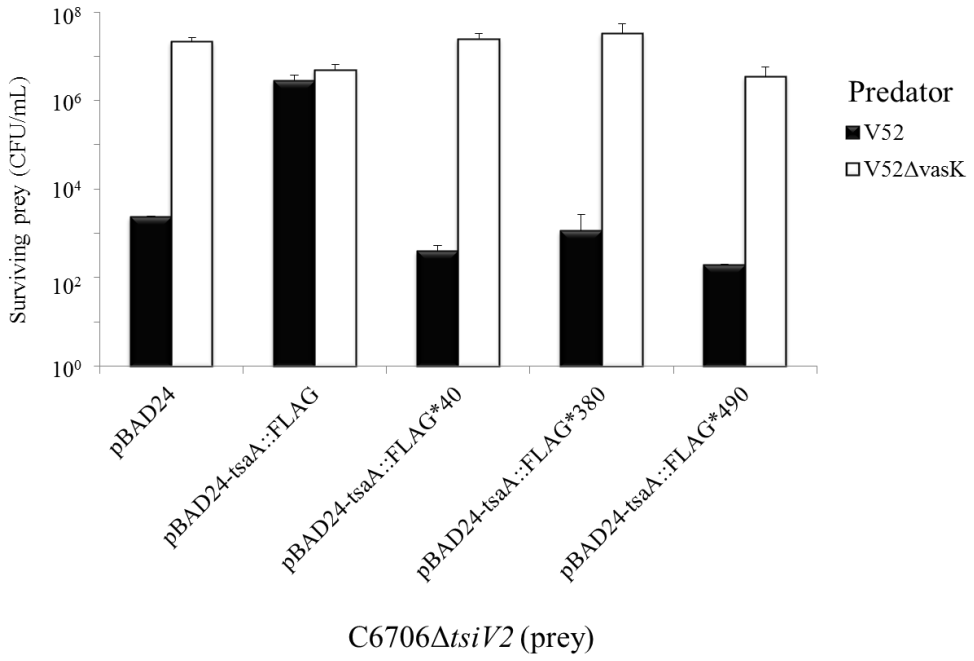

Figure 5-4. Site-directed mutants of *tsiV2* fail to protect C6706Δ*tsiV2* when challenged with V52. Survival of rifampicin-resistant prey (listed on the *x*-axis) was determined by enumerating CFU/mL following exposure to the indicated rifampicin-sensitive predator (legend). Error bars indicate the standard deviation.

5.2.4 Over-expression of TsiV2 is toxic

I noted in Figure 5-2 that expression of TsiV2::FLAG in C6706Δ*tsiV2* resulted in less CFU/mL recovered compared to the same strain grown in the absence of arabinose or the presence of glucose. I hypothesized this is because

over-expression of *tsiV2* is toxic to the producer cell. I performed a time course to determine the CFU/mL of C6706Δ*tsiV2*/pBAD24 (empty vector) and C6706Δ*tsiV2*/pBAD24-tsiV2::FLAG grown in the presence of arabinose over an 8-hour period. I observed that both strains grew until three hours post sub-inoculation; however, the recoverable CFU/mL steadily decreased thereafter for cells expressing TsiV2::FLAG eventually reaching a similar concentration to that of the starting inoculation (Figure 5-5). C6706Δ*tsiV2* harboring pBAD24 empty vector did not endure this decrease in surviving CFU/mL (Figure 5-5). Therefore, over-expression of TsiV2::FLAG is toxic to C6706Δ*tsiV2*.

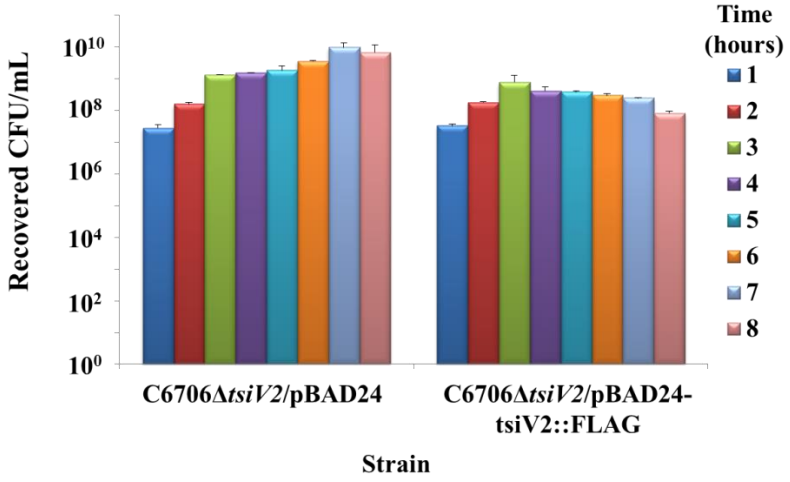

Figure 5-5. Over-expression of TsiV2::FLAG is toxic. Liquid bacterial cultures of the strains indicated on the *x*-axis were used to perform a growth curve. Samples were taken at t=0 and every hour thereafter and the recovered CFU/mL were enumerated. Error bars indicate the standard deviation.

5.2.5 TsiV2 is protective in *V. parahaemolyticus* but not *E. coli*

In Figures 4-1 and 4-3, I showed that VasX is important for V52 to kill *E. coli* (when V52 lacks *tseL* and *vgrG-3*) and other *Vibrio* species including *V. parahaemolyticus*. *E. coli* MG1655 does not encode a T6SS gene cluster;

however, *V. parahaemolyticus* encodes two T6SS gene clusters [431, 442], yet is susceptible to killing by V52. Given that TsiV2 is the VasX immunity protein, I wanted to determine whether episomal expression of *tsiV2* in both *E. coli* and *V. parahaemolyticus* would provide protection against V52 killing.

First, pBAD24-tsiV2::FLAG was transformed into *E. coli* MG1655 and this strain (MG1655/pBAD24-tsiV2::FLAG) was used as prey in a killing assay with V52 or V52Δ*vasK* predator. I observed that episomal expression of *tsiV2* in MG1655 was not protective against V52 (Figure 5-6). As expected, the T6SS-null predator strain V52Δ*vasK* was unable to kill MG1655. Since V52Δ*vasX* is able to kill MG1655 to the same extent as wild-type V52 (Figure 4-1), we then decided to test whether episomal expression of *tsiV2* could protect MG1655 challenged with V52Δ*tseL*Δ*vgrG-3* predator with VasX as the only bacterial T6SS toxin. Again, we observed that production of TsiV2 in MG1655 could not provide immunity even when VasX was the only toxin utilized by V52Δ*tseL*Δ*vgrG-3* (Figure 5-6).

To ensure that *tsiV2::FLAG* was expressed in this assay (and still failed to provide protection), a sample of the bacterial mixture of V52Δ*vasK* and MG1655/pBAD24-tsiV2::FLAG and the empty vector control were taken following the 4-hour incubation with or without arabinose. This particular sample was chosen because it was the only bacterial combination that did not result in *E. coli* being killed. Samples were boiled in protein sample buffer and subjected to SDS-PAGE followed by western blotting with DnaK (loading control) and FLAG primary antibodies. I observed a FLAG-reactive band only in the sample MG1655/pBAD24-tsiV2::FLAG in the presence of arabinose (Figure 5-6). No

FLAG-reactive band was present in the absence of arabinose, or for either condition for the empty vector control (Figure 5-6). This indicates that TsiV2::FLAG was produced under the conditions tested.

A.

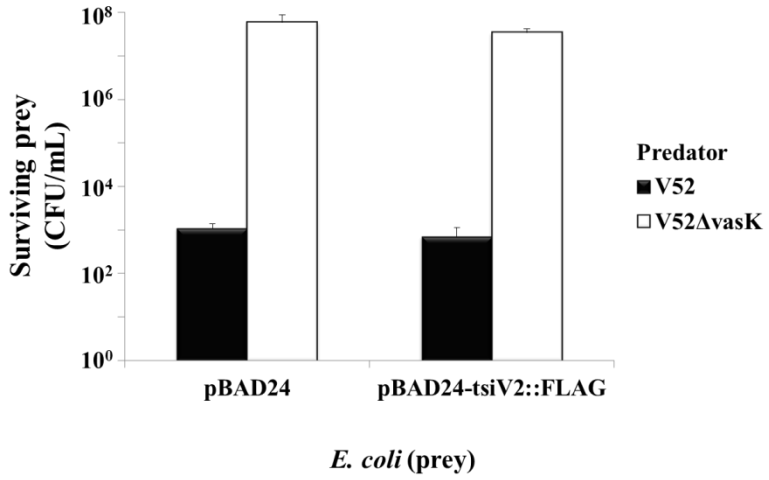

B.

C.

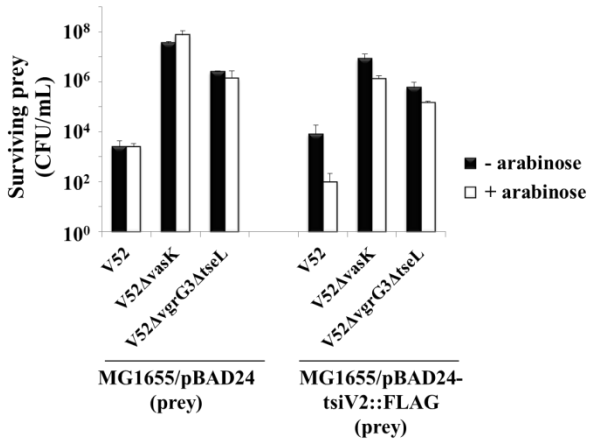

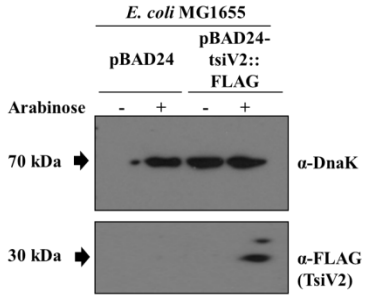

Figure 5-6. TsiV2 does not protect *E. coli* MG1655 from killing by V52. (A and B) CFU/mL of surviving prey (listed on the *x*-axis) were enumerated following exposure to the *V. cholerae* predator strains listed in the figure legend. Arabinose was included in all conditions tested in (A) and where indicated in (B) to induce expression from the P_{BAD} promoter. Error bars indicate the standard deviation. (C) A sample from the bacterial mixture of V52Δ*vasK* and MG1655/pBAD24-tsiV2::FLAG from (B) was boiled in sample buffer and subjected to SDS-PAGE followed by western blotting using DnaK (loading control) and FLAG primary antibodies.

To test whether episomal expression of *tsiV2* was protective for *V. parahaemolyticus*, pBAD33 (empty vector) and pBAD33-tsiV2::6xHis were mated into *V. parahaemolyticus* creating *V. parahaemolyticus*/pBAD33 and *V. parahaemolyticus*/pBAD33-tsiV2::6xHis, respectively. The vector pBAD33 (chloramphenicol^{R}) was used in this experiment because *V. parahaemolyticus* is inherently resistant to ampicillin which is the selectable marker used for pBAD24. *V. parahaemolyticus*/pBAD33-tsiV2::6xHis was then used as prey in a killing assay against V52 or V52Δ*vasK* predator. We observed a significant increase in surviving *V. parahaemolyticus*/pBAD33-tsiV2::6xHis compared to the empty vector control (Figure 5-7). Importantly, production of TsiV2::6xHis from pBAD33 was not able to provide complete protection in *V. parahaemolyticus*. This is likely due to the presence of the other two *V. cholerae* toxins, TseL and VgrG-3, for which *V. parahaemolyticus* was not provided the immunity gene.

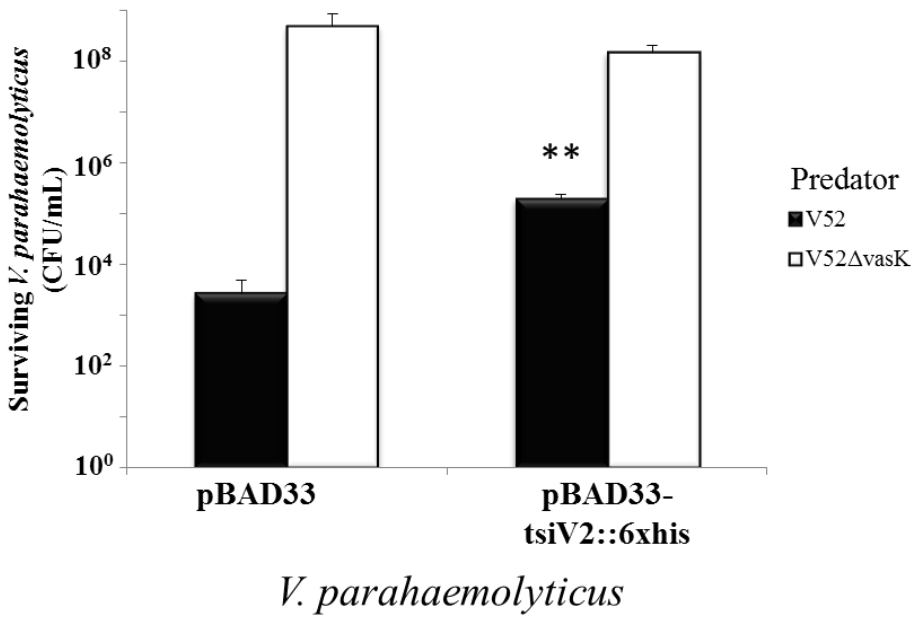

Figure 5-7. Episomal expression of *tsiV2* in *V. parahaemolyticus* results in significant protection from killing by V52. Survival of rifampicin-resistant *V. parahaemolyticus* harboring either pBAD33 empty vector or pBAD33-tsiV2::6xHis was determined by enumerating the CFU following exposure to the indicated rifampicin-sensitive predator (listed in the legend) in the presence of arabinose. Error bars indicate the standard deviation. ** = $p < 0.005$ relative to empty vector control (vs. V52). The *P*-value was calculated using the Student's one-tailed, paired T-test.

5.2.6 Bioinformatic analysis of TsiV2

BLASTp analysis indicated that TsiV2 lacks identifiable conserved domains. Aside from other *V. cholerae* strains, TsiV2 homologues were detected in *V. mimicus* (85% identity, e-value $2x10^{-147}$), *Vibrio anguillarum* (79% identity, e-value $4x10^{-138}$), *V. fischeri* (33% identity, e-value $7x10^{-30}$), *A. hydrophila* (47% identitiy, e-value $3x10^{-15}$), and *Aliivibrio salmonicida* (37% identity, e-value

$7x10^{-52}$). The most significant predictions using the secondary structure prediction software HHPred included an outer membrane insertion C-terminal signal (e-value $2x10^{-20}$) and an LPXTG-motif cell wall anchor domain (e-value $7.9x10^{-19}$). PSORTb predicted that TsiV2 localizes to the cytoplasmic membrane. TMHMM, SOSUI, and Phobius predicted that TsiV2 has three transmembrane domains; however, the results predicted by Phobius and TMHMM are opposite with respect to the topology of TsiV2 in the cytoplasmic membrane. A summary of transmembrane domain predictions is presented in Table 5-1.

Table 5-1. Summary of transmembrane (TM) regions predicted for TsiV2. The bioinformatics programs used (indicated in the left column) each suggest that TsiV2 is a membrane protein with three TM regions.

Prediction Program	Number of TM Domains Predicted	Coordinates (amino acids) of Predicted TM Domains
TMHMM	3	39-61 66-85 117-139
SOSUI	3	37-59 66-87 125-147
Phobius	3	36-54 66-84 118-151

5.2.7 Subcellular localization of TsiV2

The PSORTb bioinformatic analysis program suggested that TsiV2 localizes to the inner membrane (section 5.2.6). To determine where TsiV2 localizes within the cell, C6706Δ*tsiV2*/pBAD24-tsiV2::FLAG (grown under

inducing conditions) was subjected to subcellular fractionation. Whole cell lysates, permeabilized cells, periplasmic, cytoplasmic, and membrane fractions were analyzed by western blotting with DnaK (cytoplasm), OmpU (membrane), β-lactamase (periplasm), and FLAG (TsiV2) antibodies. I observed that TsiV2::FLAG is present in the whole cell lysate, permeabilized cells, cytoplasm, and membrane but not the periplasm (Figure 5-8). Although there is contamination of the periplasm fraction with the membrane protein OmpU, the fact that TsiV2 is absent from this fraction suggests that this data is still reliable.

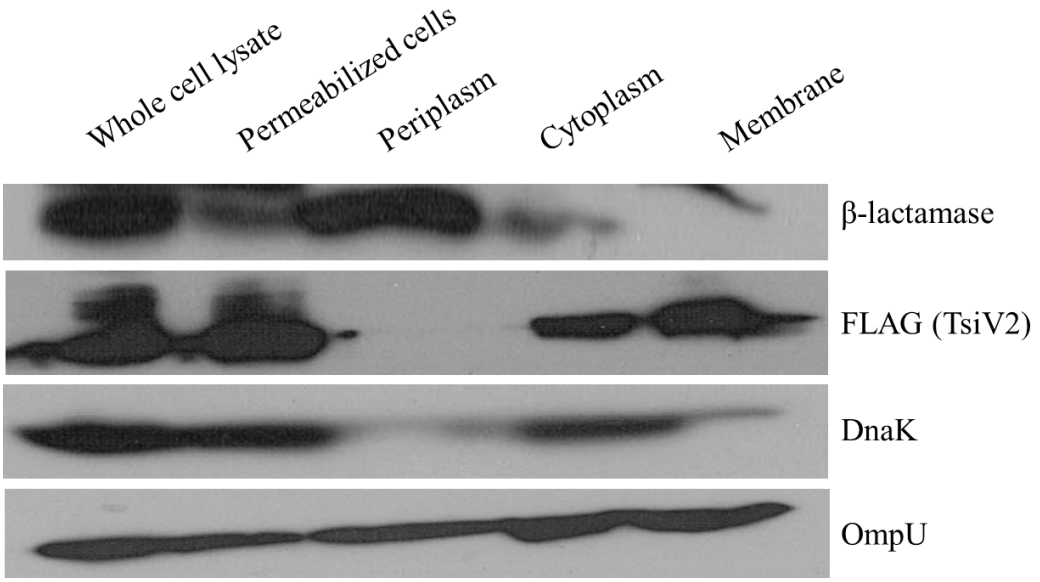

Figure 5-8. TsiV2 is present in the cytoplasm and membrane. C6706Δ*tsiV2*/pBAD24-tsiV2::FLAG was grown to late logarithmic phase and subjected to subcellular fractionation. Various fractions were separated by SDS-PAGE followed by western blotting with VasX, OmpU (membrane control), DnaK (cytosol control), and β-lactamase (Bla; periplasm control) primary antibodies.

To determine whether TsiV2 localizes to the bacterial inner or outer membrane, I performed sucrose-gradient fractionation of the total membrane fraction. Samples were assayed for NADH oxidase activity (indicative of the inner membrane) and then subjected to western blotting with OmpU (outer membrane), EpsL (inner membrane), and FLAG (TsiV2) primary antibodies. The resulting blot indicated that both EpsL and TsiV2 are present in fractions 8 and 9 and OmpU is most abundant in fraction 11. EpsL, OmpU, and TsiV2::FLAG were all detected in the whole cell lysate sample. The results of the NADH oxidase assay indicated that fractions 8 and 9 had NADH oxidase activity which corresponds to the presence of EpsL in the western blot. Taken together these data suggest that TsiV2 localizes to the inner membrane.

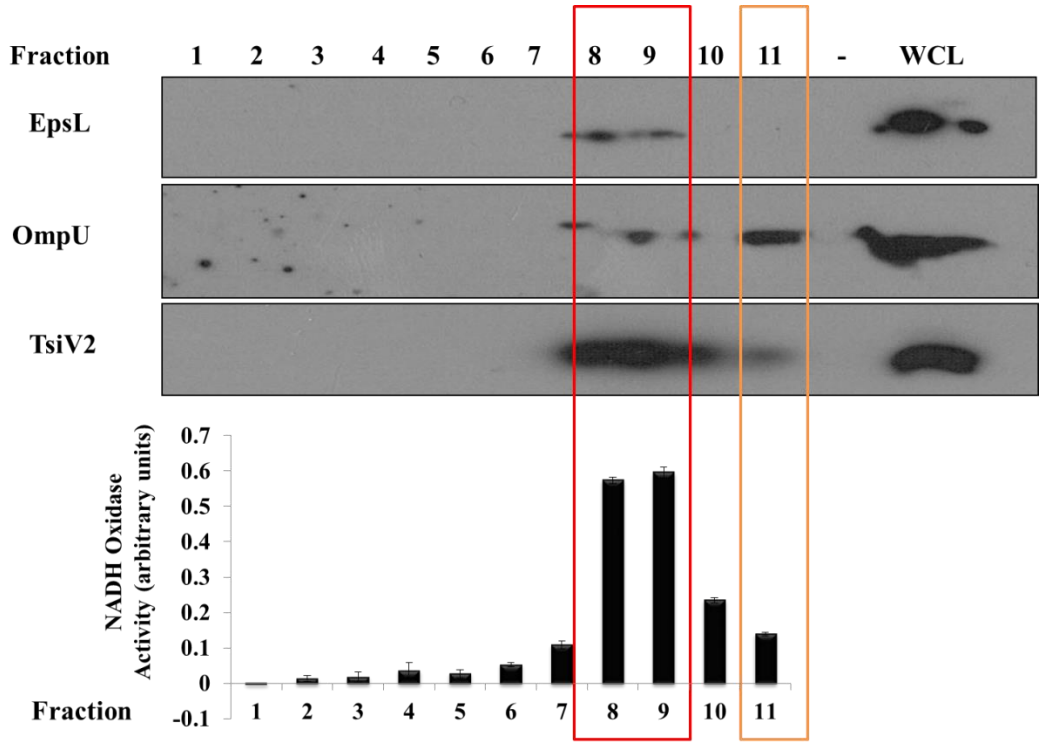

Figure 5-9. TsiV2 localizes to the inner membrane. C6706Δ*tsiV2*/pBAD24-tsiV2::FLAG total membranes were isolated and subjected sucrose-gradient fractionation to separate inner and outer membranes. Samples were subjected to western blotting with EpsL (inner membrane), OmpU (outer membrane), and FLAG (TsiV2) primary antibodies. NADH oxidase activity is plotted in the lower panel (values calculated relative to fraction 1). The red box indicates the inner membrane fractions and the orange box indicates the outer membrane. WCL; whole cell lysate sample.

5.2.8 *TsiV2* is under a dual regulatory mechanism

C6706 does not have an active T6SS under laboratory conditions (i.e. no expression of VasX or Hcp), yet is resistant to killing by V52 and we therefore wondered how immunity was maintained in the absence of T6SS gene expression. I hypothesized that the immunity gene *tsiV2* is subject to a dual regulatory mechanism. We and others previously identified a promoter which drives expression of the *vasX/tsiV2*-containing gene cluster that is located in the 400

base pairs upstream of *hcp-2* [370-372]. The T6SS regulator VasH and the alternate sigma factor σ^{54} have been shown to work at this promoter driving expression of *hcp-2*, *vgrG-2*, and *vasX* [370, 371]; however this promoter is not active in C6706 as evidenced by a lack of Hcp expression under standard laboratory conditions [365]. I hypothesized that there exists a promoter within *vasX* capable of driving transcription (in a VasH-independent manner) of the downstream gene *tsiV2* independently from the rest of the genes within the *tsiV2* gene cluster (Figure 5-10). This hypothesis provides a logical explanation as to why wild-type C6706 is immune to killing by V52.

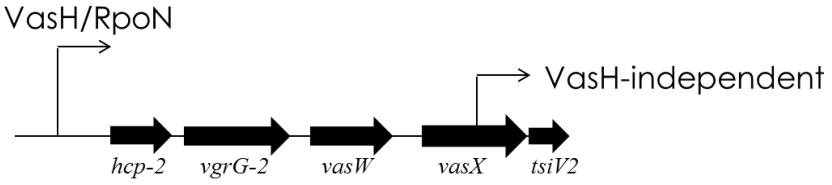

Figure 5-10. Schematic representation of the *vasX*-encoding gene cluster indicating the location of the two promoters involved in dual regulation of *tsiV2*. The first promoter is located upstream of *hcp-2* and transcription from this promoter is dependent on VasH. The second putative promoter is located within *vasX* and drives expression solely of *tsiV2* in a VasH-independent manner.

To test this, I made transcriptional fusions of full-length *vasX*, or different *vasX* truncations (nucleotides 1-1345, 1575-3258, and 2208-3258) to promoterless *lacZ* in the plasmid pAH6. The *hcp-2* promoter region ($P_{hcp,}$ basepairs -1 to -400) was also fused to *lacZ* as a control. Plasmids were transformed into V52, V52Δ*vasH*, and C6706, and β-galactosidase assays were performed to determine the level of LacZ production within the cells.

In V52 (constitutive expression of T6SS genes via the promoter upstream of *hcp-2*), I observed a significant amount of LacZ production with P_{hcp}, full length *vasX*, *vasX*(1575-3258), and *vasX*(2208-3258) compared to the empty vector control (Figure 5-11). V52Δ*vasH* which is unable to initiate transcription via the *hcp-2* promoter produced significant LacZ levels with full length *vasX*, *vasX*(1575-3258), and *vasX*(2208-3258) but not with P_{hcp}, nor *vasX*(1-1345) (Figure 5-11). In C6706, similar to V52Δ*vasH*, we observed significant LacZ production from full length *vasX*, *vasX*(1575-3258), and *vasX*(2208-3258) but not with P_{hcp}, or *vasX*(1-1345) (Figure 5-11). These data suggest a promoter exists within the 3' end of *vasX* that can drive low-level expression (compared to P_{hcp}) of *tsiV2* independently of VasH. Further to the data presented here, I also showed that internal promoters for the other two V52 immunity protein-encoding genes (*tsiV1* and *tsiV3*) are encoded within their cognate toxin genes *tseL* and *vgrG-3*, respectively (Appendix Figure 9-6).

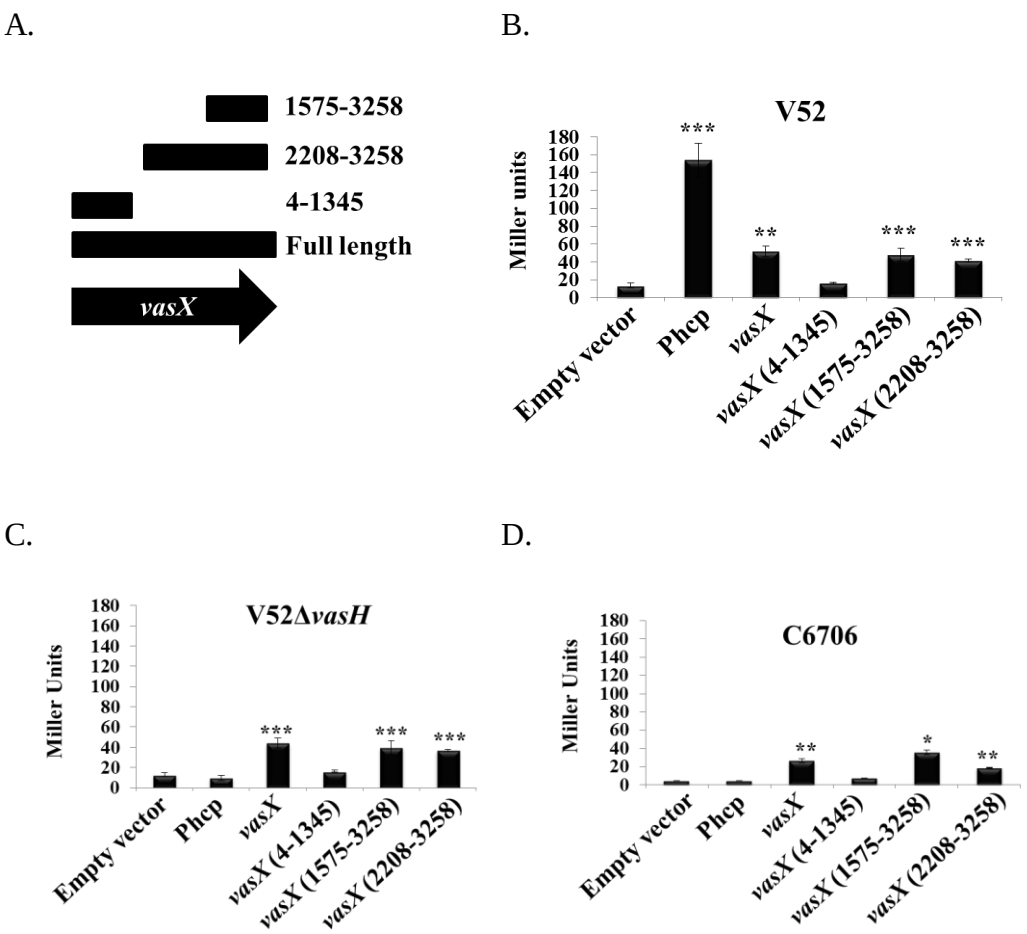

Figure 5-11. Expression of *tsiV2* is controlled by a dual regulatory mechanism. (A) Schematic representation of the *vasX* fragments cloned upstream of *lacZ* in plasmid pAH6. (B, C, and D) Overnight cultures of the strains indicated at the top of the graph harboring plasmids indicated on the *x*-axis were used to assay for the production of β-galactosidase. Miller units are a function of LacZ production combined with optical density of the starting culture and incubation time. Error bars indicate the standard deviation. ***= $p < 0.001$, **= $p < 0.005$, *= $p < 0.01$ relative to the empty vector control. *P*-values were calculated based on the Student's one-tailed, paired T-Test.

To determine whether the internal *vasX* promoter was functional in *V. cholerae* strains other than V52 and C6706, the plasmids pAH6 (empty vector) and pAH6-vasX(2208-3258) were transformed into the *V. cholerae* strains C6709 (O1 El Tor), NIH41 (O1 Classical), O395 (O1 Classical), MAK757 (Pre-7th pandemic O1 El Tor), and N16961 (O1 El Tor) each of which was mutated to possess a non-functional chromosomal *lacZ* (as described in the Materials & Methods). The plasmid pAH6-vasX(2208-3258) was chosen for this experiment because it contains the most 3' fragment of *vasX* that results in increased *lacZ* transcription according to the data presented in Figure 5-11. The amount of β-galactosidase produced by each strain was assayed and indicates the level of *lacZ* expression driven by the 3' 1050 nucleotides of *vasX*. I observed that pAH6-vasX(2208-3258) resulted in significantly more β-galactosidase production compared to the empty vector control in the strains C6709, NIH41, MAK757, and N16961 but not O395 (Figure 5-12). This data indicates that the 3' end of *vasX* possesses promoter activity that is functional in a variety of *V. cholerae* strains.

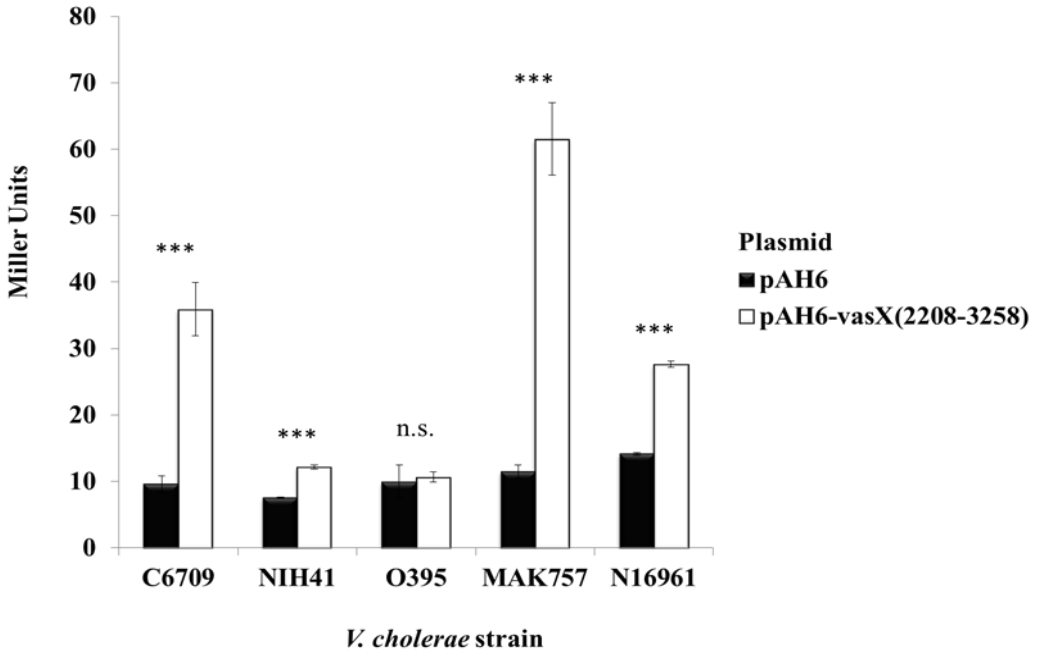

Figure 5-12. The 3' 1050 nucleotides of *vasX* drive expression of *lacZ* in *V. cholerae* O1 strains C6709, NIH41, MAK757, and N16961. Overnight cultures of the strains indicated on the *x*-axis harboring plasmids indicated in the legend were used to assay for the production of β-galactosidase. Miller units are a function of LacZ production combined with optical density of the starting culture and incubation time. n.s; no significant difference. Error bars indicate the standard deviation. ***= $p < 0.005$, **= $p < 0.01$, *= $p < 0.05$ relative to the empty vector control. *P*-values were calculated based on the Student's one-tailed, paired T-Test.

To further confirm the presence of a promoter within *vasX*, I performed two independent killing assays. First, I challenged V52 predator against rifampicin-resistant V52, V52Δ*vasH*, V52Δ*vasX*, V52Δ*vasX*Δ*vasH*, or MG1655 (control) prey. I hypothesized that V52 lacking both *vasH* and *vasX* would be unable to produce TsiV2 and would therefore become susceptible to killing by wild-type V52. When exposed to V52, MG1655 endured a ~4 log reduction in

surviving bacteria compared to the T6SS-null strain V52Δ*vasK* (Figure 5-13). V52 and V52Δ*vasH* maintained immunity to killing by wild-type V52; however, there were fewer surviving V52Δ*vasX* compared to both V52 and V52Δ*vasH* and a further reduction in surviving prey was observed when V52Δ*vasH*Δ*vasX* was exposed to wild-type V52 (Figure 5-13). This implies that the strain V52Δ*vasH* maintains basal expression of *tsiV2* to prevent VasX-mediated toxicity.

In the second assay, I created an *in-frame* C6706 *vasX* mutant and used this strain as prey in a killing assay with V52 predator. In this strain, the putative *tsiV2* promoter is deleted and this would render C6706Δ*vasX* susceptible to killing by V52. When challenged with wild-type V52, C6706Δ*vasX* (with empty vector pBAD24) was killed (Figure 5-13). Episomal expression of *vasX* was unable to restore immunity to killing by V52 because expression from pBAD24 does not restore promoter function to drive expression of *tsiV2* on the C6706 chromosome (Figure 5-13). On the other hand, expression of *tsiV2::FLAG* from pBAD24 prevented V52 from killing C6706Δ*vasX* (Figure 5-13). Taken together, these data indicate that the promoter within *vasX* can drive transcription of *tsiV2* and expression of *tsiV2* from the *vasX* internal promoter occurs in a VasH-independent manner.

A.

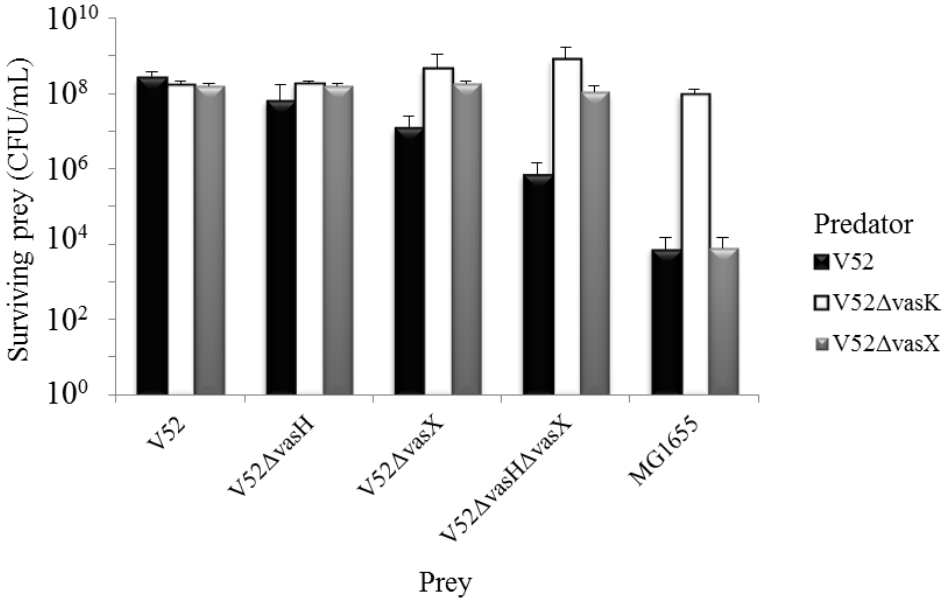

B.

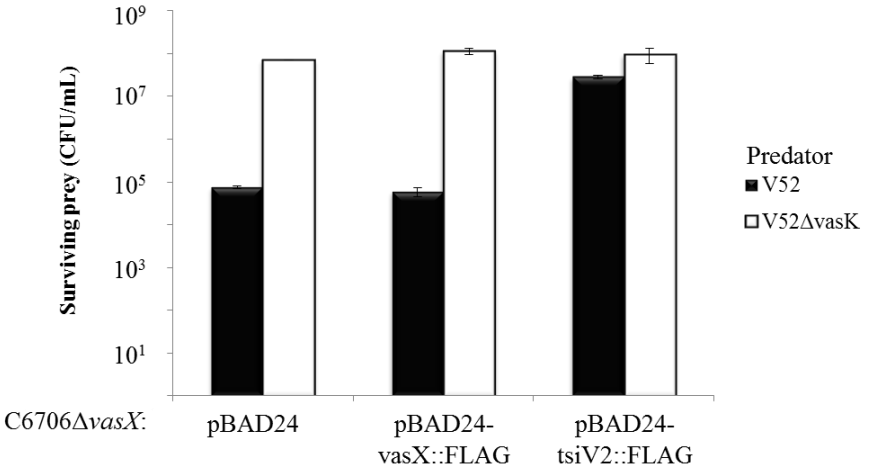

Figure 5-13. *VasX* contains a promoter to drive expression of *tsiV2*. (A and B) Survival of rifampicin-resistant prey listed on the *x*-axis was determined by enumerating the CFU following exposure to the indicated rifampicin-sensitive predator (listed in the legend). The assay in (B) was performed in the presence of arabinose to induce expression from the P_{BAD} promoter. Error bars indicate the standard deviation.

5.2.9 Internal *vasX* promoter prediction

In an attempt to map the location of the internal *vasX* promoter, we used the Neural Network Promoter Prediction Software (0.95 cut-off) and identified 5 putative promoters within *vasX* that could drive transcription of *tsiV2* (Figure 5-14). Of note, one of the predicted promoters with the highest confidence scores spans nucleotides 3191-3236 which is toward the 3' end of *vasX*. This region was subsequently used to perform an alignment among different *V. cholerae* strains to determine whether the putative promoter region was conserved. We observed that this region was 100% conserved among the *V. cholerae* strains used for the alignment (Figure 5-14).

A.

Start	End	Score	Promoter Sequence
900	945	0.96	TCTTGAAGAAAAAGAAATTCCCGATTTTGTAAAACAAGATCCGATCCGTA
919	964	0.99	CCCGATTTTGTAAAACAAGATCCGATCCGTATTTTAGAGCTAGAAAGAGC
1166	1211	0.97	TTATTGATGAAGTGCGTTGGGCGGATTTAGATAACTTTTTGGTGGAGCAT
2193	2238	1.00	GGTTTTGGAGAATATCCGCTATAAGGTCGCACAATACCCCAGTTGGAATC
3191	3236	1.00	AATTGGATTTACAATCTGCAGAGGCGAATGATATTGCCACAAGAAATCTC

B.

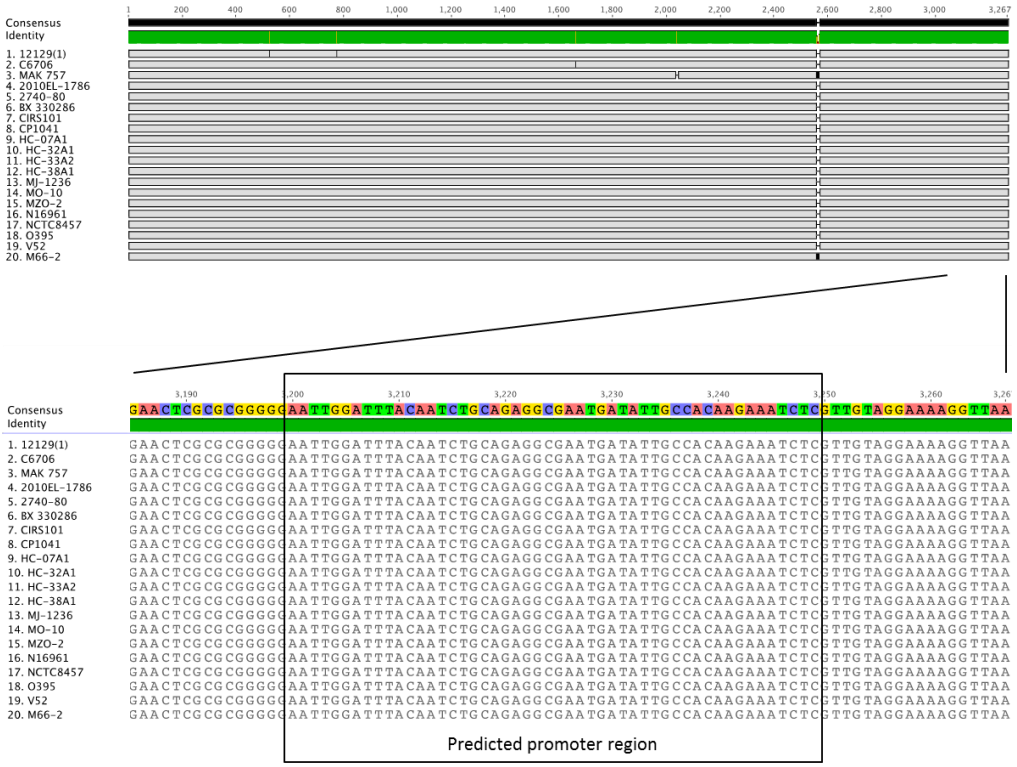

Figure 5-14. Putative *vasX* internal promoter predictions. (A) Promoter predictions within *vasX* determined by the Neural Network Promoter Prediction Software. The nucleotides encoding the putative promoter are indicated by the coordinates on the left, followed by the statistical probability. The predicted transcriptional start site is noted in the larger font. (B) The putative promoter region closest to the 3' end of *vasX* (3191-3236) was used as the basis for an alignment comparing the same region among a variety of *V. cholerae* strains. The black box indicates the predicted promoter region. Strains used for the alignment are noted on the left.

5.2.10 Physical interaction between VasX and TsiV2

To prevent VasX from disrupting the bacterial inner membrane, I hypothesized that TsiV2 physically interacts with VasX in the inner membrane of prey bacteria. I previously demonstrated that episomal expression of *tsiV2* restores immunity to VasX in C6706Δ*tsiV2* in a killing assay (Figure 5-2). If TsiV2 and VasX interact in the prey cell inner membrane, then this must occur in the course of the killing assay. I performed a killing assay where V52Δ*vasX*/pBAD24-vasX::FLAG and C6706Δ*tsiV2*/pBAD33-tsiV2::6xHis (and their respective empty vector controls) were mixed and incubated for 4 hours on an LB plate. In a standard killing assay, 2 spots of bacterial mixture are placed onto the LB agar plate; however in this assay, 15 spots were used such that my crude lysates would contain a higher protein concentration for nickel pull-down. The bacterial spots were harvested and cell lysates were incubated with Ni^{2+} NTA resin to pull out 6xHis-tagged TsiV2, as well as any proteins strongly associated with TsiV2. Protein samples were boiled and subjected to SDS-PAGE followed by western blotting using α-FLAG and α-6xHis primary antibodies. I observed that while TsiV2::6xHis was pulled out of solution using the nickel resin, VasX::FLAG was pulled out of solution in the presence and absence of TsiV2::6xHis (Figure 5-15). This implies that VasX is pelleting out of solution on its own and therefore I cannot conclude whether TsiV2 and VasX interact from these results. I also noted the presence of a ~70 kDa band that reacted with 6xHis antibody in the samples where *tsiV2::6xHis* was expressed (Figure 5-15).

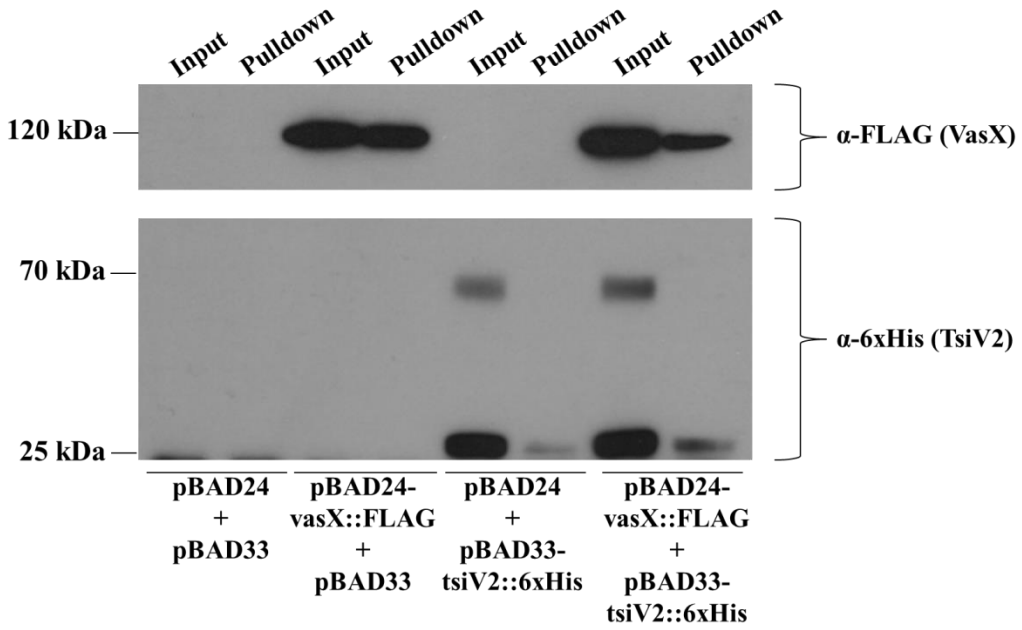

Figure 5-15. Pulldown of TsiV2::6xHis. V52Δ*vasX*/pBAD24-vasX::FLAG or V52Δ*vasX*/pBAD24 were mixed with C6706Δ*tsiV2*/pBAD33-tsiV2::6xHis or C6706Δ*tsiV2*/pBAD33 and incubated on an agar plate. Cell lysates were mixed with Ni^{2+} NTA resin to pull down 6xHis-tagged TsiV2 and protein samples were subjected to SDS-PAGE followed by western blotting using α-FLAG (VasX) and α-6xHis (TsiV2) antibodies.

Next I tried mixing purified recombinant VasX::6xHis and TsiV2::6xHis in the presence of the cross-linker dithiobis (succinimidyl) propionate (DSP). DSP is an amine-reactive cross-linker that forms amide bonds between primary amines in lysine residues. Cross-linking between proteins can be cleaved by boiling the samples in the presence of β-mercaptoethanol (βME). VasX and TsiV2 were mixed at an equal mass ratio in the presence or absence of DSP. All samples were boiled in SDS sample buffer with or without βME, subjected to SDS-PAGE, and stained with Coomassie Blue. When VasX alone was incubated

in the presence of DSP, I observed a high molecular weight complex that was incapable of migrating through the SDS-PAGE separating gel (Figure 5-16). Upon boiling this sample in the presence of βME, I saw the appearance of 4 bands including one corresponding to the expected molecular weight of monomeric VasX (~120 kDa), two smaller bands at ~70 kDa and the high molecular weight band at the top of the separating gel (Figure 5-16). In the absence of DSP, VasX still formed the high molecular weight complex; however, this band disappeared upon boiling in sample buffer containing βME (Figure 5-16). Therefore, VasX forms the high molecular weight complex in solution regardless of the presence of DSP.

When TsiV2 was incubated in the presence of DSP, I observed the formation of a high molecular weight complex that failed to migrate through the SDS-PAGE separating gel (Figure 5-16) similar to VasX. When boiled in the presence of βME, a single band at ~70 kDa was present (Figure 5-16) similar to that observed in Figure 5-15. In the absence of DSP and βME, TsiV2 bands were present at ~70 and ~100 kDa; however this was reduced to one band at ~70 kDa upon boiling with BME-containing buffer. Monomeric TsiV2 is ~30 kDa and therefore, TsiV2 also forms a stable high molecular weight complex when left in solution.

When TsiV2 and VasX were mixed together in solution with DSP, I again witnessed the formation of a high molecular weight complex that failed to migrate through the SDS-PAGE separating gel. When this mixture was boiled in the presence of βME, I observed bands corresponding to the molecular weight of each

band seen with VasX and TsiV2 alone as well as a band corresponding to the size of monomeric TsiV2 (~30 kDa) (Figure 5-16). In the absence of DSP, I observed bands corresponding to every band from both the VasX and TsiV2 alone samples including the high molecular weight complex (Figure 5-16). Upon boiling with βME^{+} buffer, these bands were reduced to the same protein bands observed for VasX and TsiV2 alone samples (-DSP, +βME).

Based on my observation of the high molecular weight complexes formed by both TsiV2 and VasX, I decided to repeat this experiment and subject the samples to 7.5% SDS-PAGE to determine whether the complexes could migrate through the lower percentage acrylamide gel (Figure 5-16). In the presence of DSP, I observed the presence of high molecular weight complexes that were unable to migrate through the separating gel (Figure 5-16). Taken together, these data indicate that VasX and TsiV2 individually can multimerize resulting in the formation of large complexes that cannot be resolved by SDS-PAGE. Furthermore, TsiV2 forms a ~60 kDa complex that is stable even after boiling in sample buffer containing βME. Due to the presence of the protein complexes formed by both TsiV2 and VasX independently, it was not possible to deduce whether the two purified proteins interacted in solution.

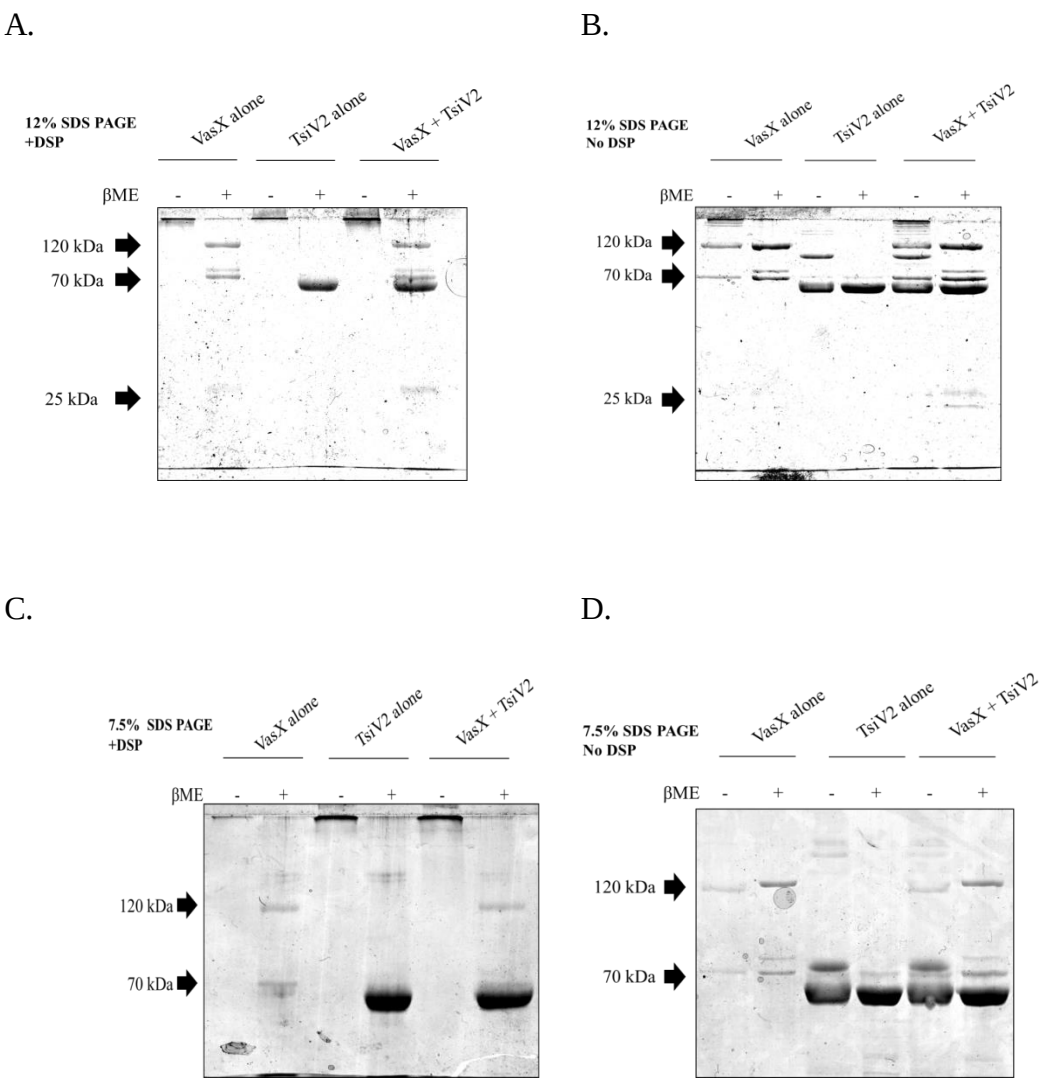

Figure 5-16. VasX and TsiV2 form LPCxs in solution. Purified, recombinant VasX and TsiV2 were mixed at an equal mass ratio in the presence (A and C) or absence (B and D) of the cross-linker DSP. Samples were boiled in sample buffer +/- βME and were subjected to 12% SDS-PAGE (A and B) or 7.5% SDS-PAGE (C and D) followed by staining with Coomassie Blue.

In my final attempt to determine whether VasX and TsiV2 physically interact, I performed far dot blots where TsiV2 was immobilized on a nitrocellulose membrane (1,000 ng, 100 ng, and 10 ng) and purified, recombinant VasX was used as the bait protein. Purified VasX and TsiV3 (VgrG-3 immunity protein) were spotted directly onto the membrane as positive and negative controls, respectively. Membranes were incubated overnight in various concentrations of bait protein (0, 2.5, 5, 7.5, 10 $\mu g \cdot mL^{-1}$) followed by incubation in α-VasX primary antibody, and α-rabbit-HRP secondary antibody. The VasX positive control spot was detected under all conditions tested, whereas TsiV3 was never detected (Figure 5-17). The spot corresponding to 1,000 ng of TsiV2 was detected; however, it was also detected on the membrane incubated with no VasX bait protein (Figure 5-17). Therefore, nitrocellulose-bound TsiV2 binds in a non-specific manner to either α-VasX or α-rabbit-HRP. Therefore it was not possible from these results to determine whether VasX and TsiV2 interact using far dot blot analysis.

A.

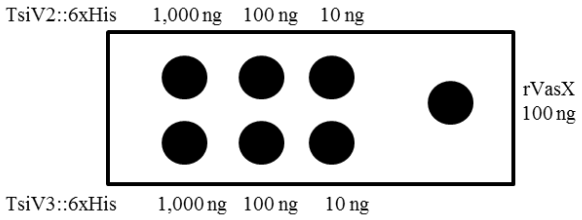

B.

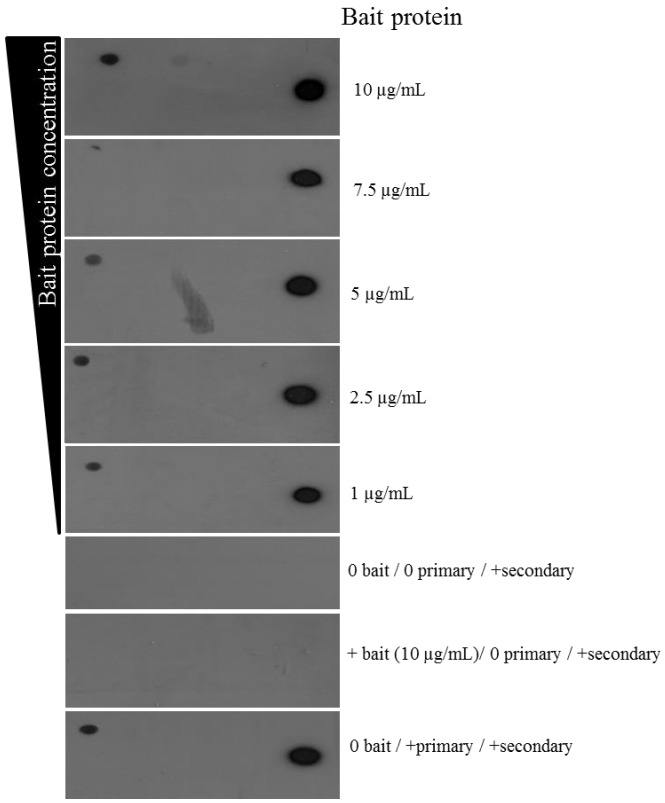

Figure 5-17. Far dot blot analysis using immobilized TsiV2 and VasX bait protein. (A) Schematic representation of proteins TsiV2, TsiV3, and VasX spotted onto nitrocellulose membrane for far dot blotting. (B) Far dot blots with TsiV2, TsiV3 (negative control), and VasX (positive control) spotted onto nitrocellulose membranes. The bait protein (purified, recombinant VasX) was diluted at the concentrations noted to the right of the blots and incubated with the nitrocellulose membranes. Bound protein was detected using α-VasX primary antibody and anti-rabbit-HRP secondary antibody.

5.2.11 TsiV2 forms a LPCx

I observed the presence of a TsiV2 LPCx in Figures 5-15 and 5-16. To confirm that the formation of the LPCx occurred *in-vivo*, I grew V52/pBAD24-tsiV2::6xHis and V52/pBAD24 under inducing conditions and whole cell lysate samples were boiled in protein sample buffer. Upon western blot analysis using α-6xHis primary antibody, I again observed monomeric TsiV2 (~30 kDa) and the presence of a LPCx (~70 kDa) strictly in samples expressing *tsiV2::6xHis* (Figure 5-18). Neither band was present in the empty vector control lane. Interestingly, these samples had been boiled, implying that the TsiV2 LPCx does not dissociate at high temperatures in the presence of SDS and βME.

To confirm LPCx formation was not an artifact mediated by the 6xHis tag, I grew the strains C6706Δ*tsiV2*/pBAD24 and C6706Δ*tsiV2*/pBAD24-tsiV2::FLAG under inducing conditions. Boiled and non-boiled whole cell lysate samples were prepared and subjected to western blot analysis using α-FLAG M_2 primary antibody. Again, I observed the presence of monomeric TsiV2 (~30 kDa) and the formation of a TsiV2 LPCx (~70 kDa); however a stronger LPCx band was present in the boiled sample containing TsiV2::FLAG compared to the non-boiled sample (Figure 5-18). Neither band was present in the empty vector control lanes indicating that the LPCx band did not occur due to cross-reactivity of the antibody. Taken together, these data suggest that boiling samples containing TsiV2 induces the formation of a stable complex with itself, or in combination with other unidentified proteins.

A.

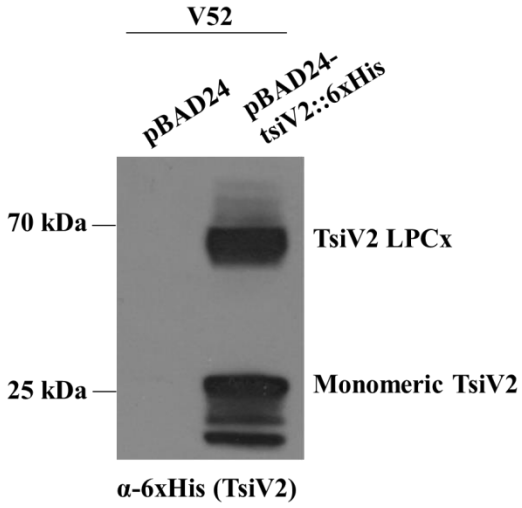

B.

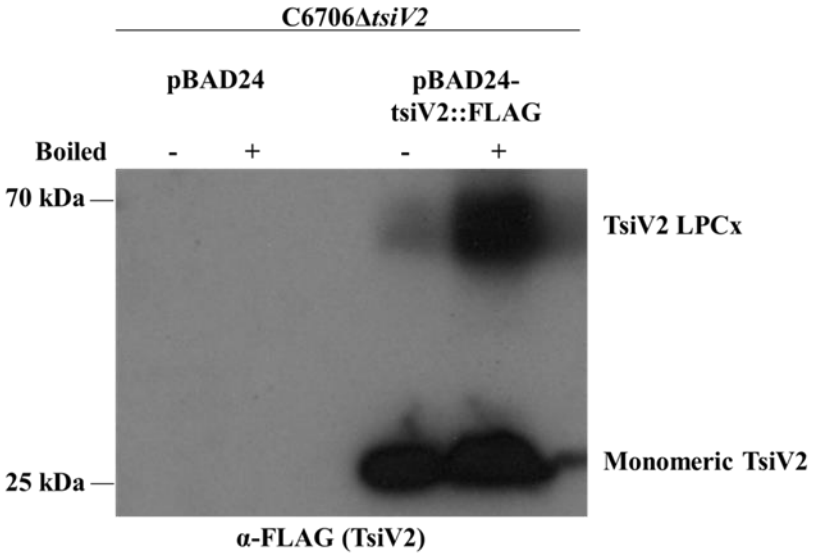

Figure 5-18. TsiV2 forms a LPCx. The strains C6706Δ*tsiV2*/pBAD24-tsiV2::FLAG or C6706Δ*tsiV2*/pBAD24 (empty vector) (A) or C6706Δ*tsiV2*/pBAD24-tsiV2::6xHis and C6706Δ*tsiV2*/pBAD24 (empty vector) (B) were grown under inducing conditions and boiled and non-boiled bacterial pellet samples were subjected to SDS-PAGE followed by western blotting with α-FLAG M_2 (A) or α-6xHis (B) primary antibody.

5.2.12 *Trans*-expression of TsiV2::FLAG does not protect against periplasmic VasX

In Figure 5-2, I demonstrated that episomal expression of TsiV2 can protect C6706Δ*tsiV2* from an oncoming attack by V52 even though over-expression of TsiV2 is slightly toxic. I also devised a system (described in section 4.2.5) where targeting VasX to the periplasm (LS::vasX) is toxic to the producing cell (Figure 4-6). I hypothesized that expression of *tsiV2* in C6706Δ*tsiV2* concomitantly expressing *LS::vasX* would be protective against periplasmic VasX. To test this, I generated the strain C6706Δ*tsiV2*/pBAD24-LS::vasX+pBAD33-tsiV2::6xHis. pBAD24 (amp^R) and pBAD33 ($chlor^R$) possess different origins of replication and can therefore be maintained within the same bacterial cell.

This strain was grown in the presence of arabinose (inducing conditions for both pBAD24 and pBAD33) and recovered the surviving CFU every 2 hours over a period of 8 hours. For C6706Δ*tsiV2*/pBAD24-LS::vasX+pBAD33-tsiV2::6xHis, the number of recovered cells increased up until the 4-hour time point; however, at the 6- and 8-hour time points I observed a drop in surviving CFU/mL (Figure 5-19). Strains expressing either *tsiV2* or *LS::vasX* alone also increased in recovered CFU/mL until the 4-hour time point, followed by a drop in recoverable cells (Figure 5-19) which was also observed previously (Figures 4-6, and 5-5). C6706Δ*tsiV2* harboring either pBAD24 or pBAD33 empty vector did not experience a drop in recovered CFU over the 8-hour time period. Taken

together, these results indicate that expression of TsiV2 does not protect C6706Δ*tsiV2* from periplasmic VasX.

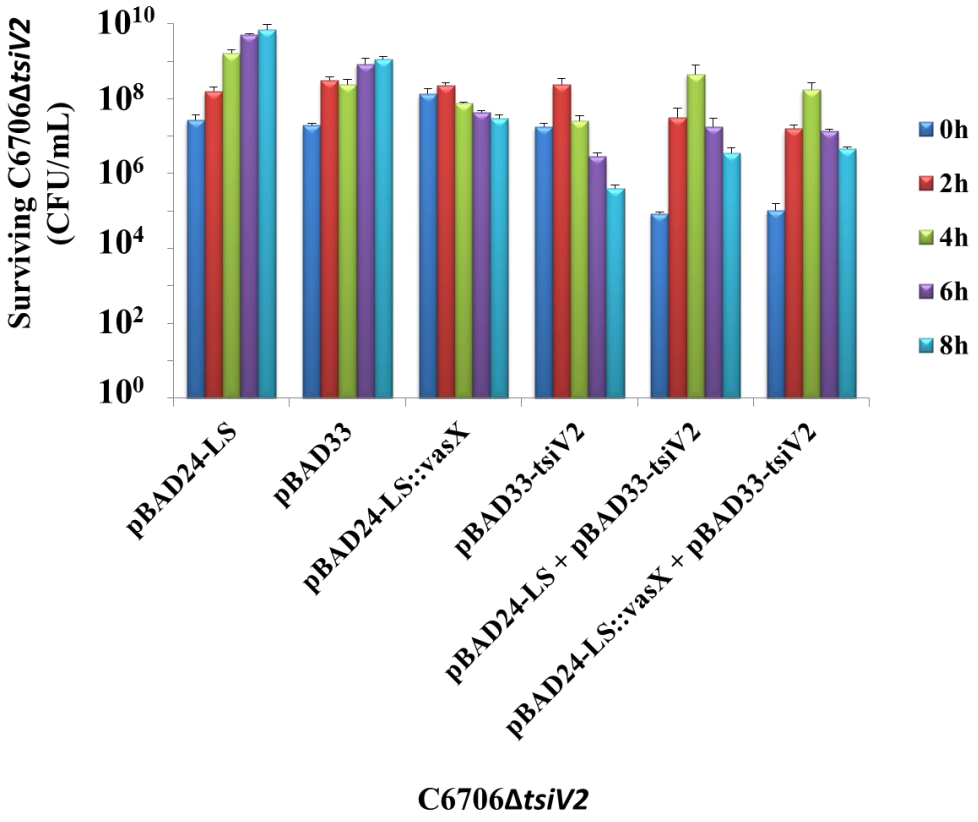

Figure 5-19. Episomal expression of *tsiV2* is not protective against periplasmic VasX. Overnight cultures of the strains indicated on the *x*-axis were grown for 8 hours under inducing conditions. At 0, 2, 4, 6, and 8 hours, a sample was taken from each strain and the CFU were recovered and enumerated.

In Figure 5-3, I demonstrated that pJET-tsiV2::6xHis was protective against VasX-mediated toxicity even though pJET1.2 has a promoter that is inactive in V52 and *tsiV2* is cloned in the reverse orientation. The results presented in Figures 5-5 and 5-19 suggest that over-expression of *tsiV2* is toxic

and it cannot protect against periplasmic VasX. I hypothesized that only very small amounts of TsiV2 are required to protect against periplasmic VasX. To test this, I transformed C6706Δ*tsiV2* with both pJET-tsiV2::6xHis and pBAD33-LS::vasX and performed an 8-hour time course where CFU were recovered every 2 hours. pJET1.2 (amp^R) and pBAD24 have the same origin of replication and so they cannot be maintained within the same cell. pJET1.2 containing super-folded GFP (sfGFP) was used as a negative control since pJET1.2 empty vector is toxic to cells (due to the design of the blunt-ended cloning vector). When grown in the presence of arabinose (to induce expression from pBAD33), C6706Δ*tsiV2* harboring pBAD33-LS::vasX, pBAD33-LS::vasX+pJET-GFP, and pBAD33-LS::vasX+pJET-tsiV2::6xHis all decreased in the number of recoverable CFU/mL over an 8-hour time period (Figure 5-20) whereas C6706Δ*tsiV2* harboring control plasmids increased in cell density over the 8-hour period. Therefore, providing pJET-tsiV2::6xHis, which does not result in over-expression of *tsiV2*, is not protective against periplasmic VasX.

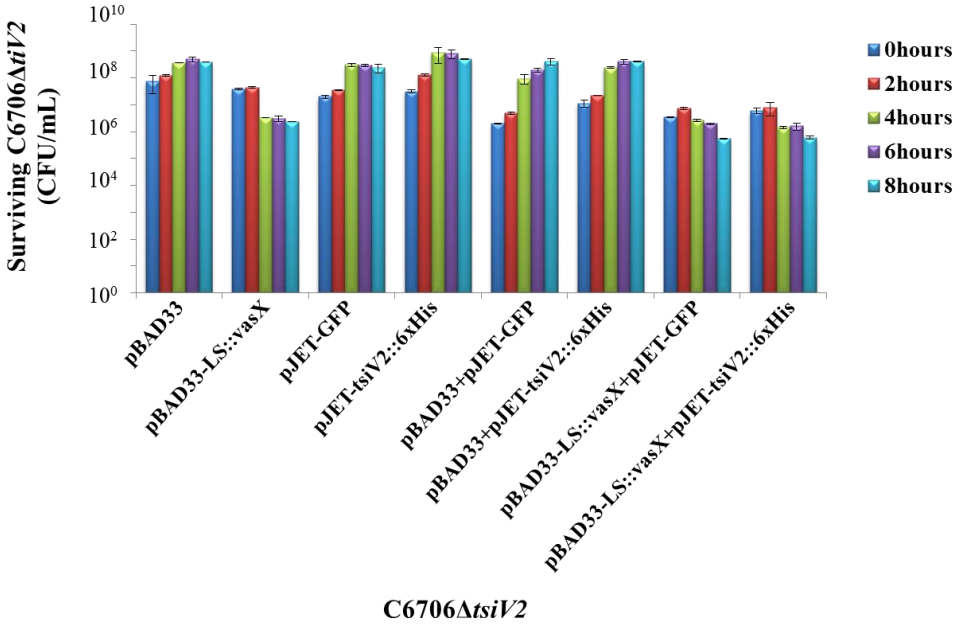

Figure 5-20. pJET-tsiV2::6xHis is not protective against periplasmic VasX. Overnight cultures of the strains indicated on the *x*-axis were grown for 8 hours at and samples were harvested at 0, 2, 4, 6, and 8 hours. CFUs from each sample were recovered and enumerated.

5.2.13 Co-incubation of TsiV2 and VasX does not prevent leakage of carboxyfluorescein from large unilammelar vesicles

In section 4.2.10 I presented data indicating that purified, recombinant VasX could disrupt CF-LUVs resulting in the release of CF from liposomes (Figure 4-11). Knowing that TsiV2 is the VasX immunity protein, I hypothesized that when mixed with TsiV2 in solution, VasX would become inactivated and therefore unable to disturb LUV integrity. To test this, purified recombinant VasX and TsiV2 were added independently, or mixed together and were incubated with CF-LUVs similar to the experiment presented in section 4.2.10.

The detergent Triton X-100 was used as a positive control for LUV disruption. Negative controls included buffer alone, BSA, and purified, recombinant TsiV3. Similar to Figure 4-11, I observed that Triton X-100 and VasX cause significant release of CF into solution compared to BSA, buffer alone, and TsiV3 controls (Figure 5-21). Interestingly, the addition of TsiV2 alone, and TsiV2 in combination with VasX, also caused a significant amount of CF release from LUVs indicating that these proteins were capable of disrupting the liposome integrity (Figure 5-21)

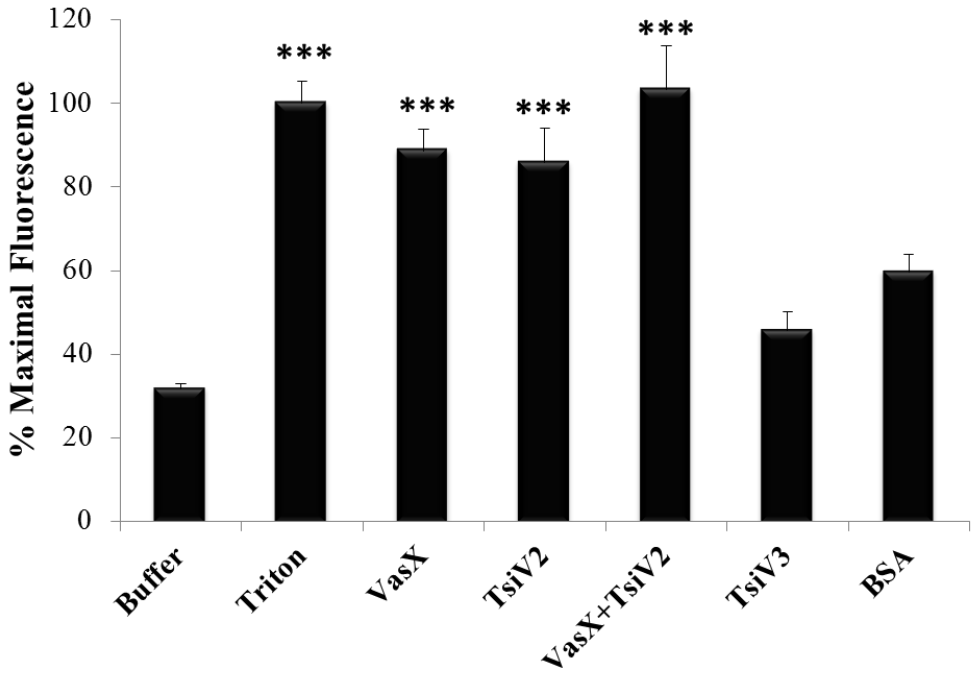

Figure 5-21. Co-incubation of TsiV2 and VasX does not prevent leakage of carboxyfluorescein from large unilamellar vesicles. The substrates listed on the *x*-axis were mixed with CF-encapsulating LUVs followed by measurement of the fluorescence intensity. The detergent Triton X-100 is a positive control for LUV disruption and this sample was used as the value for maximal fluorescence. Buffer alone, purified, recombinant TsiV3, and BSA constitute negative controls. Error bars indicate the standard deviation. *** denotes $p < 0.001$ relative to BSA control.

5.3 **Discussion**

By screening a C6706 T6SS transposon library for susceptibility to V52 killing, we determined *V. cholerae* encodes T6SS immunity proteins that specifically protect against their cognate T6SS toxin (i.e. VasX, VgrG-3, or TseL) (D. Unterweger, unpublished observation). More specifically, we identified TsiV2 as the immunity protein that specifically protects against the toxic effects of VasX (Figure 5-1). In the context of the T6SS, the production of immunity proteins is necessary to protect cells against an oncoming attack by neighboring $T6SS^+$ bacteria. This is in contrast to colicins where the immunity proteins protect against both self-intoxication and against colicins produced by sister cells.

Interestingly, episomal expression of *tsiV2* in *V. parahaemolyticus* provided significant protection against killing by V52 (Figure 5-7). On the other hand, episomal expression of *tsiV2* in *E. coli* did not provide protection against T6SS-mediated killing even when VasX was the only bacterial toxin employed (Figure 5-6). Importantly, *V. parahaemolyticus* is $T6SS^+$ but does not encode homologues of VasX or TsiV2 according to BLASTn and BLASTp analysis. *E. coli* MG1655 also does not encode homologues of VasX and TsiV2. Therefore, I postulate that even though this strain encodes T6SS gene clusters, putative *V. parahaemolyticus* immunity proteins are not cross-protective against V52 toxins. Furthermore, I suggest TsiV2 provides protection in *V. parahaemolyticus*, but not in *E. coli* because TsiV2 requires other T6SS proteins or co-factors for proper function and/or localization within the prey cell that are encoded by *V. parahaemolyticus* but not *E. coli*.

The gene encoding the VasX immunity protein, *tsiV2*, is located directly downstream of *vasX* (in both V52 and C6706) and I determined that a promoter (P_{vasX}) exists within the 3' 1050 nucleotides of *vasX* that can drive expression of *lacZ* in V52, V52Δ*vasH*, C6706, C6709, NIH41, N16961, and MAK757, (Figures 5-11, 5-12, and 5-14). Promoter prediction analysis suggested the presence of a promoter within nucleotides 3191-3236 of *vasX* and an alignment of *vasX* among other *V. cholerae* strains suggested this region is highly conserved (Figure 5-14) and that the promoter is recognized in a variety of *V. cholerae* strains.

By fusing *vasX* and the *hcp-2* promoter to *lacZ*, I demonstrated that the amount of β-galactosidase production driven by P_{vasX} is much lower than that driven by P_{hcp} (Figure 5-11). As expected, expression of *lacZ* was significantly reduced from P_{hcp} in both V52Δ*vasH* and C6706, which do not engage in VasH-mediated transcription of the *vasX*-encoding operon. Expression driven by P_{vasX} implies that C6706 expresses this immunity gene at low levels under laboratory conditions independent from the remaining T6SS genes to mediate protection against a T6SS-onslaught by bacterial neighbors. This was demonstrated experimentally by showing that deletion of *vasX* and *vasH* renders V52 susceptible to killing by wild-type V52 because the double mutant is unable to drive transcription of *tsiV2* from either promoter. Furthermore, deletion of *vasX* in C6706 rendered this strain susceptible to killing by V52 because it lacks VasH-mediated transcription, and the putative promoter encoded within *vasX*. Taken together, I conclude that *tsiV2* is under the control of a dual regulatory mechanism that ensures basal expression under all conditions. I speculate that maintaining

constitutive expression of immunity genes independently from other T6SS genes provides the bacterium with a fitness advantage in the event it engages in T6SS dueling with another T6SS^{+} bacterium.

In all TA and colicin systems, the presence of an immunity protein or anti-toxin prevents auto-intoxication and/or sororicide. Commonly, the immunity protein is encoded directly adjacent to the colicin/toxin gene or in some cases within a distinct operon on the opposite strand of DNA [231, 443, 444]. The genetic organization of *vasX* and *tsiV2* is in accordance with the chromosomal organization of colicin genes where the colicin/immunity gene-containing operon is regulated by a promoter upstream of the colicin gene; however, a second promoter exists within the colicin gene that specifically drives low-level expression of the immunity gene to protect against auto-toxicity [278, 282, 293, 294]. Interestingly, with regards to colicin genetics, this dual regulatory mechanism is common for nuclease colicins, and not pore-forming colicins [241, 257, 258, 283, 289-292, 438]. Typically, the immunity proteins of pore-forming colicins are encoded within a separate operon and on the opposite strand of DNA [231, 443, 444]. Therefore, VasX and TsiV2 do not fall within the canonical genetic organization for a membrane-targeting toxin/immunity system.

Constitutive low-level expression of immunity proteins is common with regards to colicin biology [231, 285] and it is currently unclear how such a small amount of protein can be protective against incoming colicin molecules. Along these lines, I observed that expression of *tsiV2* need not be induced to protect C6706Δ*tsiV2* from attack by V52 (Figure 5-2) and incredibly, that *tsiV2* was

protective when cloned into the plasmid pJET1.2/blunt which should not result in *tsiV2* expression (Figure 5-3). However, mutated forms of *tsiV2* (with premature stop codons, or lacking a start codon) failed to protect C6706Δ*tsiV2* implying that *tsiV2* must undergo transcription and translation into a protein in order to be protective. Contrary to these results, I also observed that over-expression of *tsiV2* is toxic to the producing cell (Figure 5-5). Because TsiV2 localizes to the inner membrane (Figure 5-9) and forms a LPCx (Figures 5-15, 5-16, and 5-18), I speculate that over-expression of this protein results in the formation of large TsiV2 complexes that insert into, and disrupt the inner membrane resulting in the reduction of surviving bacteria. This idea is supported by the results presented in Figure 5-21 where purified, recombinant TsiV2 was capable of disrupting LUVs resulting in CF release. This would also account for the toxicity observed when LS::vasX and TsiV2 are over-produced within the same cell. Simultaneous over-production of two proteins that disrupt the inner membrane would act as a double-edged sword and logically, this would result in auto-toxicity. Obviously, production of TsiV2 must be strictly regulated in order to create a fine balance of TsiV2 within the cell: enough to provide protection against incoming VasX but not enough to induce membrane damage and auto-toxicity.

Attempting to protect C6706Δ*tsiV2* from periplasmic VasX using pJET-tsiV2::6xHis also failed and I propose this resulted from the over-production of LS::vasX. Exporting a large amount of toxin to the periplasm could easily overwhelm the producer cell and present it with too many toxic molecules to counteract. Therefore I propose that T6SS-mediated killing by V52 results in less

VasX being injected into the inner membrane of the target cell compared to over-production of periplasmic VasX.

Although I was unable to demonstrate a direct interaction between VasX and TsiV2 (Figures 5-16, 5-17, and 5-18), I observed that TsiV2 localizes to the inner membrane (Figure 5-9), and that VasX disrupts the inner membrane of its target cells (Figures 4-7, 4-8, and 4-10). Therefore, it is likely that TsiV2 mediates its immunity function by interacting with VasX in the inner membrane. The pore-forming colicin Colicin A and its immunity protein have previously been shown to interact in the inner membrane of target bacteria [432]. The exact mechanism by which immunity proteins to pore-forming colicins prevent toxicity is unknown; however, it has been postulated that they either insert into the colicin pore in the inner membrane acting like a molecular plug, or bind the colicin and prevent pore formation from occurring in the first place.

The immunity protein for colicin A has been shown to form a dimer [445]. I propose that TsiV2 also forms a dimer based on the ~70 kDa LPCx observed in Figures 5-15, 5-16, and 5-18 which is approximately double the size of monomeric TsiV2. TsiV2 is capable of forming higher molecular weight complexes when mixed in solution in the presence of DSP and these complexes dissociate into the ~70 kDa form of the protein upon boiling in sample buffer containing βME. In Figure 5-18B, I observed the presence of a strong ~70 kDa band in boiled samples containing TsiV2::FLAG and a much fainter band in samples that were not boiled. In this case, I purport that boiling the samples resulted in reduction of TsiV2 protein complexes to the stable 70 kDa complex

resulting in a strong band on the western blot. In the case of the non-boiled samples, I believe that the TsiV2 protein complexes were too large to migrate through the SDS gel stacking region and were therefore not detected by western blotting. Overall, these results indicate that the 70 kDa LPCx is a very stable protein complex that resists the reducing and denaturing abilities of βME and SDS.

Based on the results presented in this section, I propose that TsiV2 localizes to the inner membrane and forms a dimer. Upon injection of the T6SS injectosome into the periplasmic space, VasX inserts into the inner membrane of the target cell where it interacts with the TsiV2 LPCx which prevents VasX-mediated disruption of the inner membrane. A model summarizing this proposed model is presented in Figure 5-22.

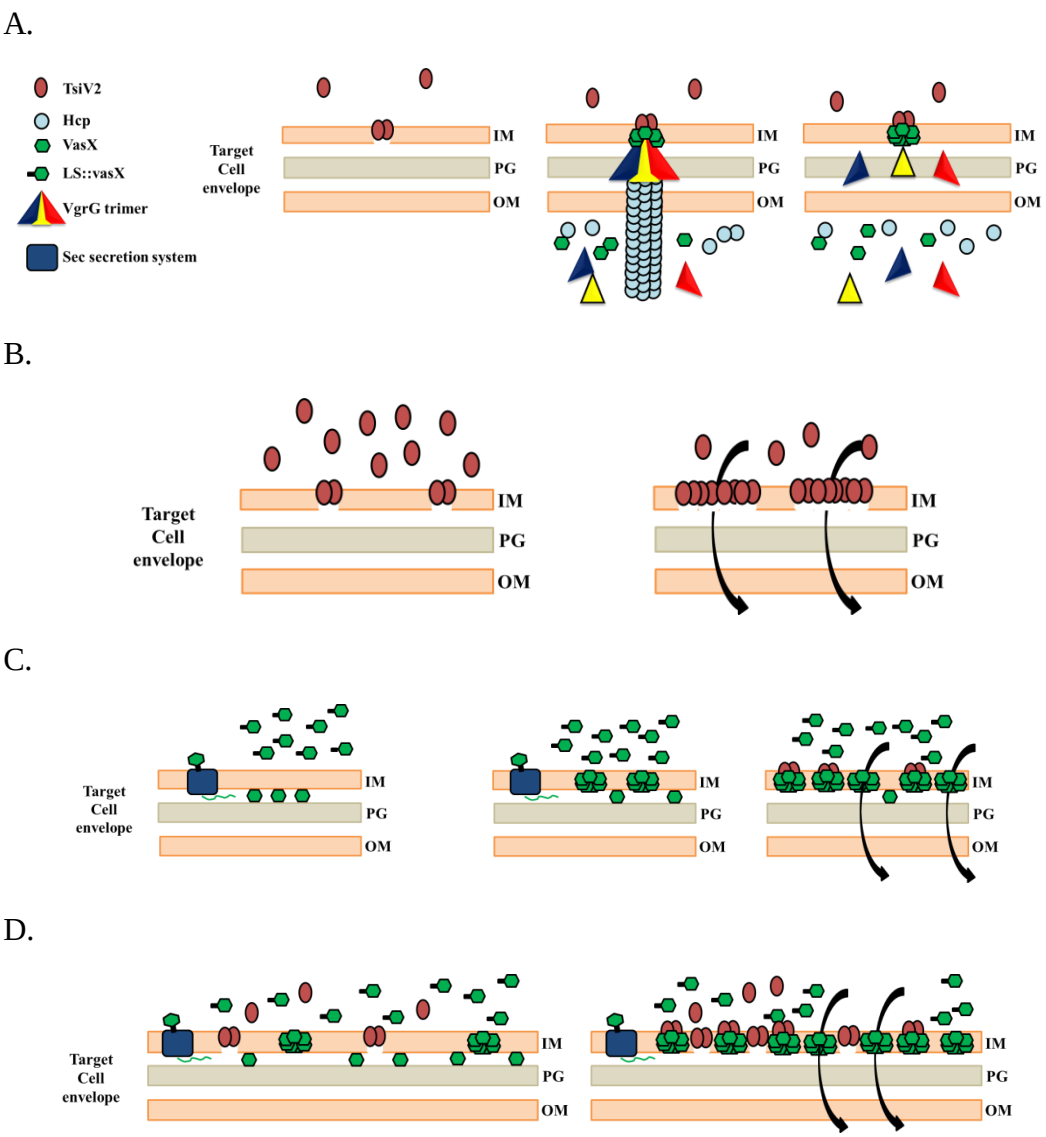

Figure 5-22. Model summarizing the proposed model by which TsiV2 inhibits VasX toxicity. (A) The target cell produces low levels of TsiV2 to protect against VasX toxicity. The cell is injected by the T6SS secretory apparatus from a neighboring bacterium and VasX is delivered to the inner membrane of the target cell. The TsiV2 LPCx in the inner membrane interacts with VasX and prevents membrane disruption. (B) Over-production of TsiV2 results in formation of very large TsiV2 LPCxs in the inner membrane and perturbs the membrane integrity. (C) Over-production of LS::vasX results in excess VasX insertion in the producing cell's inner membrane leading to dissipation of the membrane potential. (D) Over-production of both TsiV2 and LS::vasX results in auto-toxicity due to disruption of the inner membrane by both proteins. Arrows indicate pores through which ions can leak out of the cell. IM; inner membrane, OM; outer membrane, PG; peptidoglycan.

CHAPTER 6

VasW is an accessory component for VasX-mediated killing

The data for Figures 6-2 and 6-3 was provided by Sydney Rudko.

6. VasW is an accessory component for VasX-mediated killing

6.1 Introduction

V. cholerae V52 uses its T6SS to kill both prokaryotic and eukaryotic cells [194, 211, 218, 219]. Some toxins produced by V52, such as VgrG-3 with its peptidoglycan degrading capabilities, appear to strictly target prokaryotes. Conversely, some toxins are targeted more specifically toward eukaryotes (i.e. VgrG-1 and its actin cross-linking domain). On the other hand, VasX has dual capabilities and is important for killing both prokaryotes and eukaryotes.

VasX is encoded within a T6SS satellite gene cluster that also encodes *hcp-2*, *vgrG-2*, *vasW*, and *tsiV2*. With the exception of VasW, I have presented evidence that each of the proteins encoded within this gene cluster are involved in VasX-mediated toxicity. I demonstrated that VgrG-2 and Hcp are crucial for VasX secretion (Figure 2-4) and that VasX physically interacts with both of these proteins (Figure 2-8). Chapter 5 was dedicated to characterizing TsiV2 as the VasX immunity protein. Given that *vasW* is located directly upstream of *vasX*, I asked whether VasW was important for VasX-mediated toxicity toward eukaryotes and prokaryotes.

According to bioinformatics analysis of various *V. cholerae* strains, the gene located directly upstream of a T6SS toxin, the gene for the toxin itself, and the gene encoding the corresponding immunity proteins are organized in genetic "modules" that are always found together (D. Unterweger, unpublished

observation). For example, *vasW*, *vasX*, and *tsiV2* are one such module found in the *V. cholerae* chromosome and any *V. cholerae* strain that encodes VasX also encodes VasW and TsiV2 (D. Unterweger, unpublished observation). These modules have a significantly lower G-C content than the flanking DNA regions suggesting that entire modules may be exchanged via horizontal gene transfer. Furthermore, the modular organization of T6SS toxin and immunity protein genes provides a plausible explanation as to why some *V. cholerae* strains kill other *V. cholerae* strains [369] but others, such as C6706, are resistant [211]. That is, if two neighboring bacteria encode the same T6SS module, they possess the same toxin and immunity protein genes and will therefore not kill one another. On the other hand, if two neighboring bacteria harbor different T6SS modules then they will engage in T6SS-mediated competition because they are not immune to the toxin utilized by the neighboring strain (D. Unterweger, unpublished observation).

VasW, VasX, and TsiV2 are all encoded within a T6SS module on the *V. cholerae* small chromosome. In *V. cholerae* strains where *vasX* is replaced by a different gene, *vasW* also differs (D. Unterweger, unpublished observation) and this led me to postulate that VasW is an accessory protein, or chaperone, for VasX. Here I present evidence that VasW is important for T6SS-mediated killing of *D. discoideum* and Gram-negative bacteria. The data suggests that VasW is an accessory protein that is necessary for the proper localization and/or function of VasX.

6.2 Results

6.2.1 Bioinformatics analysis of VasW

BLASTp analysis determined that VasW is a conserved hypothetical protein containing the domain of unknown function, DUF4123. No characterized homologues were identified. The subcellular localization prediction tool PSORTb failed to identify a specific cellular compartment to which VasW is likely targeted. Analysis of the VasW amino acid sequence by TMHMM, SOSUI, and Phobius did not identify any trans-membrane helices, and analysis using SignalP suggested that VasW does not possess a canonical secretion signal peptide. HHPred indicated secondary structure similarity between VasW and a sortase localization domain. Taken together, the bioinformatics analysis for VasW was largely inconclusive and indicates that VasW is an uncharacterized protein with no characterized, conserved domains or predicted function with respect to the T6SS.

6.2.2 VasW is required for virulence toward *D. discoideum*

I previously demonstrated that VasX is required for V52 virulence toward the amoeboid host model *D. discoideum* (Figure 3-2). Because *vasW* is located directly upstream of *vasX*, I wondered whether VasW also played a role in the killing of *D. discoideum*. To test this, I created a V52 *vasW* deletion strain (V52Δ*vasW*). In addition, *vasW::FLAG* was cloned into pBAD24 to allow for arabinose-inducible expression of *vasW* (pBAD24-vasW::FLAG). The virulence

of V52Δ*vasW* and V52Δ*vasW*/pBAD24-vasW::FLAG toward amoebae was assessed using the *D. discoideum* plaque assay. No plaques developed in a lawn of wild-type V52; however, the lawn of the T6SS-null strain V52Δ*vasK* had ~200 plaques. As observed previously (Figure 3-2), V52Δ*vasX* was attenuated in its virulence toward *D. discoideum* but not to the extent of V52Δ*vasK* (Figure 6-1). Interestingly, V52Δ*vasW* was also attenuated in its virulence toward *D. discoideum* and the number of plaques in the lawn of V52Δ*vasW* was more similar to that of V52Δ*vasX* compared to V52Δ*vasK* (Figure 6-1). Virulence of V52Δ*vasW* was restored upon expression of *vasW in-trans* (in the presence of arabinose) indicating that deletion of *vasW* did not result in a polar mutation (Figure 6-1). This data suggests that VasW is important for V52 to kill *D. discoideum*.

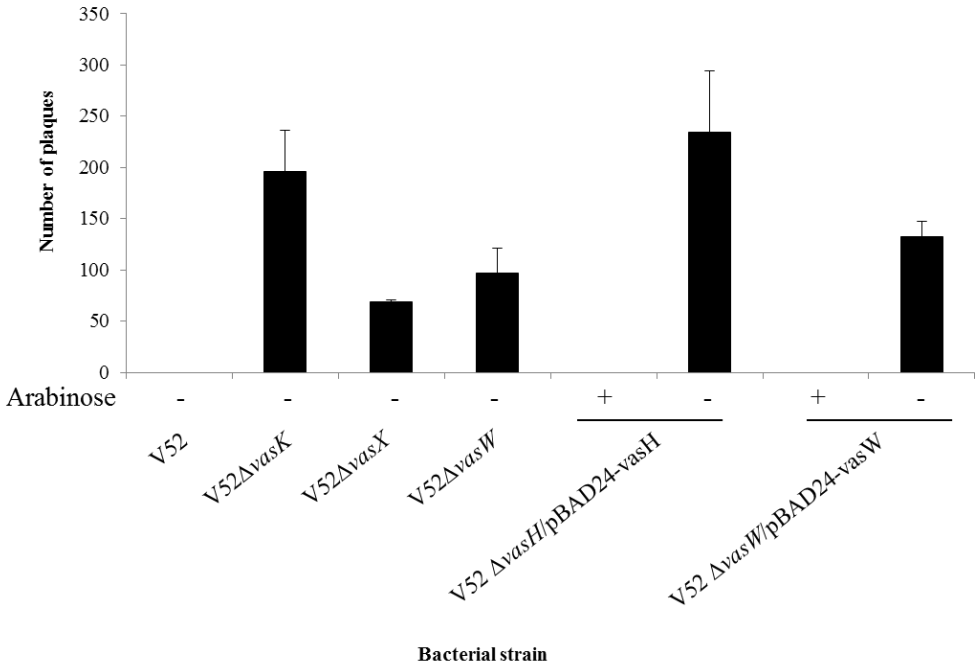

Figure 6-1. VasW is important for V52 virulence towards *D. discoideum*. Cultures of the strains indicated on the *x*-axis were mixed with *D. discoideum* amoebae and spread onto SM/5 nutrient agar plates (+/- arabinose). Plaques resulting in the bacterial lawn indicate zones of clearing where the bacteria have been preyed upon. Error bars indicate the standard deviation.

6.2.3 VasW is required for T6SS-mediated bacterial killing

Given that VasW is important for V52 to kill *D. discoideum*, we wondered whether VasW was also involved in T6SS-mediated killing of *E. coli*. Killing assays were performed using V52Δ*vasW* predator and *E. coli* prey. I observed that wild-type V52, V52Δ*vasX*, and V52Δ*vasW* retained the ability to kill *E. coli*; however, the T6SS-null mutant V52Δ*vasK* did not (Figure 6-2). Therefore, similar to VasX, VasW is not required for V52 to kill *E. coli*.

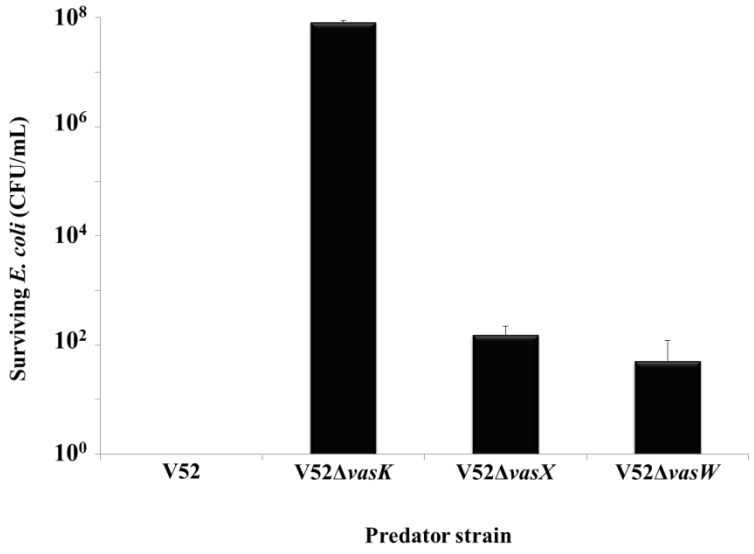

Figure 6-2. VasW is not required for V52 to kill *E. coli*. Survival of rifampicin-resistant *E. coli* was determined by measuring CFU following exposure to the indicated rifampicin-sensitive predator listed on the *x*-axis. Arabinose was included to induce expression from the P_{BAD} promoter where indicated (inducing conditions). Error bars indicate the standard deviation.

I previously demonstrated that *V. parahaemolyticus* was susceptible to killing by V52 in a VasX-dependent manner and that the other two T6SS toxins TseL and VgrG-3 did not mask the VasX killing phenotype when using *V. parahaemolyticus* as prey (Figure 4-3). Given my hypothesis that VasW is an accessory to VasX-mediated toxicity, we therefore decided to test the ability of V52Δ*vasW* to kill *V. parahaemolyticus*. As expected, co-incubation of *V. parahaemolyticus* with V52 resulted in a large (~6-log) reduction in surviving prey whereas the T6SS-null strain V52Δ*vasK* was unable to kill *V. parahaemolyticus* (Figure 6-3). As observed previously, episomal expression of *vasX* provided V52Δ*vasX* the ability to kill *V. parahaemolyticus* (Figures 4-3 and 6-3). I observed that V52Δ*vasW* is attenuated in its ability to kill *V.*

parahaemolyticus and this can be complemented by expressing *vasW in-trans* (Figure 6-3). Interestingly, over-expressing *vasX* in V52Δ*vasW* was unable to complement for the lack of *vasW* (Figure 6-3).

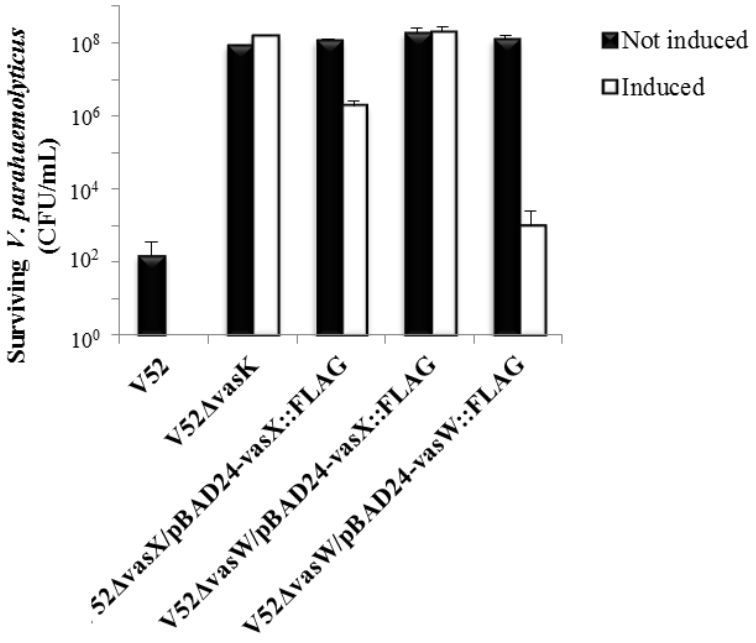

Figure 6-3. VasW is required for V52 to kill *V. parahaemolyticus*. Survival of rifampicin-resistant *V. parahaemolyticus* was determined by measuring CFU following exposure to the indicated rifampicin-sensitive predator listed on the *x*-axis. Arabinose was included to induce expression from the P_{BAD} promoter where indicated (i.e. inducing conditions). Error bars indicate the standard deviation.

To determine whether VasW is important specifically for VasX-mediated bacterial killing, I performed a killing assay using V52Δ*vasW*/pBAD24-vasW::FLAG predator and C6706Δ*tsiV2* prey. We previously determined that TsiV2 specifically inhibits VasX toxicity (Figures 5-1 and 5-2). Thus, if V52Δ*vasW* is unable to kill C6706Δ*tsiV2*, this explicitly implicates VasW as a factor in VasX toxicity. I observed that V52 and V52Δ*vasK* controls behaved as expected and V52Δ*vasX*/pBAD24-vasX killed C6706Δ*tsiV2* under inducing conditions (Figure 6-4). Under non-inducing conditions, V52Δ*vasW*/pBAD24-vasW::FLAG was attenuated towards C6706Δ*tsiV2* whereas in the presence of arabinose, the killing phenotype was restored to the same levels as wild-type V52 (Figure 6-4). Therefore, mutation of *vasW* affects the ability of VasX to function and/or localize properly in V52 as V52Δ*vasW* is attenuated in its killing against C6706Δ*tsiV2*.

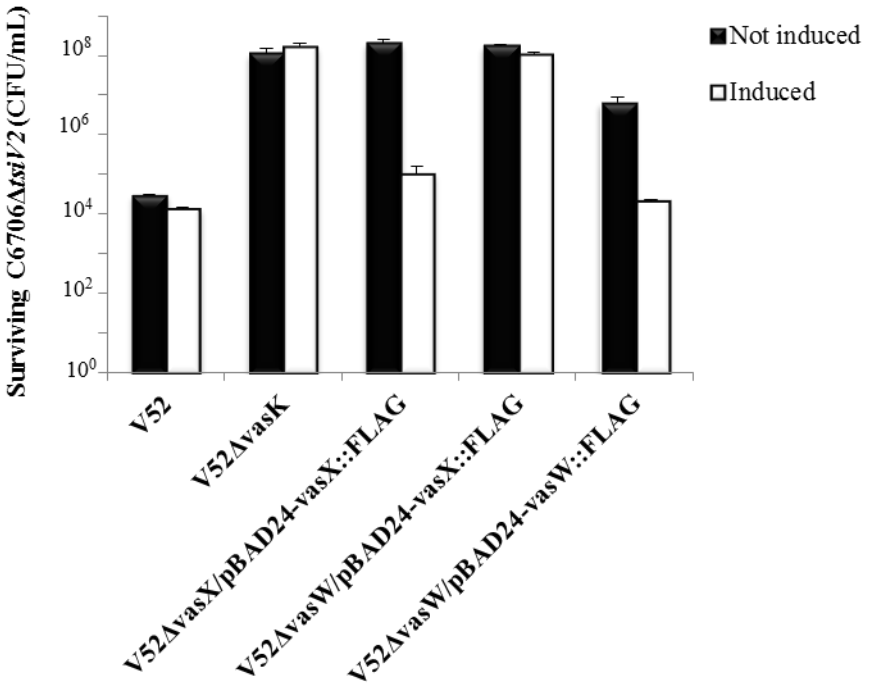

Figure 6-4. VasW is required for V52 to kill C6706Δ*tsiV2*. Survival of rifampicin-resistant C6706Δ*tsiV2* was determined by measuring CFU following exposure to the indicated rifampicin-sensitive predator listed on the *x*-axis. Arabinose was included to induce expression from the P_{BAD} promoter where indicated (i.e. inducing conditions). Error bars indicate the standard deviation.

6.2.4 Analysis of the V52Δ*vasW* secretion profile

Since VasW is an important protein for the proper functioning of the *V. cholerae* T6SS, we wondered what effect deletion of *vasW* had on the mutant bacterium's secretion profile. Secretion of Hcp is the hallmark of a functional T6SS apparatus and therefore I wondered whether V52Δ*vasW* was capable of

secreting Hcp into culture supernatants. Furthermore, we and others previously observed that V52Δ*vgrG-3*Δ*vasX* lacks Hcp secretion (Figure 6-5 and [374]). Given that VasW is imperative for VasX to function, I wondered whether V52Δ*vgrG-3*Δ*vasW* lacks Hcp secretion similar to V52Δ*vgrG-3*Δ*vasX*. Bacterial pellet and supernatant samples were subjected to western blotting using α-Hcp and α-DnaK (loading and lysis control) antibodies. As expected, V52, V52Δ*vasX*, and V52Δ*vgrG-3* produced and secreted Hcp, while Hcp was present in the pellet of V52Δ*vasK* but was not secreted (Figure 6-5). Similar to V52Δ*vgrG-3* and V52Δ*vasX*, V52Δ*vasW* retained the ability to secrete Hcp (Figure 6-5). On the other hand, although V52Δ*vgrG-3*Δ*vasW* produced Hcp, this strain was unable to export Hcp into culture supernatants (Figure 6-5).

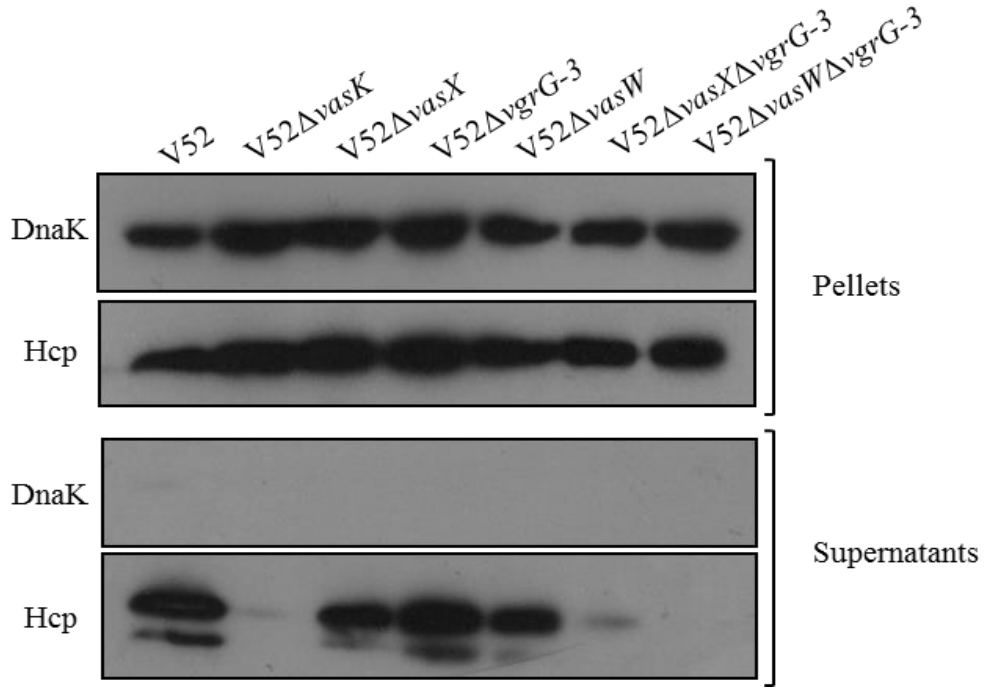

Figure 6-5. V52Δ*vgrG-3* with deletions in *vasW* or *vasX* does not secrete Hcp. Overnight bacterial cultures were grown to mid-logarithmic phase in the presence

of arabinose (to induce expression from the P_{BAD} promoter). Bacterial pellet and supernatant samples were subjected to western blotting with α-Hcp and α-DnaK (loading and lysis control) antibodies.

Since I hypothesized that VasW is an accessory protein for proper VasX function/localization, I also wondered whether V52Δ*vasW* was able to secrete VasX. Bacterial pellet and supernatant samples (grown in the presence of arabinose) were subjected to western blotting with α-VasX and α-DnaK (loading and lysis control) antibodies. VasX is present in the cell pellet of all strains analyzed but was only secreted by V52 (containing empty vector pBAD24), V52Δ*vasX*/pBAD24-vasX, and V52Δ*vasW*/pBAD24-vasW::FLAG (Figure 6-6). V52Δ*vasK* and V52Δ*vasW* (both containing empty vector pBAD24) failed to secrete VasX into culture supernatants (Figure 6-6). Therefore, VasW is imperative for VasX secretion and this defect can be complemented by expressing *vasW in-trans*.

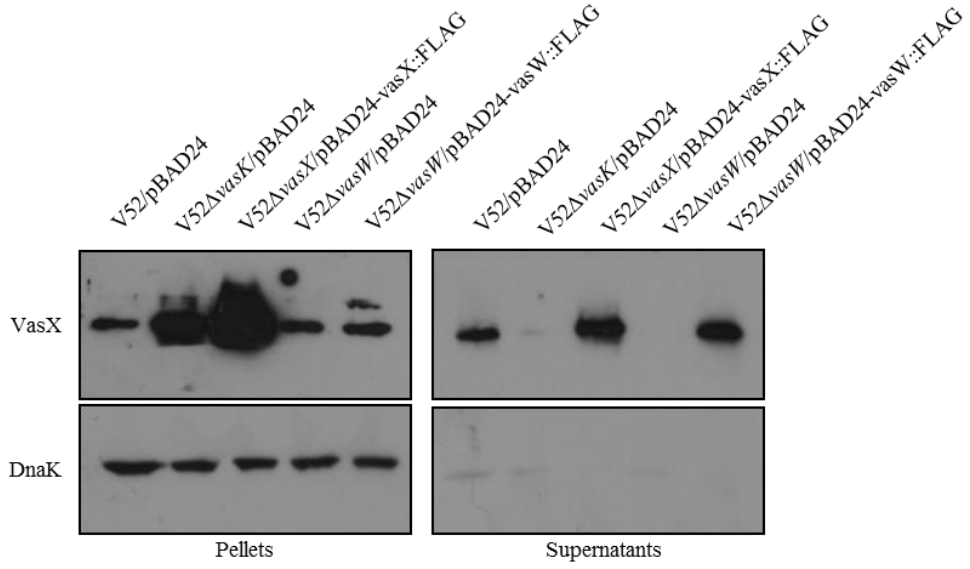

Figure 6-6. V52Δ*vgrG-3*Δ*vasW* does not secrete VasX. Overnight bacterial cultures were grown to mid-logarithmic phase. Bacterial pellet and supernatant samples were subjected to SDS-PAGE followed by western blotting with α-VasX antibody and α-DnaK (loading and lysis control) antibodies.

6.2.5 VasW is not required for formation of the VasX LPCx

VasX depends on VasW for secretion which likely accounts for the similar phenotypes observed between V52Δ*vasX* and V52Δ*vasW* in the bacterial killing assay and *D. discoideum* plaque assay. I previously demonstrated that VasX is present strictly in the forms of a LPCx in the V52 membrane (Figure 2-11). Because I propose that VasW acts as a chaperone to VasX, I tested whether VasW is required for formation of the VasX LPCx. Non-boiled V52, V52Δ*vasX*, and V52Δ*vasW* lysate samples were subjected to SDS-PAGE followed by western blotting with α-VasX primary antibody. As expected, VasX was present in both monomeric form and as the LPCx in V52 lysates, but not in V52Δ*vasX* (Figure 6-7). V52Δ*vasW* produced both monomeric VasX and the VasX LPCx (Figure 6-7). Therefore, VasW is not required for formation of the VasX LPCx.

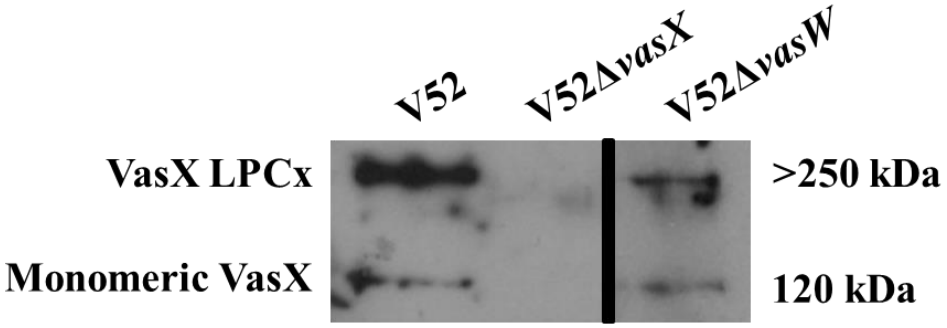

Figure 6-7. VasW is not required for formation of the VasX LPCx. Bacterial cultures were grown to mid-logarithmic phase and pellet samples were resuspended in protein sample buffer, but not boiled. Samples were subjected to SDS-PAGE followed by western blotting with α-VasX primary antibody.

6.3 Discussion

Directly upstream of *vasX* is the gene *vasW* which encodes a previously uncharacterized protein. Here, we demonstrated that VasW is important for VasX-mediated killing of amoebae and bacteria. According to bioinformatic analysis of the *V. cholerae* T6SS gene clusters, *vasW* and *vasX* are always encoded together (D. Unterweger, Unpublished) and we therefore hypothesized that the two gene products work together to mediate VasX toxicity. In accordance with this hypothesis, I observed that V52Δ*vasW* exhibits the same phenotype as V52Δ*vasX* when used as predator in the bacterial killing assay (Figures 6-2, 6-3, and 6-4), and when challenged with *D. discoideum* in the plaque assay (Figure 6-1). Furthermore, we demonstrated that both V52Δ*vgrG-3*Δ*vasW* and V52Δ*vgrG-3*Δ*vasX* are unable to secrete Hcp into culture supernatants (Figure 6-5) which lends additional support to the idea that deletion of *vasW* results in similar phenotypes compared to deletion of *vasX* in V52. Taken together, these data indicated that deletion of *vasW* likely interferes with VasX toxicity. Importantly, we observed that V52Δ*vasW* had a reduced ability to kill C6706Δ*tsiV2* and that this phenotype could be complemented by expression of *vasW in-trans.* This result confirmed that deletion of *vasW* abrogates the toxic effects of VasX

because TsiV2 specifically inhibits VasX-mediated bacterial killing (Figures 5-1 and 5-2, and [221]).

Interestingly, episomal expression of *vasX* did not restore the killing ability of V52Δ*vasW* indicating that the *vasW* mutation did not result in polar effects on *vasX*, and that even when over-produced, VasX is non-toxic toward target cells in the absence of *vasW* (Figures 6-3 and 6-4). Western blotting for Hcp and VasX indicated that V52Δ*vasW* retained the ability to secrete Hcp and produce the VasX LPCx, but does not secrete VasX (Figures 6-6 and 6-7). This implies that VasW is not required for proper formation of the T6SS injectosome (similar to VasX) or for multimerization of VasX in the bacterial membrane; however, VasW is crucial for exporting VasX out of the cell.

The data presented in this chapter lead me to propose a model whereby VasW acts as a chaperone and is responsible for localizing VasX to the T6SS secretory apparatus. The use of accessory proteins in bacterial toxin secretion has been previously documented for *B. pertussis* and *A. tumefaciens*. Pertussis toxin is a major virulence factor produced by *B. pertussis* that is exported into the periplasm via the general secretory pathway. Once in the periplasm, pertussis toxin relies on the accessory protein PtlC for secretion across the outer membrane [446]. In *A. tumefaciens*, the VirB operon encodes 11 proteins, 10 of which are essential for T4SS-mediated virulence [447]. The accessory protein VirB4 is essential for the proper localization of other VirB proteins to the inner and outer membranes [447].

In the case of the T6SS, I propose that VasW bridges the interaction between the VasX membrane-associated LPCx and the tip of the secretion apparatus consisting of VgrG proteins. In V52Δ*vasW*, the VasX LPCx is unable to localize to the T6SS injectosome. The absence of VasX association with the secretory apparatus does not impair VipA/VipB contraction and ejection of the VgrG/Hcp tube from the cell. Hcp and VgrG proteins sloughed from the secretion apparatus result in the presence of these proteins in culture supernatants and VasX-independent T6SS toxicity toward prey cells (mediated by TseL and VgrG-3). Figure 6-8 summarizes the proposed model for the role of VasW in VasX-mediated toxicity.

A.

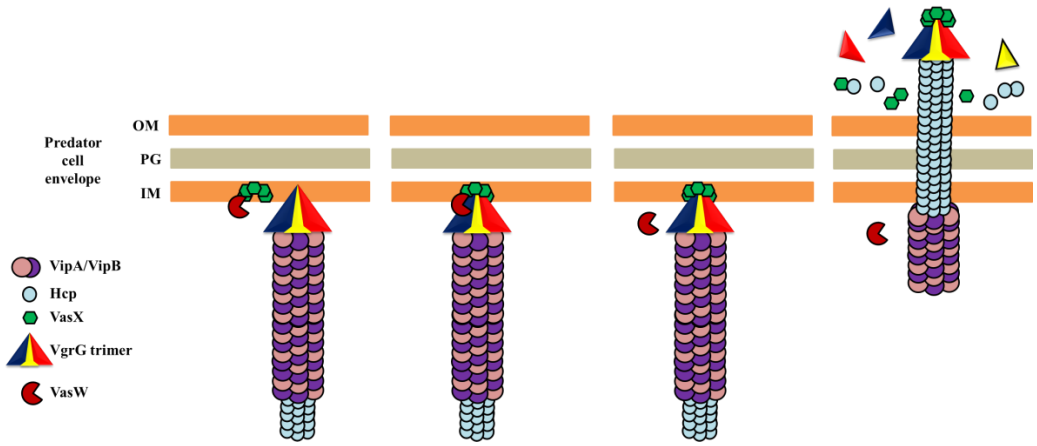

B.

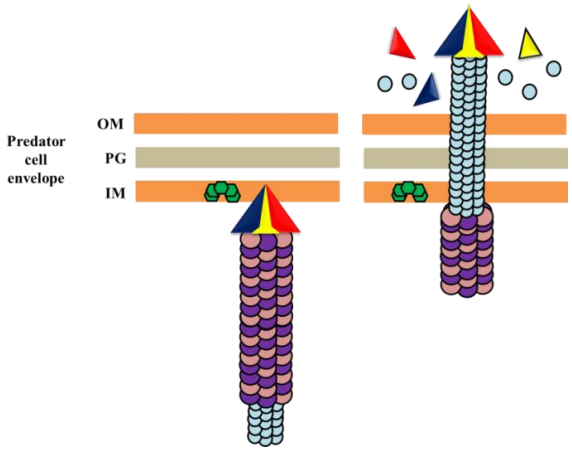

Figure 6-8. Proposed model where VasW bridges the interaction between VasX and the T6SS secretory apparatus. (A) VasW interacts with the VasX LPCx in the inner membrane of the T6SS^{+} cell and brings the LPCx into contact with the VgrG cap of the T6SS needle complex. After VasX is associated with the T6SS injectosome, VasW dissociates and the VipA/VipB outer sheath contracts. The Hcp inner tube capped with the VgrG/VasX protein complex is ejected from the cell resulting in sloughing of VasX, Hcp, and VgrG proteins into culture supernatants. (B) In the absence of VasW, the VasX LPCx fails to interact with the VrgG trimer. Contraction of the VipA/VipB sheath ejects the Hcp/VgrG tube from the cell but VasX remains in the inner membrane.

CHAPTER 7

7. General Discussion

7.1 Benefits conferred to *V. cholerae* by the T6SS

The T6SS is used by a variety of Gram-negative bacteria to target eukaryotes and/or prokaryotes. Initially, the T6SS was described as a virulence mechanism used by bacteria to target host cells; however, advances in the field have identified this secretion system as a mechanism also used to mediate bacterial killing. In some T6SS$^+$ bacteria such as *E. tarda* and *B. mallei*, the T6SS has been described solely as a killing mechanism targeting host cells [226-229]. On the other hand, *S. marcescens* and *A. baumannii* use their T6SS to kill other bacteria [212, 217]. *B. thailandensis* possesses five T6SS gene clusters, one of

which is known to target eukaryotes and another targets prokaryotes (the function of the other three is currently unclear, but bioinformatics analysis suggests they likely target prokaryotes) [213]. *V. cholerae* is unique in that it possesses one T6SS gene set, the products of which can target both eukaryotes and prokaryotes. This ability likely confers a significant evolutionary advantage to this organism both in its natural environment and during infection of the human host. As a marine organism, *V. cholerae* is constantly exposed to a variety of other microorganisms with which it competes for space and nutrients. The T6SS is one way by which *V. cholerae* could out-compete microbial neighbors to foster its own survival under conditions of low nutrient availability.

Bacteriocins represent one field of inter-bacterial interactions that has been extensively studied involving the secretion of toxic peptides for the purpose of killing closely-related microorganisms. However, the majority of this research was carried out in the 1970s-1990s and has since tapered off. Interest in studying inter-bacterial interactions has been revived in recent years with the observation that the T6SS is used as a bacterial killing machine. Future studies on the T6SS could lead to manipulation of the inherent toxin/immunity systems resulting in sororicide and self-elimination from a given niche.

When humans ingest food or water contaminated with *V. cholerae,* the bacteria enter the small intestine where they encounter the host microbiota and invading cells of the immune system. Here, the T6SS could be used to establish infection by killing members of the resident microflora and by warding off professional phagocytes. In either case, the presence of immunity proteins

protects *V. cholerae* from eliminating itself in the environment or during host infection due to sororicide.

The majority of the data presented here involve VasX – one of the four T6SS toxins used by *V. cholerae* to mediate killing of eukaryotes and prokaryotes. *V. cholerae* possesses an arsenal of toxins that target different cell types and different cellular compartments of the same cell. For instance, VgrG-3 degrades peptidoglycan in the bacterial cell wall causing lysis whereas VgrG-1 cross-links host cell actin. At this time we cannot rule out the possibility that VgrG-1 has a dual function targeting the actin homologue, MreB, in prokaryotes; however the fact that *vgrG-1* is not followed by an immunity protein-encoding gene (D. Unterweger, unpublished observation) supports the idea that VgrG-1 does not target bacteria. Both TseL and VasX are toxic toward both prokaryotes and eukaryotes and both act at the cytoplasmic membrane carrying out different toxic functions. VasX is the first T6SS toxin described that disrupts the integrity of the cytoplasmic membrane, possibly via pore-formation. T6SS toxins target cellular structures that are important for survival – the actin cytoskeleton, peptidoglycan cell wall, and cytoplasmic membrane. These targets, as opposed to a single protein/receptor, provide an evolutionarily advantageous mechanism employed by bacterial toxins since developing resistance to this toxic mechanism would prove challenging for target cells. It is likely that in both the environment and during host infection the T6SS provides a fitness advantage for $T6SS^{+}$ bacteria.

7.2 VasX: summary and future studies

The data presented here largely pertain to the characterization of VasX – a secreted protein encoded within an auxiliary T6SS gene cluster in *V. cholerae*. I have presented experimental data suggesting that VasX is a T6SS toxin used to mediate virulence toward *D. discoideum* (Chapter 3) and killing of Gram-negative bacteria (Chapter 4). With regards to VasX-mediated toxicity toward eukaryotic cells, it remains unclear why VasX is important for virulence toward *D. discoideum* and not macrophages. The first step to understanding this paradox would be to determine whether phagocytosis is required for *V. cholerae* T6SS-mediated virulence toward *D. discoideum*. This could be achieved by infecting *D. discoideum* with V52 in the presence of the phagocytosis inhibitor cytochalasin D and enumerating the surviving cells following infection. Gentamicin protection assays could also help determine whether *V. cholerae* is indeed phagocytosed by *D. discoideum*.

To ascertain whether VasX acts from the exterior (as proposed in Figure 3-14), *D. discoideum* could be incubated with purified, recombinant VasX followed by enumeration of cells with damaged membranes using PI and flow cytometry. Furthermore, expressing *vasX* from a eukaryotic expression vector within *D. discoideum* and subsequently measuring toxicity would help rectify whether VasX acts from the exterior or interior of the host cell. Multiple lines of evidence (Chapter 4) indicate that VasX acts as a bacterial toxin that targets the cytoplasmic membrane of target bacteria. Because VasX has the ability to target both prokaryotes and eukaryotes, it is likely that both targets share a common

target upon which VasX acts. Prokaryotes and eukaryotes both have cytoplasmic membranes. Since VasX must be presented to target bacteria from the periplasmic space in order to be toxic, I propose that VasX also acts from the exterior of *D. discoideum* where it can insert into and disrupt the integrity of the cytoplasmic membrane resulting in toxicity.

It is clear that VasX possesses the ability to disrupt the cytoplasmic membrane of target cells. VasX inserts into MLVs (Figure 3-8), is able to elicit release of CF from LUVs (Figure 4-11) and makes the target cell more permeable to PI (Figure 4-10); however it does not cause complete lysis of cells as DnaK is not released by cells producing LS::vasX (Figure 4-9). Based on these observations I propose that VasX forms pores in the inner membrane of target cells thereby dissipating the cell's energy reserves and eventually causing cell death.

Pore-formation by VasX could be demonstrated by monitoring the flow of ions across a lipid bi-layer *in-vitro* using a potassium electrode. I propose that addition of purified, recombinant VasX to planar lipid bi-layers would result in the flow of ions between the two solutions; however, larger molecules would not be able to traverse the VasX pores. The result of this experiment would determine whether VasX forms pores large enough to permit ion flow but too small to allow passage of larger molecules. Atomic force microscopy could also be used to physically visualize the pores formed in the inner membrane of target cells.

It also remains unclear how exactly VasX is secreted from the producing cell. When I first identified VasX, I proposed that it traversed the inner tube of the T6SS needle complex *en route* out of the producing bacterium. Three other T6SS toxins have been identified (TseL, VgrG-3, and VgrG-1): all of which are large proteins (i.e. > 70 kDa) and are secreted into culture supernatants [209, 210, 221, 319]. It seems unlikely that all *V. cholerae* T6SS toxins independently traverse the tube created by Hcp hexamers, especially given that the VgrG proteins at the tip of the Hcp tube form a cap that lacks a pore through which T6SS toxins could be secreted. Secretion through the Hcp tube would require significant rearrangements to the proteins' secondary structures and would therefore be energetically unfavorable for the cell. Thus, I propose that the T6SS toxins TseL and VasX associate with the T6SS structural components Hcp and VgrG and are ejected from the bacterium upon contraction of the VipA/VipB outer sheath. This contrasts with the translocation of effector molecules mediated by the T3SS whereby effectors are translocated through the secretion machinery and into host cells [448-450].

7.3 TsiV2: summary and future studies

TsiV2 is a protein that specifically inhibits the toxic effects mediated by VasX. Providing *tsiV2 in-trans* was able to elicit protection against VasX in *V. parahaemolyticus* (Figure 5-7) and C6706Δ*tsiV2* (Figure 5-2) even when expression of the gene was not induced. However, site-directed mutagenesis

studies (Figure 5-4) introducing premature stop codons in *tsiV2* resulted in the inability to protect against an oncoming T6SS attack. It would be interesting to determine how, exactly, such small amounts of TsiV2 are capable of protecting bacteria against VasX-mediated toxicity.

To address this, one could determine where TsiV2 localizes within the cell. Subcellular fractionation indicated that TsiV2 localized to the bacterial inner membrane (Figure 5-9); however these studies could not determine whether TsiV2 clustered in one area of the membrane (such is the case with lipid rafts), or if small amounts of TsiV2 were evenly distributed around the inner membrane. Immunofluorescence microscopy using antibodies to TsiV2, or immunogold labeling of TsiV2 followed by transmission electron microscopy, could determine the spatial distribution of TsiV2 within the bacterial cell. The result of this experiment would provide insight not only into the mechanism behind TsiV2 immunity but also the physiological dynamics involved in a T6SS attack.

If TsiV2 is clustered in foci within the membrane, this would suggest that the *V. cholerae* T6SS injects the secretory apparatus at a specific site into the target cell. For example, this site could be defined by a receptor present on the bacterial membrane to which the T6SS injectosome is targeted. On the other hand, if TsiV2 is distributed evenly throughout the inner membrane, this would suggest that the cell is protected against a T6SS attack regardless of the point of entry of the attacking cell.

Constitutive expression of *tsiV2* is maintained by the promoter located within the 3' 1050 nucleotides of *vasX* (Figures 5-11, 5-12, and 5-143). I speculate that maintaining constitutive expression of immunity genes independently from other T6SS genes provides the bacterium with a fitness advantage in the event it engages in T6SS dueling with another $T6SS^+$ bacterium either in its natural environment or upon encountering the gut microbiota within the human host. Confirming the promoter prediction presented in Figure 5-14 could be accomplished by cloning the ~65 basepair fragment of *vasX* upstream of a reporter gene such as *lacZ* and determining the transcriptional start site could be achieved using 5' rapid amplification of cDNA ends (5' RACE).

Despite numerous attempts, I was unable to determine whether VasX and TsiV2 physically interact. One would assume, based on the data presented in Chapter 5, that the two proteins must interact in order for TsiV2 to inhibit the toxic effects of VasX. If VasX forms a pore in the inner membrane, it is likely that TsiV2 binds VasX and plugs the VasX pore, or TsiV2 binds VasX in the membrane and prevents pore formation from occurring. Further experiments could be performed to test whether TsiV2 and VasX interact, including a bacterial two-hybrid approach, fluorescence resonance energy transfer (FRET), or split GFP.

7.4 VasW: summary and future studies

The data presented in Chapter 6 suggests that VasW acts as an accessory protein involved in VasX-mediated toxicity. VasW is required for secretion of VasX and therefore, I proposed a model whereby VasW mediates the interaction between VasX and the T6SS secretory apparatus. To confirm this model, nickel pull-downs, co-immunoprecipitations, or a bacterial two-hybrid approach involving VasW and VasX should be performed to determine whether the two proteins physically interact. These same experiments could also be used to determine whether VasX still interacts with Hcp and VgrG proteins in V52Δ*vasW*, or in combination with mass spectrometry, these techniques could identify other interacting partners of VasW (either T6SS-related or unrelated).

Bioinformatics analysis of VasW failed to provide clues indicating where VasW localized within the bacterium. As a VasX chaperone, I hypothesize that VasW is present in the cytoplasm and membrane fractions. Analysis of culture supernatants by western blotting would indicate whether VasW is a secreted protein and subcellular fractionation experiments would delineate where VasW localizes within the cell and could provide insight into the molecular mechanism by which VasW affects secretion of VasX.

7.5 Overall summary of conclusions

The data presented herein describes a mechanism by which *V. cholerae* mediates competition between other bacteria and host cells. I identified the protein VasX and determined its toxic mechanism involves disruption of the

cytoplasmic membrane of target bacteria. *V. cholerae* likely uses VasX, and the other two T6SS bacterial toxins, VgrG-3 and TseL, during microbial competition that arises in the bacterium's marine environment, and/or during host infection when it encounters bacteria belonging to the host microflora. *V. cholerae* avoids killing off its kin by employing an immunity protein that inhibits the action of its cognate toxin. TsiV2 is a membrane protein that protects *V. cholerae* specifically against VasX toxicity. I also identified the protein VasW which is imperative for VasX secretion via the T6SS. It is likely that VasW mediates the interaction between VasX and proteins of the T6SS structural apparatus such as Hcp and VgrGs. Taken together, this work has contributed to our understanding of the structural assembly, and the toxic and immunity mechanisms of the T6SS utilized by *V. cholerae* to mediate both host-pathogen and inter-bacterial interactions.

CHAPTER 8

Materials and methods

Strains and Culture Conditions

The bacterial strains and plasmids used in these studies are presented in Table 8-1 and Table 8-2, respectively. Unless otherwise stated, all bacterial strains were grown in Luria-Bertani (LB) broth at 37 ^{o}C with shaking. *E. coli* strains DH5α λpir and SM10 λpir were used for cloning and mating of suicide vectors, respectively. Top10 *E. coli* was used for all other cloning purposes. Antibiotic concentrations used for bacterial selection were 100 $\mu g \cdot mL^{-1}$ ampicillin, 100 $\mu g \cdot mL^{-1}$ streptomycin, 50 $\mu g \cdot mL^{-1}$ kanamycin, 50 $\mu g \cdot mL^{-1}$ rifampicin, and 10 $\mu g \cdot mL^{-1}$ chloramphenicol. *V. parahaemolyticus* and *V. alginolyticus* were grown in LB containing 3% NaCl at 37^{o}C. *V. fischeri* was grown in GVM medium at room temperature.

D. discoideum AX3 were purchased from the Dicty Stock Center (Northwestern University, IL, U.S.A) and were grown in shaking liquid culture (150 rpm) in HL/5 medium (Table 8-6 and [396]) at 22^{o}C.

Murine RAW 264.7 macrophages, a gift from Dr. Hanne Ostergaard (University of Alberta), were maintained at 37 ^{o}C in a 5% CO_2 atmosphere in Eagle's minimum essential media (Sigma-Aldrich) supplemented with 10% fetal bovine serum, 4 mM L-glutamine, 1 mM sodium pyruvate, 100 $units \cdot mL^{-1}$ penicillin, and 100 $\mu g \cdot mL^{-1}$ streptomycin (Sigma-Aldrich).

Western Blotting

The acrylamide concentration used for SDS-PAGE was 10% unless otherwise noted. SDS-PAGE was performed at 200 volts in Laemmli running buffer (Table 8-6) and transferred to BioRad 0.45 µm nitrocellulose membrane using the BioRad Mini Protean II wet transfer apparatus or the Amersham Biosciences TE 77 semi-dry transfer apparatus. Membranes were blocked for 30-60 minutes in TBS-T containing 5% or 2.5% skim milk powder. Primary antibodies were diluted in 5% or 2.5% milk/TBS-T to the concentrations noted in Table 8-5 and were incubated for at least one hour with shaking. Membranes were then washed 3x 5 minutes in TBS-T. HRP-conjugated secondary antibodies were diluted in 5% milk/TBS-T to the concentrations noted in Table 8-5 and were incubated for 30-60 minutes with shaking. Membranes were washed 3x 5 minutes in TBS-T and bound protein was detected using the SuperSignalWest Pico Chemiluminescent Substrate (Thermo Fisher) according to the manufacturer's instructions and Fuji X-Ray film. Film was developed using a Kodak M35A X-OMAT Processor.

Subcellular Fractionation

Bacterial strains were grown to OD_{600} ~0.8-1.0 in 200mL LB (in the presence of 0.1% arabinose where appropriate) and pelleted by centrifugation at 3,000 x g for 20 minutes. The pellet was resuspended in LB with 1 $mg \cdot mL^{-1}$ polymyxin B and incubated at room temperature for 20 minutes to release periplasmic contents. Permeabilized V52 (lacking periplasmic content) were

pelleted at 3,000 x g for 20 minutes at room temperature. The resulting supernatant was collected as the periplasmic fraction. Permeabilized V52 was washed with 5 mL LB and pelleted at 3,000 x g for 20 minutes at room temperature. The pellet was resuspended in 4 mL PBS and passed twice through a French pressure cell at 8000 psi. Unbroken cells were pelleted and the membrane/cytosolic fraction was retained. Membrane and cytosolic fractions were separated by centrifugation of the resulting supernatant in a Beckman L-30 Optima ultracentrifuge at 100,000 x g for 30 minutes at 4^{o}C in a SW55Ti swinging bucket rotor. Membranes were washed once in 5 mL PBS and pelleted at 100,000xg for 30 minutes at 4^{o}C in a SW55Ti rotor. Protein concentrations of all fractions were determined using the Pierce BCA protein assay. 12 µg of protein was loaded per well on SDS-PAGE for western blot analysis.

Inner and Outer Membrane Fractionation

The indicated bacterial strains were grown to OD_{600} ~ 0.8-1.0 (in the presence of 0.1% arabinose where appropriate) and pelleted by centrifugation at 3,000 x g for 20 minutes. The pellet was resuspended in 4 mL PBS and passed twice through a French pressure cell at 8000 psi. Unbroken cells were pelleted and cell membranes were harvested by centrifugation in a Beckman L-30 Optima ultracentrifuge at 100,000 x g for 30 minutes at 4 ^{o}C in a SW55Ti swinging bucket rotor. The membrane pellet was resuspended in 200 µL PBS and further purified by loading the membranes on top of a discontinuous sucrose gradient

consisting of 4 mL 50% sucrose placed on top of 2mL 75% sucrose. The visible membrane fraction was isolated using a 1 mL syringe and 26.5 gage needle punctured into the side of the ultracentrifuge tube. The purified membrane fraction was diluted in PBS such that the sucrose concentration was less than 20% and was then loaded onto a discontinuous sucrose gradient consisting of 32, 35, 38, 41, 44, 47, 50, 53, and 56% sucrose cushioned by 0.6 mL of 75% sucrose. Ultracentrifugation was performed at 325,000 rpm for 40 hours at 4 ^{o}C in a Beckman L-30 Optima ultracentrifuge. The membranes were collected using a syringe by puncturing the side of the tube every ~500 µL to collect fractions from top to bottom.

Assay for NADH Oxidase activity

Samples resulting from sucrose gradient fractionation were mixed 1:10 in assay buffer (50 mM Tris HCl pH 7.5, 0.12 mM NADH (Roche Applied Science), 0.2 mM DTT) and incubated for 20 minutes at room temperature. NADH oxidase activity (indicative of the inner membrane fraction) was recorded as the drop in OD_{340} read by an XMark microplate spectrophotometer (BioRad). Arbitrary units were determined using the following equation (1- (sample OD_{340} – blank OD_{340})). NADH oxidase values for TsiV2 inner and outer membrane fractionation were calculated with activity of Fraction 1 set to zero.

Mass Spectrometry, Bioinformatic Analysis, Statistical Analysis, and DNA Sequencing and Analysis

Liquid Chromatography/Mass Spectrometry (LC-MS/MS) analysis was performed at the University of Alberta Mass Spectrometry Facility (Department of Chemistry). In-gel proteins were reduced with 4 mM dithiothreitol and carbidomethylated with 10 mM iodoacetamide followed by tryptic digestion overnight with 0.06 $\mu g \cdot \mu L^{-1}$ modified bovine trypsin (Promega, Madison, WI) at $30^{o}C$. Peptides were subjected to LC-MS/MS analysis on a NanoAcquity Ultra Performance Liquid Chromatography System (Waters, Milford, MA) coupled with a Q-TOF Premier mass spectrometer (Waters, Milford, MA). Obtained MS/MS data were analyzed by PEAKS proteomic software (Bioinformatics Solutions Inc., Waterloo, Ontario, Canada).

Secondary structure prediction was performed using the HHpred server [382] and the Phyre server [383, 384]. Bioinformatic prediction of protein subcellular localization was performed using PSORTb (http://www.psort.org/psortb/). The number and position of transmembrane helices for VasX and TsiV2 were predicted using TMHMM (http://www.cbs.dtu.dk/services/TMHMM/), Phobius (http://phobius.sbc.su.se/) and SOSUI (http://bp.nuap.nagoya-u.ac.jp/sosui/sosui_submit.html). Bioinformatics analyses were also performed using BLASTp, psiBLAST, and BLASTn (http://blast.ncbi.nlm.nih.gov/Blast.cgi). The presence or absence of signal peptides was predicted using SignalP (http://www.cbs.dtu.dk/services/SignalP/).

DNA sequencing was performed by Eurofins MWG Operon (Huntsville, Alabama) or The Applied Genomics Centre (University of Alberta). All nucleotide sequence analyses and alignments were performed using Clone Manager Suite Software (version 6.0).

Statistical significance for experimental data was determined using the Tukey's multiple comparison test (95% confidence interval) or the Student's one-tailed, paired T-test (95% confidence interval) (as indicated in the figure legends).

RAW 264.7 Macrophage Infections and Actin Crosslinking

Murine RAW 264.7 macrophages were seeded into 24-well tissue culture plates at a density of 1×10^5 cells per well 18 hours prior to infection. Two hours prior to infection, the penicillin/streptomycin-containing medium was aspirated and the cells were washed twice in pre-warmed PBS. Macrophages were then incubated for two hours in antibiotic-free medium. Cells were infected with V52 and the given T6SS mutants at a multiplicity of infection (MOI) of 10 for two hours at 37^oC. Cells were harvested, supernatants were aspirated, and cells were resuspended in 50 µL of SDS protein sample buffer and boiled for 10 minutes. 10 µL of each sample was analyzed by western blot using actin primary antiserum.

Expression Plasmid Construction

Plasmid minipreps were performed using Qiagen or Thermo Fisher miniprep kits according to the manufacturer's instructions. DNA gel extraction was performed using Qiagen or Thermo Fisher Gel Extraction Kits according the manufacturer's instructions.

The primers used for expression plasmid construction are presented in Table 8-3. The polymerase chain reaction (PCR) was used to amplify chromosomal or plasmid DNA for cloning into the appropriate expression vector (noted in Table 8-2). PCR was performed using Accuprime Pfx (Invitrogen), Platinum Pfx (Invitrogen), or Phusion High Fidelity DNA Polymerase (Thermo Fisher Scientific) and the resulting PCR product was cloned into the TOPO-TA vector pCR2.1 (Invitrogen) or the blunt cloning vector pJET1.2/blunt (Thermo Fisher Scientific) and transformed into Top10 *E. coli* competent cells. Prior to cloning into the TOPO-TA vector, the PCR product was incubated with 1 µL TopTaq DNA polymerase (Qiagen) for 10 minutes at 72 ^{o}C to add adenine overhangs. The cloned fragments were excised using the appropriate restriction enzymes (noted in Table 8-3), subcloned into the appropriate expression vector and transformed into Top10 *E. coli* (Invitrogen).

The periplasmic expression vector pBAD24-LS was constructed by inserting the N-terminal signal sequence of *E. coli* thioredoxin downstream of the AraC promoter of pBAD24. The VasX and VgrG3core (residues 1-726) genes were cloned in-frame with this secretion signal using *Xba*I and *Hind*III, and *Pst*I

and *Xba*I restriction sites, respectively. The resulting constructs were transformed into Top10 *E. coli* (Invitrogen) for expression analysis.

Plasmid pBAD24-tsiV2::FLAG was created using the Gateway recombination system. The LR recombination site, including the *ccdB* negative selection sequence, was amplified out of pBAD-DEST-49 using the primers listed in Table 8-3 (forward primer adds a *Kpn*I site, reverse primer adds a stop codon, *Xba*I site and FLAG epitope tag sequence**.** The PCR product was digested with *Xba*I and *Kpn*I and ligated into the corresponding sites of pBAD24 to create pBAD24gw::FLAG. The Gateway recombination reaction between pDONR221-*tsiV2* (Harvard Institute of Proteomics) and pBAD24gw::FLAG was performed according to the manufacturer's protocol (Invitrogen; Carlsbad, CA) . The resulting plasmid, pBAD24-tsiV2::FLAG, was transformed into Top10 *E. coli.*

Gene Knockout Constructs

In-frame deletion of T6SS genes was performed as described by Metcalf et al. [451]. Primers used to create the knockout construct are presented in Table 8-4. PCR products resulting from primer combinations A/B and C/D were stitched together by overlapping PCR. The resulting knockout construct was cloned into TOPO-TA (Invitrogen) or pJET1.2/blunt (Thermo Fisher Scientific) vectors. Prior to cloning into the TOPO-TA vector, the PCR product was incubated with 1 µL TopTaq DNA polymerase (Qiagen) for 10 minutes at 72 ^{o}C to add adenine overhangs. The knockout fragment was excised from the cloning vector by

digestion with *Bam*HI, cloned into the suicide plasmid pWM91 [451] and transformed into *E. coli* DH5α λpir followed by *E. coli* SM10 λpir.

Bacterial Transformations and Matings

Plasmids were transformed into electrocompetent *E. coli* Top10 using a BioRad Gene Pulser set to 200 ohms, 2.5 kVolts, and 25 µFD capacity. Chemically competent Top10 cells were mixed with plasmid DNA and incubated for 30 minutes on ice followed by heat shock at 40 ^{o}C for 30 seconds. Transformed cells were recovered for 30-60 minutes at 37 ^{o}C with shaking in S.O.C medium.

A tri-parental mating technique was used to introduce pBAD33-tsiV2::6xHis into *V. parahaemolyticus* RIMD2210633. Top10/pBAD33-tsiV2::6xHis (Cm^{R}), *V. parahaemolyticus* (Rif^{R}), and DH5α/pRK2013 (helper plasmid containing *tra* and *mob* genes) were mixed at a 1:1:1 ratio and spotted onto a non-selective LB(3% NaCl) plate for 6 hours at 37 ^{o}C. The spot was harvested into 1 mL LB (3% NaCl) and pelleted at 13,000 rpm for 5 minutes. Cells were resuspended in 100 µL LB(3% NaCl) and plated onto thiosulfate-citrate-bile salts-sucrose (TCBS) agar plates (BD Biosciences) containing rifampicin and chloramphenicol to select for *V. parahaemolyticus*/pBAD33-tsiV2::6xHis. Plates were incubated overnight at 37 ^{o}C. Resulting colonies were re-streaked onto TCBS rif^{50} $chlor^{10}$ to exclude false positive transformants.

Gene Knockouts

SM10 λpir *E. coli* (donor) harboring pWM91 containing the specific gene knockout construct was mixed at a 1:1 ratio with *V. cholerae* recipient cells (10^8:10^8) and centrifuged to pellet cells. The bacterial mixture was resuspended in 50 µL LB broth and spotted onto a pre-warmed LB agar plate and incubated for 5 hours at 37 ^{o}C. Mating spots were harvested and resuspended in 1mL LB broth. Five serial dilutions were prepared in LB broth and 200 µL of each dilution was spread onto an LB agar plate containing ampicillin and streptomycin. Resulting colonies were restreaked onto LB agar containing ampicillin and streptomycin. Two transconjugant colonies were picked and inoculated into LB containing streptomycin and grown with shaking at 37 ^{o}C for 5 hours. Four serial dilutions were prepared and 200 µL of each dilution was spread onto an LB plate containing streptomycin and 6% sucrose (w/v). Plates were incubated at room temperature for 2 days to select for bacteria that had excised the suicide vector backbone. Any resulting colonies that retained ampicillin resistance were discarded and ampicillin sensitive colonies were screened by PCR to determine which isolates contained the gene knockout.

Site-directed Mutagenesis of vasX and tsiV2

Amino acid substitutions were introduced into *vasX* and *tsiV2* using the QuickChange II XL Site-directed Mutagenesis Kit (Stratagene) according to the manufacturer's instructions. Plasmids pBAD24-vasX and pBAD24-tsiV2::FLAG

were used as templates in each mutagenesis reaction (PCR reaction) with a primer containing the desired nucleotide substitution. Primers used to introduce point mutations are included in Table 8-4. A PCR-amplified plasmid containing the mutation was transformed into XL-Gold *E. coli* cells. Each mutation was confirmed by sequencing at The Applied Genomics Centre (TAGC) at the University of Alberta.

Bacterial Pellet Sample Preparation and Protein Secretion Profiles

Overnight cultures of bacteria were diluted 1:100 in 3 mL LB (containing the appropriate antibiotics) and grown to an OD_{600} ~ 0.8. 200 µL pellet samples were harvested by centrifugation at 13,000 rpm for 3 min and were resuspended in 1 x SDS protein sample buffer and boiled for 10 min. The volume of SDS protein sample buffer used to resuspend pellet samples was calculated using the equation ((OD*culture volume)/2). For supernatant samples, bacterial cells were pelleted and the supernatant was filter-sterilized through Millipore 0.22 µm low protein-binding polyvinylidine fluoride (PVDF) syringe filters. Supernatant proteins were precipitated with 20% trichloroacetic acid (TCA) for 15 min at 4 ^{o}C and washed twice with acetone to remove residual TCA. Proteins were resuspended in 50 µL of 1 × SDS protein sample buffer and boiled for 10 min. Bacterial pellet fractions were resuspended in 1 × SDS-protein lysis buffer and

boiled for 10 minutes. Samples were then subjected to SDS-PAGE (10% acrylamide) and analyzed by silver staining or western blotting.

Antibodies

A list of primary and secondary antibodies along with their dilution factors are presented in Table 8-5. The polyclonal antibody against VasX was generated by New England Peptide Inc. (Gardner, MA). A synthetic peptide, comprising amino acids 271-VAKRTKAIGDETQQHKMQMAELTRT-295 of VasX was prepared and conjugated to keyhole limpet hemocyanin. The conjugated peptide was injected into rabbits (New Zealand White), boosted twice, then tested on crude cell extracts from *V. cholerae* strain V52 by western blotting to ensure antibody specificity.

Dictyostelium discoideum Plaque Assays

Mid-logarithmic *D. discoideum* cells (10^4-10^6 cells·mL^{-1}) were diluted in SorC medium [396] to 10^4 cells·mL^{-1}, 100µL was mixed with 100µL overnight culture of *Klebsiella pneumoniae* and spread on an SM/5 agar plate [396]. Where applicable, arabinose was added to a final concentration of 0.1% to induce expression from the P_{BAD} promoter. The plates were incubated for four days at 22 ^{o}C. Pictures of plaques were generated using a Kodak Gel Logic 200 Imaging System and Kodak 1D v3.6 software.

Cloning, Expression and Purification of Recombinant VasX

The full-length *vasX* gene was cloned from a Gateway entry vector (Harvard Institute of Proteomics, Clone ID: VcCD00020120) into the pET-DEST42 expression vector in-frame with a C-terminal V5 and 6xHis fusion for IPTG-inducible high-level expression. The resulting plasmid, pET-DEST42-*vasX* was transformed into *E. coli* BL21 Star (DE3) (Invitrogen) which encodes the T7 RNA polymerase required for expression from the T7 promoter. The *E. coli* BL21 Star (DE3)/ pET-DEST42-*vasX* culture was incubated at 30°C to an OD_{600} of ~0.5, induced with 0.1 mM IPTG, and harvested 4 hours post-induction by centrifugation at 5,000 x g. The N-terminal 200 residues of VasX were PCR amplified and cloned into the pET28a vector (Novagen) using the restriction sites *Nhe*I and *Xho*I to place the fragment in-frame with an N-terminal 6xHis tag. The construct, pET28a-PH, was transformed into *E. coli* BL21 Star (DE3) and grown at 25˚C to an OD_{600} of ~0.9, induced by addition of 10 µM IPTG for 16-20 hours and harvested by centrifugation at 5,000 x g.

Bacterial pellets were resuspended in 20 mM Tris-HCl, pH 8.0, 500 mM NaCl, 20mM imidazole supplemented with 1 mM phenylmethylsulfonyl fluoride and lysed by three passes through a French pressure cell at 18,000 psi. Lysates were cleared of insoluble cell debris by centrifugation at 20,000 x g and filtered through a 0.45 µm PVDF filter (Millipore). His-tagged proteins were purified using the AKTAdesign Basic system (GE Healthcare, Piscataway, NJ) mounted with a HisTrap FF Crude (GE Healthcare) column using an elution gradient of 20

mM to 500 mM imidazole. The purified protein fractions were dialyzed against PBS pH 7.4 and concentration was determined by A_{280}.

Purification of TsiV2

The full-length *tsiV2* gene was PCR-amplified from V52 genomic DNA and cloned into the pBAD33 expression vector in-frame with a C-terminal 6xHis fusion for arabinose-inducible expression. The resulting plasmid, pBAD33-tsiV2::6xHis was transformed into *E. coli* Top10. The *E. coli* Top10/pBAD33-tsiV2::6xHis culture was incubated at 37° C to an OD_{600} of ~0.5, induced with 0.1% arabinose, and harvested after 4 hours by centrifugation at 5,000 x g.

Bacterial pellets were resuspended in 20 mM Tris-HCl, pH 8.0, 500 mM NaCl, 20mM imidazole supplemented with Complete Protease Inhibitor Cocktail (Roche) and lysed by three passes through a French pressure cell at 18,000 psi. Lysates were cleared of insoluble cell debris by centrifugation at 20,000 x g and filtered through a 0.45 µm PVDF filter (Millipore). His-tagged proteins were purified using the AKTAdesign Basic system (GE Healthcare, Piscataway, NJ) mounted with a HisTrap FF Crude (GE Healthcare) column using an elution gradient of 20 mM to 500 mM imidazole. Purified protein fractions were dialyzed against 20mM HEPES, 100mM NaCl, pH 8 and the concentration was determined by A_{280}.

PIP Strip Immunoblots

PIP Strips were purchased from Echelon Biosciences (Salt Lake City, Utah). The strips were blocked with 3% BSA/PBS-T for 30 minutes at room temperature and incubated with the target protein at 2 $\mu g \cdot mL^{-1}$ in 3% BSA/PBS-T for 1 hour at room temperature. The strips were then incubated with full-length purified recombinant VasX, or the VasX fragment containing residues 1-200, according to the manufacturer's recommendations. As a positive, control purified VasX protein was spotted directly onto the nitrocellulose membrane prior to blocking. Purified *E. coli* (strain 0127:B8) LPS was purchased from Sigma-Aldrich and was spotted onto the nitrocellulose membrane in an equimolar amount (100 picomoles) as the various lipids. Bound proteins were detected with mouse-α-6xHis (Clontech) primary antibody and an α-mouse IgG-HRP secondary antibody (Santa Cruz Biotechnology Inc.).

Multilamellar Vesicle Pull-down

Membrane lipid preparations (Avanti Polar Lipids) were transferred to methanol-washed glass tubes, dried under a nitrogen stream, and rehydrated in 500 µL of PBS for 3 minutes at room temperature. Samples were vortexed for 3 minutes yielding a suspension of 5 mM MLV. 80 µL of purified recombinant VasX(full-length), VasX(1-200), or BSA at a concentration of 60 $\mu g \cdot mL^{-1}$ were added to 20 µL of MLV, gently mixed and incubated for 5 minutes at room temperature. 50µL of this mixture was centrifuged for 30 minutes at 13,000 x g at

4°C to pellet MLV-protein complexes. Fractions from each sample (total, pellet or supernatant) were mixed with 1 × SDS-protein lysis buffer, boiled and separated by SDS-PAGE. Proteins were visualized by staining with Coomassie Blue R-250 stain.

Large Unilammelar Vesicle Fluorescence Dequenching Assay

Large unilamellar vesicles (LUV) were prepared by Avanti Polar Lipids (Birmingham, AL). 98 mM carboxyfluorescein was encapsulated within 180 nm vesicles composed of *E. coli* polar lipids in 20 mM HEPES, 150 mM NaCl, pH 7.4. The unencapsulated fluorophore was removed by gel filtration and the concentration of lipid was determined by UV/Vis to be 5.67 mM. When encapsulated at greater than 50 mM, the concentration of carboxyfluorescein is self-quenching. Leakage of the fluorophore into the solvent upon vesicle disruption results in an increase in overall fluorescence.

Purified VasX, TsiV2, and relevant controls were diluted to 125ug·mL^{-1} in 20 mM HEPES, 50 mM NaCl, pH 5.4, then mixed with 50 nmol LUV in a black-framed 96-well plate (Costar No. 3603) for fluorescence measurements. The relative fluorescence units were measured by excitation at 480 nm and emission at 520 nm in a FLUOstar OPTIMA microplate reader (BMG Labtech). Triton X-100 (0.1%) was added to determine maximal fluorescence and the assayed values were expressed as % maximal fluorescence. The experiment was performed three times in duplicate.

Bacterial Killing Assays

Bacterial strains were grown on LB agar plates (unless otherwise noted) with appropriate antibiotics. Streptomycin-resistant (rifampicin-sensitive) predator and rifampicin-resistant (streptomycin-sensitive) prey were harvested and mixed at a 10:1 ratio with volumes normalized by OD_{600} readings. 25 μL of the mixed bacterial culture was spotted onto pre-warmed LB agar and incubated at 37 ^{o}C for 4 hours. Bacterial spots were harvested and the $CFU \cdot mL^{-1}$ of surviving prey and predator were measured by serial dilution and selective growth on agar containing rifampicin and streptomycin, respectively. Where applicable, arabinose was added to LB plates at a final concentration of 0.1% to induce expression from the P_{BAD} promoter during the 4 hour incubation. Killing assays with *V. parahaemolyticus* and *V. alginolyticus* were performed on LB containing 3% NaCl for 4 hours at 37 ^{o}C. Killing assays with *V. fischeri* were performed on GVM agar at room temperature for 8 hours. Killing assays with *V. communis*, *V. harveyi*, and *P. phenolica* prey were performed on ½ YTSS agar (recipe provided in Table 8-6) for 4 hours at 30 ^{o}C.

For the contact-dependent killing assay, predator and prey strains were incubated at a 10:1 ratio with the addition of a sterile 0.22-μm filter (Millipore). The filter was placed either directly on the LB-agar plate or on top of the predator cells. Prey bacteria were spotted on top of the filter. After 4 hour incubation, cells were harvested by suspending the filter in 1 mL LB and vortexing for 10 seconds. The CFU per milliliter of surviving prey were determined by serial dilution and growth on selective media as described above.

Isolation of RGVC strains, V. communis, V. harveyi, and P. phenolica

Environmental bacteria were collected by submerging a Turtox tow net (Envco, New Zealand) with a 20 mm pore-size Nitex mesh spanning a 30.48 cm diameter mouth in estuary water for one minute. Water samples (200 mL) collected from estuaries of the Rio Grande delta were blended with a handheld homogenizer (PRO Scientific; Oxford, CT), and vacuum filtered through Whatman filter paper number 3 (GE Healthcare, Little Chalfont, UK). A second vacuum filtration was performed on the filtrate through 0.45 mM pore-size membranes (Millipore, Bedford, MA). Filters were incubated separately in a small volume of 0.15 M sterile NaCl for one hour shaking at room temperature. The suspensions were plated on thiosulfate-citrate-bile salts sucrose (TCBS) agar (BD, Franklin Lakes, NJ) and/or marine agar 2216 (BD, Franklin Lakes, NJ). Following incubation for16 hours at 30 ^{o}C, colony forming units were isolated and cultured in LB or ½ YTSS broth.

Primers binding to conserved 16S ribosomal gene sequences (Table 8-4) were used to PCR-amplify the 16S ribosomal sequences from environmental bacterial isolates. Sequencing was performed at the University of Alberta Applied Genomics Center and species were identified using BLASTn.

Immunity Gene Internal Promoter Prediction

Promoter predictions were performed using the Neural Network Promoter Prediction Software with a 0.95 cut-off (http://www.fruitfly.org/seq_ tools/promoter.html), PePPER (http://pepper.molgenrug.nl/index.php/pepper-

tools/promoter-predictie-tool), PPP (http://bioinformatics.biol.rug.nl/websoftware/ppp/ppp_start.php), and BPROM (http://linux1.softberry.com/berry.phtml?topic=bprom&group=programs&subgroup=gfindb).

VasX and TsiV2 High Oligomeric Complexes

Overnight bacterial cultures were diluted 1:100 in LB containing the appropriate antibiotics and grown to OD_{600} ~0.8. 200 µL of culture was centrifuged for 3 minutes at 13, 000 rpm, the supernatant was aspirated and the pellet was resuspended in 100 µL of 1x SDS protein sample buffer which were not subjected to boiling prior to analysis by western blotting.

β-galactosidase Assay

A 1/10 dilution of overnight liquid cultures was used to measure the OD_{600}. Cultures were diluted 1/10 in Z buffer containing 2.7% β-mercaptoethanol. Using a Pasteur pipette, one drop of 0.1% SDS and two drops of chloroform were added and the mixture was vortexed for 5 seconds. Tubes were incubated in a 28 ^{o}C water bath for 10 minutes followed by addition of 200 µL *ortho*-Nitrophenyl-β-galactoside (ONPG) buffer (4 $mg \cdot mL^{-1}$ ONPG dissolved in Z buffer using a sonicating water bath). The length of time required for development of a yellow color was recorded and the reaction was halted by the addition of 500 µL 1M Na_2CO_3. The OD_{420} was measured for each sample using

an XMark microplate spectrophotometer (BioRad). Reactions that failed to turn yellow were halted after one hour. Miller units were calculated based on the equation ($OD_{420}/(OD_{600}\cdot time\cdot volume)*10^3$).

Strains V52, C6706, and V52Δ*vasH* used in this assay possess their chromosomal copy of *lacZ*. The strains O395, NIH41, MAK757, C6709, and N16961 contain a disrupted *lacZ* gene. Mutation of *lacZ* was accomplished using the suicide vector pJL1-ΔlacZ. *E. coli* SM10λpir/pJL1 was mixed at a ~1:1 ratio with the recipient *V. cholerae* strains and incubated on a pre-warmed LB agar plate for 6 hours at 37 ^oC. Bacterial mixtures were harvested and resuspended in 1 mL LB and were subjected to 4 serial dilutions of which 200 µL were spread onto selective LB agar plates. Transconjugants were re-streaked onto LB containing ampicillin and 40 $\mu g\cdot mL^{-1}$ 5-bromo-4-chloro-3-indolyl-β-D-galactopyranoside (x-gal) to ensure disruption of *lacZ* resulted in white colony formation.

CFU Recovery Time Course

Strains grown overnight were back-diluted 1:100 in selective LB broth with 0.1% arabinose. At 0, 2, 4, 6, and 8 hours a 200 µL sample was taken and serially diluted seven times. 10 µL of each dilution was spotted onto selective LB plates and incubated overnight at 37 ^oC. The recovered CFU were enumerated and plotted.

SDS Lysis Assay

Overnight bacterial cultures were back-diluted 1:25 in selective LB broth with arabinose (0.1%) and grown for 2 hours at 37 ^{o}C with shaking. 1.2 mL of each culture was dispensed into four microfuge tubes per strain. Two of these were treated with 100 µL 7.5 mg·mL^{-1} SDS and the other two received 100 µL of water (diluent) as a negative control. Microfuge tubes were placed on a nutating shaker for 10 minutes at room temperature. Samples were placed into wells of a 96-well plate, and the OD_{600} of each sample was read using an XMark microplate spectrophotometer (BioRad). OD_{600} readings in SDS were divided by OD_{600} readings in H_2O to generate the lysis ratio.

RNA Isolation and Quantitative RT-PCR

Shaking bacterial cultures were grown at 37 ^{o}C to mid-logarithmic stage in the absence or presence of 0.1% arabinose. Total mRNA was extracted using an RNeasy® Mini Kit (Qiagen) according to the manufacturer's instructions. 1 µg of RNA from each sample was subjected to DNaseI (Invitrogen) treatment to remove residual DNA, followed by a reverse transcription reaction using SuperScript™ III Reverse Transcriptase (Invitrogen). Semi-quantitative real-time PCR was performed with PerfeCTa™ SYBR® Green FastMix™ (Quanta). The C_T values were determined by Mastercycler® ep *realplex* (Eppendorf) and the fold-change was calculated using the $2^{-\Delta\Delta CT}$ method [452]. Primers used for qRT-PCR are presented in Table 8-4.

Membrane Potential Assay and Flow Cytometry

The BacLight Bacterial Membrane Potential Kit (Molecular Probes) was used to determine whether LS::vasX causes dissipation of the membrane potential. Overnight cultures of the indicated strains were back-diluted 1:30 in selective LB with arabinose (0.1%) and grown for 2 hours at 37 ^{o}C with shaking (225 rpm). Cells were diluted to ~10^{6} cells·mL^{-1} in filtered PBS. CCCP (depolarizing control) and $DiOC_2(3)$ (stain) were added (where appropriate) to final concentrations of 5 µM and 15 µM, respectively and incubated for 30 minutes in the dark. Stained cells were analyzed using a BD LSR II with a 488 nm laser, and PE-Texas Red (601 long pass and 616/23 band pass filters) and FITC (502 long pass and 525/50 band pass filters) detectors. Forward and side scatter, and fluorescence were collected with logarithmic signal amplification. Red/green ratios were calculated based on double positive (Texas Red and FITC) cells by collecting 50,000 events per strain tested.

Malachite Green Phosphatase Assay

The reagents for this experiment were purchased from Caymen Chemical and were used according to the manufacturer's recommendations. Purified, recombinant VasX and PH domain (i.e. VasX residues 1-200) were used at a final concentration of 50 µg·mL^{-1}. The lipid phosphatidylinositol-4,5-phosphate (PI(4,5)P) was purchased from Avanti Polar Lipids and used at a final concentration of 25 µM. Lipids were dried under a nitrogen stream and

resuspended in 100 mM tris-HCl (pH 7.0) by vortexing continually for 3 min. Proteins and PI(4,5)P were mixed at a final volume of 100 µL and incubated for 60 min at 37 ^{o}C. 10 µL of "MG acidic solution" was added to each sample and samples were incubated for 10 min at room temperature. 30 µL of "MG blue solution" was added to each sample and samples were incubated for 20 min at room temperature. The OD_{620} of all wells were measured using an XMark microplate spectrophotometer (BioRad).

cyaA Fusion to vasX

Plasmid pBAD24-*vasX::cyaA* was constructed to allow arabinose-inducible expression of the *vasX::cyaA* fusion. The primers used to construct the *cyaA* fusions are presented in Table 8-3. The enzymatic portion of the adenylate cyclase toxin gene *cyaA* was PCR amplified using plasmid pACYC184-espF::cyaA cells [403-406] as the template. The resulting PCR product was restricted with *Eco*RI and *Hind*III and subcloned into *Eco*RI/*Hind*III-restricted pBAD24. The resulting plasmid was restricted with *Eco*RI and *Xho*I to subclone *vasX* as an EcoRI/XhoI fragment that was previously amplified using plasmid clone VcCD00020120 (Harvard Institute of Proteomics) as the template.

cAMP Assay

RAW 264.7 murine macrophages were seeded at $5x10^4$ cells per well in a 96 well tissue culture plate 18 hours prior to infection. Mid-logarithmic *D. discoideum* were diluted to ~10^6 cells/mL in HL5 broth. Overnight bacterial cultures were back-diluted 1:50 in LB with the appropriate antibiotics (in the presence or absence of 0.1% arabinose) and grown to mid-logarithmic phase. Bacterial lysates were prepared by incubating cultures in the presence of 2 $mg \cdot mL^{-1}$ lysozyme for 30 minutes on ice and sonicating (with protease inhibitor cocktail, Fisher Scientific) using a Fisher Scientific Sonic Dismembrator (Model 500) with nine pulses for ten seconds each with an amplitude of 45%. Macrophages were infected at an MOI of 50 for 1.5 hours in a 5% CO_2 atmosphere at 37 ^oC. Amoebae were infected at an MOI of 50 for 1.5 hours at 22 ^oC. Media was aspirated and wells were washed once with pre-warmed PBS. Cells were treated with 0.1 M hydrochloric acid for 10 minutes at room temperature, the 96 well plate was centrifuged in a Beckman Coulter Allegra 25R swinging bucket centrifuge at 1500 x g for 3 minutes to pellet debris. 100 µL of sample was used to assay cAMP levels using a cAMP EIA Kit (New East Biosciences) according to the manufacturer's instructions (non-acetylated protocol for suspension cells).

Bacterial lysate samples were incubated at 37^oC in a 5% CO_2 atmosphere for 1.5 hours in the presence or absence of 2 mM Mg^{2+}/ATP and 60 nM CaM. Samples were treated with 1.5 µL concentrated hydrochloric acid for 10 minutes at room temperature, spun for 5 minutes in swinging bucket rotor at 1000 rpm and

100 µL was used to assay cAMP levels using the cAMP EIA Kit (NewEast Biosciences) according to the manufacturer's instructions (non-acetylated protocol for suspension cells).

VasX and TsiV2 Crosslinking Experiment

Purified recombinant VasX and TsiV2 were mixed at a 1:1 mass ratio in resuspension buffer (each at 0.1 $mg \cdot mL^{-1}$) and cross-linked with 2 mM dithiobis (succinimidyl) propionate (DSP) (Pierce). The protein/DSP mixture was incubated for 2 hours on ice and the reaction was quenched by adding 5 µL 1M Tris-HCl, pH 8.0. The samples were mixed with 4x SDS-PAGE sample buffer with and without β-mercaptoethanol to cleave the cross-linker, boiled for 10 minutes and separated by either 7.5% or 12% SDS-PAGE then stained with Coomassie Blue overnight.

Nickel Pull-downs of 6xHis-tagged Proteins

Bacterial strains were grown in 200 mL of selective LB broth in the presence of 0.1% arabinose to an OD_{600} ~0.8. Cells were pelleted at 14,000 rpm for 20 minutes and the supernatant was decanted. The bacterial pellet was resuspended in 10 mL PBS and lysed by three passages through a French pressure cell at 18,000 psi. Lysates were centrifuged twice at 13,000 rpm for 10 minutes to pellet unbroken cells and insoluble matter. The soluble lysate fraction was mixed

with 200 µL pre-equilibrated Ni^{2+} NTA resin (Qiagen) and incubated on a nutating shaker at 4 ^{o}C for one hour. The lysate/resin mixture was centrifuged at 1,000 rpm for 5 seconds to pellet the nickel resin along with 6xHis-tagged proteins bound to the resin and the pellet was washed 10x 5 minutes with 1mL binding buffer to remove proteins that bound non-specifically. Proteins bound to the nickel resin were eluted by adding of 400 µL elution buffer and incubating for 20 minutes at 4 ^{o}C on a nutating shaker. The resin was pelleted at 1,000 rpm for 5 seconds and eluted proteins in the supernatant were mixed with 4x protein sample buffer and boiled for 10 minutes to disrupt protein-protein interactions. Protein samples were subjected to SDS-PAGE followed by immunoblotting with the appropriate antibodies.

Far Dot Blotting

Purified recombinant proteins were diluted to 200 µg·mL^{-1} and three serial dilutions were performed so that the lowest concentration achieved was 2 µg·mL^{-1}. For TsiV2, 5 µL of each protein concentration was spotted onto nitrocellulose membrane (BioRad) so that 1,000 ng, 100 ng and 10 ng of protein were spotted onto the membrane. As positive and negative controls, 100 ng of purified recombinant VasX and TsiV3, respectively, were also spotted onto the membrane. Proteins were allowed to dry onto the membrane for 30 minutes at room temperature. The membranes were blocked in 5% skim milk TBS-T for 1 hour at room temperature with shaking. The bait protein (purified, recombinant VasX)

was prepared in the following dilutions in 5% skim milk TBS-T: 0, 2.5, 5, 7.5, 10 $\mu g \cdot mL^{-1}$. Following blocking, membranes were incubated with bait protein overnight at 4 ^{o}C with shaking. Membranes were washed 3x 5 minutes in TBS-T and incubated with primary VasX antibody for 1 hour at room temperature with shaking. Membranes were washed 3x 5 minutes in TBS-T and then incubated with anti-rabbit-HRP secondary antibody for 1 hour at room temperature with shaking. Membranes were washed 3x 5 minutes in TBS-T and bound protein was detected using the SuperSignalWest Pico Chemiluminescent Substrate (Thermo Fisher Scientific).

Flow Cytometry Analysis of Cells Incubated with Propidium Iodide

Overnight bacterial cultures were diluted 1:100 in LB containing the appropriate antibiotics in the presence of 0.1% arabinose. Cultures were grown under inducing conditions for 2 hours at 37 ^{o}C with shaking. As a positive control for PI staining dead cells were prepared by ethanol-treatment: 1 mL of bacterial culture was centrifuged for 13,000 rpm for 3 minutes. The supernatant was aspirated and the pellet was resuspended in 1 mL of 70% ethanol and incubated for 20 minutes at room temperature. Cells were pelleted by centrifugation at 13,000 rpm for 3 minutes and the pellet was resuspended in 1 mL filtered PBS. ~10^6 cells (living or dead cells) were diluted into 1 mL of filtered PBS. 1.5 µL of 20 mM PI was added to each sample followed by incubation for 15 minutes in the dark.

Stained cells were analyzed using a BD LSRFortessa Cell Analyzer with a 488 nm laser, and a PE (550 long pass and 575/26 band pass filters) detector. Forward and side scatter, and fluorescence were collected with logarithmic signal amplification. The percentage of cells permeable to P.I. was recorded by collecting 50,000 events per strain tested.

Lysis Assay Using rVasX and rTseL

This assay was performed as described previously [210]. Bacterial colonies were harvested from overnight LB agar plates and resuspended to an OD_{600} ~ 1.0 in 20 mM Tris-HCl, pH 7. Aliquots of 100 µL were transferred to a 96-well plate. 5 µg of each protein was diluted to a final volume of 10 µL with 20 mM Tris-HCl buffer. 1 µL of 4 $mg \cdot mL^{-1}$ polymyxin B (or 1 µL water) was added to the protein mixtures where appropriate. The polymyxin B/protein mixtures were added to the bacterial cultures in the 96 well plate using a multichannel pipette (VWR) and the OD_{600} at 0 minutes was measured in an xMark microplate spectrophotometer (BioRad). The plate was incubated for 5 minutes at 37 °C on a Heidolph Titromax 1000 vibrating shaker at 900 rpm, and the OD_{600} was measured again. Percent lysis was calculated as [(OD_{600} at 0 min - OD_{600} at 5 min)/OD_{600} at 0 min] *100%.

Growth Curve - Cytoplasmic expression of VasX in C6706ΔtsiV2

An overnight culture of C6706Δ*tsiV2*/pBAD24-vasX was diluted 1:100 in selective LB broth in the presence or absence of 0.1% arabinose to induce expression of *vasX*. Strains were grown in a 96 well plate on a Heidolph Titromax 1000 vibrating shaker at 900 rpm. OD_{600} readings were taken every hour for 8 hours using an XMark microplate spectrophotometer (BioRad). At the 7 hour time point, a cell lysate sample was collected from each sample, mixed with SDS protein sample buffer and boiled for 10 min. The protein samples were subjected to 10% SDS-PAGE followed by western blotting with the appropriate antibodies.

Table 8-1. Bacterial strains used in this study.

Strain	Description	Reference or source
***V. cholerae*, V52**	**O37 serogroup strain, sm^R** **O37 serogroup strain, Δ*hapA*, Δ*rtxA*, Δ*hlyA*, sm^R**	**[368]** **Isolated in Sudan, 1968**
V. cholerae*, V52Δ*vasK	**V52 mutant lacking *vasK* (VCA0120), Δ*hapA*, Δ*rtxA*, Δ*hlyA*, sm^R**	**[194]**
V. cholerae*, V52Δ*vasW	**V52 mutant lacking *vasW* (VCA0019), Δ*hapA*, Δ*rtxA*, Δ*hlyA*, sm^R**	**This study**
V. cholerae*, V52Δ*vasX	**V52 mutant lacking *vasX* (VCA0020), Δ*hapA*, Δ*rtxA*, Δ*hlyA*, sm^R**	**This study**
V. cholerae*, V52Δ*vasX*Δ*vasK	**V52 mutant lacking *vasX* and *vasK* (parent was V52Δ*vasK*), Δ*hapA*, Δ*rtxA*, Δ*hlyA*, sm^R**	**This study**
***V. cholerae*, V52ΔPHdomain**	**V52 mutant lacking PH domain within *vasX*, Δ*hapA*, Δ*rtxA*, Δ*hlyA*, sm^R**	**This study**
V. cholerae*, V52Δ*vgrG-1	**V52 mutant lacking *vgrG-1* (VC1416), Δ*hapA*, Δ*rtxA*, Δ*hlyA*, sm^R**	**[194]**
V. cholerae*, V52Δ*vgrG-2	**V52 mutant lacking *vgrG-2* (VCA0018), Δ*hapA*, Δ*rtxA*, Δ*hlyA*, sm^R**	**[194]**
V. cholerae*, V52Δ*vgrG-3	**V52 mutant lacking *vgrG-3* (VCA0123), Δ*hapA*, Δ*rtxA*, Δ*hlyA*, sm^R**	**[194]**
V. cholerae*, V52Δ*hcp1,2	**V52 mutant lacking *hcp-1* (VC1415) and *hcp-2* (VCA0017), Δ*hapA*, Δ*rtxA*, Δ*hlyA*, sm^R**	**[194]**
V. cholerae*, V52Δ*vgrG-1*Δ*vasX	**V52 mutant lacking *vgrG-1* and *vasX*, Δ*hapA*, Δ*rtxA*, Δ*hlyA*, sm^R**	**This study**
V. cholerae*, V52Δ*tseL	**V52 mutant lacking *tseL* (VC1418), sm^R**	**This study**
V. cholerae*, V52Δ*vasX*Δ*vgrG-3	**V52 mutant lacking *vasX* and *vgrG-3*, sm^R**	**This study**
V. cholerae*, V52Δ*vasX*Δ*tseL	**V52 mutant lacking *vasX* and *tseL*, sm^R**	**This study**
V. cholerae*, V52Δ*vasX*Δ*vgrG-3*Δ*tseL	**V52 mutant lacking *vasX*, *vgrG-3*, and *tseL*, sm^R**	**This study**
V. cholerae*, V52Δ*vasH	**V52 mutant lacking *vasH* (VCA0117), Δ*hapA*, Δ*rtxA*, Δ*hlyA*, sm^R**	**[194]**
V. cholerae*, V52Δ*vasH*Δ*vasX	**V52 mutant lacking *vasH* and *vasX* (parent was V52Δ*vasH*), Δ*hapA*, Δ*rtxA*, Δ*hlyA*, sm^R**	**This study**
***V. cholerae*, C6706**	**O1 El Tor, sm^R** **O1 El Tor, sm^R, Rif^R**	**[430]**

V. cholerae*, C6706Δ*tsiV2	**C6706 mutant lacking *tsiV2*, sm^R, Rif^R**	**This study**
V. cholerae*, C6706Δ*vasX	**C6706 mutant lacking *vasX*, sm^R, Rif^R**	**This study**
***V. cholerae*, N16961**	**O1 El Tor, sm^R, *lacZ*$^-$**	**[453] Isolated in Bangladesh, 1975**
***V. cholerae*, NIH41**	**O1 Classical, sm^R, *lacZ*$^-$**	**[454]**
***V. cholerae*, C6709**	**O1 El Tor, sm^R, *lacZ*$^-$**	**[67]**
***V. cholerae*, O395**	**O1 Classical, sm^R, *lacZ*$^-$**	**[455] Isolated in India, 1965**
***V. cholerae*, MAK757**	**O1 El Tor, sm^R, *lacZ*$^-$**	**[456] Isolated in Indonesia, 1937**
***V. parahaemolyticus* RIMD2210633**	**$rif^{R'}$ amp^R**	**[457]**
V. parahaemolyticus	**$rif^{R'}$ amp^R**	**Dr. R. DeVinney, University of Calgary**
V. alginolyticus	**$rif^{R'}$ amp^R**	**Dr. R. DeVinney, University of Calgary**
V. mimicus	**rif^R**	**Dr. K. Ellison, University of Alberta**
***V. fischeri*, MJ1**	**rif^R**	**Fotodyne, Inc.**
***E. coli*, DH5α λpir**	**fhuA2 D(argF-lacZ)U169 phoA glnV44 W80 D(lacZ)M15 gyrA96 recA1 relA1 endA1 thi-1 hsdR17**	**[458]**
***E. coli*, SM10 λpir**	**KmR, thi-1, thr, leu, tonA, lacY, supE, recA::RP4-2-Tc::Mu, pir**	**[459]**
***E. coli*, Top10**	**F- mcrA Δ(mrr-hsdRMS-mcrBC) φ80lacZΔM15 ΔlacX74 nupG recA1 araD139 Δ(ara-leu)7697 galE15 galK16 rpsL(Str^R) endA1 λ$^-$**	**Invitrogen**
***E. coli*, MG1655**	**F- lambda- ilvG- rfb-50 rph-1, rif^R**	**[460]**
Enteropathogenic *E. coli*, E2348/69	**rif^R**	**[461]**
Klebsiella pneumoniae		**Dr. R. Kessin, Columbia University**
XL Gold *E. coli*	**endA1 glnV44 recA1 thi-1 gyrA96 relA1 lac Hte Δ(mcrA)183 Δ(mcrCB-hsdSMR-mrr)173 tet^R F'[proAB $lacI^q$ZΔM15 Tn10(Tet^R)**	**QuickChange II XL Site-Directed Mutagenesis Kit**

	Amy Cm^R)]	**(Stratagene)**
***E. coli* BL21 Star**	**F^- ompT gal dcm lon $hsdS_B(r_B^- m_B^-)$ λ(DE3 [lacI lacUV5-T7 gene 1 ind1 sam7 nin5])**	**Invitrogen**
Enterohemorrhagic *E. coli* O157:H7	**rif^R**	**[211]**
C. rodentium	**rif^R**	**[211]**
***S. enterica* sv. Typhimurium**	**rif^R**	**[211]**
***P. aeruginosa* PAO1**	**rif^R**	**[462]**
S. aureus	**rif^R**	**[211]**
L. monocytogenes	**rif^R**	**[211]**
B. subtilis	**rif^R**	**[211]**
E. fecaelis	**rif^R**	**[211]**
P. phenolica	**Environmental isolate, Rif^R**	**[369]**
V. communis	**Environmental isolate, Rif^R**	**[369]**
V. harveyi	**Environmental isolate, Rif^R**	**[369]**
DL4211 (RGVC) **DL4211Δ*vasK***	**Environmental *V. cholerae* isolate, sm^R** **DL4211 lacking *vasK***	**[369]**
DL4215 (RGVC) **DL4215Δ*vasK***	**Environmental *V. cholerae* isolate, sm^R** **DL4215 lacking *vasK***	**[369]**

sm; streptomycin, rif; rifampicin, km; kanamycin, amp; ampicillin

Table 8-2. Plasmids used in this study.

Plasmid	Description	Source
pBAD24	pBAD vector, pBR322 ori, araC, Amp^R	[399]
pBAD24-vasX	pBAD24 carrying *vasX* (VCA0020) of the *V. cholerae* strain V52	This study
pBAD24-vasX::FLAG	pBAD24 carrying *vasX* from V52, C-terminal FLAG tag	This study
pBAD24-vasX(1-218)::FLAG	pBAD24 encoding amino acids 1-218 of *vasX*	This study
pBAD24-vasX(1-542)::FLAG	pBAD24 encoding amino acids 1-542 of *vasX*	This study
pBAD24-vasX(76-542)::FLAG	pBAD24 encoding amino acids 76-542 of *vasX*	This study
pBAD24-vasX(543-1085)::FLAG	pBAD24 encoding amino acids 543-1085 of *vasX*	This study
pBAD24-vasX(167-700)::FLAG	pBAD24 encoding amino acids 167-700 of *vasX*	This study
pBAD24-tsiV2::FLAG	pBAD24 carrying *tsiV2* from V52, C-terminal FLAG tag	This study
pBAD24-tsiV2*14	pBAD24 carrying *tsiV2* site directed mutant, residue 14→TAA	This study
pBAD24-tsiV2*127	pBAD24 carrying *tsiV2* site directed mutant, residue 127→TAA	This study
pBAD24-tsiV2*164	pBAD24 carrying *tsiV2* site directed mutant, residue 164→TAA	This study
pBAD24-LS	pBAD24 with periplasmic targeting sequence	This study
pBAD24-LS::vasX	pBAD24-LS carrying *vasX* from V52	This study
pBAD24-LS::core	pBAD24-LS carrying *vgrG-3* (VCA0123) core (lacks PBD)	[210]
pBAD24-vasX::cyaA	pBAD24 carrying *vasX* fused to *cyaA* (adenylate cyclase)	This study
pBAD24-vasX(W144A)	pBAD24 carrying *vasX* with Trp144→Ala	This study
pBAD24-vasX(W146A)	pBAD24 carrying *vasX* with Trp146→Ala	This study
pBAD24-vgrG2::6xHis	pBAD24 carrying *vgrG-2*, C-terminal hexa-histidine tag	This study
pBAD24-vgrG-1::6xHis	pBAD24 carrying *vgrG-1*, C-terminal hexa-histidine tag	This study
pBAD24-hcp-2::6xHis	pBAD24 carrying *hcp-2*, C-terminal hexa-histidine tag	This study
pBAD24-vasW::FLAG	pBAD24 carrying *vasW*, C-terminal FLAG tag	This study
pBAD24-vasW::6xHis	pBAD24 carrying *vasW*, C-terminal hexa-histidine tag	This study
pBAD24-vasH	pBAD24 carrying *vasH* from *V. cholerae* V52	[369]
pBAD24-vasK	pBAD24 carrying *vasK* from *V. cholerae* V52	[369]
pBAD33	pBAD vector, pACYC184 ori, araC, Cm^R	[399]
pBAD33-tsiV2::6xHis	pBAD33 carrying *tsiV2*, C-terminal hexa-histidine tag	This study
pBAD33-LS::vasX	pBAD33 carrying LS::vasX amplified from pBAD24-LS::vasX	This study
pAH6	pAH6 vector, pACYC184 ori, Cm^R	[463]
pAH6-P_{hcp}	pAH6 carrying *hcp-2* promoter (-1 to -400)	This study
pAH6-vasX	pAH6 carrying *vasX* from *V. cholerae* V52 (lacking start codon)	This study
pAH6-vasX(1-1345)	pAH6 carrying *vasX* (nucleotides 1-1345) from V52	This study
pAH6-vasX(1575-3258)	pAH6 carrying *vasX* (nucleotides 1575-3258) from V52	This study
pAH6-vasX(2208-3258)	pAH6 carrying *vasX* (nucleotides 2208-3258) from V52	This study
pAH6-tseL	pAH6 carrying *tseL* from V52	This study

pAH6-vgrG-3	**pAH6 carrying *vgrG-3* from V52**	**This study**
pWM91	**oriR6K mobRP4 lacI ptac tnp mini-Tn10Km; Km^R Amp^R**	**[451]**
pRK2013	**Col E1 rep, tra^+ mob^+, Kan^R**	**Clontech**
pDONR221-tsiV2	**Col E1 rep, Kan^R carrying *tsiV2***	**Harvard Institute of Proteomics**
pJET1.2/blunt	**Vector for cloning blunt ended PCR products, Amp^R**	**Thermo-Fisher Scientific**
pJET-GFP	**pJET1.2/blunt carrying superfolded GFP**	**This study**
pJET-tsiV2::6xHis	**pJET1.2/blunt carrying *tsiV2* (from N16961) in reverse orientation from the T7 promoter**	**This study**
pJET-tsiV2(ATG)::6xHis	**pJET1.2/blunt carrying *tsiV2* (from N16961) in reverse orientation from the T7 promoter, lacking a start codon**	**This study**
pCR2.1-TOPO TA	**Vector for cloning PCR products, Amp^R**	**Invitrogen**
pACYC184	**p15A ori, Cm^R**	**Dr. N. Thomas, Dalhousie University**
pACYC184-espF::cyaA	**pACYC184 carrying *espF* (T3SS effector) fused to *cyaA* (adenylate cyclase)**	
pJL1-ΔlacZ	**ori6K, mob^+, Amp^R**	**Dr. D. Provenzano, University of Texas at Brownsville**

Table 8-3. Cloning primers used in this study.

Primer name	Destination plasmid	Direction[a]	Sequence[b]
5' *vasX*	pBAD24	F	GGTACC CATGAGTAATCCCAAT
3' vasX::FLAG		R	TCTAGATTATTTATCATCATCATCTTTATAA TCACCTTTTCCTACAACGAG
3' vasX::6xHis		R	TCTAGATTAGTGGTGATGGTGATGATGACC TTTTCCTACAACGAG
3' vasX(1-542)::FLAG		R	TCTAGATTATTTATCATCATCATCTTTATAA TCCTGAATACGTTCATCCCC
3' vasX(1-218)::FLAG		R	TCTAGATTATTTATCATCATCATCTTTATAA TCGCGTTCTTCACTTTTCTCTACCGG
3' vasX(76-542)::FLAG		R	TCTAGATTATTTATCATCATCATCTTTATAA TCCTGAATACGTTCATCCCC
3' vasX(167-700)::FLAG		R	TCTAGATTATTTATCATCATCATCTTTATAA TCCGATAGCGCGCTCAGTTTC
5' vasX(543-1085)::FLAG		F	TCTAGATTATTTATCATCATCATCTTTATAA TCACCTTTTCCTACAAC
5' pBAD-DEST49		F	GGTACC AAGTTTGTACAAAAAAGCTGAAC
3' pBAD-DEST49::FLAG		R	TCTAGATCATTTATCATCATCATCTTTATAA TCCACCACTTTGTACAAGAAAGCTG
5' *cyaA*		F	GAATTCACCATGCTCGAGCAGCAATCGCAT CAG
3' cyaA		R	AAGCTTTTAGCGTTCCACTGCGCCCAGCGA
5'*vasX(1-213)*		F	GAATTCACCATGAGTAATCCC
3'vasX(2722-3255)		R	CTCGAGACCTTTTCCTACAAC
5' *vgrG-1*		F	GAATTCACCATGGCGACATTAGCGTACAGC
3' *vgrG-1::6xHis*		R	GTCGACCTAGTGGTGATGGTGATGATGAGC AATAATGCGTTG
5' vgrG-2		F	GAATTCACCATGGCGACATTAGCGTAC
3' vgrG-2::6xHis		R	TCTAGATTAGTGGTGATGGTGATGATGATT TCCCTTGGCCTCTTC
5' hcp-2		F	GAATTCCTAGCATGCCAACTCCATGTTATAT C
3' hcp-2::6xHis		R	AAGCTTTTAGTGGTGATGGTGATGATGCGC TTCGATTGGCTTACG
5' vasH		F	GAATTC ACCATGAGTCAATGGCTGGCG
3' vasH		R	CTCGAG TTAACCTTTTCCTACAACGAG
3' vasX (no TAA) – cyaA		R	AAGCTT TTAACCTTTTCCTACAACGAG
5' vasW		F	GAATTC ATGCGTTCAACAAATTCC

3' vasW::FLAG		R	TCTAGATTATTTATCATCATCATCTTTATAA TCTCCTTGTACCTCCTGTGA
5' vasK		F	GAATTCACCATGTGGAAATTCATT
3' vasK		R	TCTAGATTAATAGAGTGTTTTAGAC
5' *vasX*	pAH6	F	AAGCTT AGTAATCCCAATCAAGCTGCG
3' *vasX*		R	TCTAGA TTAACCTTTTCCTACAAC
3' *vasX* (1345)		R	TCTAGA ACGCTTGCTGAACCTCATCT
5' *vasX* (1575)		F	AAGCTT TGCGACCGCAATCGCTAACT
5' *vasX* (2208)		F	AAGCTT CCGCTATAAGTCGCACAAT
5' P_{hcp}		F	AAGCTTGCTCTTCCCGTTTGTCGTTATATAC
3' P_{hcp}		R	TCTAGA GGCTATTTCCTTTCAATAAATC
5' *tseL*		F	TCTAGA GATTCATTTAATTATTGC
3' *tseL*		R	GTCGAC TCATCTTATTTGCACCTTG
5' *vgrG-3*		F	TCTAGA GCAAGGTTACAGTTTCAATTA
3' *vgrG-3*		R	TCTAGA TCATTTTATATCAACCTCCAAAC
5' *vasX*	pBAD24-LS	F	TCTAGA AGTAATCCCAATCAAGCTGCG
3' *vasX*		R	AAGCTT TTAACCTTTTCCTACAAC
5' *tsiV2*	pBAD33	F	AAGCTT GATGTTAATTGATAAAAATGAG
3' t*siV2::6xHis*		R	TCTAGA TTAGTCTTTTAATTCTTG
5' *LS::vasX*		F	GGTACCAGGAGGAATTCACCATGAAAAAGA TTTGGCTGG
3' *vasX*		R	TCTAGATTAACCTTTTCCTACAACGAG
5' GFP	pJET1.2/ blunt	F	GAATTC ATGCGTAAAGGCGAAGAGCT
3' GFP		R	TCTAGA TCATTTGTACAGTTCATCC
5' tsiV2(ATG)		F	CCCGGG TTAATTGATAAAAATGAGTTAG
3' tsiV2::6xHis		R	TCTAGATTAGTGGTGATGGTGATGATGTTC CTCTTTTAATTCTTG
5' tsiV2		F	AAGCTT GATGTTAATTGATAAAAATGAG
3' tsiV2::6xHis		R	TCTAGATTAGTGGTGATGGTGATGATGTTC CTCTTTTAATTCTTG
5' vasX	pUC19	F	AAGCTTAAGTAATCCCAATCAAGCTGCG
3' vasX		R	TCTAGATTAACCTTTTCCTACAACGAG
5' idsD		F	GTCGACTACTGGAGAAGTGAATGAG
3' idsD::myc		R	GGATCCTTATAAATCTTCTTCAGAAATTAAT TTTTGTTCGATATTCTCACTGTTAAT

[a] F, forward; R, reverse, [b] Restriction sites are underlined

Table 8-4. List of primers used for knockout constructs, site-directed mutagenesis, 16S sequencing, and qRT-PCR.

Primer Name	Direction[a]	Sequence[b]
Knockout constructs		
***vasX* k/o A**	**F**	**GGATCCCTTCTTTAGATTCTATTG**
***vasX* k/o B**	**R**	**ACATTTAACCTTTTCCTACATTGGGATTACTCATCCTT**
***vasX* k/o C**	**F**	**AAGGATGAGTAATCCCAATGTAGGAAAAGGTTAAATGT**
***vasX* k/o D**	**R**	**GGATCCTTATTATGAATACTCTTC**
***tsiV2* k/o A**	**F**	**GGATCCAACCGATCTTGAAC**
***tsiV2* k/o B**	**R**	**TGAGCTATTCCTCTTTTAATTTATCAATTAACATTTAA**
***tsiV2* k/o C**	**F**	**TTAAATGTTAATTGATAAATTAAAAGAGGAATAGCTCA**
***tsiV2* k/o D**	**R**	**GGATCCCTTATCTACTCGTTA**
***vasW* k/o A**	**F**	**GGATCCATCGGTCATGAAG**
***vasW* k/o B**	**R**	**TTACTCATCCTTGTACCTCATTTGTTGAACGCATTAAT**
***vasW* k/o C**	**F**	**ATTAATGCGTTCAACAAATGAGGTACAAGGATGAGTAA**
***vasW* k/o D**	**R**	**GGATCCCATTCAGCGCCAC**
PHdomain k/o A	**F**	**GGATCCGAGATTGCTGAACAAC**
PHdomain k/o B	**R**	**GGCTCACTTTACGCATCACATCACGCAGTTGCCTTAAA**
PHdomain k/o C	**F**	**TTTAAGGCAACTGCGTGATGTGATGCGTAAAGTGAGCC**
PHdomain k/o D	**R**	**GGATCCGCTTGCTGAACCTC**
***vgrG-3* k/o A**	**F**	**GGATCC CCACAAGTGAGCGTGCG**
***vgrG-3* k/o B**	**R**	**TTATTCATTTTATATCAACCTGTAACCTTGCCATGCTG**
***vgrG-3* k/o C**	**F**	**CAGCATGGCAAGGTTACAGGTTGATATAAAATGAATAA**
***vgrG-3* k/o D**	**R**	**GGATCC GTAATGAAGATTTGATGAGG**
***tseL* k/o A**	**F**	**GGATCC CGTTTAAACAGGCGGTGGCG**
***tseL* k/o B**	**R**	**GATAACCATGATTTCACAGCAAACCTTACC**
***tseL* k/o C**	**F**	**GCTGTGAAATCATGGTTATCCCCTTAGTTC**
***tseL* k/o D**	**R**	**GGATCC CACCGGCATTAATTATCATCAGATACC**
Site-directed mutagenesis		
PH Domain W144A	**F**	**GGTTATGCGCATCAACGAGCAACGTGGCGAGTGTGTG**
	R	**CACACACTCGCCACGTTGCTCGTTGATGCGCATAACC**
PH Domain W146A	**F**	**GCGCATCAACGATGGACGGCACGAGTGTGTGAGCATATG**
	R	**CATATGCTCACACACTCGTGCCGTCCATCGTTGATGCGC**
tsiV2*14	**F**	**GTTAAAGGTATAATTACACAG**
tsiV2*127	**F**	**CGGGGATTTAATATACGGATC**
tsiV2*164	**F**	**AAGAGGTTTAATTTGCTGACC**
qRT-PCR		
qRT-PCR – vasX	**F**	**TCCTTTACCCAAAGCGGATCGACA**
qRT-PCR – vasX	**R**	**GCCATCACGCAGTTG CCTTAAAGT**
qRT-PCR – ompW	**F**	**GGACTTGCTGCTAACGTTGGCTTT**
qRT-PCR – ompW	**R**	**CCTGCTTTGTAGGTTGCCGTTGTT**
16S Universal	**F**	**AGAGTTTGATCCTGGCTCAG**
	R	**AGGGTTGCGCTCGTTG**

[a] F, forward; R, reverse, [b] Restriction sites are underlined

Table 8-5. Antibodies used in this study.

Antibody	Source	Dilution	Company/Reference
α-VasX	Rabbit	1:1,000	This study
α-Hcp	Rabbit	1:500	[194]
α-6xHis	Mouse	1:1,000	Santa Cruz Biotechnology Inc. (Dallas, TX)
α-RNA Polymerase	Mouse	1:1,000	Neoclone (Madison, WI)
α-β-lactamase	Mouse	1:500	Millipore/Chemicon International (Temecula, CA)
α-FLAG M_2	Mouse	1:1,000	Sigma Aldrich (St. Louis, MO)
α-DnaK	Mouse	1:10,000	Stressgen (Ann Arbor, MI)
α-OmpU	Goat	1:200	Santa Cruz Biotechnology Inc. (Dallas, TX)
α-EpsL	Rabbit	1:20,000	Dr. M. Patrick, University of Michigan Medical School
α-Actin	Mouse	1:1,000	Santa Cruz Biotechnology Inc. (Dallas, TX)
α-Rabbit(HRP)	Goat	1:3,000	Santa Cruz Biotechnology Inc. (Dallas, TX)
α-Goat(HRP)	Donkey	1:3,000	Santa Cruz Biotechnology Inc. (Dallas, TX)
α-Mouse(HRP)	Goat	1:3,000	Santa Cruz Biotechnology Inc. (Dallas, TX)

Table 8-6. Recipes of reagents used in this study

Name	Purpose	Recipe
Luria Bertani (LB) broth and agar plates	Bacterial growth medium	Per liter: 5 g NaCl, 10 g Tryptone, 5 g Yeast extract, (+15 g agar)
S.O.C medium	Recovery of transformed *E. coli*	Per Litre: 20 g tryptone, 5 g yeast extract, 2 mL 5M NaCl, 2.5 mL 1M KCl, 10 mL 1M $MgCl_2$, 10 mL 1M $MgSO_4$, 20 mL 1M glucose
3% NaCl LB broth and agar plates	Growth medium for *Vibrio parahaemolyticus* and *Vibrio alginolyticus*	Per liter: 30 g NaCl, 10 g tryptone, 5 g yeast extract, (+15 g agar)
GVM nutrient broth and agar plates	Growth of *V. fischeri*	Per 200 mL: 2 g tryptone, 1 g casamino acids, 5 g NaCl, 0.8 g $MgCl_2$, 0.2 g KCl (+ 3 g agar), pH 7.4
HL/5 nutrient broth	Axenic growth medium for *D discoideum*	Per liter: 10 g glucose, 5 g yeast extract, 5 g proteose peptone, 5 g thiotone peptone, 0.67 g Na_2HPO_4, 0.34 g KH_2PO_4
Sorensen's Buffer (SorC)	Salt solution for dilution of *D. discoideum*	Per liter: 2 g KH_2PO_4, 0.29 g Na_2HPO_4, 1 mL 50mM calcium chloride pH 6.0
SM/5 agar plates	*D. Discoideum* plaque assay	Per liter: 2 g glucose, 2 g bactopeptone, 0.2 g yeast extract, 0.1g $MgSO_4$, 1.9 g KH_2PO_4, 1.0 g K_2HPO_4, 2.92 g NaCl, 7.5 g agar, pH 6.5
Eagle's Minimum Essential Medium	Growth medium for RAW 264.7 macrophages	500 mL Eagle's minimal essential medium (Sigma Aldrich, St. Louis, MO) 50 mL Fetal bovine serum 10 mL 200 mM L-glutamine 5 mL 100mM Sodium pyruvate 0.5 mL 100mg/mL streptomycin
Laemmli running buffer	SDS-PAGE running buffer	Per liter: 3 g Tris, 14.4 g Glycine, 1 g SDS
Coomassie Blue Stain	Total protein staining of SDS gels	0.25% Coomassie Brilliant Blue R-250 40% methanol 7% acetic acid
Coomassie Blue Destaining Solution	De-staining coomassie blue stained gels to reduce background	Per liter: 100 mL Glacial acetic acid, 300 mL methanol, 600 mL dH_2O
Phosphate-buffered saline	Diluent	Per liter: 8 g NaCl, 0.2 g KCl, 1.4 g Na_2HPO_4, 0.24 g KH_2PO_4
Transfer buffer	Transfer of proteins from polyacrylamide gel to nitrocellulose membrane for western blotting	Per liter: 2.4 g Tris, 11.25 g Glycine, 200 mL Methanol

4x SDS protein sample buffer	Resuspension of bacterial pellet and supernatant samples for SDS-PAGE	40 % glycerol (v/v), 0.24 M Tris-HCl (pH 6.8), 8% SDS (w/v), 0.04% bromophenol blue (w/v), 5% β-mercaptoethanol (v/v)
6x DNA loading dye	Preparation of DNA samples for agarose gel anaylsis.	Per 100 mL: 60 mL 100% Glycerol, 6 mL 1M Tris HCl pH 8.0, 1.2 mL 0.5M EDTA pH 8.0, 34 mL dH_2O, 60 mg Bromophenol blue
Ni^{2+} NTA elution buffer	Elution of 6xHis-tagged proteins bound to Ni^{2+} NTA resin	20mM Tris, 125 mM NaCl, 500 mM Imidazole, pH 8.0
Binding buffer	Washing Ni^{2+} NTA resin with bound 6xHis-tagged proteins	20 mM Tris, 125 mM NaCl, 20 mM Imidazole, pH 8.0
TAE	Preparation and running of agarose gels for DNA fragment analysis.	Per liter: 4.84g Tris, 1.14 mL acetic acid, 2 mL 0.5M EDTA (pH 8.0)
10% SDS-PAGE Separating Gel	Protein analysis	5 mL Acrylamide/Bis (29:1), 3.75 mL 4x Tris pH 8.8, 150 µL 10% SDS (w/v), 6 mL dH_2O, 75 µL 10% ammonium persulfate (w/v), 5 µL TEMED
7.5% SDS-PAGE Separating Gel	Protein analysis	3.75 mL Acrylamide/Bis (29:1), 3.75 mL 4x Tris pH 8.8 (separating buffer), 150 µL 10% SDS (w/v), 7.25 mL dH_2O, 75 µL 10% ammonium persulfate (w/v), 5 µL TEMED
SDS-PAGE Stacking Gel	Protein analysis	1.3 mL Acrylamide/Bis (29:1), 2.5 mL 4x Tris pH 6.8 (stacking buffer), 100 µL 10% SDS, 6 mL dH_2O, 70 µL 10% ammonium persulfate (w/v), 7 µL TEMED
4x Tris pH 8.8 Separating buffer	SDS-PAGE separating gel	400 mL dH_2O, 72.6 g Tris, pH 8.8
4x Tris pH 6.8 Stacking buffer	SDS-PAGE stacking gel	200 mL dH_2O, 12 g Tris, pH 6.8
TBS-T	Western blotting wash buffer and preparation of 5% milk-TBS-T western blotting blocking buffer.	Per liter: 12.11 g Tris, 52 g NaCl, 5 mL Tween-20, pH 8.0
Skim milk TBST (2.5 or 5%)	Blocking buffer for western blot membranes	Skim milk powder to 2.5% or 5% (w/v) in TBS-T
Ponceau S	Visualization of total protein content transferred to nitrocellulose membrane	0.4 g Ponceau S, 2 mL Glacial acetic acid, 198 mL dH_2O
Z Buffer	Dilutent for β-galactosidase assays	0.06 M Na_2HPO_4, 0.04M NaH_2PO_4, 0.01 M KCl, 0.001 M $MgSO_4$, pH 7.0
½ YTSS nutrient broth and agar plates	Growth of environmental isolates *V. communis*, *V. harveyi*, and *P. phenolica*	Per litre: 2.5 g tryptone, 4 g yeast extract, 20 g sea salts (Sigma Aldrich)

CHAPTER 9

Appendix

Portions of this chapter have been published as:

MacIntyre, D., Miyata, S.T., Kitaoka, M., and Pukatzki, S. (2010) The *Vibrio cholerae* type VI secretion system displays antimicrobial properties. *Proceedings of the National Academy of Sciences U.S.A*, 107(45):19520-4.

Unterweger, D., Kitaoka, M., Miyata, S.T., Bachmann, V., Brooks, T.M., Moloney, J., Sosa, O., Silva, D., Duran-Gonzalez, J., Provenzano, D. and Pukatzki, S. (2012) Constitutive type VI secretion system expression gives *Vibrio cholerae* intra- and inter-specific competitive advantages. *PLoS One*, 7(10): e48320.

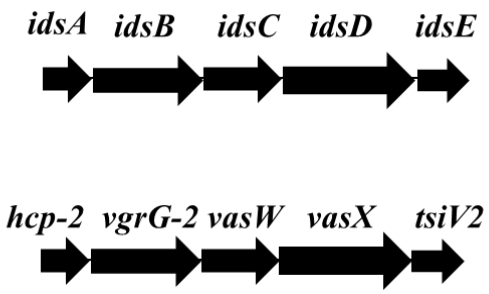

Figure 9-1. Alignment of *P. mirabilis ids* and *V. cholerae* VasX-encoding gene clusters. The *ids* gene cluster is known to encode proteins involved in self/non-self recognition between *P. mirabilis* swarms. IdsD encodes a crucial molecular identifier in self-recognition and shares similarity with VasX.

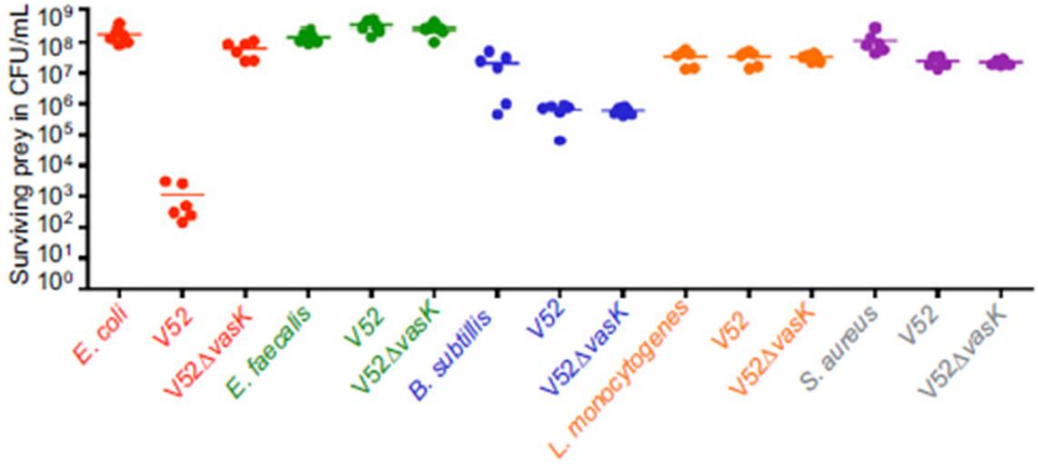

Figure 9-2. *V. cholerae* is unable to kill Gram-positive bacteria using its T6SS. Survival of rifampicin-resistant bacteria is shown: *E. coli* MG1655 (red, positive control), *E. fecaelis* (green), *B. subtilis* (blue), *L. monocytogenes* (orange), and *S. aureus* (grey) was determined by measuring CFU following exposure to the indicated rifampicin-sensitive predator listed on the *x*-axis. Each prey was exposed to itself, V52, and V52Δ*vasK*.

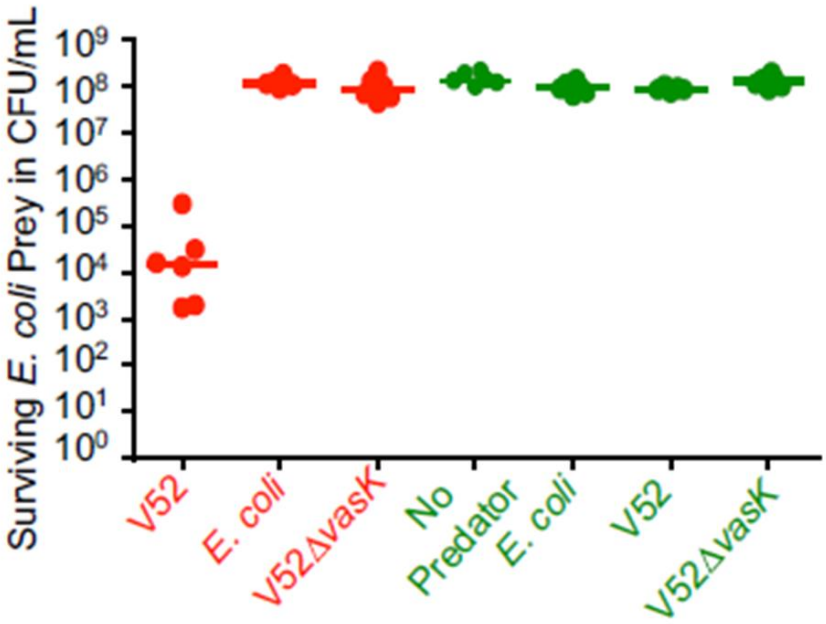

Figure 9-3. T6SS-mediated bacterial killing by V52 is contact-dependent. Survival of rifampicin-resistant *E. coli* was determined by measuring CFU following exposure to the indicated rifampicin-sensitive predator listed on the *x*-axis with (green) or without (red) separation of predator and prey by a 0.22-µm filter.

A.

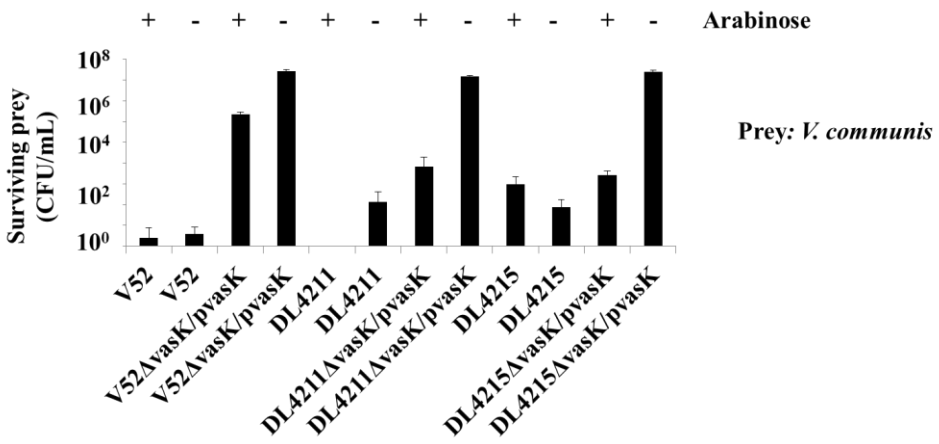

B.

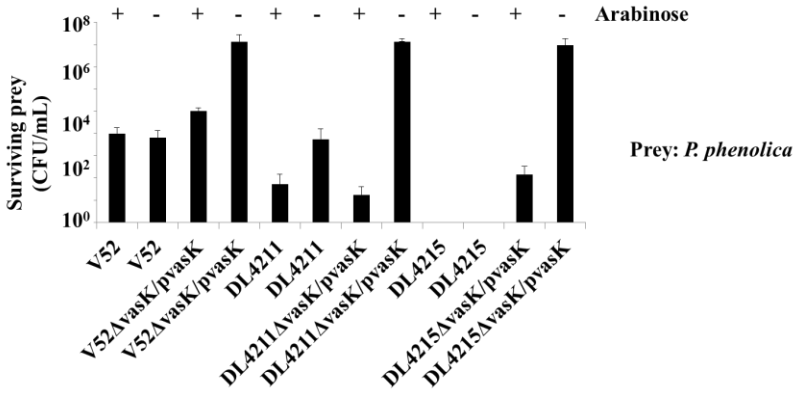

C.

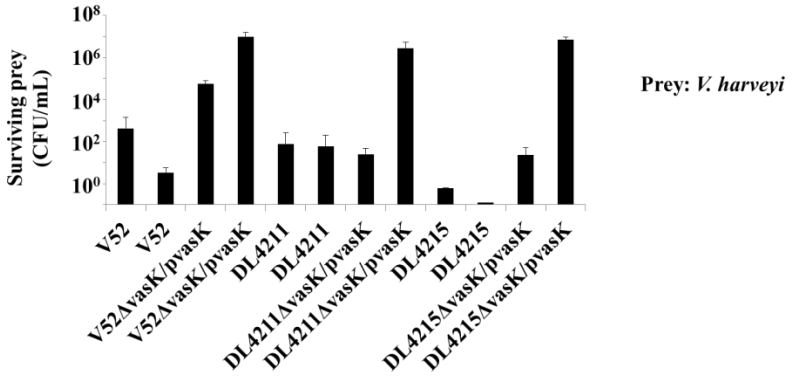

Figure 9-4. Rio Grande *V. cholerae* kill bacterial neighbors in a T6SS-dependent manner. Survival of rifampicin-resistant prey (listed in the legend) following exposure to rifampicin-sensitive predator (*x*-axis). Arabinose was added where indicated to induce expression from the P_{BAD} promoter. Killing assays, growth, and selection of prey was performed on ½ YTSS agar at 30 ^{o}C.

A.

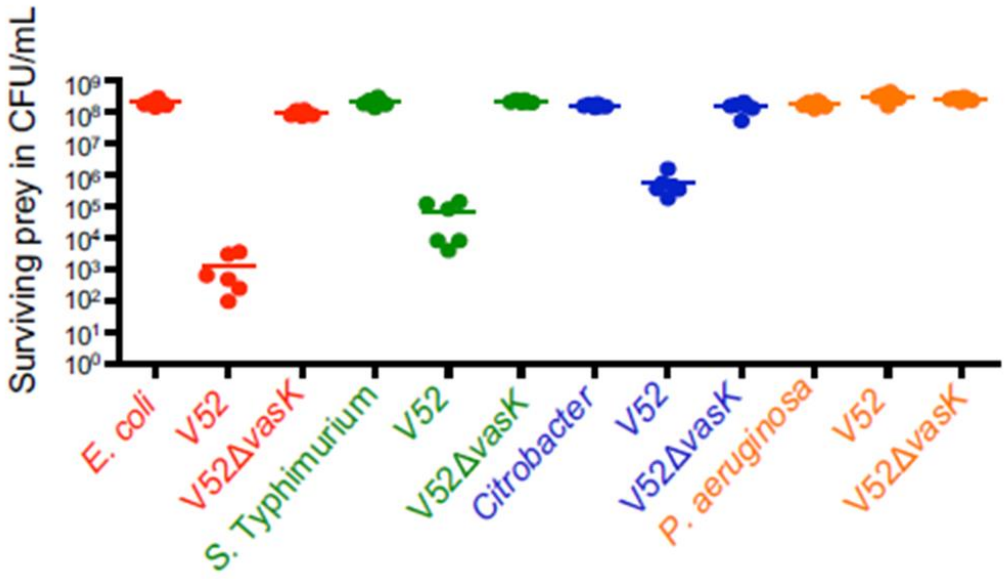

B.

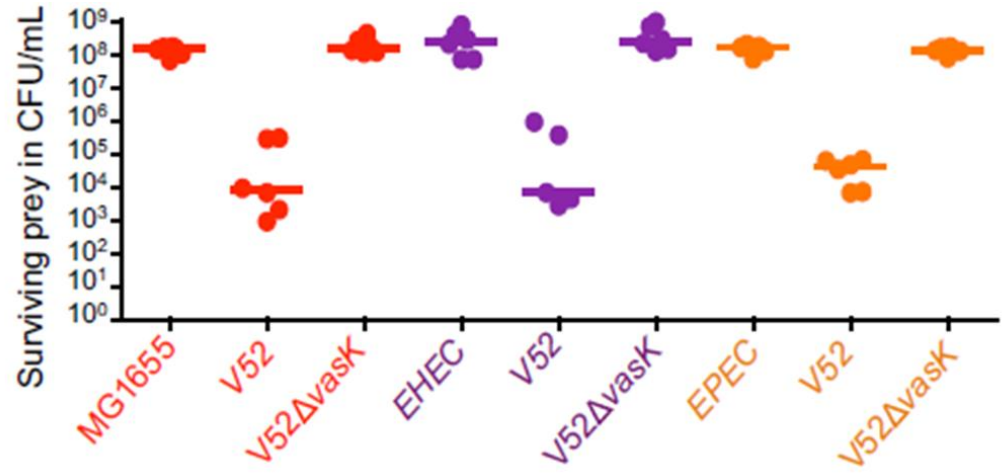

Figure 9-5. *V. cholerae* uses its T6SS to kill other Gram-negative bacteria. (A) Survival of rifampicin-resistant bacteria is shown: *E. coli* MG1655 (red, positive control), *S.* Typhimurium (green), *C. rodentium* (blue) and *P. aeruginosa* (orange) was determined by measuring CFU following exposure to the indicated rifampicin-sensitive predator listed on the *x*-axis. Each prey was exposed to itself, V52, and V52Δ*vasK*. (B) Survival of rifampicin-resistant bacteria is shown: *E. coli* MG1655 (red, positive control), Enterohemorrhagic *E coli.* (EHEC, purple), Enteropathogenic *E. coli* (EPEC, orange) was determined by measuring CFU following exposure to the indicated rifampicin-sensitive predator listed on the *x*-axis. Each prey was exposed to itself, V52, and V52Δ*vasK*.

A.

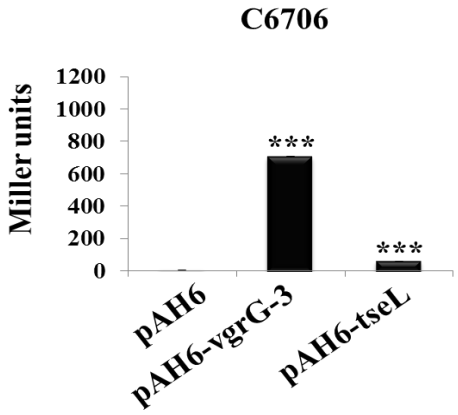

B.

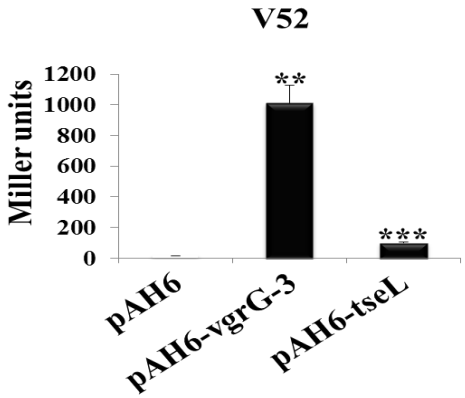

C.

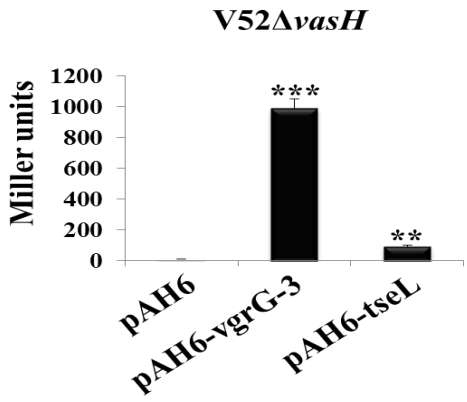

Figure 9-6. Promoters are present within *tseL* and *vgrG-3* that drive expression of their cognate immunity protein genes. (A, B, and C) Overnight cultures of the strains indicated at the top of the graph harboring plasmids indicated on the *x*-axis were used to assay for the production of β-galactosidase. Miller units are a function of LacZ production combined with optical density of the starting culture and incubation time. Error bars indicate the standard deviation. ***= $p < 0.001$, **= $p < 0.005$, *= $p < 0.01$ relative to the empty vector control. *P*-values were calculated based on the Student's one-tailed, paired T-Test.

Bibliography

1. Bentivoglio, M. and P. Pacini, *Filippo Pacini: a determined observer.* Brain Res Bull, 1995. **38**(2): p. 161-5.
2. Pollitzer, R., S. Swaroop, and W. Burrows, *Cholera.* Monogr Ser World Health Organ, 1959. **58**(43): p. 1001-19.
3. Kaper, J., H. Lockman, R.R. Colwell, and S.W. Joseph, *Ecology, serology, and enterotoxin production of Vibrio cholerae in Chesapeake Bay.* Appl Environ Microbiol, 1979. **37**(1): p. 91-103.
4. Hase, C.C., *Analysis of the role of flagellar activity in virulence gene expression in Vibrio cholerae.* Microbiology, 2001. **147**(Pt 4): p. 831-7.
5. Guentzel, M.N. and L.J. Berry, *Motility as a virulence factor for Vibrio cholerae.* Infect Immun, 1975. **11**(5): p. 890-7.
6. Jones, G.W., G.D. Abrams, and R. Freter, *Adhesive properties of Vibrio cholerae: adhesion to isolated rabbit brush border membranes and hemagglutinating activity.* Infect Immun, 1976. **14**(1): p. 232-39.
7. Attridge, S.R. and D. Rowley, *The role of the flagellum in the adherence of Vibrio cholerae.* J Infect Dis, 1983. **147**(5): p. 864-72.
8. Butler, S.M. and A. Camilli, *Both chemotaxis and net motility greatly influence the infectivity of Vibrio cholerae.* Proc Natl Acad Sci U S A, 2004. **101**(14): p. 5018-23.
9. Baker, R.M., F.L. Singleton, and M.A. Hood, *Effects of nutrient deprivation on Vibrio cholerae.* Appl Environ Microbiol, 1983. **46**(4): p. 930-40.
10. Faruque, S.M., K. Biswas, S.M. Udden, Q.S. Ahmad, D.A. Sack, G.B. Nair, and J.J. Mekalanos, *Transmissibility of cholera: in vivo-formed biofilms and their relationship to infectivity and persistence in the environment.* Proc Natl Acad Sci U S A, 2006. **103**(16): p. 6350-5.
11. Sack, D.A., R.B. Sack, G.B. Nair, and A.K. Siddique, *Cholera.* Lancet, 2004. **363**(9404): p. 223-33.
12. Ritchie, J.M. and M.K. Waldor, *Vibrio cholerae interactions with the gastrointestinal tract: lessons from animal studies.* Curr Top Microbiol Immunol, 2009. **337**: p. 37-59.
13. Faruque, S.M., M.J. Islam, Q.S. Ahmad, A.S. Faruque, D.A. Sack, G.B. Nair, and J.J. Mekalanos, *Self-limiting nature of seasonal cholera epidemics: Role of host-mediated amplification of phage.* Proc Natl Acad Sci U S A, 2005. **102**(17): p. 6119-24.
14. Faruque, S.M., I.B. Naser, M.J. Islam, A.S. Faruque, A.N. Ghosh, G.B. Nair, D.A. Sack, and J.J. Mekalanos, *Seasonal epidemics of cholera inversely correlate with the prevalence of environmental cholera phages.* Proc Natl Acad Sci U S A, 2005. **102**(5): p. 1702-7.
15. Jensen, M.A., S.M. Faruque, J.J. Mekalanos, and B.R. Levin, *Modeling the role of bacteriophage in the control of cholera outbreaks.* Proc Natl Acad Sci U S A, 2006. **103**(12): p. 4652-7.
16. Waldor, M.K. and J.J. Mekalanos, *Lysogenic conversion by a filamentous phage encoding cholera toxin.* Science, 1996. **272**(5270): p. 1910-4.
17. Seed, K.D., S.M. Faruque, J.J. Mekalanos, S.B. Calderwood, F. Qadri, and A. Camilli, *Phase variable O antigen biosynthetic genes control expression of the*

major protective antigen and bacteriophage receptor in Vibrio cholerae O1. PLoS Pathog, 2012. **8**(9): p. e1002917.
18. Pierce, N.F., J.G. Banwell, S.L. Gorbach, R.C. Mitra, and A. Mondal, *Convalescent carriers of Vibrio cholerae. Detection and detailed investigation.* Ann Intern Med, 1970. **72**(3): p. 357-64.
19. Miller, C.E., K.H. Wong, J.C. Feeley, and M.E. Forlines, *Immunological conversion of Vibrio chorlerae in gnotobiotic mice.* Infect Immun, 1972. **6**(5): p. 739-42.
20. Herrington, D.A., R.H. Hall, G. Losonsky, J.J. Mekalanos, R.K. Taylor, and M.M. Levine, *Toxin, toxin-coregulated pili, and the toxR regulon are essential for Vibrio cholerae pathogenesis in humans.* J Exp Med, 1988. **168**(4): p. 1487-92.
21. Taylor, R.K., V.L. Miller, D.B. Furlong, and J.J. Mekalanos, *Use of phoA gene fusions to identify a pilus colonization factor coordinately regulated with cholera toxin.* Proc Natl Acad Sci U S A, 1987. **84**(9): p. 2833-7.
22. Vanden Broeck, D., C. Horvath, and M.J. De Wolf, *Vibrio cholerae: cholera toxin.* Int J Biochem Cell Biol, 2007. **39**(10): p. 1771-5.
23. Levine, M.M., J.B. Kaper, R.E. Black, and M.L. Clements, *New knowledge on pathogenesis of bacterial enteric infections as applied to vaccine development.* Microbiol Rev, 1983. **47**(4): p. 510-50.
24. De, S.N., *Enterotoxicity of bacteria-free culture-filtrate of Vibrio cholerae.* Nature, 1959. **183**(4674): p. 1533-4.
25. Dutta, N.K., M.V. Panse, and D.R. Kulkarni, *Role of cholera a toxin in experimental cholera.* J Bacteriol, 1959. **78**: p. 594-5.
26. Sharma, D.P., U.H. Stroeher, C.J. Thomas, P.A. Manning, and S.R. Attridge, *The toxin-coregulated pilus (TCP) of Vibrio cholerae: molecular cloning of genes involved in pilus biosynthesis and evaluation of TCP as a protective antigen in the infant mouse model.* Microb Pathog, 1989. **7**(6): p. 437-48.
27. Levine, M.M., J.B. Kaper, D. Herrington, G. Losonsky, J.G. Morris, M.L. Clements, R.E. Black, B. Tall, and R. Hall, *Volunteer studies of deletion mutants of Vibrio cholerae O1 prepared by recombinant techniques.* Infect Immun, 1988. **56**(1): p. 161-7.
28. Ghosh, C., R.K. Nandy, S.K. Dasgupta, G.B. Nair, R.H. Hall, and A.C. Ghose, *A search for cholera toxin (CT), toxin coregulated pilus (TCP), the regulatory element ToxR and other virulence factors in non-01/non-0139 Vibrio cholerae.* Microb Pathog, 1997. **22**(4): p. 199-208.
29. Sarkar, A., R.K. Nandy, G.B. Nair, and A.C. Ghose, *Vibrio pathogenicity island and cholera toxin genetic element-associated virulence genes and their expression in non-O1 non-O139 strains of Vibrio cholerae.* Infect Immun, 2002. **70**(8): p. 4735-42.
30. Datta-Roy, K., K. Banerjee, S.P. De, and A.C. Ghose, *Comparative study of expression of hemagglutinins, hemolysins, and enterotoxins by clinical and environmental isolates of non-O1 Vibrio cholerae in relation to their enteropathogenicity.* Appl Environ Microbiol, 1986. **52**(4): p. 875-9.
31. Mukhopadhyay, A.K., S. Chakraborty, Y. Takeda, G.B. Nair, and D.E. Berg, *Characterization of VPI pathogenicity island and CTXphi prophage in environmental strains of Vibrio cholerae.* J Bacteriol, 2001. **183**(16): p. 4737-46.
32. Mukhopadhyay, A.K., P.K. Saha, S. Garg, S.K. Bhattacharya, T. Shimada, T. Takeda, Y. Takeda, and G.B. Nair, *Distribution and virulence of Vibrio cholerae*

belonging to serogroups other than O1 and O139: a nationwide survey. Epidemiol Infect, 1995. **114**(1): p. 65-70.
33. Organization, W.H., *Manual for Laboratory Investigations of Acute Enteric Infections.* 1987.
34. Kaper, J.B., J.G. Morris, Jr., and M.M. Levine, *Cholera.* Clin Microbiol Rev, 1995. **8**(1): p. 48-86.
35. Ghosh-Banerjee, J., M. Senoh, T. Takahashi, T. Hamabata, S. Barman, H. Koley, A.K. Mukhopadhyay, T. Ramamurthy, S. Chatterjee, M. Asakura, S. Yamasaki, G.B. Nair, and Y. Takeda, *Cholera toxin production by the El Tor variant of Vibrio cholerae O1 compared to prototype El Tor and classical biotypes.* J Clin Microbiol, 2010. **48**(11): p. 4283-6.
36. Safa, A., J. Sultana, P. Dac Cam, J.C. Mwansa, and R.Y. Kong, *Vibrio cholerae O1 hybrid El Tor strains, Asia and Africa.* Emerg Infect Dis, 2008. **14**(6): p. 987-8.
37. Nair, G.B., F. Qadri, J. Holmgren, A.M. Svennerholm, A. Safa, N.A. Bhuiyan, Q.S. Ahmad, S.M. Faruque, A.S. Faruque, Y. Takeda, and D.A. Sack, *Cholera due to altered El Tor strains of Vibrio cholerae O1 in Bangladesh.* J Clin Microbiol, 2006. **44**(11): p. 4211-3.
38. Ansaruzzaman, M., N.A. Bhuiyan, B.G. Nair, D.A. Sack, M. Lucas, J.L. Deen, J. Ampuero, and C.L. Chaignat, *Cholera in Mozambique, variant of Vibrio cholerae.* Emerg Infect Dis, 2004. **10**(11): p. 2057-9.
39. Faruque, S.M., V.C. Tam, N. Chowdhury, P. Diraphat, M. Dziejman, J.F. Heidelberg, J.D. Clemens, J.J. Mekalanos, and G.B. Nair, *Genomic analysis of the Mozambique strain of Vibrio cholerae O1 reveals the origin of El Tor strains carrying classical CTX prophage.* Proc Natl Acad Sci U S A, 2007. **104**(12): p. 5151-6.
40. Stroeher, U.H., L.E. Karageorgos, R. Morona, and P.A. Manning, *Serotype conversion in Vibrio cholerae O1.* Proc Natl Acad Sci U S A, 1992. **89**(7): p. 2566-70.
41. Sakazaki, R., *Bacteriology of Vibrio and related organisms*, in *Cholera*, D. Barua, and Greenough, W.B., Editor 1992, Plenum Medical Book Co, New York. p. 37-35.
42. Burrows, W., A.N. Mather, and et al., *Studies on immunity to Asiatic cholera; the O and H antigenic structure of the cholera and related vibrios.* J Infect Dis, 1946. **79**(2): p. 168-97.
43. Villeneuve, S., H. Souchon, M.M. Riottot, J.C. Mazie, P. Lei, C.P. Glaudemans, P. Kovac, J.M. Fournier, and P.M. Alzari, *Crystal structure of an anti-carbohydrate antibody directed against Vibrio cholerae O1 in complex with antigen: molecular basis for serotype specificity.* Proc Natl Acad Sci U S A, 2000. **97**(15): p. 8433-8.
44. Villeneuve, S., A. Boutonnier, L.A. Mulard, and J.M. Fournier, *Immunochemical characterization of an Ogawa-Inaba common antigenic determinant of Vibrio cholerae O1.* Microbiology, 1999. **145 (Pt 9)**: p. 2477-84.
45. Gunn, S.W.A., and Masellis, M, *Concepts and Practice of Humanitarian Medicine*2008: Springer Science.
46. Yoon, S.S. and J.J. Mekalanos, *2,3-butanediol synthesis and the emergence of the Vibrio cholerae El Tor biotype.* Infect Immun, 2006. **74**(12): p. 6547-56.
47. Bik, E.M., A.E. Bunschoten, R.D. Gouw, and F.R. Mooi, *Genesis of the novel epidemic Vibrio cholerae O139 strain: evidence for horizontal transfer of genes involved in polysaccharide synthesis.* EMBO J, 1995. **14**(2): p. 209-16.

48. Roberts, N.C., Siebeling, R.J., Kaper, J.B., and Bradford, H.B. Jr., *Vibrios in the Louisiana Gulf Coast Environment.* Microbial Ecology, 1982. **8**: p. 299-312.
49. Swerdlow, D.L. and A.A. Ries, *Vibrio cholerae non-O1--the eighth pandemic?* Lancet, 1993. **342**(8868): p. 382-3.
50. Control, C.f.D., *Imported cholera associated with a newly described toxigenic Vibrio cholerae O139 strain - California, 1993.* Morbidity and Mortality Weekly Report, 1993. **42**: p. 501-503.
51. Group, C.W., *Large epidemic of cholera-like disease in Bangladesh caused by Vibrio cholerae O139 synonym Bengal.* Lancet, 1993. **342**: p. 387-390.
52. Service, P.H.L., *Vibrio cholerae O139 and epidemic cholera.* Communicable Disease Report Weekly, 1993. **3**: p. 173.
53. Morris, J.G., Jr., *Non-O group 1 Vibrio cholerae: a look at the epidemiology of an occasional pathogen.* Epidemiol Rev, 1990. **12**: p. 179-91.
54. Hughes, J.M., D.G. Hollis, E.J. Gangarosa, and R.E. Weaver, *Non-cholera vibrio infections in the United States. Clinical, epidemiologic, and laboratory features.* Ann Intern Med, 1978. **88**(5): p. 602-6.
55. Morris, J.G., Jr. and R.E. Black, *Cholera and other vibrioses in the United States.* N Engl J Med, 1985. **312**(6): p. 343-50.
56. Morris, J.G., Jr., R. Wilson, B.R. Davis, I.K. Wachsmuth, C.F. Riddle, H.G. Wathen, R.A. Pollard, and P.A. Blake, *Non-O group 1 Vibrio cholerae gastroenteritis in the United States: clinical, epidemiologic, and laboratory characteristics of sporadic cases.* Ann Intern Med, 1981. **94**(5): p. 656-8.
57. Ceccarelli, D., M. Spagnoletti, P. Cappuccinelli, V. Burrus, and M.M. Colombo, *Origin of Vibrio cholerae in Haiti.* Lancet Infect Dis, 2011. **11**(4): p. 262.
58. Chin, C.S., J. Sorenson, J.B. Harris, W.P. Robins, R.C. Charles, R.R. Jean-Charles, J. Bullard, D.R. Webster, A. Kasarskis, P. Peluso, E.E. Paxinos, Y. Yamaichi, S.B. Calderwood, J.J. Mekalanos, E.E. Schadt, and M.K. Waldor, *The origin of the Haitian cholera outbreak strain.* N Engl J Med, 2011. **364**(1): p. 33-42.
59. Hasan, N.A., S.Y. Choi, M. Eppinger, P.W. Clark, A. Chen, M. Alam, B.J. Haley, E. Taviani, E. Hine, Q. Su, L.J. Tallon, J.B. Prosper, K. Furth, M.M. Hoq, H. Li, C.M. Fraser-Liggett, A. Cravioto, A. Huq, J. Ravel, T.A. Cebula, and R.R. Colwell, *Genomic diversity of 2010 Haitian cholera outbreak strains.* Proc Natl Acad Sci U S A, 2012. **109**(29): p. E2010-7.
60. Sack, D.A., C.O. Tacket, M.B. Cohen, R.B. Sack, G.A. Losonsky, J. Shimko, J.P. Nataro, R. Edelman, M.M. Levine, R.A. Giannella, G. Schiff, and D. Lang, *Validation of a volunteer model of cholera with frozen bacteria as the challenge.* Infect Immun, 1998. **66**(5): p. 1968-72.
61. Nelson, E.J., J.B. Harris, J.G. Morris, Jr., S.B. Calderwood, and A. Camilli, *Cholera transmission: the host, pathogen and bacteriophage dynamic.* Nat Rev Microbiol, 2009. **7**(10): p. 693-702.
62. Harris, J.B., R.C. LaRocque, F. Chowdhury, A.I. Khan, T. Logvinenko, A.S. Faruque, E.T. Ryan, F. Qadri, and S.B. Calderwood, *Susceptibility to Vibrio cholerae infection in a cohort of household contacts of patients with cholera in Bangladesh.* PLoS Negl Trop Dis, 2008. **2**(4): p. e221.
63. Harris, J.B., A.I. Khan, R.C. LaRocque, D.J. Dorer, F. Chowdhury, A.S. Faruque, D.A. Sack, E.T. Ryan, F. Qadri, and S.B. Calderwood, *Blood group, immunity, and risk of infection with Vibrio cholerae in an area of endemicity.* Infect Immun, 2005. **73**(11): p. 7422-7.

64. Alam, M., M. Sultana, G.B. Nair, A.K. Siddique, N.A. Hasan, R.B. Sack, D.A. Sack, K.U. Ahmed, A. Sadique, H. Watanabe, C.J. Grim, A. Huq, and R.R. Colwell, *Viable but nonculturable Vibrio cholerae O1 in biofilms in the aquatic environment and their role in cholera transmission.* Proc Natl Acad Sci U S A, 2007. **104**(45): p. 17801-6.
65. Finkelstein, R.A., S. Mukerjee, and B.C. Rudra, *Demonstration and Quantitation of Antigen in Cholera Stool Filtrates.* J Infect Dis, 1963. **113**: p. 99-104.
66. Organization, W.H. *Cholera*. 2013; Available from: http://www.who.int/topics/cholera/about/en/.
67. Merrell, D.S., D.L. Hava, and A. Camilli, *Identification of novel factors involved in colonization and acid tolerance of Vibrio cholerae.* Mol Microbiol, 2002. **43**(6): p. 1471-91.
68. Colwell, R.R., A. Huq, M.S. Islam, K.M. Aziz, M. Yunus, N.H. Khan, A. Mahmud, R.B. Sack, G.B. Nair, J. Chakraborty, D.A. Sack, and E. Russek-Cohen, *Reduction of cholera in Bangladeshi villages by simple filtration.* Proc Natl Acad Sci U S A, 2003. **100**(3): p. 1051-5.
69. Levine, M.M., R.E. Black, M.L. Clements, L. Cisneros, D.R. Nalin, and C.R. Young, *Duration of infection-derived immunity to cholera.* J Infect Dis, 1981. **143**(6): p. 818-20.
70. Levine, M.M., D.R. Nalin, J.P. Craig, D. Hoover, E.J. Bergquist, D. Waterman, H.P. Holley, R.B. Hornick, N.P. Pierce, and J.P. Libonati, *Immunity of cholera in man: relative role of antibacterial versus antitoxic immunity.* Trans R Soc Trop Med Hyg, 1979. **73**(1): p. 3-9.
71. Cash, R.A., S.I. Music, J.P. Libonati, J.P. Craig, N.F. Pierce, and R.B. Hornick, *Response of man to infection with Vibrio cholerae. II. Protection from illness afforded by previous disease and vaccine.* J Infect Dis, 1974. **130**(4): p. 325-33.
72. Organization, W.H., *Cholera vaccines: WHO position paper.* Weekly epidemiological record, 2010. **85**(13): p. 117-128.
73. Sinclair, D., K. Abba, K. Zaman, F. Qadri, and P.M. Graves, *Oral vaccines for preventing cholera.* Cochrane Database Syst Rev, 2011(3): p. CD008603.
74. Graves, P.M., J.J. Deeks, V. Demicheli, and T. Jefferson, *Vaccines for preventing cholera: killed whole cell or other subunit vaccines (injected).* Cochrane Database Syst Rev, 2010(8): p. CD000974.
75. Finkelstein, R.A., *Vibriocidal antibody inhibition (VAI) analysis: a technique for the identification of the predominant vibriocidal antibodies in serum and for the detection and identification of Vibrio cholerae antigens.* Journal of Immunology, 1962. **89**: p. 264-271.
76. Neoh, S.H. and D. Rowley, *The antigens of Vibrio cholerae involved in the vibriocidal action of antibody and complement.* J Infect Dis, 1970. **121**(5): p. 505-13.
77. Harris, A.M., M.S. Bhuiyan, F. Chowdhury, A.I. Khan, A. Hossain, E.A. Kendall, A. Rahman, R.C. LaRocque, J. Wrammert, E.T. Ryan, F. Qadri, S.B. Calderwood, and J.B. Harris, *Antigen-specific memory B-cell responses to Vibrio cholerae O1 infection in Bangladesh.* Infect Immun, 2009. **77**(9): p. 3850-6.
78. Bishop, A.L. and A. Camilli, *Vibrio cholerae: lessons for mucosal vaccine design.* Expert Rev Vaccines, 2011. **10**(1): p. 79-94.

79. Provenzano, D., P. Kovac, and W.F. Wade, *The ABCs (Antibody, B cells, and Carbohydrate epitopes) of cholera immunity: considerations for an improved vaccine.* Microbiol Immunol, 2006. **50**(12): p. 899-927.
80. Organization, W.H. *Cholera Fact Sheet*. 2012; Available from: http://www.who.int/mediacentre/factsheets/fs107/en/index.html.
81. Greenough, W.B., 3rd, R.S. Gordon, Jr., I.S. Rosenberg, B.I. Davies, and A.S. Benenson, *Tetracycline in the Treatment of Cholera.* Lancet, 1964. **1**(7329): p. 355-7.
82. Lindenbaum, J., W.B. Greenough, and M.R. Islam, *Antibiotic therapy of cholera.* Bull World Health Organ, 1967. **36**(6): p. 871-83.
83. Pierce, N.F., J.G. Banwell, R.C. Mitra, G.J. Caranasos, R.I. Keimowitz, J. Thomas, and A. Mondal, *Controlled comparison of tetracycline and furazolidone in cholera.* Br Med J, 1968. **3**(5613): p. 277-80.
84. Kitaoka, M., S.T. Miyata, D. Unterweger, and S. Pukatzki, *Antibiotic resistance mechanisms of Vibrio cholerae.* J Med Microbiol, 2011. **60**(Pt 4): p. 397-407.
85. Mhalu, F.S., P.W. Mmari, and J. Ijumba, *Rapid emergence of El Tor Vibrio cholerae resistant to antimicrobial agents during first six months of fourth cholera epidemic in Tanzania.* Lancet, 1979. **1**(8112): p. 345-7.
86. Towner, K.J., N.J. Pearson, F.S. Mhalu, and F. O'Grady, *Resistance to antimicrobial agents of Vibrio cholerae E1 Tor strains isolated during the fourth cholera epidemic in the United Republic of Tanzania.* Bull World Health Organ, 1980. **58**(5): p. 747-51.
87. Zhu, J. and J.J. Mekalanos, *Quorum sensing-dependent biofilms enhance colonization in Vibrio cholerae.* Dev Cell, 2003. **5**(4): p. 647-56.
88. Kirn, T.J., M.J. Lafferty, C.M. Sandoe, and R.K. Taylor, *Delineation of pilin domains required for bacterial association into microcolonies and intestinal colonization by Vibrio cholerae.* Mol Microbiol, 2000. **35**(4): p. 896-910.
89. Rhine, J.A. and R.K. Taylor, *TcpA pilin sequences and colonization requirements for O1 and O139 vibrio cholerae.* Mol Microbiol, 1994. **13**(6): p. 1013-20.
90. Taylor, R., C. Shaw, K. Peterson, P. Spears, and J. Mekalanos, *Safe, live Vibrio cholerae vaccines?* Vaccine, 1988. **6**(2): p. 151-4.
91. Karaolis, D.K., J.A. Johnson, C.C. Bailey, E.C. Boedeker, J.B. Kaper, and P.R. Reeves, *A Vibrio cholerae pathogenicity island associated with epidemic and pandemic strains.* Proc Natl Acad Sci U S A, 1998. **95**(6): p. 3134-9.
92. Karaolis, D.K., S. Somara, D.R. Maneval, Jr., J.A. Johnson, and J.B. Kaper, *A bacteriophage encoding a pathogenicity island, a type-IV pilus and a phage receptor in cholera bacteria.* Nature, 1999. **399**(6734): p. 375-9.
93. Karaolis, D.K., R. Lan, J.B. Kaper, and P.R. Reeves, *Comparison of Vibrio cholerae pathogenicity islands in sixth and seventh pandemic strains.* Infect Immun, 2001. **69**(3): p. 1947-52.
94. Hase, C.C. and J.J. Mekalanos, *TcpP protein is a positive regulator of virulence gene expression in Vibrio cholerae.* Proc Natl Acad Sci U S A, 1998. **95**(2): p. 730-4.
95. Carroll, P.A., K.T. Tashima, M.B. Rogers, V.J. DiRita, and S.B. Calderwood, *Phase variation in tcpH modulates expression of the ToxR regulon in Vibrio cholerae.* Mol Microbiol, 1997. **25**(6): p. 1099-111.
96. DiRita, V.J., *Co-ordinate expression of virulence genes by ToxR in Vibrio cholerae.* Mol Microbiol, 1992. **6**(4): p. 451-8.

97. DiRita, V.J., C. Parsot, G. Jander, and J.J. Mekalanos, *Regulatory cascade controls virulence in Vibrio cholerae.* Proc Natl Acad Sci U S A, 1991. **88**(12): p. 5403-7.
98. Faruque, S.M., J. Zhu, Asadulghani, M. Kamruzzaman, and J.J. Mekalanos, *Examination of diverse toxin-coregulated pilus-positive Vibrio cholerae strains fails to demonstrate evidence for Vibrio pathogenicity island phage.* Infect Immun, 2003. **71**(6): p. 2993-9.
99. Waldor, M.K., E.J. Rubin, G.D. Pearson, H. Kimsey, and J.J. Mekalanos, *Regulation, replication, and integration functions of the Vibrio cholerae CTXphi are encoded by region RS2.* Mol Microbiol, 1997. **24**(5): p. 917-26.
100. Spangler, B.D., *Structure and function of cholera toxin and the related Escherichia coli heat-labile enterotoxin.* Microbiol Rev, 1992. **56**(4): p. 622-47.
101. King, C.A. and W.E. Van Heyningen, *Deactivation of cholera toxin by a sialidase-resistant monosialosylganglioside.* J Infect Dis, 1973. **127**(6): p. 639-47.
102. Majoul, I.V., P.I. Bastiaens, and H.D. Soling, *Transport of an external Lys-Asp-Glu-Leu (KDEL) protein from the plasma membrane to the endoplasmic reticulum: studies with cholera toxin in Vero cells.* J Cell Biol, 1996. **133**(4): p. 777-89.
103. Moss, J. and M. Vaughan, *Mechanism of action of choleragen. Evidence for ADP-ribosyltransferase activity with arginine as an acceptor.* J Biol Chem, 1977. **252**(7): p. 2455-7.
104. Kahn, R.A. and A.G. Gilman, *ADP-ribosylation of Gs promotes the dissociation of its alpha and beta subunits.* J Biol Chem, 1984. **259**(10): p. 6235-40.
105. Cassel, D. and Z. Selinger, *Mechanism of adenylate cyclase activation by cholera toxin: inhibition of GTP hydrolysis at the regulatory site.* Proc Natl Acad Sci U S A, 1977. **74**(8): p. 3307-11.
106. Tsai, B. and T.A. Rapoport, *Unfolded cholera toxin is transferred to the ER membrane and released from protein disulfide isomerase upon oxidation by Ero1.* J Cell Biol, 2002. **159**(2): p. 207-16.
107. Hazes, B. and R.J. Read, *Accumulating evidence suggests that several AB-toxins subvert the endoplasmic reticulum-associated protein degradation pathway to enter target cells.* Biochemistry, 1997. **36**(37): p. 11051-4.
108. Sanchez, J. and J. Holmgren, *Virulence factors, pathogenesis and vaccine protection in cholera and ETEC diarrhea.* Curr Opin Immunol, 2005. **17**(4): p. 388-98.
109. Fuqua, W.C., S.C. Winans, and E.P. Greenberg, *Quorum sensing in bacteria: the LuxR-LuxI family of cell density-responsive transcriptional regulators.* J Bacteriol, 1994. **176**(2): p. 269-75.
110. Miller, M.B. and B.L. Bassler, *Quorum sensing in bacteria.* Annu Rev Microbiol, 2001. **55**: p. 165-99.
111. More, M.I., L.D. Finger, J.L. Stryker, C. Fuqua, A. Eberhard, and S.C. Winans, *Enzymatic synthesis of a quorum-sensing autoinducer through use of defined substrates.* Science, 1996. **272**(5268): p. 1655-8.
112. Val, D.L. and J.E. Cronan, Jr., *In vivo evidence that S-adenosylmethionine and fatty acid synthesis intermediates are the substrates for the LuxI family of autoinducer synthases.* J Bacteriol, 1998. **180**(10): p. 2644-51.
113. Parsek, M.R. and E.P. Greenberg, *Quorum sensing signals in development of Pseudomonas aeruginosa biofilms.* Methods Enzymol, 1999. **310**: p. 43-55.

114. Gould, T.A., H.P. Schweizer, and M.E. Churchill, *Structure of the Pseudomonas aeruginosa acyl-homoserinelactone synthase LasI.* Mol Microbiol, 2004. **53**(4): p. 1135-46.
115. Gould, T.A., W.T. Watson, K.H. Choi, H.P. Schweizer, and M.E. Churchill, *Crystallization of Pseudomonas aeruginosa AHL synthase LasI using beta-turn crystal engineering.* Acta Crystallogr D Biol Crystallogr, 2004. **60**(Pt 3): p. 518-20.
116. Bottomley, M.J., E. Muraglia, R. Bazzo, and A. Carfi, *Molecular insights into quorum sensing in the human pathogen Pseudomonas aeruginosa from the structure of the virulence regulator LasR bound to its autoinducer.* J Biol Chem, 2007. **282**(18): p. 13592-600.
117. Schuster, M. and E.P. Greenberg, *Early activation of quorum sensing in Pseudomonas aeruginosa reveals the architecture of a complex regulon.* BMC Genomics, 2007. **8**: p. 287.
118. Schuster, M., C.P. Lostroh, T. Ogi, and E.P. Greenberg, *Identification, timing, and signal specificity of Pseudomonas aeruginosa quorum-controlled genes: a transcriptome analysis.* J Bacteriol, 2003. **185**(7): p. 2066-79.
119. Balaban, N. and R.P. Novick, *Translation of RNAIII, the Staphylococcus aureus agr regulatory RNA molecule, can be activated by a 3'-end deletion.* FEMS Microbiol Lett, 1995. **133**(1-2): p. 155-61.
120. Novick, R.P., S.J. Projan, J. Kornblum, H.F. Ross, G. Ji, B. Kreiswirth, F. Vandenesch, and S. Moghazeh, *The agr P2 operon: an autocatalytic sensory transduction system in Staphylococcus aureus.* Mol Gen Genet, 1995. **248**(4): p. 446-58.
121. Vuong, C., H.L. Saenz, F. Gotz, and M. Otto, *Impact of the agr quorum-sensing system on adherence to polystyrene in Staphylococcus aureus.* J Infect Dis, 2000. **182**(6): p. 1688-93.
122. Pang, Y.Y., J. Schwartz, M. Thoendel, L.W. Ackermann, A.R. Horswill, and W.M. Nauseef, *agr-Dependent interactions of Staphylococcus aureus USA300 with human polymorphonuclear neutrophils.* J Innate Immun, 2010. **2**(6): p. 546-59.
123. Thoendel, M. and A.R. Horswill, *Identification of Staphylococcus aureus AgrD residues required for autoinducing peptide biosynthesis.* J Biol Chem, 2009. **284**(33): p. 21828-38.
124. Bassler, B.L., M. Wright, and M.R. Silverman, *Multiple signalling systems controlling expression of luminescence in Vibrio harveyi: sequence and function of genes encoding a second sensory pathway.* Mol Microbiol, 1994. **13**(2): p. 273-86.
125. Bassler, B.L., M. Wright, and M.R. Silverman, *Sequence and function of LuxO, a negative regulator of luminescence in Vibrio harveyi.* Mol Microbiol, 1994. **12**(3): p. 403-12.
126. Freeman, J.A. and B.L. Bassler, *A genetic analysis of the function of LuxO, a two-component response regulator involved in quorum sensing in Vibrio harveyi.* Mol Microbiol, 1999. **31**(2): p. 665-77.
127. Freeman, J.A. and B.L. Bassler, *Sequence and function of LuxU: a two-component phosphorelay protein that regulates quorum sensing in Vibrio harveyi.* J Bacteriol, 1999. **181**(3): p. 899-906.
128. Henke, J.M. and B.L. Bassler, *Three parallel quorum-sensing systems regulate gene expression in Vibrio harveyi.* J Bacteriol, 2004. **186**(20): p. 6902-14.

129. Henke, J.M. and B.L. Bassler, *Quorum sensing regulates type III secretion in Vibrio harveyi and Vibrio parahaemolyticus.* J Bacteriol, 2004. **186**(12): p. 3794-805.
130. Lenz, D.H., K.C. Mok, B.N. Lilley, R.V. Kulkarni, N.S. Wingreen, and B.L. Bassler, *The small RNA chaperone Hfq and multiple small RNAs control quorum sensing in Vibrio harveyi and Vibrio cholerae.* Cell, 2004. **118**(1): p. 69-82.
131. Surette, M.G., M.B. Miller, and B.L. Bassler, *Quorum sensing in Escherichia coli, Salmonella typhimurium, and Vibrio harveyi: a new family of genes responsible for autoinducer production.* Proc Natl Acad Sci U S A, 1999. **96**(4): p. 1639-44.
132. Deziel, E., S. Gopalan, A.P. Tampakaki, F. Lepine, K.E. Padfield, M. Saucier, G. Xiao, and L.G. Rahme, *The contribution of MvfR to Pseudomonas aeruginosa pathogenesis and quorum sensing circuitry regulation: multiple quorum sensing-regulated genes are modulated without affecting lasRI, rhlRI or the production of N-acyl-L-homoserine lactones.* Mol Microbiol, 2005. **55**(4): p. 998-1014.
133. Juhas, M., L. Eberl, and B. Tummler, *Quorum sensing: the power of cooperation in the world of Pseudomonas.* Environ Microbiol, 2005. **7**(4): p. 459-71.
134. Lesic, B., M. Starkey, J. He, R. Hazan, and L.G. Rahme, *Quorum sensing differentially regulates Pseudomonas aeruginosa type VI secretion locus I and homologous loci II and III, which are required for pathogenesis.* Microbiology, 2009. **155**(Pt 9): p. 2845-55.
135. Rampioni, G., M. Schuster, E.P. Greenberg, I. Bertani, M. Grasso, V. Venturi, E. Zennaro, and L. Leoni, *RsaL provides quorum sensing homeostasis and functions as a global regulator of gene expression in Pseudomonas aeruginosa.* Mol Microbiol, 2007. **66**(6): p. 1557-65.
136. Southey-Pillig, C.J., D.G. Davies, and K. Sauer, *Characterization of temporal protein production in Pseudomonas aeruginosa biofilms.* J Bacteriol, 2005. **187**(23): p. 8114-26.
137. Benson, M.A., S. Lilo, G.A. Wasserman, M. Thoendel, A. Smith, A.R. Horswill, J. Fraser, R.P. Novick, B. Shopsin, and V.J. Torres, *Staphylococcus aureus regulates the expression and production of the staphylococcal superantigen-like secreted proteins in a Rot-dependent manner.* Mol Microbiol, 2011. **81**(3): p. 659-75.
138. Boles, B.R. and A.R. Horswill, *Agr-mediated dispersal of Staphylococcus aureus biofilms.* PLoS Pathog, 2008. **4**(4): p. e1000052.
139. Queck, S.Y., M. Jameson-Lee, A.E. Villaruz, T.H. Bach, B.A. Khan, D.E. Sturdevant, S.M. Ricklefs, M. Li, and M. Otto, *RNAIII-independent target gene control by the agr quorum-sensing system: insight into the evolution of virulence regulation in Staphylococcus aureus.* Mol Cell, 2008. **32**(1): p. 150-8.
140. Freeman, J.A., B.N. Lilley, and B.L. Bassler, *A genetic analysis of the functions of LuxN: a two-component hybrid sensor kinase that regulates quorum sensing in Vibrio harveyi.* Mol Microbiol, 2000. **35**(1): p. 139-49.
141. Neiditch, M.B., M.J. Federle, S.T. Miller, B.L. Bassler, and F.M. Hughson, *Regulation of LuxPQ receptor activity by the quorum-sensing signal autoinducer-2.* Mol Cell, 2005. **18**(5): p. 507-18.
142. Neiditch, M.B., M.J. Federle, A.J. Pompeani, R.C. Kelly, D.L. Swem, P.D. Jeffrey, B.L. Bassler, and F.M. Hughson, *Ligand-induced asymmetry in histidine sensor kinase complex regulates quorum sensing.* Cell, 2006. **126**(6): p. 1095-108.

143. Ng, W.L., L.J. Perez, Y. Wei, C. Kraml, M.F. Semmelhack, and B.L. Bassler, *Signal production and detection specificity in Vibrio CqsA/CqsS quorum-sensing systems.* Mol Microbiol, 2011. **79**(6): p. 1407-17.
144. Miller, M.B., K. Skorupski, D.H. Lenz, R.K. Taylor, and B.L. Bassler, *Parallel quorum sensing systems converge to regulate virulence in Vibrio cholerae.* Cell, 2002. **110**(3): p. 303-14.
145. Zhu, J., M.B. Miller, R.E. Vance, M. Dziejman, B.L. Bassler, and J.J. Mekalanos, *Quorum-sensing regulators control virulence gene expression in Vibrio cholerae.* Proc Natl Acad Sci U S A, 2002. **99**(5): p. 3129-34.
146. Rutherford, S.T., J.C. van Kessel, Y. Shao, and B.L. Bassler, *AphA and LuxR/HapR reciprocally control quorum sensing in vibrios.* Genes Dev, 2011. **25**(4): p. 397-408.
147. Shao, Y. and B.L. Bassler, *Quorum-sensing non-coding small RNAs use unique pairing regions to differentially control mRNA targets.* Mol Microbiol, 2012. **83**(3): p. 599-611.
148. Ng, W.L., Y. Wei, L.J. Perez, J. Cong, T. Long, M. Koch, M.F. Semmelhack, N.S. Wingreen, and B.L. Bassler, *Probing bacterial transmembrane histidine kinase receptor-ligand interactions with natural and synthetic molecules.* Proc Natl Acad Sci U S A, 2010. **107**(12): p. 5575-80.
149. Rutherford, S.T. and B.L. Bassler, *Bacterial quorum sensing: its role in virulence and possibilities for its control.* Cold Spring Harb Perspect Med, 2012. **2**(11).
150. Merrell, D.S., S.M. Butler, F. Qadri, N.A. Dolganov, A. Alam, M.B. Cohen, S.B. Calderwood, G.K. Schoolnik, and A. Camilli, *Host-induced epidemic spread of the cholera bacterium.* Nature, 2002. **417**(6889): p. 642-5.
151. Finkelstein, R.A., M. Boesman-Finkelstein, and P. Holt, *Vibrio cholerae hemagglutinin/lectin/protease hydrolyzes fibronectin and ovomucin: F.M. Burnet revisited.* Proc Natl Acad Sci U S A, 1983. **80**(4): p. 1092-5.
152. Hase, C.C. and R.A. Finkelstein, *Cloning and nucleotide sequence of the Vibrio cholerae hemagglutinin/protease (HA/protease) gene and construction of an HA/protease-negative strain.* J Bacteriol, 1991. **173**(11): p. 3311-7.
153. Wu, Z., D. Milton, P. Nybom, A. Sjo, and K.E. Magnusson, *Vibrio cholerae hemagglutinin/protease (HA/protease) causes morphological changes in cultured epithelial cells and perturbs their paracellular barrier function.* Microb Pathog, 1996. **21**(2): p. 111-23.
154. Mel, S.F., K.J. Fullner, S. Wimer-Mackin, W.I. Lencer, and J.J. Mekalanos, *Association of protease activity in Vibrio cholerae vaccine strains with decreases in transcellular epithelial resistance of polarized T84 intestinal epithelial cells.* Infect Immun, 2000. **68**(11): p. 6487-92.
155. Gutierrez, M.G., H.A. Saka, I. Chinen, F.C. Zoppino, T. Yoshimori, J.L. Bocco, and M.I. Colombo, *Protective role of autophagy against Vibrio cholerae cytolysin, a pore-forming toxin from V. cholerae.* Proc Natl Acad Sci U S A, 2007. **104**(6): p. 1829-34.
156. Olson, R. and E. Gouaux, *Vibrio cholerae cytolysin is composed of an alpha-hemolysin-like core.* Protein Sci, 2003. **12**(2): p. 379-83.
157. Saka, H.A., C. Bidinost, C. Sola, P. Carranza, C. Collino, S. Ortiz, J.R. Echenique, and J.L. Bocco, *Vibrio cholerae cytolysin is essential for high enterotoxicity and apoptosis induction produced by a cholera toxin gene-negative V. cholerae non-O1, non-O139 strain.* Microb Pathog, 2008. **44**(2): p. 118-28.

158. Saka, H.A., M.G. Gutierrez, J.L. Bocco, and M.I. Colombo, *The autophagic pathway: a cell survival strategy against the bacterial pore-forming toxin Vibrio cholerae cytolysin.* Autophagy, 2007. **3**(4): p. 363-5.
159. Zitzer, A., M. Palmer, U. Weller, T. Wassenaar, C. Biermann, J. Tranum-Jensen, and S. Bhakdi, *Mode of primary binding to target membranes and pore formation induced by Vibrio cholerae cytolysin (hemolysin).* Eur J Biochem, 1997. **247**(1): p. 209-16.
160. Mitra, R., P. Figueroa, A.K. Mukhopadhyay, T. Shimada, Y. Takeda, D.E. Berg, and G.B. Nair, *Cell vacuolation, a manifestation of the El tor hemolysin of Vibrio cholerae.* Infect Immun, 2000. **68**(4): p. 1928-33.
161. Coelho, A., J.R. Andrade, A.C. Vicente, and V.J. Dirita, *Cytotoxic cell vacuolating activity from Vibrio cholerae hemolysin.* Infect Immun, 2000. **68**(3): p. 1700-5.
162. Alm, R.A., G. Mayrhofer, I. Kotlarski, and P.A. Manning, *Amino-terminal domain of the El Tor haemolysin of Vibrio cholerae O1 is expressed in classical strains and is cytotoxic.* Vaccine, 1991. **9**(8): p. 588-94.
163. Ichinose, Y., K. Yamamoto, N. Nakasone, M.J. Tanabe, T. Takeda, T. Miwatani, and M. Iwanaga, *Enterotoxicity of El Tor-like hemolysin of non-O1 Vibrio cholerae.* Infect Immun, 1987. **55**(5): p. 1090-3.
164. Ikigai, H., A. Akatsuka, H. Tsujiyama, T. Nakae, and T. Shimamura, *Mechanism of membrane damage by El Tor hemolysin of Vibrio cholerae O1.* Infect Immun, 1996. **64**(8): p. 2968-73.
165. Fullner, K.J. and J.J. Mekalanos, *In vivo covalent cross-linking of cellular actin by the Vibrio cholerae RTX toxin.* EMBO J, 2000. **19**(20): p. 5315-23.
166. Lin, W., K.J. Fullner, R. Clayton, J.A. Sexton, M.B. Rogers, K.E. Calia, S.B. Calderwood, C. Fraser, and J.J. Mekalanos, *Identification of a vibrio cholerae RTX toxin gene cluster that is tightly linked to the cholera toxin prophage.* Proc Natl Acad Sci U S A, 1999. **96**(3): p. 1071-6.
167. Fullner, K.J., W.I. Lencer, and J.J. Mekalanos, *Vibrio cholerae-induced cellular responses of polarized T84 intestinal epithelial cells are dependent on production of cholera toxin and the RTX toxin.* Infect Immun, 2001. **69**(10): p. 6310-7.
168. Sheahan, K.L., C.L. Cordero, and K.J. Satchell, *Identification of a domain within the multifunctional Vibrio cholerae RTX toxin that covalently cross-links actin.* Proc Natl Acad Sci U S A, 2004. **101**(26): p. 9798-803.
169. Olivier, V., N.H. Salzman, and K.J. Satchell, *Prolonged colonization of mice by Vibrio cholerae El Tor O1 depends on accessory toxins.* Infect Immun, 2007. **75**(10): p. 5043-51.
170. Somarny, W.M.Z., Mariana, N.S., Neela, V., Rozita, R., and A.R. Raha, *Optimization of Parameters for Accessory Cholera Enterotoxin (Ace) Protein Expression.* Journal of Medical Science, 2002. **2**(2): p. 74-76.
171. Chatterjee, T., D. Mukherjee, S. Dey, A. Pal, K.M. Hoque, and P. Chakrabarti, *Accessory cholera enterotoxin, Ace, from Vibrio cholerae: structure, unfolding, and virstatin binding.* Biochemistry, 2011. **50**(14): p. 2962-72.
172. Fasano, A., B. Baudry, D.W. Pumplin, S.S. Wasserman, B.D. Tall, J.M. Ketley, and J.B. Kaper, *Vibrio cholerae produces a second enterotoxin, which affects intestinal tight junctions.* Proc Natl Acad Sci U S A, 1991. **88**(12): p. 5242-6.
173. Alam, A., K.A. Miller, M. Chaand, J.S. Butler, and M. Dziejman, *Identification of Vibrio cholerae type III secretion system effector proteins.* Infect Immun, 2011. **79**(4): p. 1728-40.

174. Tam, V.C., D. Serruto, M. Dziejman, W. Brieher, and J.J. Mekalanos, *A type III secretion system in Vibrio cholerae translocates a formin/spire hybrid-like actin nucleator to promote intestinal colonization.* Cell Host Microbe, 2007. **1**(2): p. 95-107.
175. Shin, O.S., V.C. Tam, M. Suzuki, J.M. Ritchie, R.T. Bronson, M.K. Waldor, and J.J. Mekalanos, *Type III secretion is essential for the rapidly fatal diarrheal disease caused by non-O1, non-O139 Vibrio cholerae.* MBio, 2011. **2**(3): p. e00106-11.
176. Madueno, F., S.A. Bradshaw, and J.C. Gray, *The thylakoid-targeting domain of the chloroplast Rieske iron-sulfur protein is located in the N-terminal hydrophobic region of the mature protein.* J Biol Chem, 1994. **269**(26): p. 17458-63.
177. Papanikou, E., S. Karamanou, and A. Economou, *Bacterial protein secretion through the translocase nanomachine.* Nat Rev Microbiol, 2007. **5**(11): p. 839-51.
178. Stephenson, K., *Sec-dependent protein translocation across biological membranes: evolutionary conservation of an essential protein transport pathway (review).* Mol Membr Biol, 2005. **22**(1-2): p. 17-28.
179. Martoglio, B. and B. Dobberstein, *Signal sequences: more than just greasy peptides.* Trends Cell Biol, 1998. **8**(10): p. 410-5.
180. Muller, M., *Twin-arginine-specific protein export in Escherichia coli.* Res Microbiol, 2005. **156**(2): p. 131-6.
181. Filloux, A., *The underlying mechanisms of type II protein secretion.* Biochim Biophys Acta, 2004. **1694**(1-3): p. 163-79.
182. Ali, A., J.A. Johnson, A.A. Franco, D.J. Metzger, T.D. Connell, J.G. Morris, Jr., and S. Sozhamannan, *Mutations in the extracellular protein secretion pathway genes (eps) interfere with rugose polysaccharide production in and motility of Vibrio cholerae.* Infect Immun, 2000. **68**(4): p. 1967-74.
183. Davis, B.M., E.H. Lawson, M. Sandkvist, A. Ali, S. Sozhamannan, and M.K. Waldor, *Convergence of the secretory pathways for cholera toxin and the filamentous phage, CTXphi.* Science, 2000. **288**(5464): p. 333-5.
184. Sandkvist, M., L.O. Michel, L.P. Hough, V.M. Morales, M. Bagdasarian, M. Koomey, and V.J. DiRita, *General secretion pathway (eps) genes required for toxin secretion and outer membrane biogenesis in Vibrio cholerae.* J Bacteriol, 1997. **179**(22): p. 6994-7003.
185. Connell, T.D., D.J. Metzger, J. Lynch, and J.P. Folster, *Endochitinase is transported to the extracellular milieu by the eps-encoded general secretory pathway of Vibrio cholerae.* J Bacteriol, 1998. **180**(21): p. 5591-600.
186. Cianciotto, N.P., *Type II secretion: a protein secretion system for all seasons.* Trends Microbiol, 2005. **13**(12): p. 581-8.
187. Jacob-Dubuisson, F., R. Fernandez, and L. Coutte, *Protein secretion through autotransporter and two-partner pathways.* Biochim Biophys Acta, 2004. **1694**(1-3): p. 235-57.
188. Dautin, N. and H.D. Bernstein, *Protein secretion in gram-negative bacteria via the autotransporter pathway.* Annu Rev Microbiol, 2007. **61**: p. 89-112.
189. Henderson, I.R., F. Navarro-Garcia, M. Desvaux, R.C. Fernandez, and D. Ala'Aldeen, *Type V protein secretion pathway: the autotransporter story.* Microbiol Mol Biol Rev, 2004. **68**(4): p. 692-744.

190. Holland, I.B., L. Schmitt, and J. Young, *Type 1 protein secretion in bacteria, the ABC-transporter dependent pathway (review).* Mol Membr Biol, 2005. **22**(1-2): p. 29-39.
191. Gerlach, R.G. and M. Hensel, *Protein secretion systems and adhesins: the molecular armory of Gram-negative pathogens.* Int J Med Microbiol, 2007. **297**(6): p. 401-15.
192. Brodin, P., L. Majlessi, L. Marsollier, M.I. de Jonge, D. Bottai, C. Demangel, J. Hinds, O. Neyrolles, P.D. Butcher, C. Leclerc, S.T. Cole, and R. Brosch, *Dissection of ESAT-6 system 1 of Mycobacterium tuberculosis and impact on immunogenicity and virulence.* Infect Immun, 2006. **74**(1): p. 88-98.
193. Mougous, J.D., M.E. Cuff, S. Raunser, A. Shen, M. Zhou, C.A. Gifford, A.L. Goodman, G. Joachimiak, C.L. Ordonez, S. Lory, T. Walz, A. Joachimiak, and J.J. Mekalanos, *A virulence locus of Pseudomonas aeruginosa encodes a protein secretion apparatus.* Science, 2006. **312**(5779): p. 1526-30.
194. Pukatzki, S., A.T. Ma, D. Sturtevant, B. Krastins, D. Sarracino, W.C. Nelson, J.F. Heidelberg, and J.J. Mekalanos, *Identification of a conserved bacterial protein secretion system in Vibrio cholerae using the Dictyostelium host model system.* Proc Natl Acad Sci U S A, 2006. **103**(5): p. 1528-33.
195. Cornelis, G.R., *The type III secretion injectisome.* Nat Rev Microbiol, 2006. **4**(11): p. 811-25.
196. Christie, P.J. and E. Cascales, *Structural and dynamic properties of bacterial type IV secretion systems (review).* Mol Membr Biol, 2005. **22**(1-2): p. 51-61.
197. Blocker, A.J., J.E. Deane, A.K. Veenendaal, P. Roversi, J.L. Hodgkinson, S. Johnson, and S.M. Lea, *What's the point of the type III secretion system needle?* Proc Natl Acad Sci U S A, 2008. **105**(18): p. 6507-13.
198. Burns, D.L., *Biochemistry of type IV secretion.* Curr Opin Microbiol, 1999. **2**(1): p. 25-9.
199. Stein, M., R. Rappuoli, and A. Covacci, *Tyrosine phosphorylation of the Helicobacter pylori CagA antigen after cag-driven host cell translocation.* Proc Natl Acad Sci U S A, 2000. **97**(3): p. 1263-8.
200. Jakubowski, S.J., V. Krishnamoorthy, E. Cascales, and P.J. Christie, *Agrobacterium tumefaciens VirB6 domains direct the ordered export of a DNA substrate through a type IV secretion System.* J Mol Biol, 2004. **341**(4): p. 961-77.
201. Toro, N., A. Datta, O.A. Carmi, C. Young, R.K. Prusti, and E.W. Nester, *The Agrobacterium tumefaciens virC1 gene product binds to overdrive, a T-DNA transfer enhancer.* J Bacteriol, 1989. **171**(12): p. 6845-9.
202. Alvarez-Martinez, C.E. and P.J. Christie, *Biological diversity of prokaryotic type IV secretion systems.* Microbiol Mol Biol Rev, 2009. **73**(4): p. 775-808.
203. Das, S., A. Chakrabortty, R. Banerjee, S. Roychoudhury, and K. Chaudhuri, *Comparison of global transcription responses allows identification of Vibrio cholerae genes differentially expressed following infection.* FEMS Microbiol Lett, 2000. **190**(1): p. 87-91.
204. Marra, A., S.J. Blander, M.A. Horwitz, and H.A. Shuman, *Identification of a Legionella pneumophila locus required for intracellular multiplication in human macrophages.* Proc Natl Acad Sci U S A, 1992. **89**(20): p. 9607-11.
205. Berger, K.H., J.J. Merriam, and R.R. Isberg, *Altered intracellular targeting properties associated with mutations in the Legionella pneumophila dotA gene.* Mol Microbiol, 1994. **14**(4): p. 809-22.

206. Segal, G., M. Purcell, and H.A. Shuman, *Host cell killing and bacterial conjugation require overlapping sets of genes within a 22-kb region of the Legionella pneumophila genome.* Proc Natl Acad Sci U S A, 1998. **95**(4): p. 1669-74.
207. Das, S. and K. Chaudhuri, *Identification of a unique IAHP (IcmF associated homologous proteins) cluster in Vibrio cholerae and other proteobacteria through in silico analysis.* In Silico Biol, 2003. **3**(3): p. 287-300.
208. Leiman, P.G., M. Basler, U.A. Ramagopal, J.B. Bonanno, J.M. Sauder, S. Pukatzki, S.K. Burley, S.C. Almo, and J.J. Mekalanos, *Type VI secretion apparatus and phage tail-associated protein complexes share a common evolutionary origin.* Proc Natl Acad Sci U S A, 2009. **106**(11): p. 4154-9.
209. Pukatzki, S., A.T. Ma, A.T. Revel, D. Sturtevant, and J.J. Mekalanos, *Type VI secretion system translocates a phage tail spike-like protein into target cells where it cross-links actin.* Proc Natl Acad Sci U S A, 2007. **104**(39): p. 15508-13.
210. Brooks, T.M., D. Unterweger, V. Bachmann, B. Kostiuk, and S. Pukatzki, *Lytic Activity of the Vibrio cholerae Type VI Secretion Toxin VgrG-3 is Inhibited by the Antitoxin TsaB.* J Biol Chem, 2013.
211. MacIntyre, D.L., S.T. Miyata, M. Kitaoka, and S. Pukatzki, *The Vibrio cholerae type VI secretion system displays antimicrobial properties.* Proc Natl Acad Sci U S A, 2010. **107**(45): p. 19520-4.
212. Murdoch, S.L., K. Trunk, G. English, M.J. Fritsch, E. Pourkarimi, and S.J. Coulthurst, *The opportunistic pathogen Serratia marcescens utilizes type VI secretion to target bacterial competitors.* J Bacteriol, 2011. **193**(21): p. 6057-69.
213. Schwarz, S., T.E. West, F. Boyer, W.C. Chiang, M.A. Carl, R.D. Hood, L. Rohmer, T. Tolker-Nielsen, S.J. Skerrett, and J.D. Mougous, *Burkholderia type VI secretion systems have distinct roles in eukaryotic and bacterial cell interactions.* PLoS Pathog, 2010. **6**(8).
214. Hood, R.D., P. Singh, F. Hsu, T. Guvener, M.A. Carl, R.R. Trinidad, J.M. Silverman, B.B. Ohlson, K.G. Hicks, R.L. Plemel, M. Li, S. Schwarz, W.Y. Wang, A.J. Merz, D.R. Goodlett, and J.D. Mougous, *A type VI secretion system of Pseudomonas aeruginosa targets a toxin to bacteria.* Cell Host Microbe, 2010. **7**(1): p. 25-37.
215. Russell, A.B., R.D. Hood, N.K. Bui, M. LeRoux, W. Vollmer, and J.D. Mougous, *Type VI secretion delivers bacteriolytic effectors to target cells.* Nature, 2011. **475**(7356): p. 343-7.
216. Russell, A.B., P. Singh, M. Brittnacher, N.K. Bui, R.D. Hood, M.A. Carl, D.M. Agnello, S. Schwarz, D.R. Goodlett, W. Vollmer, and J.D. Mougous, *A Widespread Bacterial Type VI Secretion Effector Superfamily Identified Using a Heuristic Approach.* Cell Host Microbe, 2012. **11**(5): p. 538-49.
217. Carruthers, M.D., P.A. Nicholson, E.N. Tracy, and R.S. Munson, Jr., *Acinetobacter baumannii Utilizes a Type VI Secretion System for Bacterial Competition.* PLoS One, 2013. **8**(3): p. e59388.
218. Basler, M., B.T. Ho, and J.J. Mekalanos, *Tit-for-tat: type VI secretion system counterattack during bacterial cell-cell interactions.* Cell, 2013. **152**(4): p. 884-94.
219. Basler, M. and J.J. Mekalanos, *Type 6 secretion dynamics within and between bacterial cells.* Science, 2012. **337**(6096): p. 815.
220. Basler, M., M. Pilhofer, G.P. Henderson, G.J. Jensen, and J.J. Mekalanos, *Type VI secretion requires a dynamic contractile phage tail-like structure.* Nature, 2012. **483**(7388): p. 182-6.

221. Dong, T.G., B.T. Ho, D.R. Yoder-Himes, and J.J. Mekalanos, *Identification of T6SS-dependent effector and immunity proteins by Tn-seq in Vibrio cholerae.* Proc Natl Acad Sci U S A, 2013.
222. Ma, A.T., S. McAuley, S. Pukatzki, and J.J. Mekalanos, *Translocation of a Vibrio cholerae type VI secretion effector requires bacterial endocytosis by host cells.* Cell Host Microbe, 2009. **5**(3): p. 234-43.
223. Miyata, S.T., M. Kitaoka, T.M. Brooks, S.B. McAuley, and S. Pukatzki, *Vibrio cholerae requires the type VI secretion system virulence factor VasX to kill Dictyostelium discoideum.* Infect Immun, 2011. **79**(7): p. 2941-9.
224. Aubert, D.F., R.S. Flannagan, and M.A. Valvano, *A novel sensor kinase-response regulator hybrid controls biofilm formation and type VI secretion system activity in Burkholderia cenocepacia.* Infect Immun, 2008. **76**(5): p. 1979-91.
225. Burtnick, M.N., P.J. Brett, S.V. Harding, S.A. Ngugi, W.J. Ribot, N. Chantratita, A. Scorpio, T.S. Milne, R.E. Dean, D.L. Fritz, S.J. Peacock, J.L. Prior, T.P. Atkins, and D. Deshazer, *The cluster 1 type VI secretion system is a major virulence determinant in Burkholderia pseudomallei.* Infect Immun, 2011. **79**(4): p. 1512-25.
226. Burtnick, M.N., D. DeShazer, V. Nair, F.C. Gherardini, and P.J. Brett, *Burkholderia mallei cluster 1 type VI secretion mutants exhibit growth and actin polymerization defects in RAW 264.7 murine macrophages.* Infect Immun, 2010. **78**(1): p. 88-99.
227. Schell, M.A., R.L. Ulrich, W.J. Ribot, E.E. Brueggemann, H.B. Hines, D. Chen, L. Lipscomb, H.S. Kim, J. Mrazek, W.C. Nierman, and D. Deshazer, *Type VI secretion is a major virulence determinant in Burkholderia mallei.* Mol Microbiol, 2007. **64**(6): p. 1466-85.
228. Wang, X., Q. Wang, J. Xiao, Q. Liu, H. Wu, L. Xu, and Y. Zhang, *Edwardsiella tarda T6SS component evpP is regulated by esrB and iron, and plays essential roles in the invasion of fish.* Fish Shellfish Immunol, 2009. **27**(3): p. 469-77.
229. Zheng, J. and K.Y. Leung, *Dissection of a type VI secretion system in Edwardsiella tarda.* Mol Microbiol, 2007. **66**(5): p. 1192-206.
230. Gratia, A., *Sur un remarquable exemple d'antagonism entre deux souches de colibacille.* Comptes Rendus des Seances et Memoires de la Societe de Biologie, 1925. **93**: p. 1040-41.
231. Cascales, E., S.K. Buchanan, D. Duche, C. Kleanthous, R. Lloubes, K. Postle, M. Riley, S. Slatin, and D. Cavard, *Colicin biology.* Microbiol Mol Biol Rev, 2007. **71**(1): p. 158-229.
232. Kageyama, M. and F. Egami, *On the purification and some properties of a pyocin, a bacteriocin produced by Pseudomonas aeruginosa.* Life Sci, 1962. **1**: p. 471-6.
233. de Graaf, F.K., *Effects of cloacin DF13 on the functioning of the cytoplasmic membrane.* Antonie Van Leeuwenhoek, 1973. **39**(1): p. 109-19.
234. de Graaf, F.K., H.G. Niekus, and J. Klootwijk, *Inactivation of bacterial ribosomes in vivo and in vitro by cloacin DF13.* FEBS Lett, 1973. **35**(1): p. 161-5.
235. de Graaf, F.K., M.J. Stukart, F.C. Boogerd, and K. Metselaar, *Limited proteolysis of cloacin DF13 and characterization of the cleavage products.* Biochemistry, 1978. **17**(6): p. 1137-42.
236. Fuller, A.T. and J.M. Horton, *Marcescin, an antibiotic substance from Serratia marcescens.* J Gen Microbiol, 1950. **4**(3): p. 417-33.

237. Jayawardene, A. and H. Farkas-Himsley, *Particulate nature of vibriocin: a bacteriocin from Vibrio comma.* Nature, 1968. **219**(5149): p. 79-80.
238. Jayawardene, A. and H. Farkas-Himsley, *Mode of action of vibriocin.* J Bacteriol, 1970. **102**(2): p. 382-8.
239. Farkas-Himsley, H. and P.L. Seyfried, *Lethal biosynthesis of a new antibacterial principle: vibriocin.* Nature, 1962. **193**: p. 1193-4.
240. Von Tersch, M.A. and B.C. Carlton, *Megacinogenic plasmids of Bacillus megaterium.* J Bacteriol, 1983. **155**(2): p. 872-7.
241. Chak, K.F., W.S. Kuo, F.M. Lu, and R. James, *Cloning and characterization of the ColE7 plasmid.* J Gen Microbiol, 1991. **137**(1): p. 91-100.
242. Cooper, P.C. and R. James, *Two new E colicins, E8 and E9, produced by a strain of Escherichia coli.* J Gen Microbiol, 1984. **130**(1): p. 209-15.
243. Schaller, K. and M. Nomura, *Colicin E2 is DNA endonuclease.* Proc Natl Acad Sci U S A, 1976. **73**(11): p. 3989-93.
244. Senior, B.W. and I.B. Holland, *Effect of colicin E3 upon the 30S ribosomal subunit of Escherichia coli.* Proc Natl Acad Sci U S A, 1971. **68**(5): p. 959-63.
245. Bowman, C.M., J.E. Dahlberg, T. Ikemura, J. Konisky, and M. Nomura, *Specific inactivation of 16S ribosomal RNA induced by colicin E3 in vivo.* Proc Natl Acad Sci U S A, 1971. **68**(5): p. 964-8.
246. Bowman, C.M., J. Sidikaro, and M. Nomura, *Specific inactivation of ribosomes by colicin E3 in vitro and mechanism of immunity in colicinogenic cells.* Nat New Biol, 1971. **234**(48): p. 133-7.
247. Boon, T., *Inactivation of ribosomes in vitro by colicin E 3 and its mechanism of action.* Proc Natl Acad Sci U S A, 1972. **69**(3): p. 549-52.
248. Schaller, K., J.V. Holtje, and V. Braun, *Colicin M is an inhibitor of murein biosynthesis.* J Bacteriol, 1982. **152**(3): p. 994-1000.
249. Elkins, P., A. Bunker, W.A. Cramer, and C.V. Stauffacher, *A mechanism for toxin insertion into membranes is suggested by the crystal structure of the channel-forming domain of colicin E1.* Structure, 1997. **5**(3): p. 443-58.
250. Vetter, I.R., M.W. Parker, A.D. Tucker, J.H. Lakey, F. Pattus, and D. Tsernoglou, *Crystal structure of a colicin N fragment suggests a model for toxicity.* Structure, 1998. **6**(7): p. 863-74.
251. Reeves, P., *Mode of action of colicins of types E1, E2, E3, and K.* J Bacteriol, 1968. **96**(5): p. 1700-3.
252. Luria, S.E., *On the Mechanisms of Action of Colicins.* Ann Inst Pasteur (Paris), 1964. **107**: p. SUPPL:67-73.
253. Cavard, D.a.L., C., *Involvement of BtuB and OmpF proteins in binding and uptake of colicin A.* FEMS Microbiol Lett, 1981. **12**: p. 311-316.
254. Ozeki, H., B.A. Stocker, and H. De Margerie, *Production of colicine by single bacteria.* Nature, 1959. **184**: p. 337-9.
255. Lwoff, A., F. Jacob, E. Ritz, and M. Gage, *[Induction of bacteriophage production and of a colicine by peroxides, ethyleneimines and halogenated alkylamines].* C R Hebd Seances Acad Sci, 1952. **234**(23): p. 2308-10.
256. Hakkaart, M.J., E. Veltkamp, and H.J. Nijkamp, *Protein H encoded by plasmid Clo DF13 involved in lysis of the bacterial host. II. Functions and regulation of synthesis of the gene H product.* Mol Gen Genet, 1981. **183**(2): p. 326-32.
257. Hakkaart, M.J., E. Veltkamp, and H.J. Nijkamp, *Protein H encoded by plasmid Clo DF13 involved in lysis of the bacterial host. I. Localisation of the gene and*

identification and subcellular localisation of the gene H product. Mol Gen Genet, 1981. **183**(2): p. 318-25.
258. Jakes, K.S. and N.D. Zinder, *Plasmid ColE3 specifies a lysis protein.* J Bacteriol, 1984. **157**(2): p. 582-90.
259. Oudega, B., F. Stegehuis, G.J. van Tiel-Menkveld, and F.K. de Graaf, *Protein H encoded by plasmid CloDF13 is involved in excretion of cloacin DF13.* J Bacteriol, 1982. **150**(3): p. 1115-21.
260. Pugsley, A.P. and M. Schwartz, *Expression of a gene in a 400-base-pair fragment of colicin plasmid ColE2-P9 is sufficient to cause host cell lysis.* J Bacteriol, 1983. **156**(1): p. 109-14.
261. Sabik, J.F., J.L. Suit, and S.E. Luria, *cea-kil operon of the ColE1 plasmid.* J Bacteriol, 1983. **153**(3): p. 1479-85.
262. van der Wal, F.J., J. Luirink, and B. Oudega, *Bacteriocin release proteins: mode of action, structure, and biotechnological application.* FEMS Microbiol Rev, 1995. **17**(4): p. 381-99.
263. van der Wal, F.J., C.M. ten Hagen, B. Oudega, and J. Luirink, *The stable bacteriocin release protein signal peptide, expressed as a separate entity, functions in the release of cloacin DF13.* FEMS Microbiol Lett, 1995. **131**(2): p. 173-7.
264. Jacob, F., Siminovitch, L., and Wollman, E., *Sur la biosynthese d'une colicine et sur son mode d'action.* Annales de l'Institut Pasteur (Paris), 1952. **83**: p. 295-315.
265. Jakes, K.S. and P. Model, *Mechanism of export of colicin E1 and colicin E3.* J Bacteriol, 1979. **138**(3): p. 770-8.
266. Cavard, D., A. Bernadac, and C. Lazdunski, *Exclusive localization of colicin A in cell cytoplasm of producing bacteria.* Eur J Biochem, 1981. **119**(1): p. 125-31.
267. Lazdunski, C.J., E. Bouveret, A. Rigal, L. Journet, R. Lloubes, and H. Benedetti, *Colicin import into Escherichia coli cells.* J Bacteriol, 1998. **180**(19): p. 4993-5002.
268. Braun, V., S.I. Patzer, and K. Hantke, *Ton-dependent colicins and microcins: modular design and evolution.* Biochimie, 2002. **84**(5-6): p. 365-80.
269. Cao, Z. and P.E. Klebba, *Mechanisms of colicin binding and transport through outer membrane porins.* Biochimie, 2002. **84**(5-6): p. 399-412.
270. Fredericq, P., *Sur la pluralite des recepteurs d'antibiose de E. coli.* Comptes Rendus des Seances et Memoires de la Societe de Biologie (Paris), 1946. **140**: p. 1189-1194.
271. Baty, D., M. Frenette, R. Lloubes, V. Geli, S.P. Howard, F. Pattus, and C. Lazdunski, *Functional domains of colicin A.* Mol Microbiol, 1988. **2**(6): p. 807-11.
272. Dankert, J.R., Y. Uratani, C. Grabau, W.A. Cramer, and M. Hermodson, *On a domain structure of colicin E1. A COOH-terminal peptide fragment active in membrane depolarization.* J Biol Chem, 1982. **257**(7): p. 3857-63.
273. Escuyer, V. and M. Mock, *DNA sequence analysis of three missense mutations affecting colicin E3 bactericidal activity.* Mol Microbiol, 1987. **1**(1): p. 82-5.
274. Martinez, M.C., C. Lazdunski, and F. Pattus, *Isolation, molecular and functional properties of the C-terminal domain of colicin A.* EMBO J, 1983. **2**(9): p. 1501-7.
275. Ohno-Iwashita, Y. and K. Imahori, *Assignment of the functional loci in colicin E2 and E3 molecules by the characterization of their proteolytic fragments.* Biochemistry, 1980. **19**(4): p. 652-9.

276. Ohno-Iwashita, Y. and K. Imahori, *Assignment of the functional loci in the colicin E1 molecule by characterization of its proteolytic fragments.* J Biol Chem, 1982. **257**(11): p. 6446-51.
277. Boon, T., *Inactivation of ribosomes in vitro by colicin E 3.* Proc Natl Acad Sci U S A, 1971. **68**(10): p. 2421-5.
278. Jakes, K., N.D. Zinder, and T. Boon, *Purification and properties of colicin E3 immunity protein.* J Biol Chem, 1974. **249**(2): p. 438-44.
279. Duche, D., A. Frenkian, V. Prima, and R. Lloubes, *Release of immunity protein requires functional endonuclease colicin import machinery.* J Bacteriol, 2006. **188**(24): p. 8593-600.
280. Sidikaro, J. and M. Nomura, *E3 immunity substance. A protein from e3-colicinogenic cells that accounts for their immunity to colicin E3.* J Biol Chem, 1974. **249**(2): p. 445-53.
281. Weaver, C.A., A.H. Redborg, and J. Konisky, *Plasmid-determined immunity of Escherichia coli K-12 to colicin Ia Is mediated by a plasmid-encoded membrane protein.* J Bacteriol, 1981. **148**(3): p. 817-28.
282. Chak, K.F. and R. James, *Analysis of the promoters for the two immunity genes present in the ColE3-CA38 plasmid using two new promoter probe vectors.* Nucleic Acids Res, 1985. **13**(7): p. 2519-31.
283. Cole, S.T., B. Saint-Joanis, and A.P. Pugsley, *Molecular characterisation of the colicin E2 operon and identification of its products.* Mol Gen Genet, 1985. **198**(3): p. 465-72.
284. Ebina, Y., F. Kishi, and A. Nakazawa, *Direct participation of lexA protein in repression of colicin E1 synthesis.* J Bacteriol, 1982. **150**(3): p. 1479-81.
285. Lloubes, R., D. Baty, and C. Lazdunski, *The promoters of the genes for colicin production, release and immunity in the ColA plasmid: effects of convergent transcription and Lex A protein.* Nucleic Acids Res, 1986. **14**(6): p. 2621-36.
286. Mankovich, J.A., C.H. Hsu, and J. Konisky, *DNA and amino acid sequence analysis of structural and immunity genes of colicins Ia and Ib.* J Bacteriol, 1986. **168**(1): p. 228-36.
287. Lloubes, R., M. Granger-Schnarr, C. Lazdunski, and M. Schnarr, *LexA repressor induces operator-dependent DNA bending.* J Mol Biol, 1988. **204**(4): p. 1049-54.
288. Lloubes, R., M. Granger-Schnarr, C. Lazdunski, and M. Schnarr, *Interaction of a regulatory protein with a DNA target containing two overlapping binding sites.* J Biol Chem, 1991. **266**(4): p. 2303-12.
289. Curtis, M.D., R. James, and A. Coddington, *An evolutionary relationship between the ColE5-099 and the ColE9-J plasmids revealed by nucleotide sequencing.* J Gen Microbiol, 1989. **135**(10): p. 2783-8.
290. Lau, P.C. and J.A. Condie, *Nucleotide sequences from the colicin E5, E6 and E9 operons: presence of a degenerate transposon-like structure in the ColE9-J plasmid.* Mol Gen Genet, 1989. **217**(2-3): p. 269-77.
291. Roos, U., R.E. Harkness, and V. Braun, *Assembly of colicin genes from a few DNA fragments. Nucleotide sequence of colicin D.* Mol Microbiol, 1989. **3**(7): p. 891-902.
292. Uchimura, T. and P.C. Lau, *Nucleotide sequences from the colicin E8 operon: homology with plasmid ColE2-P9.* Mol Gen Genet, 1987. **209**(3): p. 489-93.
293. Masaki, H. and T. Ohta, *Colicin E3 and its immunity genes.* J Mol Biol, 1985. **182**(2): p. 217-27.

294. Soong, B.W., S.Y. Hsieh, and K.F. Chak, *Mapping of transcriptional start sites of the cea and cei genes of the ColE7 operon.* Mol Gen Genet, 1994. **243**(4): p. 477-81.
295. Chak, K.F. and R. James, *Localization and characterization of a gene on the ColE3-CA38 plasmid that confers immunity to colicin E8.* J Gen Microbiol, 1984. **130**(3): p. 701-10.
296. Lloubes, R., D. Baty, and C. Lazdunski, *Transcriptional terminators in the caa-cal operon and cai gene.* Nucleic Acids Res, 1988. **16**(9): p. 3739-49.
297. van den Elzen, P.J., R.N. Konings, E. Veltkamp, and H.J. Nijkamp, *Transcription of bacteriocinogenic plasmid CloDF13 in vivo and in vitro: structure of the cloacin immunity operon.* J Bacteriol, 1980. **144**(2): p. 579-91.
298. Hayes, F., *Toxins-antitoxins: plasmid maintenance, programmed cell death, and cell cycle arrest.* Science, 2003. **301**(5639): p. 1496-9.
299. Rawlings, D.E., *Proteic toxin-antitoxin, bacterial plasmid addiction systems and their evolution with special reference to the pas system of pTF-FC2.* FEMS Microbiol Lett, 1999. **176**(2): p. 269-77.
300. Syed, M.A. and C.M. Levesque, *Chromosomal bacterial type II toxin-antitoxin systems.* Can J Microbiol, 2012. **58**(5): p. 553-62.
301. Lehnherr, H., E. Maguin, S. Jafri, and M.B. Yarmolinsky, *Plasmid addiction genes of bacteriophage P1: doc, which causes cell death on curing of prophage, and phd, which prevents host death when prophage is retained.* J Mol Biol, 1993. **233**(3): p. 414-28.
302. Hiraga, S., *Chromosome and plasmid partition in Escherichia coli.* Annu Rev Biochem, 1992. **61**: p. 283-306.
303. Nordstrom, K. and S.J. Austin, *Mechanisms that contribute to the stable segregation of plasmids.* Annu Rev Genet, 1989. **23**: p. 37-69.
304. Williams, D.R. and C.M. Thomas, *Active partitioning of bacterial plasmids.* J Gen Microbiol, 1992. **138**(1): p. 1-16.
305. Engelberg-Kulka, H. and G. Glaser, *Addiction modules and programmed cell death and antideath in bacterial cultures.* Annu Rev Microbiol, 1999. **53**: p. 43-70.
306. Aoki, S.K., R. Pamma, A.D. Hernday, J.E. Bickham, B.A. Braaten, and D.A. Low, *Contact-dependent inhibition of growth in Escherichia coli.* Science, 2005. **309**(5738): p. 1245-8.
307. Aoki, S.K., J.S. Webb, B.A. Braaten, and D.A. Low, *Contact-dependent growth inhibition causes reversible metabolic downregulation in Escherichia coli.* J Bacteriol, 2009. **191**(6): p. 1777-86.
308. Aoki, S.K., J.C. Malinverni, K. Jacoby, B. Thomas, R. Pamma, B.N. Trinh, S. Remers, J. Webb, B.A. Braaten, T.J. Silhavy, and D.A. Low, *Contact-dependent growth inhibition requires the essential outer membrane protein BamA (YaeT) as the receptor and the inner membrane transport protein AcrB.* Mol Microbiol, 2008. **70**(2): p. 323-40.
309. Diner, E.J., C.M. Beck, J.S. Webb, D.A. Low, and C.S. Hayes, *Identification of a target cell permissive factor required for contact-dependent growth inhibition (CDI).* Genes Dev, 2012. **26**(5): p. 515-25.
310. Morse, R.P., K.C. Nikolakakis, J.L. Willett, E. Gerrick, D.A. Low, C.S. Hayes, and C.W. Goulding, *Structural basis of toxicity and immunity in contact-dependent*

growth inhibition (CDI) systems. Proc Natl Acad Sci U S A, 2012. **109**(52): p. 21480-5.
311. Nikolakakis, K., S. Amber, J.S. Wilbur, E.J. Diner, S.K. Aoki, S.J. Poole, A. Tuanyok, P.S. Keim, S. Peacock, C.S. Hayes, and D.A. Low, *The toxin/immunity network of Burkholderia pseudomallei contact-dependent growth inhibition (CDI) systems.* Mol Microbiol, 2012. **84**(3): p. 516-29.
312. Poole, S.J., E.J. Diner, S.K. Aoki, B.A. Braaten, C. t'Kint de Roodenbeke, D.A. Low, and C.S. Hayes, *Identification of functional toxin/immunity genes linked to contact-dependent growth inhibition (CDI) and rearrangement hotspot (Rhs) systems.* PLoS Genet, 2011. **7**(8): p. e1002217.
313. Ruhe, Z.C., D.A. Low, and C.S. Hayes, *Bacterial contact-dependent growth inhibition.* Trends Microbiol, 2013.
314. Webb, J.S., K.C. Nikolakakis, J.L. Willett, S.K. Aoki, C.S. Hayes, and D.A. Low, *Delivery of CdiA nuclease toxins into target cells during contact-dependent growth inhibition.* PLoS One, 2013. **8**(2): p. e57609.
315. Aoki, S.K., E.J. Diner, C.T. de Roodenbeke, B.R. Burgess, S.J. Poole, B.A. Braaten, A.M. Jones, J.S. Webb, C.S. Hayes, P.A. Cotter, and D.A. Low, *A widespread family of polymorphic contact-dependent toxin delivery systems in bacteria.* Nature, 2010. **468**(7322): p. 439-42.
316. Aoki, S.K., S.J. Poole, C.S. Hayes, and D.A. Low, *Toxin on a stick: modular CDI toxin delivery systems play roles in bacterial competition.* Virulence, 2011. **2**(4): p. 356-9.
317. Koskiniemi, S., J.G. Lamoureux, K.C. Nikolakakis, C. T'Kint de Roodenbeke, M.D. Kaplan, D.A. Low, and C.S. Hayes, *Rhs proteins from diverse bacteria mediate intercellular competition.* Proc Natl Acad Sci U S A, 2013. **110**(17): p. 7032-7.
318. Lin, R.J., M. Capage, and C.W. Hill, *A repetitive DNA sequence, rhs, responsible for duplications within the Escherichia coli K-12 chromosome.* J Mol Biol, 1984. **177**(1): p. 1-18.
319. Pukatzki, S., S.B. McAuley, and S.T. Miyata, *The type VI secretion system: translocation of effectors and effector-domains.* Curr Opin Microbiol, 2009. **12**(1): p. 11-7.
320. Chow, A.W., P.R. Taylor, T.T. Yoshikawa, and L.B. Guze, *A nosocomial outbreak of infections due to multiply resistant Proteus mirabilis: role of intestinal colonization as a major reservoir.* J Infect Dis, 1979. **139**(6): p. 621-7.
321. O'Hara, C.M., F.W. Brenner, and J.M. Miller, *Classification, identification, and clinical significance of Proteus, Providencia, and Morganella.* Clin Microbiol Rev, 2000. **13**(4): p. 534-46.
322. Mobley, H.L. and R. Belas, *Swarming and pathogenicity of Proteus mirabilis in the urinary tract.* Trends Microbiol, 1995. **3**(7): p. 280-4.
323. Budding, A.E., C.J. Ingham, W. Bitter, C.M. Vandenbroucke-Grauls, and P.M. Schneeberger, *The Dienes phenomenon: competition and territoriality in Swarming Proteus mirabilis.* J Bacteriol, 2009. **191**(12): p. 3892-900.
324. Dienes, L., *Further observations on the reproduction of bacilli from large bodies in Proteus cultures.* Proc Soc Exp Biol Med, 1947. **66**(1): p. 97.
325. Sourek, J., *On some findings concerning Dienes's phenomenon in swarming proteus strains.* Zentralbl Bakteriol Orig, 1968. **208**(3): p. 419-27.
326. Gibbs, K.A., M.L. Urbanowski, and E.P. Greenberg, *Genetic determinants of self identity and social recognition in bacteria.* Science, 2008. **321**(5886): p. 256-9.

327. Dienes, L., *Reproductive processes in Proteus cultures.* Proc Soc Exp Biol Med, 1946. **63**(2): p. 265-70.
328. Gibbs, K.A. and E.P. Greenberg, *Territoriality in Proteus: advertisement and aggression.* Chem Rev, 2011. **111**(1): p. 188-94.
329. Gibbs, K.A., L.M. Wenren, and E.P. Greenberg, *Identity gene expression in Proteus mirabilis.* J Bacteriol, 2011. **193**(13): p. 3286-92.
330. Boyer, F., G. Fichant, J. Berthod, Y. Vandenbrouck, and I. Attree, *Dissecting the bacterial type VI secretion system by a genome wide in silico analysis: what can be learned from available microbial genomic resources?* BMC Genomics, 2009. **10**: p. 104.
331. Shrivastava, S. and S.S. Mande, *Identification and functional characterization of gene components of Type VI Secretion system in bacterial genomes.* PLoS One, 2008. **3**(8): p. e2955.
332. Russell, A.B., M. LeRoux, K. Hathazi, D.M. Agnello, T. Ishikawa, P.A. Wiggins, S.N. Wai, and J.D. Mougous, *Diverse type VI secretion phospholipases are functionally plastic antibacterial effectors.* Nature, 2013. **496**(7446): p. 508-12.
333. Ma, A.T. and J.J. Mekalanos, *In vivo actin cross-linking induced by Vibrio cholerae type VI secretion system is associated with intestinal inflammation.* Proc Natl Acad Sci U S A, 2010. **107**(9): p. 4365-70.
334. Shalom, G., J.G. Shaw, and M.S. Thomas, *In vivo expression technology identifies a type VI secretion system locus in Burkholderia pseudomallei that is induced upon invasion of macrophages.* Microbiology, 2007. **153**(Pt 8): p. 2689-99.
335. Chakraborty, S., J. Sivaraman, K.Y. Leung, and Y.K. Mok, *Two-component PhoB-PhoR regulatory system and ferric uptake regulator sense phosphate and iron to control virulence genes in type III and VI secretion systems of Edwardsiella tarda.* J Biol Chem, 2011. **286**(45): p. 39417-30.
336. Rogge, M.L. and R.L. Thune, *Regulation of the Edwardsiella ictaluri type III secretion system by pH and phosphate concentration through EsrA, EsrB, and EsrC.* Appl Environ Microbiol, 2011. **77**(13): p. 4293-302.
337. Folkesson, A., S. Lofdahl, and S. Normark, *The Salmonella enterica subspecies I specific centisome 7 genomic island encodes novel protein families present in bacteria living in close contact with eukaryotic cells.* Res Microbiol, 2002. **153**(8): p. 537-45.
338. Mulder, D.T., C.A. Cooper, and B.K. Coombes, *Type VI secretion system-associated gene clusters contribute to pathogenesis of Salmonella enterica serovar Typhimurium.* Infect Immun, 2012. **80**(6): p. 1996-2007.
339. Blondel, C.J., J.C. Jimenez, I. Contreras, and C.A. Santiviago, *Comparative genomic analysis uncovers 3 novel loci encoding type six secretion systems differentially distributed in Salmonella serotypes.* BMC Genomics, 2009. **10**: p. 354.
340. Blondel, C.J., H.J. Yang, B. Castro, S. Chiang, C.S. Toro, M. Zaldivar, I. Contreras, H.L. Andrews-Polymenis, and C.A. Santiviago, *Contribution of the type VI secretion system encoded in SPI-19 to chicken colonization by Salmonella enterica serotypes Gallinarum and Enteritidis.* PLoS One, 2010. **5**(7): p. e11724.
341. Suarez, G., J.C. Sierra, T.E. Erova, J. Sha, A.J. Horneman, and A.K. Chopra, *A type VI secretion system effector protein, VgrG1, from Aeromonas hydrophila that induces host cell toxicity by ADP ribosylation of actin.* J Bacteriol, 2010. **192**(1): p. 155-68.

342. Suarez, G., J.C. Sierra, M.L. Kirtley, and A.K. Chopra, *Role of Hcp, a type 6 secretion system effector, of Aeromonas hydrophila in modulating activation of host immune cells.* Microbiology, 2010. **156**(Pt 12): p. 3678-88.
343. Suarez, G., J.C. Sierra, J. Sha, S. Wang, T.E. Erova, A.A. Fadl, S.M. Foltz, A.J. Horneman, and A.K. Chopra, *Molecular characterization of a functional type VI secretion system from a clinical isolate of Aeromonas hydrophila.* Microb Pathog, 2008. **44**(4): p. 344-61.
344. Chow, J. and S.K. Mazmanian, *A pathobiont of the microbiota balances host colonization and intestinal inflammation.* Cell Host Microbe, 2010. **7**(4): p. 265-76.
345. de Bruin, O.M., J.S. Ludu, and F.E. Nano, *The Francisella pathogenicity island protein IglA localizes to the bacterial cytoplasm and is needed for intracellular growth.* BMC Microbiol, 2007. **7**: p. 1.
346. Ludu, J.S., O.M. de Bruin, B.N. Duplantis, C.L. Schmerk, A.Y. Chou, K.L. Elkins, and F.E. Nano, *The Francisella pathogenicity island protein PdpD is required for full virulence and associates with homologues of the type VI secretion system.* J Bacteriol, 2008. **190**(13): p. 4584-95.
347. Broms, J.E., L. Meyer, M. Lavander, P. Larsson, and A. Sjostedt, *DotU and VgrG, core components of type VI secretion systems, are essential for Francisella LVS pathogenicity.* PLoS One, 2012. **7**(4): p. e34639.
348. Broms, J.E., L. Meyer, K. Sun, M. Lavander, and A. Sjostedt, *Unique substrates secreted by the type VI secretion system of Francisella tularensis during intramacrophage infection.* PLoS One, 2012. **7**(11): p. e50473.
349. Blondel, C.J., J.C. Jimenez, L.E. Leiva, S.A. Alvarez, B.I. Pinto, F. Contreras, D. Pezoa, C.A. Santiviago, and I. Contreras, *The type VI secretion system encoded in Salmonella pathogenicity island 19 is required for Salmonella enterica serotype Gallinarum survival within infected macrophages.* Infect Immun, 2013. **81**(4): p. 1207-20.
350. Lindgren, H., I. Golovliov, V. Baranov, R.K. Ernst, M. Telepnev, and A. Sjostedt, *Factors affecting the escape of Francisella tularensis from the phagolysosome.* J Med Microbiol, 2004. **53**(Pt 10): p. 953-8.
351. Barker, J.R., A. Chong, T.D. Wehrly, J.J. Yu, S.A. Rodriguez, J. Liu, J. Celli, B.P. Arulanandam, and K.E. Klose, *The Francisella tularensis pathogenicity island encodes a secretion system that is required for phagosome escape and virulence.* Mol Microbiol, 2009. **74**(6): p. 1459-70.
352. Wu, C.F., J.S. Lin, G.C. Shaw, and E.M. Lai, *Acid-induced type VI secretion system is regulated by ExoR-ChvG/ChvI signaling cascade in Agrobacterium tumefaciens.* PLoS Pathog, 2012. **8**(9): p. e1002938.
353. Chen, Y., J. Wong, G.W. Sun, Y. Liu, G.Y. Tan, and Y.H. Gan, *Regulation of type VI secretion system during Burkholderia pseudomallei infection.* Infect Immun, 2011. **79**(8): p. 3064-73.
354. Gueguen, E. and E. Cascales, *Promoter swapping unveils the role of the Citrobacter rodentium CTS1 type VI secretion system in interbacterial competition.* Appl Environ Microbiol, 2013. **79**(1): p. 32-8.
355. Zheng, J., B. Ho, and J.J. Mekalanos, *Genetic Analysis of Anti-Amoebae and Anti-Bacterial Activities of the Type VI Secretion System in Vibrio cholerae.* PLoS One, 2011. **6**(8): p. e23876.

356. Barret, M., F. Egan, E. Fargier, J.P. Morrissey, and F. O'Gara, *Genomic analysis of the type VI secretion systems in Pseudomonas spp.: novel clusters and putative effectors uncovered.* Microbiology, 2011. **157**(Pt 6): p. 1726-39.
357. Hachani, A., N.S. Lossi, A. Hamilton, C. Jones, S. Bleves, D. Albesa-Jove, and A. Filloux, *Type VI secretion system in Pseudomonas aeruginosa: secretion and multimerization of VgrG proteins.* J Biol Chem, 2011. **286**(14): p. 12317-27.
358. Mougous, J.D., C.A. Gifford, T.L. Ramsdell, and J.J. Mekalanos, *Threonine phosphorylation post-translationally regulates protein secretion in Pseudomonas aeruginosa.* Nat Cell Biol, 2007. **9**(7): p. 797-803.
359. Weber, B.S., S.T. Miyata, J.A. Iwashkiw, B.L. Mortensen, E.P. Skaar, S. Pukatzki, and M.F. Feldman, *Genomic and functional analysis of the type VI secretion system in Acinetobacter.* PLoS One, 2013. **8**(1): p. e55142.
360. Wu, H.Y., P.C. Chung, H.W. Shih, S.R. Wen, and E.M. Lai, *Secretome analysis uncovers an Hcp-family protein secreted via a type VI secretion system in Agrobacterium tumefaciens.* J Bacteriol, 2008. **190**(8): p. 2841-50.
361. Ma, L.S., J.S. Lin, and E.M. Lai, *An IcmF family protein, ImpLM, is an integral inner membrane protein interacting with ImpKL, and its walker a motif is required for type VI secretion system-mediated Hcp secretion in Agrobacterium tumefaciens.* J Bacteriol, 2009. **191**(13): p. 4316-29.
362. Bonemann, G., A. Pietrosiuk, A. Diemand, H. Zentgraf, and A. Mogk, *Remodelling of VipA/VipB tubules by ClpV-mediated threading is crucial for type VI protein secretion.* EMBO J, 2009. **28**(4): p. 315-25.
363. Bladergroen, M.R., K. Badelt, and H.P. Spaink, *Infection-blocking genes of a symbiotic Rhizobium leguminosarum strain that are involved in temperature-dependent protein secretion.* Mol Plant Microbe Interact, 2003. **16**(1): p. 53-64.
364. Ishikawa, T., P.K. Rompikuntal, B. Lindmark, D.L. Milton, and S.N. Wai, *Quorum sensing regulation of the two hcp alleles in Vibrio cholerae O1 strains.* PLoS One, 2009. **4**(8): p. e6734.
365. Ishikawa, T., D. Sabharwal, J. Broms, D.L. Milton, A. Sjostedt, B.E. Uhlin, and S.N. Wai, *Pathoadaptive conditional regulation of the type VI secretion system in Vibrio cholerae O1 strains.* Infect Immun, 2012. **80**(2): p. 575-84.
366. Mandlik, A., J. Livny, W.P. Robins, J.M. Ritchie, J.J. Mekalanos, and M.K. Waldor, *RNA-Seq-based monitoring of infection-linked changes in Vibrio cholerae gene expression.* Cell Host Microbe, 2011. **10**(2): p. 165-74.
367. Zheng, J., O.S. Shin, D.E. Cameron, and J.J. Mekalanos, *Quorum sensing and a global regulator TsrA control expression of type VI secretion and virulence in Vibrio cholerae.* Proc Natl Acad Sci U S A, 2010. **107**(49): p. 21128-33.
368. Zinnaka, Y. and C.C. Carpenter, Jr., *An enterotoxin produced by noncholera vibrios.* Johns Hopkins Med J, 1972. **131**(6): p. 403-11.
369. Unterweger, D., M. Kitaoka, S.T. Miyata, V. Bachmann, T.M. Brooks, J. Moloney, O. Sosa, D. Silva, J. Duran-Gonzalez, D. Provenzano, and S. Pukatzki, *Constitutive Type VI Secretion System Expression Gives Vibrio cholerae Intra- and Interspecific Competitive Advantages.* PLoS One, 2012. **7**(10): p. e48320.
370. Kitaoka, M., S.T. Miyata, T.M. Brooks, D. Unterweger, and S. Pukatzki, *VasH Is a Transcriptional Regulator of the Type VI Secretion System Functional in Endemic and Pandemic Vibrio cholerae.* J Bacteriol, 2011. **193**(23): p. 6471-82.

371. Bernard, C.S., Y.R. Brunet, M. Gavioli, R. Lloubes, and E. Cascales, *Regulation of type VI secretion gene clusters by sigma54 and cognate enhancer binding proteins.* J Bacteriol, 2011. **193**(9): p. 2158-67.
372. Dong, T.G. and J.J. Mekalanos, *Characterization of the RpoN regulon reveals differential regulation of T6SS and new flagellar operons in Vibrio cholerae O37 strain V52.* Nucleic Acids Res, 2012.
373. Pukatzki, S., R.H. Kessin, and J.J. Mekalanos, *The human pathogen Pseudomonas aeruginosa utilizes conserved virulence pathways to infect the social amoeba Dictyostelium discoideum.* Proc Natl Acad Sci U S A, 2002. **99**(5): p. 3159-64.
374. Dong, T.G., B.T. Ho, D.R. Yoder-Himes, and J.J. Mekalanos, *Identification of T6SS-dependent effector and immunity proteins by Tn-seq in Vibrio cholerae.* Proc Natl Acad Sci U S A, 2013. **110**(7): p. 2623-8.
375. Miyata, S.T., M. Kitaoka, L. Wieteska, C. Frech, N. Chen, and S. Pukatzki, *The Vibrio Cholerae Type VI Secretion System: Evaluating its Role in the Human Disease Cholera.* Front Microbiol, 2010. **1**: p. 117.
376. Clatworthy, A.E., E. Pierson, and D.T. Hung, *Targeting virulence: a new paradigm for antimicrobial therapy.* Nat Chem Biol, 2007. **3**(9): p. 541-8.
377. Dong, T.G. and J.J. Mekalanos, *Characterization of the RpoN regulon reveals differential regulation of T6SS and new flagellar operons in Vibrio cholerae O37 strain V52.* Nucleic Acids Res, 2012. **40**(16): p. 7766-75.
378. Williams, S.G., L.T. Varcoe, S.R. Attridge, and P.A. Manning, *Vibrio cholerae Hcp, a secreted protein coregulated with HlyA.* Infect Immun, 1996. **64**(1): p. 283-9.
379. Bernard, C.S., Y.R. Brunet, E. Gueguen, and E. Cascales, *Nooks and crannies in type VI secretion regulation.* J Bacteriol, 2010. **192**(15): p. 3850-60.
380. Lindquist, S., *The heat-shock response.* Annu Rev Biochem, 1986. **55**: p. 1151-91.
381. Nandi, B., R.K. Nandy, A. Sarkar, and A.C. Ghose, *Structural features, properties and regulation of the outer-membrane protein W (OmpW) of Vibrio cholerae.* Microbiology, 2005. **151**(Pt 9): p. 2975-86.
382. Soding, J., A. Biegert, and A.N. Lupas, *The HHpred interactive server for protein homology detection and structure prediction.* Nucleic Acids Res, 2005. **33**(Web Server issue): p. W244-8.
383. Bennett-Lovsey, R.M., A.D. Herbert, M.J. Sternberg, and L.A. Kelley, *Exploring the extremes of sequence/structure space with ensemble fold recognition in the program Phyre.* Proteins, 2008. **70**(3): p. 611-25.
384. Kelley, L.A. and M.J. Sternberg, *Protein structure prediction on the Web: a case study using the Phyre server.* Nat Protoc, 2009. **4**(3): p. 363-71.
385. Lemmon, M.A., *Pleckstrin homology domains: not just for phosphoinositides.* Biochem Soc Trans, 2004. **32**(Pt 5): p. 707-11.
386. Gray, M.D., M. Bagdasarian, W.G. Hol, and M. Sandkvist, *In vivo cross-linking of EpsG to EpsL suggests a role for EpsL as an ATPase-pseudopilin coupling protein in the Type II secretion system of Vibrio cholerae.* Mol Microbiol, 2011. **79**(3): p. 786-98.
387. Aubert, D., D.K. MacDonald, and M.A. Valvano, *BcsKC is an essential protein for the type VI secretion system activity in Burkholderia cenocepacia that forms an outer membrane complex with BcsLB.* J Biol Chem, 2010. **285**(46): p. 35988-98.
388. Shimada, H. and S. Kitada, *Mega assemblages of oligomeric aerolysin-like toxins stabilized by toxin-associating membrane proteins.* J Biochem, 2011. **149**(1): p. 103-15.

389. Fussle, R., S. Bhakdi, A. Sziegoleit, J. Tranum-Jensen, T. Kranz, and H.J. Wellensiek, *On the mechanism of membrane damage by Staphylococcus aureus alpha-toxin.* J Cell Biol, 1981. **91**(1): p. 83-94.
390. Chou, S., N.K. Bui, A.B. Russell, K.W. Lexa, T.E. Gardiner, M. LeRoux, W. Vollmer, and J.D. Mougous, *Structure of a peptidoglycan amidase effector targeted to Gram-negative bacteria by the type VI secretion system.* Cell Rep, 2012. **1**(6): p. 656-64.
391. Morita, Y.S., Y. Yamaryo-Botte, K. Miyanagi, J.M. Callaghan, J.H. Patterson, P.K. Crellin, R.L. Coppel, H. Billman-Jacobe, T. Kinoshita, and M.J. McConville, *Stress-induced synthesis of phosphatidylinositol 3-phosphate in mycobacteria.* J Biol Chem, 2010. **285**(22): p. 16643-50.
392. Gordesky, S.E. and G.V. Marinetti, *The asymetric arrangement of phospholipids in the human erythrocyte membrane.* Biochem Biophys Res Commun, 1973. **50**(4): p. 1027-31.
393. Bretscher, M.S., *Asymmetrical lipid bilayer structure for biological membranes.* Nat New Biol, 1972. **236**(61): p. 11-2.
394. Cavard, D., P. Sauve, F. Heitz, F. Pattus, C. Martinez, R. Dijkman, and C. Lazdunski, *Hydrodynamic properties of colicin A. Existence of a high-affinity lipid-binding site and oligomerization at acid pH.* Eur J Biochem, 1988. **172**(2): p. 507-12.
395. Benz, R., A. Schmid, W. Wagner, and W. Goebel, *Pore formation by the Escherichia coli hemolysin: evidence for an association-dissociation equilibrium of the pore-forming aggregates.* Infect Immun, 1989. **57**(3): p. 887-95.
396. Sussman, M., *Cultivation and synchronous morphogenesis of Dictyostelium under controlled experimental conditions.* Methods Cell Biol, 1987. **28**: p. 9-29.
397. Abrams, C.S., H. Wu, W. Zhao, E. Belmonte, D. White, and L.F. Brass, *Pleckstrin inhibits phosphoinositide hydrolysis initiated by G-protein-coupled and growth factor receptors. A role for pleckstrin's PH domains.* J Biol Chem, 1995. **270**(24): p. 14485-92.
398. Deak, M., A. Casamayor, R.A. Currie, C.P. Downes, and D.R. Alessi, *Characterisation of a plant 3-phosphoinositide-dependent protein kinase-1 homologue which contains a pleckstrin homology domain.* FEBS Lett, 1999. **451**(3): p. 220-6.
399. Guzman, L.M., D. Belin, M.J. Carson, and J. Beckwith, *Tight regulation, modulation, and high-level expression by vectors containing the arabinose PBAD promoter.* J Bacteriol, 1995. **177**(14): p. 4121-30.
400. Solomon, J.M., A. Rupper, J.A. Cardelli, and R.R. Isberg, *Intracellular growth of Legionella pneumophila in Dictyostelium discoideum, a system for genetic analysis of host-pathogen interactions.* Infect Immun, 2000. **68**(5): p. 2939-47.
401. Cosson, P., L. Zulianello, O. Join-Lambert, F. Faurisson, L. Gebbie, M. Benghezal, C. Van Delden, L.K. Curty, and T. Kohler, *Pseudomonas aeruginosa virulence analyzed in a Dictyostelium discoideum host system.* J Bacteriol, 2002. **184**(11): p. 3027-33.
402. Maroun, C.R., D.K. Moscatello, M.A. Naujokas, M. Holgado-Madruga, A.J. Wong, and M. Park, *A conserved inositol phospholipid binding site within the pleckstrin homology domain of the Gab1 docking protein is required for epithelial morphogenesis.* J Biol Chem, 1999. **274**(44): p. 31719-26.

403. McNamara, B.P., A. Koutsouris, C.B. O'Connell, J.P. Nougayrede, M.S. Donnenberg, and G. Hecht, *Translocated EspF protein from enteropathogenic Escherichia coli disrupts host intestinal barrier function.* J Clin Invest, 2001. **107**(5): p. 621-9.
404. Kanack, K.J., J.A. Crawford, I. Tatsuno, M.A. Karmali, and J.B. Kaper, *SepZ/EspZ is secreted and translocated into HeLa cells by the enteropathogenic Escherichia coli type III secretion system.* Infect Immun, 2005. **73**(7): p. 4327-37.
405. Garcia-Angulo, V.A., W. Deng, N.A. Thomas, B.B. Finlay, and J.L. Puente, *Regulation of expression and secretion of NleH, a new non-locus of enterocyte effacement-encoded effector in Citrobacter rodentium.* J Bacteriol, 2008. **190**(7): p. 2388-99.
406. Elliott, S.J., C.B. O'Connell, A. Koutsouris, C. Brinkley, M.S. Donnenberg, G. Hecht, and J.B. Kaper, *A gene from the locus of enterocyte effacement that is required for enteropathogenic Escherichia coli to increase tight-junction permeability encodes a chaperone for EspF.* Infect Immun, 2002. **70**(5): p. 2271-7.
407. Taylor, G.S. and J.E. Dixon, *PTEN and myotubularins: families of phosphoinositide phosphatases.* Methods Enzymol, 2003. **366**: p. 43-56.
408. Minagawa, T., T. Ijuin, Y. Mochizuki, and T. Takenawa, *Identification and characterization of a sac domain-containing phosphoinositide 5-phosphatase.* J Biol Chem, 2001. **276**(25): p. 22011-5.
409. Taylor, G.S., T. Maehama, and J.E. Dixon, *Myotubularin, a protein tyrosine phosphatase mutated in myotubular myopathy, dephosphorylates the lipid second messenger, phosphatidylinositol 3-phosphate.* Proc Natl Acad Sci U S A, 2000. **97**(16): p. 8910-5.
410. Broberg, C.A., L. Zhang, H. Gonzalez, M.A. Laskowski-Arce, and K. Orth, *A Vibrio effector protein is an inositol phosphatase and disrupts host cell membrane integrity.* Science, 2010. **329**(5999): p. 1660-2.
411. Niebuhr, K., S. Giuriato, T. Pedron, D.J. Philpott, F. Gaits, J. Sable, M.P. Sheetz, C. Parsot, P.J. Sansonetti, and B. Payrastre, *Conversion of PtdIns(4,5)P(2) into PtdIns(5)P by the S.flexneri effector IpgD reorganizes host cell morphology.* EMBO J, 2002. **21**(19): p. 5069-78.
412. Hernandez, L.D., K. Hueffer, M.R. Wenk, and J.E. Galan, *Salmonella modulates vesicular traffic by altering phosphoinositide metabolism.* Science, 2004. **304**(5678): p. 1805-7.
413. Dowler, S., R.A. Currie, D.G. Campbell, M. Deak, G. Kular, C.P. Downes, and D.R. Alessi, *Identification of pleckstrin-homology-domain-containing proteins with novel phosphoinositide-binding specificities.* Biochem J, 2000. **351**(Pt 1): p. 19-31.
414. Rebecchi, M.J. and S. Scarlata, *Pleckstrin homology domains: a common fold with diverse functions.* Annu Rev Biophys Biomol Struct, 1998. **27**: p. 503-28.
415. Ferguson, K.M., M.A. Lemmon, P.B. Sigler, and J. Schlessinger, *Scratching the surface with the PH domain.* Nat Struct Biol, 1995. **2**(9): p. 715-8.
416. Strassmann, J.E., O.M. Gilbert, and D.C. Queller, *Kin discrimination and cooperation in microbes.* Annu Rev Microbiol, 2011. **65**: p. 349-67.
417. Zhang, Y., A. Ducret, J. Shaevitz, and T. Mignot, *From individual cell motility to collective behaviors: insights from a prokaryote, Myxococcus xanthus.* FEMS Microbiol Rev, 2012. **36**(1): p. 149-64.

418. Hibbing, M.E., C. Fuqua, M.R. Parsek, and S.B. Peterson, *Bacterial competition: surviving and thriving in the microbial jungle.* Nat Rev Microbiol, 2010. **8**(1): p. 15-25.
419. Jani, A.J. and P.A. Cotter, *Type VI secretion: not just for pathogenesis anymore.* Cell Host Microbe, 2010. **8**(1): p. 2-6.
420. Huq, A., E.B. Small, P.A. West, M.I. Huq, R. Rahman, and R.R. Colwell, *Ecological relationships between Vibrio cholerae and planktonic crustacean copepods.* Appl Environ Microbiol, 1983. **45**(1): p. 275-83.
421. Schwarz, S., T.E. West, F. Boyer, W.C. Chiang, M.A. Carl, R.D. Hood, L. Rohmer, T. Tolker-Nielsen, S.J. Skerrett, and J.D. Mougous, *Burkholderia type VI secretion systems have distinct roles in eukaryotic and bacterial cell interactions.* PLoS Pathog, 2010. **6**(8): p. e1001068.
422. Espesset, D., Y. Corda, K. Cunningham, H. Benedetti, R. Lloubes, C. Lazdunski, and V. Geli, *The colicin A pore-forming domain fused to mitochondrial intermembrane space sorting signals can be functionally inserted into the Escherichia coli plasma membrane by a mechanism that bypasses the Tol proteins.* Mol Microbiol, 1994. **13**(6): p. 1121-31.
423. Lazdunski, C.J., D. Baty, V. Geli, D. Cavard, J. Morlon, R. Lloubes, S.P. Howard, M. Knibiehler, M. Chartier, S. Varenne, and et al., *The membrane channel-forming colicin A: synthesis, secretion, structure, action and immunity.* Biochim Biophys Acta, 1988. **947**(3): p. 445-64.
424. Fields, K.L. and S.E. Luria, *Effects of colicins E1 and K on cellular metabolism.* J Bacteriol, 1969. **97**(1): p. 64-77.
425. Greig, S.L., M. Radjainia, and A.K. Mitra, *Oligomeric structure of colicin ia channel in lipid bilayer membranes.* J Biol Chem, 2009. **284**(24): p. 16126-34.
426. Schein, S.J., B.L. Kagan, and A. Finkelstein, *Colicin K acts by forming voltage-dependent channels in phospholipid bilayer membranes.* Nature, 1978. **276**(5684): p. 159-63.
427. Zakharov, S.D. and W.A. Cramer, *Insertion intermediates of pore-forming colicins in membrane two-dimensional space.* Biochimie, 2002. **84**(5-6): p. 465-75.
428. Stroud, R., *Ion channel forming colicins.* Curr Opin Struct Biol, 1995. **5**(4): p. 514-20.
429. Abrams, C.K., K.S. Jakes, A. Finkelstein, and S.L. Slatin, *Identification of a translocated gating charge in a voltage-dependent channel. Colicin E1 channels in planar phospholipid bilayer membranes.* J Gen Physiol, 1991. **98**(1): p. 77-93.
430. Cameron, D.E., J.M. Urbach, and J.J. Mekalanos, *A defined transposon mutant library and its use in identifying motility genes in Vibrio cholerae.* Proc Natl Acad Sci U S A, 2008. **105**(25): p. 8736-41.
431. Ma, L., Y. Zhang, X. Yan, L. Guo, L. Wang, J. Qiu, R. Yang, and D. Zhou, *Expression of the type VI secretion system 1 component Hcp1 is indirectly repressed by OpaR in Vibrio parahaemolyticus.* ScientificWorldJournal, 2012. **2012**: p. 982140.
432. Espesset, D., D. Duche, D. Baty, and V. Geli, *The channel domain of colicin A is inhibited by its immunity protein through direct interaction in the Escherichia coli inner membrane.* EMBO J, 1996. **15**(10): p. 2356-64.
433. Mukherjee, S., H. Yakhnin, D. Kysela, J. Sokoloski, P. Babitzke, and D.B. Kearns, *CsrA-FliW interaction governs flagellin homeostasis and a checkpoint on flagellar morphogenesis in Bacillus subtilis.* Mol Microbiol, 2011. **82**(2): p. 447-61.

434. Perrett, C.A. and D. Zhou, *Type three secretion system effector translocation: one step or two?* Front Microbiol, 2011. **2**: p. 50.
435. Lazzaroni, J.C., J.F. Dubuisson, and A. Vianney, *The Tol proteins of Escherichia coli and their involvement in the translocation of group A colicins.* Biochimie, 2002. **84**(5-6): p. 391-7.
436. Yamashita, E., M.V. Zhalnina, S.D. Zakharov, O. Sharma, and W.A. Cramer, *Crystal structures of the OmpF porin: function in a colicin translocon.* EMBO J, 2008. **27**(15): p. 2171-80.
437. Zakharov, S.D. and W.A. Cramer, *On the mechanism and pathway of colicin import across the E. Coli outer membrane.* Front Biosci, 2004. **9**: p. 1311-7.
438. Akutsu, A., H. Masaki, and T. Ohta, *Molecular structure and immunity specificity of colicin E6, an evolutionary intermediate between E-group colicins and cloacin DF13.* J Bacteriol, 1989. **171**(12): p. 6430-6.
439. Zhang, H., Z.Q. Gao, W.J. Wang, G.F. Liu, J.H. Xu, X.D. Su, and Y.H. Dong, *Structure of the type VI effector-immunity complex (Tae4-Tai4) provides novel insights into the inhibition mechanism of the effector by its immunity protein.* J Biol Chem, 2013.
440. Miyada, C.G., L. Stoltzfus, and G. Wilcox, *Regulation of the araC gene of Escherichia coli: catabolite repression, autoregulation, and effect on araBAD expression.* Proc Natl Acad Sci U S A, 1984. **81**(13): p. 4120-4.
441. Studier, F.W. and B.A. Moffatt, *Use of bacteriophage T7 RNA polymerase to direct selective high-level expression of cloned genes.* J Mol Biol, 1986. **189**(1): p. 113-30.
442. Gode-Potratz, C.J. and L.L. McCarter, *Quorum sensing and silencing in Vibrio parahaemolyticus.* J Bacteriol, 2011. **193**(16): p. 4224-37.
443. Dougan, G., Saul, M., Warren, G., Sherratt, D., *A Functional Map of Plasmid ColE1.* Molecular and General Genetics, 1978. **158**(3): p. 325-7.
444. Andreoli, P.M., N. Overbeeke, E. Veltkamp, J.D. van Embden, and H.J. Nijkamp, *Genetic map of the bacteriocinogenic plasmid CLO DF13 derived by insertion of the transposon Tn901.* Mol Gen Genet, 1978. **160**(1): p. 1-11.
445. Zhang, X.Y., R. Lloubes, and D. Duche, *Channel domain of colicin A modifies the dimeric organization of its immunity protein.* J Biol Chem, 2010. **285**(49): p. 38053-61.
446. Covacci, A. and R. Rappuoli, *Pertussis toxin export requires accessory genes located downstream from the pertussis toxin operon.* Mol Microbiol, 1993. **8**(3): p. 429-34.
447. Jones, A.L., K. Shirasu, and C.I. Kado, *The product of the virB4 gene of Agrobacterium tumefaciens promotes accumulation of VirB3 protein.* J Bacteriol, 1994. **176**(17): p. 5255-61.
448. Sory, M.P., A. Boland, I. Lambermont, and G.R. Cornelis, *Identification of the YopE and YopH domains required for secretion and internalization into the cytosol of macrophages, using the cyaA gene fusion approach.* Proc Natl Acad Sci U S A, 1995. **92**(26): p. 11998-2002.
449. Rosqvist, R., K.E. Magnusson, and H. Wolf-Watz, *Target cell contact triggers expression and polarized transfer of Yersinia YopE cytotoxin into mammalian cells.* EMBO J, 1994. **13**(4): p. 964-72.
450. Cornelis, G.R. and F. Van Gijsegem, *Assembly and function of type III secretory systems.* Annu Rev Microbiol, 2000. **54**: p. 735-74.

451. Metcalf, W.W., W. Jiang, L.L. Daniels, S.K. Kim, A. Haldimann, and B.L. Wanner, *Conditionally replicative and conjugative plasmids carrying lacZ alpha for cloning, mutagenesis, and allele replacement in bacteria.* Plasmid, 1996. **35**(1): p. 1-13.
452. Livak, K.J. and T.D. Schmittgen, *Analysis of relative gene expression data using real-time quantitative PCR and the 2(-Delta Delta C(T)) Method.* Methods, 2001. **25**(4): p. 402-8.
453. Heidelberg, J.F., J.A. Eisen, W.C. Nelson, R.A. Clayton, M.L. Gwinn, R.J. Dodson, D.H. Haft, E.K. Hickey, J.D. Peterson, L. Umayam, S.R. Gill, K.E. Nelson, T.D. Read, H. Tettelin, D. Richardson, M.D. Ermolaeva, J. Vamathevan, S. Bass, H. Qin, I. Dragoi, P. Sellers, L. McDonald, T. Utterback, R.D. Fleishmann, W.C. Nierman, O. White, S.L. Salzberg, H.O. Smith, R.R. Colwell, J.J. Mekalanos, J.C. Venter, and C.M. Fraser, *DNA sequence of both chromosomes of the cholera pathogen Vibrio cholerae.* Nature, 2000. **406**(6795): p. 477-83.
454. Parker, C., S.H. Richardson, and W.R. Romig, *Production of Bacteriophage-Associated Materials by Vibrio cholerae: Possible Correlation with Pathogenicity.* Infect Immun, 1970. **1**(4): p. 417-20.
455. Mekalanos, J.J., R.J. Collier, and W.R. Romig, *Enzymic activity of cholera toxin. I. New method of assay and the mechanism of ADP-ribosyl transfer.* J Biol Chem, 1979. **254**(13): p. 5849-54.
456. Chakrabarti, B.K., K. Si, and D. Chattopadhyay, *Characterization of Vibrio cholerae EIT or typing phage D10.* J Gen Virol, 1996. **77 (Pt 11)**: p. 2881-4.
457. Makino, K., K. Oshima, K. Kurokawa, K. Yokoyama, T. Uda, K. Tagomori, Y. Iijima, M. Najima, M. Nakano, A. Yamashita, Y. Kubota, S. Kimura, T. Yasunaga, T. Honda, H. Shinagawa, M. Hattori, and T. Iida, *Genome sequence of Vibrio parahaemolyticus: a pathogenic mechanism distinct from that of V cholerae.* Lancet, 2003. **361**(9359): p. 743-9.
458. Elliott, S.J. and J.B. Kaper, *Role of type 1 fimbriae in EPEC infections.* Microb Pathog, 1997. **23**(2): p. 113-8.
459. Simon, R., Priefer, U., and Puhler, A., *A Broad Host Range Mobilization System for In Vivo Genetic Engineering: Transposon Mutagenesis in Gram Negative Bacteria.* Nature Biotechnology, 1983. **1**: p. 784-791.
460. Blattner, F.R., G. Plunkett, 3rd, C.A. Bloch, N.T. Perna, V. Burland, M. Riley, J. Collado-Vides, J.D. Glasner, C.K. Rode, G.F. Mayhew, J. Gregor, N.W. Davis, H.A. Kirkpatrick, M.A. Goeden, D.J. Rose, B. Mau, and Y. Shao, *The complete genome sequence of Escherichia coli K-12.* Science, 1997. **277**(5331): p. 1453-62.
461. Iguchi, A., N.R. Thomson, Y. Ogura, D. Saunders, T. Ooka, I.R. Henderson, D. Harris, M. Asadulghani, K. Kurokawa, P. Dean, B. Kenny, M.A. Quail, S. Thurston, G. Dougan, T. Hayashi, J. Parkhill, and G. Frankel, *Complete genome sequence and comparative genome analysis of enteropathogenic Escherichia coli O127:H6 strain E2348/69.* J Bacteriol, 2009. **191**(1): p. 347-54.
462. Mulcahy, H., L. Charron-Mazenod, and S. Lewenza, *Extracellular DNA chelates cations and induces antibiotic resistance in Pseudomonas aeruginosa biofilms.* PLoS Pathog, 2008. **4**(11): p. e1000213.
463. Hsiao, A., Z. Liu, A. Joelsson, and J. Zhu, *Vibrio cholerae virulence regulator-coordinated evasion of host immunity.* Proc Natl Acad Sci U S A, 2006. **103**(39): p. 14542-7.